Infection of human blood-brain barrier cells in vitro by different subtypes of enterovirus a71 and its consequences on permeability and particles release

Igor Lopes Coqueiro

Université Clermont Auvergne

Année 2022 N° d'ordre

Ecole Doctorale des Sciences de la Vie, Sante, Agronomie & Environnement

Thèse

Présentée à l'Université Clermont Auvergne, Clermont-Ferrand pour l'obtention du grade de (décret du 5 juillet 1984)

DOCTEUR

Spécialité : ***Microbiologie***

Le 31 janvier 2023 par

Igor Lopes Coqueiro

INFECTION OF HUMAN BLOOD-BRAIN BARRIER CELLS IN VITRO BY DIFFERENT SUBTYPES OF ENTEROVIRUS A71 AND ITS CONSEQUENCES ON PERMEABILITY AND PARTICLES RELEASE

Devant la commission d'examen composée de :

Rapporteurs :	Professeur Fabien GOSSELET, Docteur Sylvie PILLET, Professeur Nicolas LEVEQUE
Examinateurs :	Docteur Karen COSTE
Président du jury:	Professeur Cécile HENQUELL
Directeur de Thèse :	Docteur Jean-Luc BAILLY

Laboratoire Microorganismes : Génome et Environnement, CNRS 6023
Equipe Epidémiologie et Physiopathologie des Infections à Entérovirus

À un enfant qui un jour a rêvé de faire de l'étude
de la biologie son propre métier,
Je dédis

Se essa rua
Se essa rua fosse minha
Eu mandava
Eu mandava ladrilhar
Com pedrinhas
Com pedrinhas de brilhante
Para o meu
Para o meu amor passar

Nessa rua
Nessa rua tem um bosque
Que se chama
Que se chama solidão
Dentro dele
Dentro dele mora um anjo
Que roubou
Que roubou meu coração

Se eu roubei
Se eu roubei teu coração
Tu roubaste
Tu roubaste o meu também
Se eu roubei
Se eu roubei teu coração
É porque
É porque te quero bem

(Auteur inconnu)

Remerciements

J'attribue la valeur de ce travail à la contribution de chaque employé direct et indirect dans ce cycle d'apprentissage. J'ai donc beaucoup de raisons d'être reconnaissant.

Je remercie mon encadrant Jean-Luc BAILLY de m'avoir ouvert les portes de son laboratoire. J'ai vécu une expérience unique et authentique grâce à sa générosité. Je remercie Léa GAUME, Isabelle SIMON, et Gwendoline JUGIE pour leur travail expérimental. Vous étiez les bras, les mains et les jambes qui ont contribué à générer la collecte d'informations qui constitue le corps de ce travail. Je suis reconnaissante pour l'interaction et l'échange de connaissances que j'ai eu tout au long de cette période avec l'équipe EPIE (Anais, Arnaud, Elise, Gael, Ghizlane, Hélène, Jérome, Mahya, Maxime, Nathalie, Siméon et Stéphanie). Je remercie tout particulièrement à Audrey MIRAND, Cecile HENQUELL, Christine ARCHIMBAUD, Fabien GOESSELET, Maxime BISSEUX, Nicolas LEVEQUE, et Sylvie PILETT pour les considérations précieuses qui ont permis d'affiner le travail.

Je remercie l'ensemble du secrétariat de l'Université Clermont Auvergne pour son aide dans les démarches bureaucratiques, en particulier Samira RIAD, Emmeline BLANC, Rita BOUZABOUNE, Mélanie MOULIN, Mélanie RIGAL, et Valérie LYONNET. Je remercie le laboratoire GReD, en particulier Caroline VACHIAS pour les analyses en microscopie. Je remercie le CHU et le laboratoire Neuro-Dol pour la disponibilité de leur infrastructure. Je remercie UCA, EDSVSAE et LMGE pour l’accueil.

Je remercie nos collaborateurs extérieurs pour leur accueil dans leurs établissements et pour leur formation technique :

> Au Laboratoire de la Barrière Hémato-Encéphalique, je remercie tout particulièrement Lucie Dehouck, Emmanuel Sevin et Fabien Gosselet.
>
> Et à l'Université technique du Danemark, je remercie tout particulièrement Asli Doğan, Hakan Gürbüz et Martin Dufva.

Je remercie le réseau de collaborateurs du consortium OrganoVIR, en particulier Dasja Pajkrt et Katja Wolthers pour avoir idéalisé cette initiative. Merci à l'équipe de The power of time off pour l'excellent programme de développement personnel, en

particulier à Ingrid Valks. Je remercie tous les scientifiques qui croient aux possibilités d'aller au-delà des frontières de la connaissance.

Je remercie ma famille: mon père José Orestes Coqueiro, ma mère Peônia Lopes Coqueiro et mon frère José Orestes Coqueiro Filho pour être ma fondation.

Muito obrigado!

Résumé

La barrière hémato-encéphalique (BHE) formée par la microvasculature cérébrale peut être contournée lors de l'invasion du système nerveux central (SNC) par des virus neurotropes. L'entérovirus A71 (EV-A71) est décrit comme un agent pathogène capable de migrer via les nerfs périphériques vers le cerveau par transport axonal rétrograde. Cependant, nous ne savons toujours pas si l'EV-A71 est capable d'envahir le SNC via la BHE. Dans cette thèse, nous avons utilisé un modèle in vitro de la BHE humaine co-cultivant des cellules endothéliales cérébrales (BLEC) et des péricytes. Grâce à ce modèle, nous avons montré que l'EV-A71 n'affecte pas les principales caractéristiques de la BHE telles que la perméabilité paracellulaire, car peu de cellules endotheliales sont infectées. Le virus infectieux est libéré principalement par le pôle luminal. Cependant, nous avons aussi détecté la libération de quelques particules virales infectieuses par le pôle baso-latéral et la présence d'ARN viraux dans ce compartiment baso-latéral. Ce travail ouvre des perspectives d'étude vers d'autres modes de franchissement de la BHE par l'EV-A71.

Mots-clés : Barrière hémato-encéphalique ; Entérovirus A71 ; Maladie pieds-mains-bouche ; Neuroinflammation ; Infection neurologique.

Abstract

The blood-brain barrier (BBB) formed by the brain microvasculature can be circumvented during the invasion of the central nervous system (CNS) by neurotropic viruses. Enterovirus A71 (EV-A71) is well reported as a pathogen capable of migrating to the brain through peripherical nerves via retrograde axonal transport. However, we still do not know whether EV-A71 is capable of invading the CNS through the BBB. In this thesis we used an in vitro model of the human BBB by co-culture brain-like endothelial cells (BLECs) and pericytes. With this model, we showed that EV-A71 does not affect the main characteristics of the BBB, such as paracellular permeability because few BLECs are productively infected. High amounts of infectious viruses are released from the luminal side. However, we also detected leakage of infectious viruses from the baso-lateral side and the presence of viral RNAs in the baso-lateral compartment. This work provides opportunities to the analyses of other mechanisms of BBB crossing by EV-A71.

Key words: Blood-brain barrier; Enterovirus A71; Hand, foot and mouth disease; Neuroinflammation; Neurological disease

Abbreviations

ABC	ATP-binding cassette
Akt	V-akt murine thymoma viral oncogene homolog
AMPK	AMP-activated protein kinase
Ang-1	Angiopoietin 1
APJ	Apelin Receptor
Arp2/3	Actin-related protein 2/3
ASC	Apoptosis-associated speck-like protein
ATP	Adenosine Tri-Phosphate
BBB	Blood-brain barrier
BCRP	Breast cancer resistance protein
BLECs	Brain-like endothelial cells
CB	cell buffer
CCL	chemokine ligand
CNS	Central nervous system
CPT2	Carnitine palmitoyltransferase 2
CSF	Cerebrospinal fluid
CV	Coxsackievirus
CypA	Cyclophilin A
DAMPs	Danger associated molecular patterns
DMEM	Dulbecco's Modified Eagle's Medium
dsRNA	Double-stranded RNA
E6	Echovirus 6
EBP3	End-binding protein 3
ECGS	Endothelial cell growth supplement
ECM	Endothelial cell medium
ECs	Endothelial cells
EDTA	Ethylenediaminetetraacetic acid
eIFG4	eukaryotic translation initiation factor 4G
Erk	Extracellular signal-regulated kinase
Etv2	ETS variant transcription factor 2
EV-A71	Enterovirus A71
FAK	Focal adhesion kinase

FBS	Fœtal Bovine Serum
Flk1	Fetal Liver Kinase 1
Fox	Forkhead transcription factor
Fzd	Frizzled protein
GF-AFC	Glycyl-phenylalanyl-aminofluorocoumarin
GLUT-1	Glucose transporter 1
Gpr124	Probable G-protein coupled receptor 124
h.p.i	Hours post infection
HBSS	Hank's balanced salt solution
hCMEC/D3	Human cortical microvessels endothelial cells/D3
HEPES	4-(2-hydroxyethyl)-1-piperazineethanesulfonic acid
HFMD	Hand, foot and mouth disease
HMGB1	High-mobility group protein 1
hSCARB2	Human scavenger receptor class B member 2
HSPCs	Hematopoietic stem and progenitor cells
IF	Immunofluorescence
IFN	Interferon
IFNAR	Interferon-α/β receptor
IFNs	Interferons
IkBa	Factor kappa light polypeptide gene enhancer in B-cells inhibitor, alpha
IL	Interleukin
IL-18	Interleukin 18
iNOS	Inducible nitric oxide synthase
iPSCs	Human induced pluripotent stem cell
IRAK1/4	Interleukin-1 receptor-associated kinase **4**
IRES	Internal ribosomal entry site
IRF3/7	Interferon Regulatory Factor 3/7
ISG	interferon-stimulated genes
ISRE	Interferon-sensitive response element
ITAFs	Trans-acting factors
JAK2	janus kinase-2
JAMs	Junctional adhesion molecules

LIF	Leukemia inhibitory factor
LY assay	Lucyfer Yellow assay
MAGUK	Membrane-associated guanylate kinase
MAVS	Mitochondrial antiviral-signaling
MDA5	Melanoma differentiation-associated protein 5
Mef2c	Myocyte Enhancer Factor 2C
MEK	Mitogen-activated protein kinase kinase
MLCK	Myosin light-chain kinase
MMPs	Matrix metalloproteinases
MOI	Multiplicity of infection
MPNCU	MPNCU
MRPs	Multidrug resistance proteins
MyD88	Myeloid differentiation primary response 88
N-WASP	Neural Wiskott–Aldrich syndrome protein
NEK7	NIMA related kinase 7
NF-κB	Nuclear factor-kappa beta
NLRP3	NOD-like receptor family, pyrin domain containing 3
NO	Nitric oxide
NVUs	Neurovascular units
OATPs	Organic anion transporting polypeptides
OCTs	Organic cation transporters
ORF	Open reading frame
P-gp	P-glycoprotein
PBS	Phosphate buffered saline
PCAM-1	Platelet endothelial cell adhesion molecule
Pe	Permeability coefficient
PECAM	Platelet-endothelial cell adhesion molecule
PKC	Protein kinase C
PKCδ	Protein kinase C delta
PSGL-1	P-selectin glycoprotein ligand-1
RD cells	Human rhabdomyosarcoma cells
Rho 123	Rhodamine 123
RhoK	Rho kinase

RIG-I	Retinoic acid-inducible gene 1
RT-qPCR	Reverse transcription polymerase chain reaction
S1P	Sphingosine-1-phosphate
SLC	Solute carriers
Src	Proto-Oncogene, Non-Receptor Tyrosine Kinase
STAT1/2	Signal transducer and activator of transcription 1/2
STAT3	Signal transducers and activators of transcription 3
TAB2/3	TGF-β Activated Kinase 2/3
TAK1	Janus kinase 1
TAMPs	Tight junction-associated marvel proteins
TBK1	TANK-binding kinase 1
TEER	Transendothelial electrical resistance
TGF-b1	Transforming growth factor beta 1
TGF-β	Transforming growth factor beta
Tie2	tyrosine kinase with immunoglobulin and EGF homology domains
TLR	Toll-like receptor
TNF	Tumor necrosis factor
TRAF6	TNF Receptor Associated Factor 6
TRIF	TIR-domain-containing adapter-inducing interferon-β
TYK2	Tyrosine Kinase 2
UTR	Untranslated region
VEGF	Vascular endothelial growth factor
WARS	Tryptophanyl-tRNA synthetase
YAP1	yes-associated protein 1
ZO	Zonula occludens

List of figures

List of tables

Summary

INTRODUCTION

1) Introduction

Non-polio enteroviruses represent a public health concern for causing a wide range of human infections, occasionally severe and associated with neurological complications (Baggen et al., 2018; Owino & Chu, 2019; and Harvala et al., 2021). After the almost complete eradication of poliomyelitis and wild poliovirus types, non-polio enteroviruses such as enterovirus A71 (EV-A71) emerged as a pathogens responsible for spreading a polio-like disease (**Fig. 1**) during outbreaks reported worldwide (Bitnun & Yeh, 2018; Gilsdorf, 2019; Brown et al., 2020; and Wang et al., 2022).

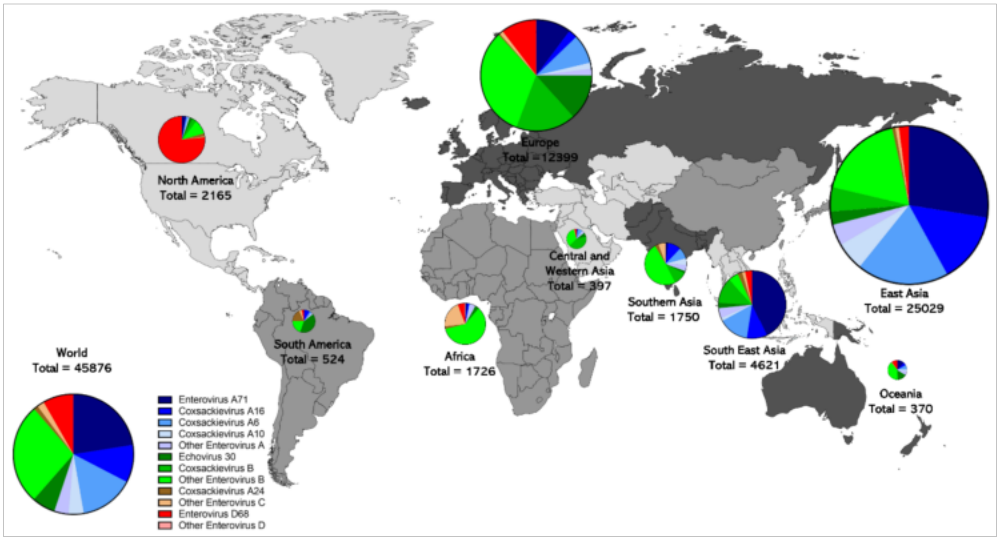

Fig. 1. Global incidence of non-polio enteroviruses. The figure indicates records of genomic sequences collected from 2000 to 2018. The sequences are classified as enterovirus species A (blue), B (green), C (brown), and D (red). The distribution pattern is highlighted in nine regions of the world. The total number of sequences within each virus group is proportional to the size of pie graphs. Figure from Brown et al., 2020.

HFMD is a highly contagious, communicable infectious disease caused by several enterovirus types – notably those assigned to the EV-A species (see below) – that affect predominantly infants and young children below 5 years (McMinn, 2014 and Zhu et al., 2014). The patients generally manifest low-grade fever, malaise and myalgia for a few days followed by appearance of rashes, vesicular and maculovesicular eruptions on hands, feet, mouth, buttocks and oral cavity (**Fig. 2**) (Goksugur & Goksugur, 2010 and Gu et al., 2017). In the most cases, HFMD is a benign illness, however, EV-A71

infections represent a high risk of developing severe neurological complications, such as aseptic meningoencephalitis, poliomyelitis-like acute flaccid paralysis, respiratory difficulties, and fatal outcomes (Tee et al., 2010; Mirand et al., 2015; and Nayak et al., 2022).

Fig. 2. Typical symptoms of hand, foot and mouth disease. HFMD may cause vesicular and maculovesicular eruptions **(a-b)**, exfoliation of soles **(c)**, maculopapular lesions **(d)**, and onychomadesis **(e)**. Figure from Ślebioda & Dorocka-Bobkowska, 2018.

The main manifestations of severe HFMD are cardiopulmonary failure in consequence of damages in the brainstem, especially medulla oblongata and hypothalamus (Shen et al., 1999; Jiang et al., 2012; and Phan et al., 2019). Children under 2 years old are more vulnerable to severe EV-A71 infections and may develop cognitive sequelae (Chang et al., 2007).

In 1998 in Taiwan, an EV-A71 outbreak was monitored and the report of clinical features served as a robust panel for characterization of severe EV-A71 infections. Patients infected with EV-A71 generally manifest persistent fever, vomiting, ulcerative lesions in buccal mucosa, oral cavity, tong, hands, and feet. These symptoms are self-limited, but it may progress to neurological complications similar those caused by

poliomyelitis. The neurological complications may be classified in three syndromes: aseptic meningitis, acute flaccid paralysis, and rhombencephalitis (Huang et al., 1999).

Aseptic meningitis is characterized by headache, vomiting, fever, and stiffness of the neck. Among the neurological syndromes characterized, aseptic meningitis presents the highest chance of favorable evolution.

Acute flaccid paralysis of the arms or the legs, may occur without loss of senses, such as pain, heat or cold. Transient symptoms of rhombencephalitis (myoclonus, tremor, and ataxia) may occur before the paralysis. The magnetic resonance imaging (MRI) shows that patients with acute flaccid paralysis may present lesions on spinal cord. A complete recovery is possible, but patients may persist with limb weakness and atrophy.

During the rhombencephalitis, the patients manifest myoclonus, jerks even during sleep, tremors, ataxia, hallucinations, and respiratory abnormalities. Patients with rhombencephalitis may present MRI with signal lesions at the brainstem. The severity of rhombencephalitis vary in three grades: romboencephalitis of grade I are characterized by generalized myoclonic jerks with tremor and ataxia. In the grade II, the myoclonus involves cranial-nerves. Patients may present ocular and facial involuntary movements. The grade III is the most severe manifestation of EV-A71 infection. Patients present a transient myoclonus followed by respiratory distress, cyanosis, apnea, loss of doll's eye reflex , shock, and coma. Patients with grade III requires mechanical ventilation after admission due the risk of fulminant pulmonary.

Overall, the location of lesions on CNS defines the severity of the infection. The white cell counting, the levels of glucose, and protein, in CSF are similar among the neurological syndromes caused by EV-A71.

A special attention in patients less than five years old presenting vomiting, restlessness, and unconsciousness is required in early diagnosis of severe HFMD (Tu et al., 2015 and van Hinsbergh et al., 2020). The main causes of medical consultation are persistent high fever, restlessness, loss of appetite, discomfort while eating, and intense cutaneous lesions for up to one week (Gu et al., 2017 and Ślebioda & Dorocka-Bobkowska, 2018). In the most severe cases, patients are admitted with neurological

symptoms such as headache, vomiting, lethargy, altered consciousness, paralysis, spasms, or convulsions (Hohmann & Kim, 2012 and Long et al., 2016). Monitoring of the blood pressure, platelets and phosphatase levels, and when possible neuroimaging and electroencephalography examinations, are important for patient management (Kovacs et al., 2001; Hohmann & Kim, 2012; and R. Li et al., 2014).

Treatments for severe HFMD are still not available, therefore developing antiviral drugs is an urgent need (Aylward et al., 2003 and Ludlam et al., 2006). There is no specific treatment for mild EV infections other than symptomatic, mostly to control the body temperature (Foli-Andersen et al., 2022). Antibiotic treatment is unnecessary and may expose the community to the risk of selection of resistant microorganisms, which have been emerging as a cause of mortality among neonates (Hollander et al., 2005; D'Acremont et al., 2014; and Saha et al., 2018). Severe EV infections require hospitalisation for specialised management.

The sequelae reported with severe CNS infections include dysfunctional aerodigestive tract, neurological sequelae, delayed neurodevelopment, impaired cognition, as well as psychosocial problems. The long-term monitoring with complete clinical assessment of young children with historic of severe HFMD or other CNS infections are recommended to improve the outcomes (van Hinsbergh et al., 2020).

EV-A71 is a common etiologic agent of HFMD. When the virus reaches the central nervous system (CNS), a neuroinflammatory process is triggered, affecting permeability of brain microvasculature, which form the blood brain barrier (BBB) (Coyne et al., 2007 and Wang et al., 2020). EV-A71 may invade the CNS by axonal retrograde transport, inside infected leukocytes or crosses the BBB of brain microvasculature (Mizutani et al., 2016 and Wiatr et al., 2019). Different EV types can effectively infect brain microvascular endothelial cells. However, in a study from our group, these cells were reported to be resistant to EV-A71 infection (Volle et al., 2015). In the present study, we reexamined whether EV-A71 can infect cerebral microvascular endothelial cells within an in vitro model of human BBB including pericytes. The results obtained are consistent with those obtained earlier (Volle et al., 2015) and suggest that EV-A71 does not cross efficiently the human BBB.

BIBLIOGRAPHY

2) Bibliography

I. Epidemiology and diversity of enterovirus A71 (EV-A71)

a. Incidence and surveillance of HFMD

The first description of HFMD and detection of EV-A71 were reported at a time when most outbreaks of EV neurological diseases were caused by poliovirus, coxsackievirus, and echovirus strains (Robinson et al., 1958; Johnson et al., 1960; Duncan, 1961; Flewett et al., 1963; and Portnoy et al., 1965). Since then, epidemiological studies of HFMD outbreaks have suggested that severe HFMD is significantly associated with an infection caused by EV-A71.

HFMD outbreaks happen due to several determinants, such as rapid population growth, climate change, socioeconomic changes, and other lifestyle changes (Puenpa et al., 2019 and Abdul Wahid et al., 2021). In countries of the Asia-Pacific region, HFMD outbreaks occur in a cyclical pattern of every three years. In this geographic region, HFMD outbreaks has been associated with the co-circulation of coxsackievirus A16 and EV-A71 (Xu et al., 2010 and Nayak et al., 2022). In China, outbreaks of HFMD associated with EV-A71 have affected millions of children, and represent a serious public health concern (Liu et al., 2011). After several large HFMD outbreaks in the Asia-Pacific region, some countries established a sentinel surveillance program for EV-A71 (Podin et al., 2006; Koh et al., 2018; Chiu et al., 2020; and F. He et al., 2022). In this epidemiological context, HFMD is a notifiable disease in several Asian countries, including Singapore since 2000 and China since 2008. Investigations in Europe are scarce because HFMD do not benefit from a specific and active surveillance. In France, the ambulatory paediatric surveillance of HFMD between 2014 and 2015 showed that the mean age of infection is 2.1 years, regardless of the EV type (Mirand et al., 2015). In addition, EV-A71 represents only sporadic cases among the reported HFMD cases.

The surveillance protocols can provide important data and information: giving support to diagnosis, monitoring virus identification and the circulation of EV-A71, and characterising clinical features in patients (Benschop et al., 2021; Harvala et al., 2021). The profiles of virus circulation in a population can be traced in the serum of individuals through seroprevalence investigations. This screening is performed by searching

neutralizing antibodies against EV-A71. In China, the low incidence of HFMD in the adult population correlates with a seroprevalence rate of 74.6 % (Koh et al., 2016). The analysis of sera collected between 2006 and 2017, in the United Kingdom, showed EV-A71 seroprevalence rates of 32% at 6 to 11 months and of >75% by the age of 10 years (Kamau et al., 2021). In Southern Vietnam, 23.5% of 1-year-old children have been infected by EV-A71, and the median age of infection was 3 years (Kuo et al., 2020). These data and other studies indicate that the lack of protective antibodies may contribute to the high susceptibility and fatality rate in the youngest children.

Public health officials can also correlate data of HFMD incidence and strain prevalence with potential risk factors for developing a predictive surveillance (He et al., 2020; Ding et al., 2021; Sun et al., 2021; and Wahid et al., 2021). Moreover, samples isolated from throat, rectal, vesicle and other swabs have been genotyped to raise precise information on circulating EV-A71 strains (Song et al., 2018; Yang et al., 2019; and Volle et al., 2020).

b. *Picornaviridae* family

Human enterovirus diseases were initially understood as enteric infections caused by pathogens that could colonize the gastro-intestinal tract, such as polioviruses, coxsackieviruses, and echoviruses. Later, the term “Picornaviruses” was attributed for grouping enteroviruses and rhinoviruses in a family of small RNA virus (Horstmann, 1965). Members of the Picornaviridae family associated with human diseases are known for causing mucocutaneous manifestations, respiratory and gastrointestinal infections, cardiopathies, hepatitis, poliomyelitis, meningitis, and encephalitis (Tapparel et al., 2013 and Zell, 2018). The Picornaviridae family includes human and animal viruses that are classified in 68 genera (https://www.picornaviridae.com/). The initial taxonomic classification was developed by considering the ecological relationships between these entities and their hosts (tropism, diseases, syndromes, symptoms…) and their physicochemical properties – temperature susceptibility, acid lability, cross antigenicity (Wenner, 1982).

c. The genus Enterovirus

Further, molecular tools and first generation sequencing were at the root of major updates in the classification of the picornavirus diversity, and notably within the Enterovirus genus (Oberste et al., 2004 and Simmonds et al., 2020). Rhinovirus strains – initially classified in a separate genus – were integrated the Enterovirus genus because of the close nucleotide similarities and were assigned to three species designated Rhinovirus A to C (Brouwer et al., 2021). Currently, the Enterovirus genus classifies the members (coxsackievirus, echovirus, and poliovirus, and enteroviruses discovered later) among four taxonomic species designated Enterovirus A (EV-A) to Enterovirus D (EV-D). EV-A71 belongs to the EV-A species.

d. The enterovirus A (specie EV-A)

Overall, the EV-A species includes 25 (sero)(geno)types designated coxsackievirus (CVA2 to CVA8, CVA10, CVA12, CVA14, and CVA16) and numbered enteroviruses (EV-A71, EV-A76, EV-A89 to EV-A92, EV-A114, EV-A119 to EV-A125) (Brouwer et al., 2021).

e. Enterovirus A71

In 1969, an outbreak of neurological manifestations in California allowed the identification of a new EV strain (designated BrCr) because its antigenic properties were different from those of the other EV types (Schmidt et al., 1974). It was designated “Enterovirus 71” (Melnick et al., 1974) and later “Enterovirus A71”. The EV-A71 strains are currently classified among eight genotypes named A to H (Bessaud et al., 2014). The prototype strain BrCr is assigned to genotype A, the vast majority of epidemic viruses reported over the world are scattered among genotypes B and C, and the other genotypes include viruses reported sporadically over the world (Bessaud et al., 2014; Mirand et al., 2015; and Mandary & Poh, 2018) (**Fig. 3**). The strains within the B and C genotypes are further assigned to subgenotypes B0 to B5, and C1 to C6, respectively (Y. Liu et al., 2022). Overall, the phylogenetic analyses are performed by comparing and clustering the VP1 capsid protein sequences; alternatively, the VP4-VP2 sequences can also be used.

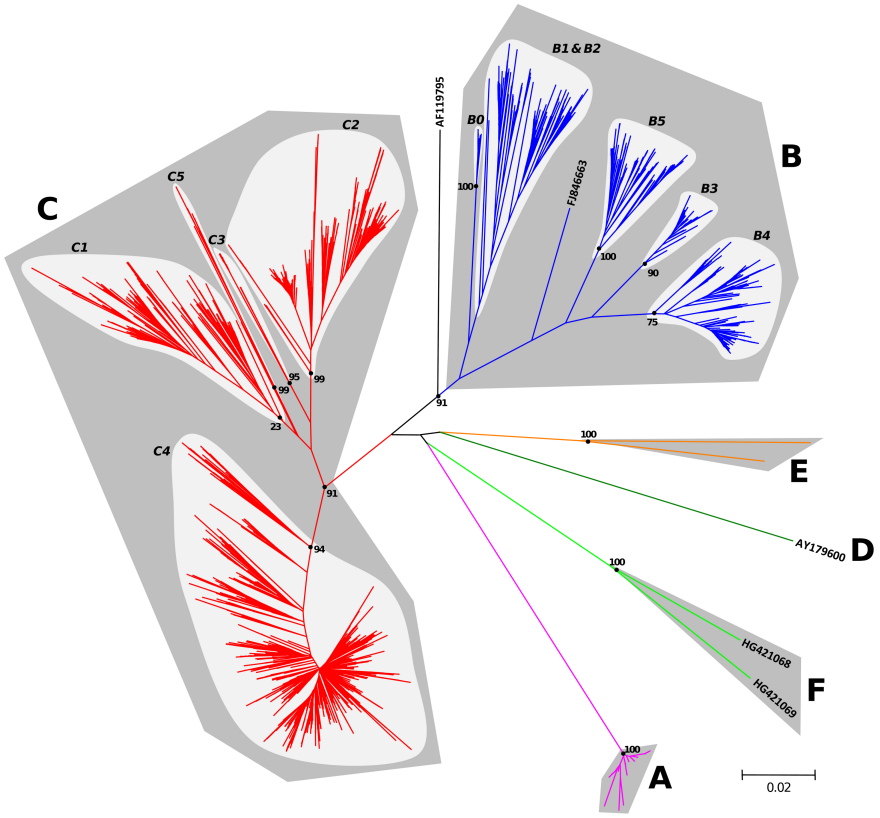

Fig. 3. Diversity of the EV-A71 species based on comparison of the complete nucleotide sequences encoding the VP1 capsid protein. The genotypes and subgenotypes are indicated with the exception of genotypes G and H for which only partial sequences were known. The scale indicates genetic distances (nucleotide substitutions per site). Figure from Bessaud et al., 2014.

II. EV-A71 circulation

Strains assigned to subgenotypes B0, B1, and B2 circulated from 1963 to 1986 affecting distant geographical regions such as USA, European countries, and Australia. A shift to the circulation of subgenotypes C1 and C2 in 1987, was reported in the Netherlands (van der Sanden et al., 2010). These two subgenotypes were found recently in Europe. Outbreaks involving C1-like virus strains are reported since 2015 (Hassel et al., 2015). The C1-like virus infections are associated with benign rapidly self-limiting infections and severe infections, highlighting the need for enhanced EV-A71 surveillance (Casas-Alba et al., 2017 and Ngangas et al., 2019).

The EV-A71 strains circulating in the Asia-Pacific region are much more diverse (**Fig. 4**). Subgenotypes B3, B4, C1, C2, and C4 are reported throughout this region, subgenotype C4 being predominant in China (Puenpa et al., 2019).

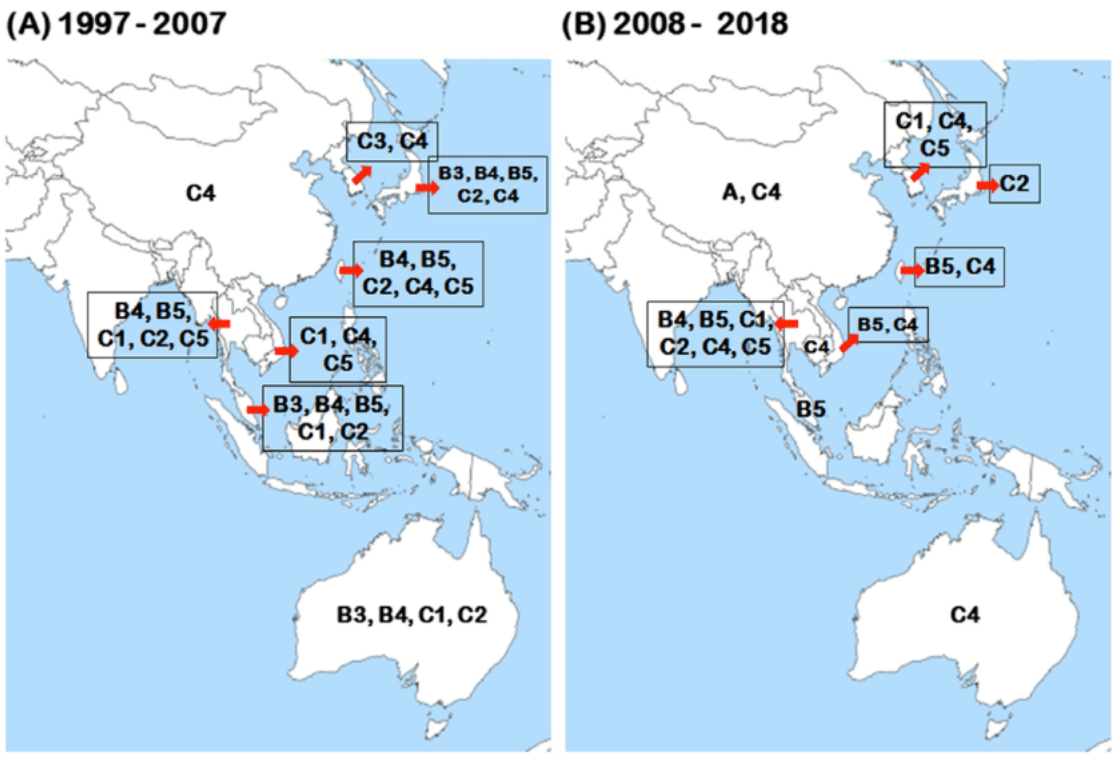

Fig. 4. Prevalence of the EV-A71 subgenotypes in South East Asia. In countries of the Asia-Pacific region, EV-A71 triggers recurrent outbreaks, mainly caused by circulation of virus strains from genogroups B and C. In countries such as China and Australia, strains of subgenotype C4 are predominant. Figure from (Puenpa et al., 2019).

The analysis of circulating strains from different outbreaks in Sarawak (Malaysia) revealed that despite the predominance of genotype B, the strains from each outbreak belong to various subgenogroups (Chua & Kasri, 2011). Nucleotide sequence analysis of the VP1 gene showed that after the emergence of subgenotype B5 in 1997, subgenotypes B4, C1, C2, C4, and C5 were reported in the years 2000s (Chua & Kasri, 2011).

III. Evolution

The worldwide circulation of EV-A71 and the error-prone RNA polymerase contribute to viral evolution and is associated with the emergence and re-emergence of genetically different strains (Bible et al., 2007; Y. Zhang et al., 2011; and Nhu et al., 2021). The analysis of genotypic changes in circulating strains revealed that amino acid variations at specific positions in capsid proteins are involved in phenotypic polymorphism and virulence of EV-A71 strains. In particular, amino acid polymorphism at position 145 in the VP1 protein is associated with variations in virus attachment to

leukocytes (see below, the paragraph “Viremia”). The A289T amino acid substitution decreases the interaction with cell surface vimentin and may contribute to a reduced infection of the CNS (Zhu et al., 2019). Evolutionary analyses of the VP1 capsid sequences provided little evidence of positive selection, but they showed continuous virus strain and lineage replacement over time, and frequent variations were detected at several immunogenic sites (Tee et al., 2010). Amino acid changes in nonstructural proteins were also reported. Notably, the N69D in the 3C protease and the V263I changes in the 3D polymerase were associated with a decrease in EV-A71 virulence (Li et al., 2017). The data indicate that single amino acid variation occurring during interindividual and intraindividual virus spread may be associated with changes in virological properties.

Genetic recombination between strains has long been recognized as a major process contributing to the evolutionary dynamics of EVs, including EV-A71 (Huang et al., 2009 and Liu et al., 2015). Analyses of full-length genome sequences indicate that CVA co-circulating with EV-A71 introduce genetic elements within the EV-A71 genome (Huang et al., 2009 and McWilliam Leitch et al., 2012). Recently a newly subgenotype C6 emerged in China. The genomic P1 region of this C6 virus displays high identity with C4 strains (Liu et al., 2022). The data indicate that C6 strain emerged through intratypic recombination within the genomic P2 and P3 regions. The P2 locus harbors evidence of recombination events between strains from the EV-A71 subgenotypes B and C. Intertypic recombination events can occur with a large array of CVA strains (CVA4, CVA5, CVA14, and CVA16) (Zhou et al., 2021).

The P2 and P3 loci are important sites of recombination. European countries like Germany and France reported the widespread circulation of a multirecombinant strain from subgenotype C1 that emerged through recombination events with strains of other CVA types such as CVA2, CVA4, CVA5, CVA6, and CVA8 (**Fig. 5**) (Karrasch et al., 2016 and Ngangas et al., 2019). Recombination may represent a potential risk for outbreaks of severe infections. The fitness and virulence of EV-A71 are associated with recombination events, mutations, and natural selection (Mandary & Poh, 2018; Huang et al., 2019; and Ang et al., 2021).

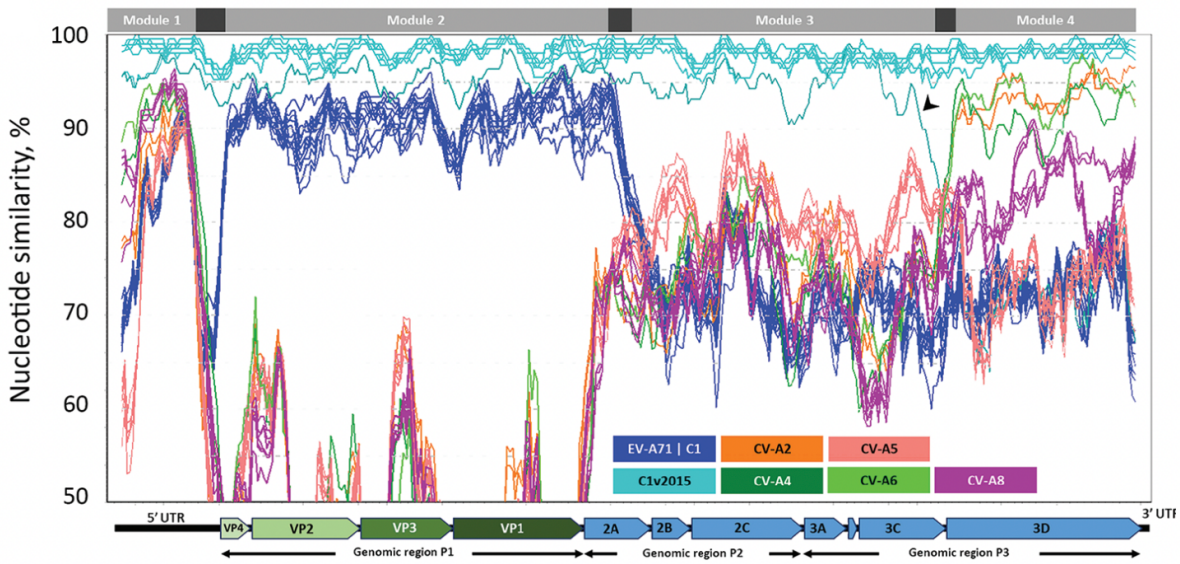

Fig. 5. Evidence of intertypic recombination. The P3 locus of a multirecombinant strain from subgenotype C1 present high level of similarity with the genomes of strains of other enterovirus types, such as coxsackievirus CVA2 and CVA6. In contrast, the P2 locus has low similarity with these two viruses and other coxsackievirus types. Figure from Ngangas et al., 2019.

IV. Genetic and epidemiological features of EV-A71 strain used in the study

The Virology Service of the University Hospital Gabriel Montpied (CHU) in Clermont-Ferrand provided all EV-A71 isolates used in this study. The EV-A71 clinical isolates used in this study were obtained from three patients: isolate CF1920113_FRA04 from a patient with meningitis and other neurological complications, isolate 09_PMB250102_FRA16 from a patient with HFMD, and isolate CR210042_FRA06 from an asymptomatic infection case (**Table 2**). The first virus is representative of the C4 subgenogroup and was designated throughout the study as C4-04. The C4 strain, has an accumulation of mutations in the gene encoding the VP1 protein, which may be associated with the high infectivity potential (He et al., 2016). The second strain is a C1-like virus (it was designated C1-16 in this study); the strain C1-16 is a multirecombinant strain reported during outbreaks, which emerged as a consequence of recombination events between viruses from subgenegroup C1 and other EV types (Ngangas et al., 2019). The third virus strain is assigned to the C1 sugenogroup, a parental C1 strain; it was designated C1-06.

Table 1. Characteristics of EV-A71 strains used in this study					
Clinical manifestation	**Specimen isolation**	**Accession number**	**Year of isolation**	**Subgenogroup**	**Designation**
Assymptomatic	Pharynx sample	CF210042/2006 (LR027547.1) (HG934219.1)	2006	C1	C1-06
Mild hand, foot and mouth disease (HFMD)	Throat swab	PMB250102/2016 (LR027524.1)	2016	C1	C1-16
Severe HFMD with neurological complication	Stool sample	CF192013/2004 (HG934208.1)	2004	C4	C4-04

Table 1. Characteristics of EV-A71 strains used in this study. The accession number indicated is linked to the nucleotide sequence of the P1 genomic region. Each strain was characterized by sequencing the complete genome. The nucleotide sequences for the complete genomes of the C1-06 and C4-04 strains have not been deposited in GenBank.

V. Vaccine

In China, three inactivated vaccines were approved by a national regulatory authority (Chiu et al., 2020 and Li et al., 2021). Following their implementation, the seasonality, geographical distribution, and etiologic agents of HFMD outbreaks changed completely (Jiang et al., 2021 and Huang et al., 2022). Outbreaks of CVA6 and CVA10, as well as re-emerging of rare serotypes such as echovirus 11 and echovirus 30 were reported (Tong et al., 2021). The current inactivated vaccines are highly protective against EV-A71, but do not offer cross-protection for other EV types. Therefore, the development of additional vaccines with polyvalent spectrum are still necessary (Mao et al., 2016; Takahashi et al., 2016; and Apostol et al., 2019).

VI. EV-A71: capsid structure and genome

EV-A71 is a non-polio EV type, formed by a nonenveloped icosahedral capsid, composed by 60 copies of the four structural proteins VP1, VP2, VP3, and VP4 (Liu et al., 2013; Zhang et al., 2017 ; Cao et al., 2019 ; and Zhao et al., 2021). VP4 forms an internal protein, while the VP2, VP3, and VP1 proteins are exposed at the virion surface (**Fig. 6**) (Li et al., 2011 and Yuan et al., 2015). The sequence of the VP4 protein is

extremely well conserved among different EV types, and is under investigation for developing broad-spectrum antivirals (Tan et al., 2016 and Cao et al., 2020). VP1 protein is also a target for drug discovery, but its variability between EV types makes development even more difficult and expensive (Ke et al., 2006 and Sun et al., 2020).

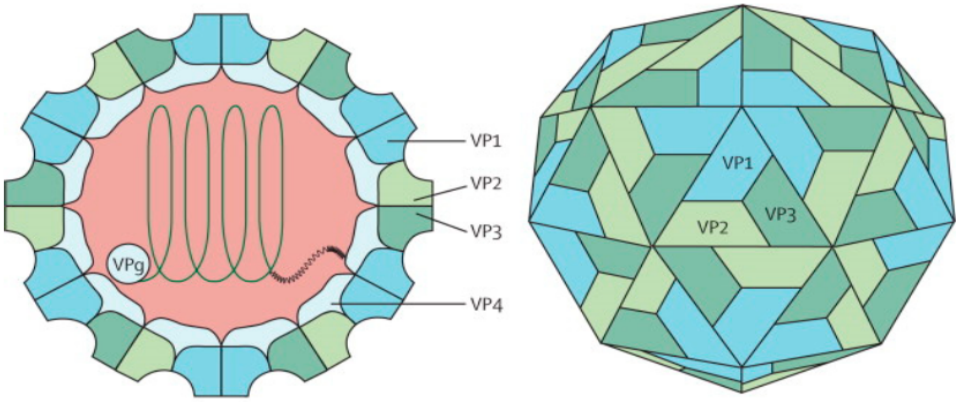

Fig. 6. Capsid structure of EV-A71. The image shows the proteins that form the icosahedral capsid of EV-A71. The structure of EV-A71 capsid is formed by an internal layer of VP4 proteins, and external units composed of the VP2, VP3, and VP1 proteins. Figure from Yee & Poh, 2015.

The tridimensional arrangement of the VP1 proteins within the viral capsid forms an excavated area (commonly designated the canyon), which interacts with cellular receptors (see below). At the bottom of the canyon, there is a local area filled with a hydrophobic, lipid, also known as 'pocket factor' that stabilizes the virion (**Fig. 7**) (Ranganathan et al., 2002). Unlike in other enterovirus types, the EV-A71 pocket has a unique conformation flushing the canyon floor (Ke et al., 2006 and Plevka et al., 2012). Accordingly, since the head of the EV-A71 pocket factor interacts with polar residues on the canyon floor, EV-A71 antivirals may require a hydrophilic head group.

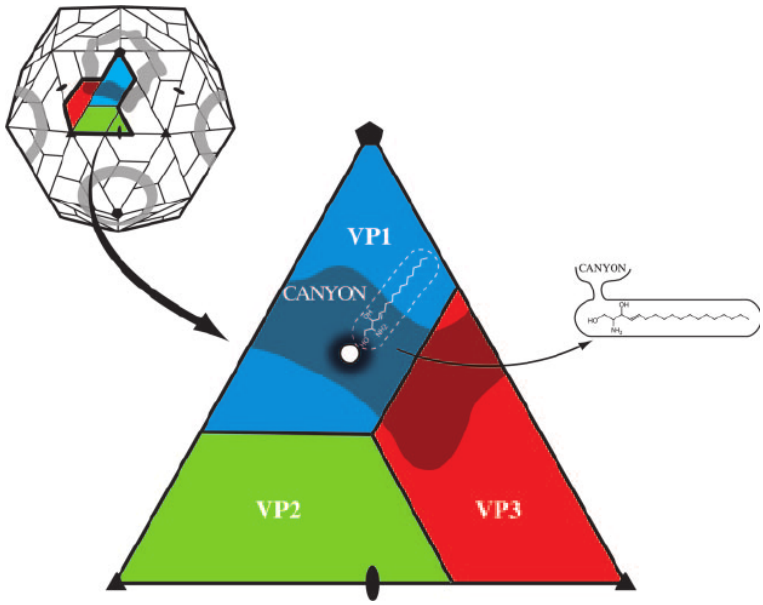

Fig. 7. Capsid canyon. The image shows specific areas of the capsid structure. In this illustration, it is highlighted regions of interaction between the VP1, VP2, and VP3 proteins. The tridimensional organisation of these proteins forms a deep area in the capsid structure (also called canyon) that passes through the VP1 and VP3 proteins, and which harbors an important lipid molecule, the pocket factor. The canyon is in contact with different molecular structures such as cellular receptors. Figure from Hafenstein et al., 2007.

The EV-A71 genome is a positive single-stranded RNA of approximately 7400 nucleotides (Han et al., 2010). The EV-A71 genome consists in a unique open reading frame (ORF) flanked by two untranslated region (UTR), the 5' and 3'-UTRs (Meng et al., 2012). The ORF region encodes the capsid (or structural) proteins VP1, VP2, VP3, and VP4, and the non-structural proteins 2A, 2B, 2C, 3A, 3B, 3C, and 3D (Guo et al., 2019 and Brown et al., 2020). The 5'-UTR contains secondary structures, formed by RNA folding generating stem loops (I–VI) that play important roles on the viral life cycle and influence directly on EV-A71 fitness and virulence (Chang et al., 2018 and Dong et al., 2019). Stem loop I is involved in the replication of the viral RNA and stem loops II–VI, in the translation of the viral RNA (**Fig. 8**). The nucleotide sequence of the 3'-UTR also forms secondary structures called X, Y, and Z that are cis-acting elements capable to interact with host cell and viral proteins (Zoll et al., 2009).

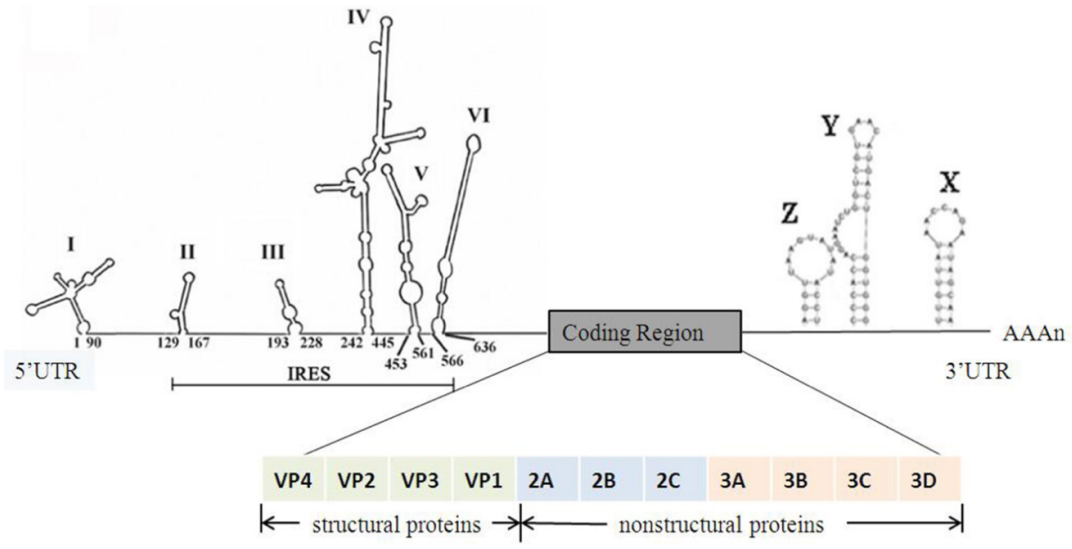

Fig. 8. Genome structure of EV-A71. The EV-A71 genome harbors genes that encode structural and non-structural proteins, and is flanked by the 5' and 3'-untranslated regions (UTR). The 5'-UTR forms secondary structure domains (stem loops I–VI). The positions of the first and last nucleotide of each stem loop, are indicated. The loops II–VI forms the internal ribosomal entry site (IRES). 3'-UTR has three secondary structure domains (Z, Y, and X) and a polyadenylated tail. Figure from Yuan et al., 2018.

VII. Life cycle

a. Surface attachment

The VP1 protein mediates the attachment of EV-A71 to several host receptors (Tseligka et al., 2018 and Earley et al., 2019). Variations in amino acid sequences of the VP1 protein at position 145 (VP1-145) showed the relevance of electrical charges in sustaining binding to the heparan sulfate residues (Fujii et al., 2018). Amino acids at VP1-145 are in close contact with conserved lysine residues, which have positive charges (Nishimura et al., 2013). Amino acids of negative or neutral charges, such as glycine and glutamine, respectively, may affect the orientation of lysine residues at VP1-145.

b. Cell entry

The human scavenger receptor class B member 2 (hSCARB2), a type III transmembrane protein classified within the CD36 family, is the main mediator of entry into the host cell for EV-A71 and most of the other EV types within the EV-A species

(Yamayoshi et al., 2012). hSCARB2 is involved in membrane transport and reorganization of the endosomal-lysosomal compartment; it is predominantly localized in the lysosomal membrane and in small amount in the plasma membrane. The structure of EV-A71 complexed to SCARB2 was determined at a 3.4 Å resolution using cryo-electron microscopy (Zhou et al., 2019). The analysis of the virion-SCARB2 complex provides evidence that SCARB2 does not bind inside the canyon but with two loops exposed at the virion surface: the VP1 G-H and the VP2 E-F loops. The analysis also revealed that the human SCARB2 helices α5 (amino acid residues 153–163) and α7 (amino acid residues 183–193) are the binding sites on the viral protein loops (**Fig. 9**).

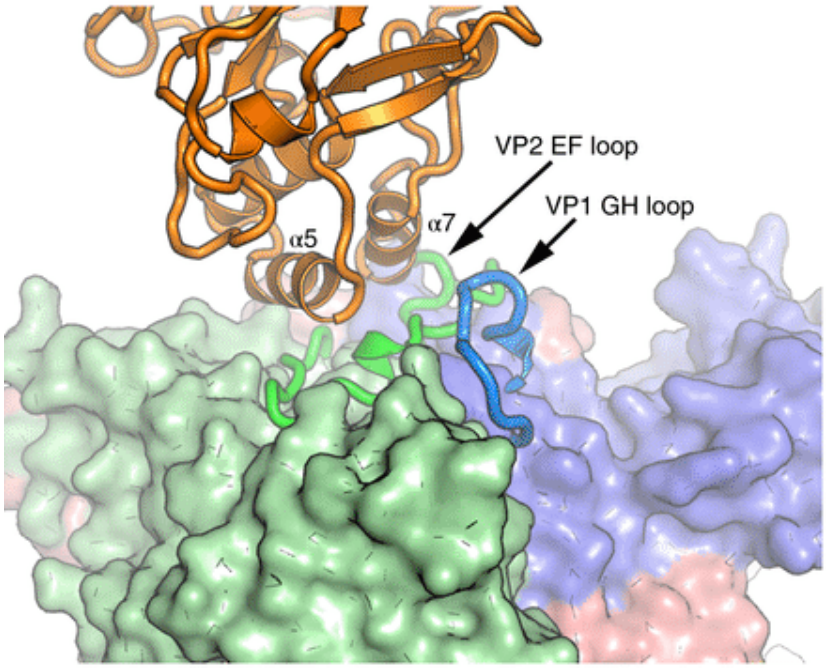

Fig. 9. Interaction between VP1 protein and human SCARB2. The loop structures of VP1 proteins sustain molecular interactions with to α-helices of hSCARB2 receptor. Figure from Zhou et al., 2019.

c. Humanization of mouse for elucidation of EV-A71 pathogenicity

Studies in transgenic mice expressing hSCARB2 allow mimicking the natural route of infection in humans, and has been performed to evaluate the potential spread, tissue tropism, pathogenesis, and neurovirulence (Lin et al., 2021). In these models, the severity of EV-A71 infection is influenced by the route of infection. Therefore, to access

properly the pathogenicity and cell tropism, infections are performed intravenously. To study the neuropathogenicity, the animals are subjected to intracranial inoculation (Zhu et al., 2018). Infections of hSCARB2 mice with a large array of mutant strains suggests that virulence determinants are located throughout the viral genome, in the regions encoding the structural and non-structural proteins, as well as in the untranslated regions (Tee et al., 2019; Ang et al., 2021; and Kobayashi et al., 2021). Even with the possibilities to reproduce infectious scenarios, the interpretation of the virulence may be controversial, because EV-A71 adapt quickly to various host environments (Kobayashi et al., 2021).

d. Uncoating

The interactions between virion surface and cellular receptor are fundamental to stabilize the complex and activate a clathrin-dependent endocytosis pathway (**Fig. 10**) (Ang et al., 2016; Chen et al., 2019; and Chang et al., 2021).

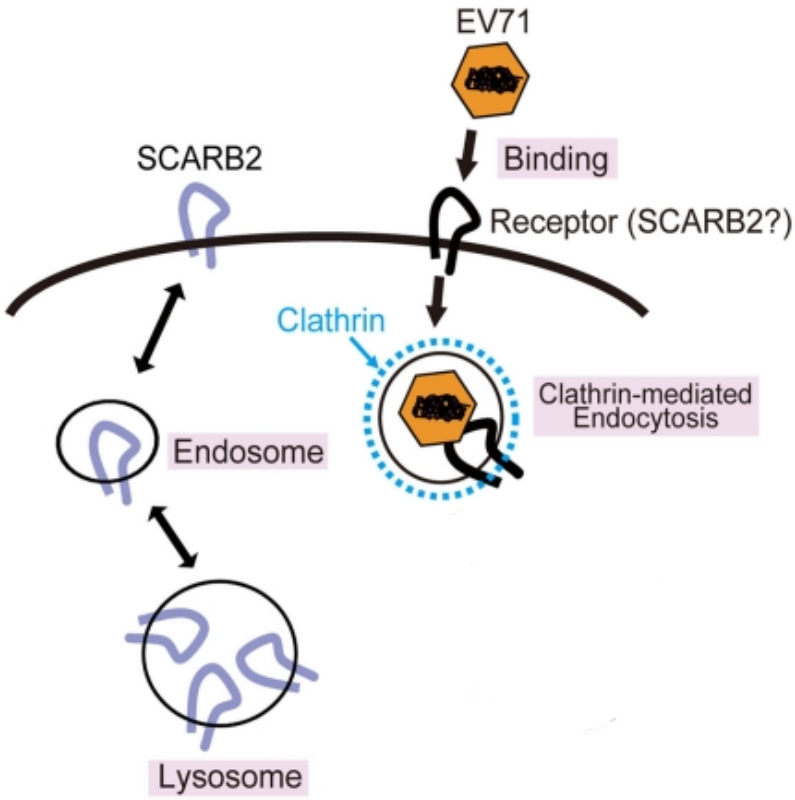

Fig. 10. Entry of EV-A71 into the host cell. The interaction between EV-A71 and surface receptors, such as hSCARB2, activates clathrin receptors that are responsible for packing extracellular content in endocytic vesicles. This clathrin-dependent endocytosis is essential for the internalization of virions. Figure from Yamayoshi et al., 2012.

The endosomal vesicle is subject to acidification, which causes alteration of the virion structure, and results in the expulsion of the VP1 pocket factor from the virion capsid (Dang et al., 2014 and Lyu et al., 2014). The lysosomal pH also regulates the activity of isomerases, such as cyclophilin A (CypA), which promotes proteolytic deformations on the virion capsid (Qing et al., 2014; Meng et al., 2019; and Swain & Mohanty, 2019). These mechanisms result in the formation of a channel in the capsid structure surrounded by negatively charged amino acid residues, essential for expulsion of viral genome (**Fig. 11**) (Shingler et al., 2013; Peters et al., 2015; Ross et al., 2018; and Ohka et al., 2022).

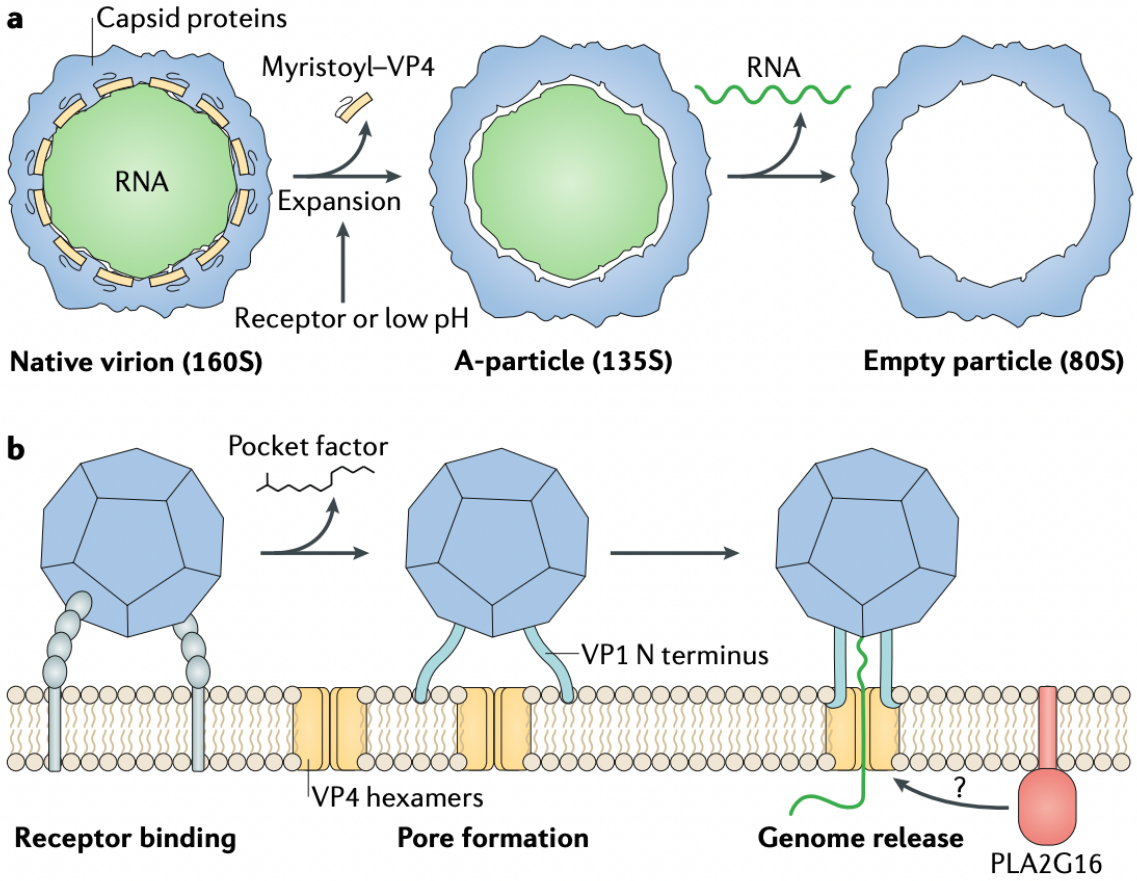

Fig. 11. Viral uncoating. The figure shows experimental observation of virion capsid. Under low pH occurs an expansion of capsid proteins and expulsion of VP4-associated factor (Myristoyl-VP4). These alterations result in the RNA expulsion and formation of empty capsid **(a)**. Further the internalization, the virion anchored at endosomal vesicles expulses the ‘’pocket factor’’. In consequence of capsid destabilization, the N terminus region of VP1 protein is exposed; establishing adhesion to endosomal vesicle, while VP4 protein forms pores that together other with host proteins (Group XVI phospholipase A2, PLA2G16) mediates the expulsion of virion genome **(b)**. Figure from Baggen et al., 2018.

e. Translation

After the uncoating stage, the viral RNA is translated through an unconventional mechanism. Within the 5’-UTR, stem loops II to VI form the internal ribosomal entry site (IRES) that initiates the translation of the EV-A71 genome (Lin & Shih, 2014 and Lai et al., 2020). The viral IRES hijacks the cell machinery for translation of viral genome (Zhang et al., 2018; Lee et al., 2017; Tolbert et al., 2017; and Gunaseelan et al., 2019). The EV-A71 interacts with several host trans-acting factors (ITAFs), some of them like Far Upstream Element-Binding Protein 1 (FBP1) result from the proteolytic activity of the viral protease 2A (**Fig. 12**). Some ITAFs are protein processors (helicases and chaperones), therefore the proteolytic activities are enhanced, driving the cell metabolism in benefit of viral replication (Dong et al., 2018 and Dan et al., 2019). The 2A protease also targets other key host components that enhance IRES activity (Li et al., 2018; Visser et al., 2019; and Fan et al., 2021).

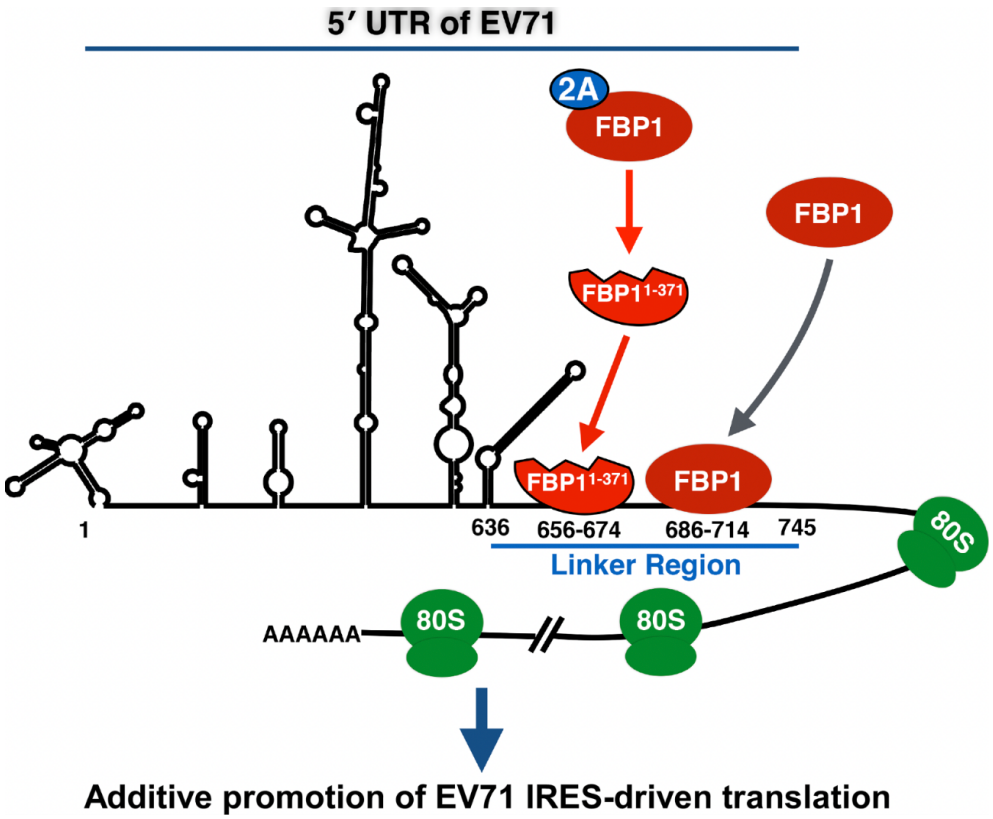

Fig. 12. IRES activity. This figure is a proposition of model that explains the IRES function. The host factor FBP1 (Far Upstream Element-Binding Protein 1) is recruited to 5'-UTR region for enhancing the translation of virion genome. As long as the levels of viral protein 2A increases the FBP1, a host factor is cleaved. The products of this protein cleavage forms functional subunits enhancing IRES translation. Figure from Hung et al., 2016.

As a consequence of viral genome translation, a single polyprotein is generated and processed into the three major precursors P1, P2, and P3 (Lai et al., 2020). Finally, ten functional proteins are produced, including the capsid (structural) proteins (VP0, VP1 and VP3), the nonstructural proteins (2A–2C and 3A–3D) (**Fig. 13**). The non-structural proteins 2A and 3C cleave the polyprotein into intermediate precursors and functional viral proteins (Kean et al., 1990 and Lin et al., 2015). Three stable protein intermediates (2BC, 3AB, and 3CD) generated during translation, are functional and recruited during viral RNA replication.

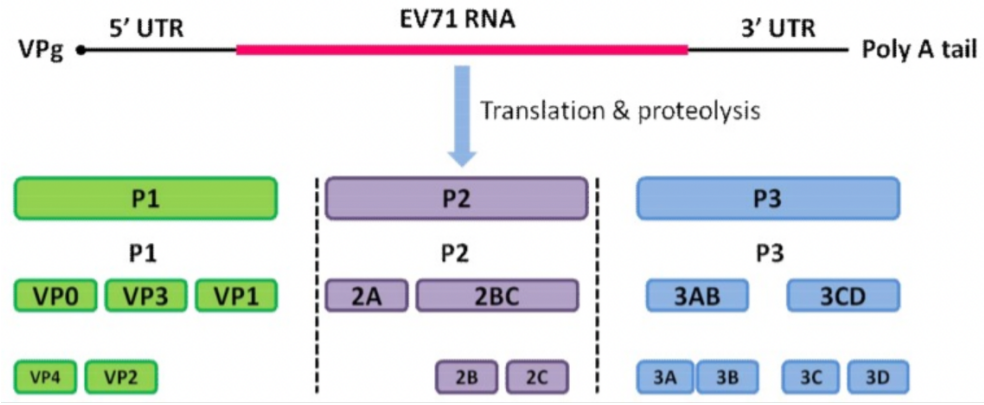

Fig. 13. Translation of the viral genome. The EV-A71 genome encodes three protein precursors (P1, P2, and P3), which are further processed into subunits of functional viral proteins. The image shows the translation of viral ORF, which results in the production of P1, P2, and P3, and the products of cleavage of these precursors. P1 encodes capsid proteins, such as VP0, VP3, and VP1. The cleavage of VP0 releases the VP4 and VP2 proteins that constitute the mature viral capsid. The P2 and P3 regions produces non-structural proteins that are involved in the replication cycle. The 2BC protein is cleaved into the 2B and 2C proteins, the cleavage of protein 3AB releases the 3A and 3B proteins, and the cleavage of protein 3CD releases the proteins 3C and 3D. Figure from Jin et al., 2018.

f. Replication of the viral genome

Non-structural proteins are involved in the replication of the EV-A71 genome (Yang et al., 2019). Owing to their hydrophobic domains, the 2BC and 3A proteins are involved in the formation of replication organelles during infection (see below). The RNA-dependent RNA polymerase 3D initiates the genome replication by synthesizing a negative-strand copy of the viral genome, generating a double-stranded (ds)RNA. The negative copies serve as templates for genome replication, and the newly-synthetized (+)RNAs may serve as template for protein synthesis or can be encapsidated to form the virus particles of a new progeny (Baggen et al., 2018). Structural proteins VP0, VP1, and VP3 assemble into pentamers to form the EV-A71 provirion. At the final stage, the viral RNA induces processing of VP0 into VP2 and VP4, which forms the mature virion (Tan et al., 2014).

Non-structural proteins 2B and 2C promote mitochondrial clustering and trigger the formation of autolysosome (Lai et al., 2017 and Yang et al., 2019). Both non-structural and structural proteins contribute for activating autophagy by regulating mTOR signaling (Zhang et al., 2018; Liu et al., 2019; and Lu et al., 2021). During the EV-A71

infectious cycle, the autophagic vesicles are hijacked and used as membranous scaffolds (replication organelles) for the replication of the viral RNA (Lin & Huang, 2020 and Rattanakomol et al., 2022). The 3A and 3D proteins mediate the assembly of replicative complexes at surface of replication organelles (**Fig. 14**) (Morosky et al., 2016; Lei et al., 2017; Wang et al., 2017; Lee et al., 2020; and Zhang et al., 2021).

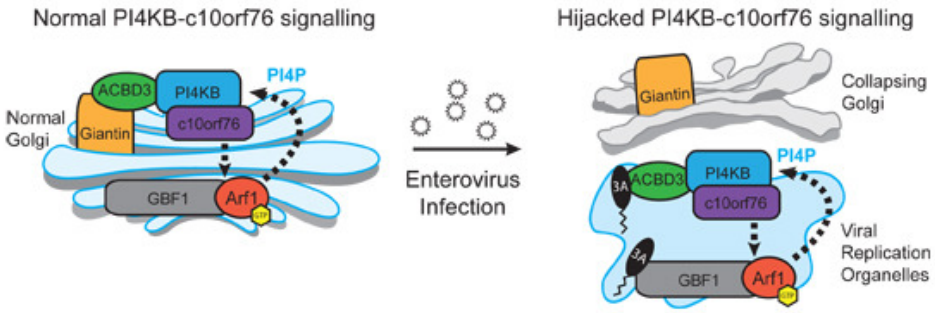

Fig. 14. Formation of replicative organelles. The figure shows host proteins associated with the Golgi complex. The complex C10orf76-PI4KB activates regulatory molecules (GBF1, Golgi Brefeldin A Resistant Guanine Nucleotide Exchange Factor 1 and Arf1, ADP-ribosylation factor 1) for increases the levels of PI4P (phosphatidylinositol-4-phosphate), an effector molecule that mediates the membrane transport. C10orf76-PI4KB complex is linked to ACBD3 (Acyl-CoA Binding Domain Containing 3), a protein that it anchors to Giantin, a resident protein of Golgi. EV-A71 hijack key proteins of Golgi, such as ACBD3 and GBF1 to form replicative organelles. Figure from McPhail et al., 2020.

Replication organelles may give the additional advantage to protect viral RNAs from cytoplasmic sensing proteins involved in early innate immune detection of viral RNAs.

g. Virion assembly

The formation of new capsids depends on cleavage of the P1 precursor. A short and highly conserved motif near C-terminus of P1 precursor is targeted by chaperones, which exposes the motif to activity of the viral 3C protease (Kristensen & Belsham, 2019). Cleavage of the P1 precursor releases three subunits (VP0, VP1, and VP3) that self-assemble into a protomer, and five protomers into a pentamer (**Fig. 15**) (Chung et al., 2006; Kim et al., 2019; and Kristensen et al., 2022).

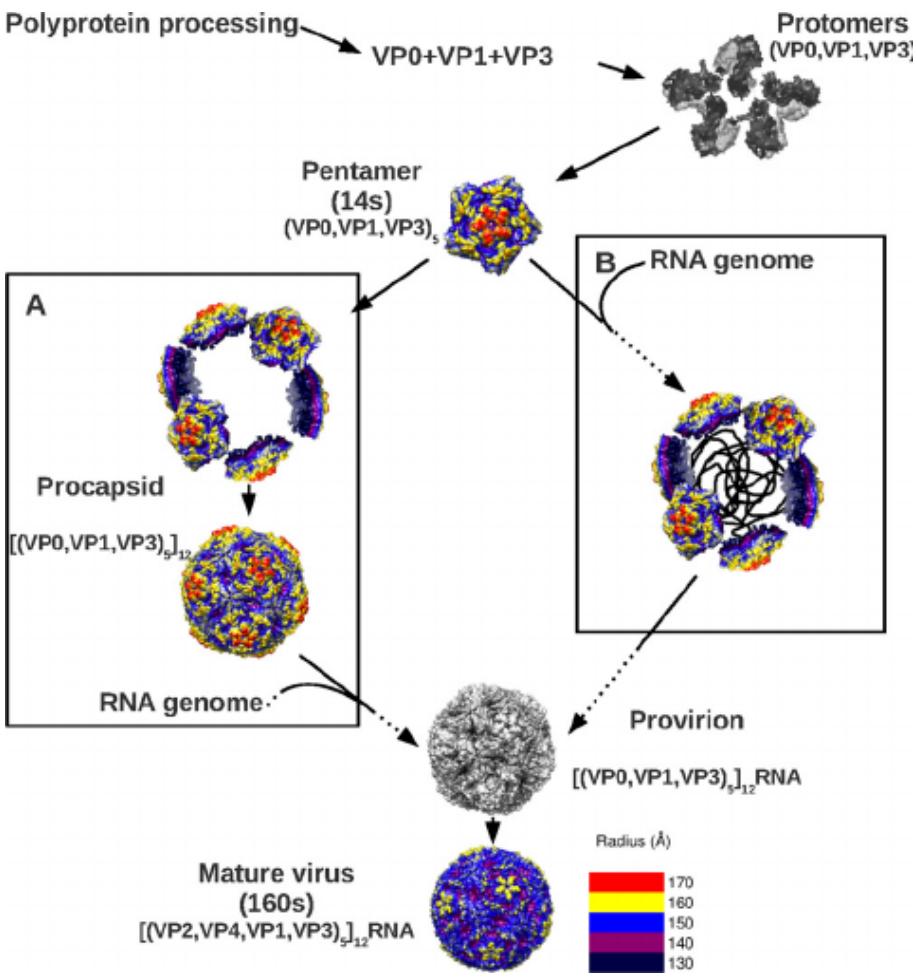

Fig. 15. Virion maturation. The processing of precursor P1 forms a protomer composed of VP0, VP1, and VP3, which self-assemble into empty capsid (pro-capsid). Two mechanisms may explain how the viral genome is integrated: (**A**) integration after the procapsid is formed and (**B**) interaction with the pentamers. This interaction catalyzes the cleavage of VP0 to generate the functional VP2 and VP4 proteins, allowing the formation of a mature virion. Figure from Cifuente et al., 2013.

The final step of maturation is characterized by the encapsidation of viral RNA to form a mature infectious virion (Ansardi & Morrow, 1993 and Vance et al., 1997). VP0, is a precursor protein containing a conserved histidine residue that participate in RNA packing (Curry et al., 1997 and Cifuente et al., 2013).

h. Virion release

EV-A71 is a cytolytic virus that can also be released through a non-lytic process (Gu et al., 2020). In few cell types, the newly formed virions inside vesicles take advantage

of autophagic flux for escaping from the extracellular environment (**Fig. 16**) (Luo et al., 2020).

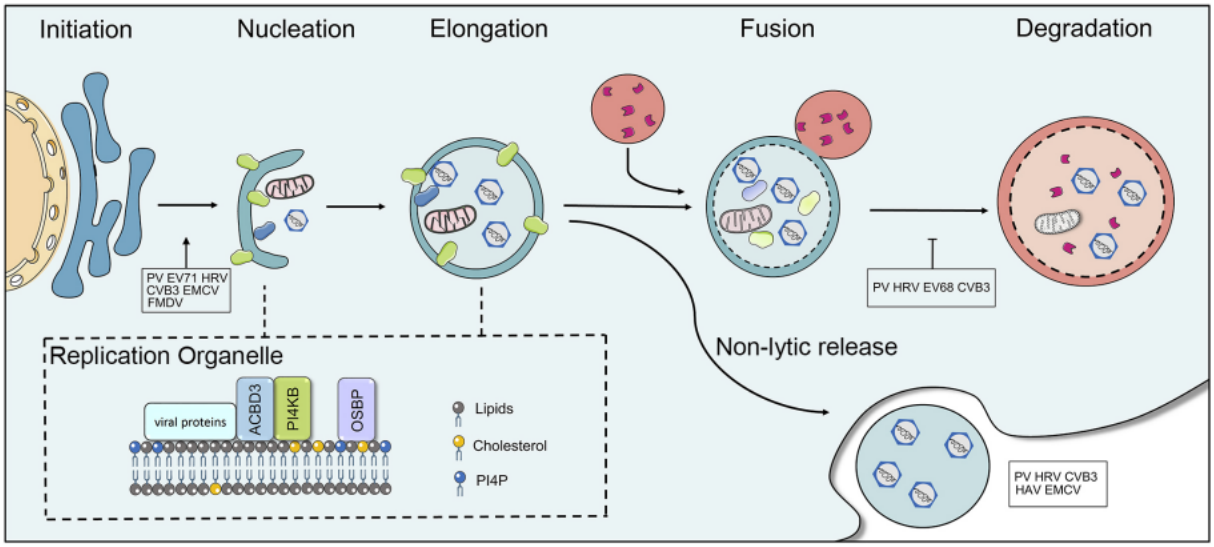

Fig. 16. Virion release. During physiological cell metabolism, the fusion of an autophagosome (double-membrane vesicles) with a lysosome induces the degradation of the autophagosome content. This stage is inhibited during the infectious cycle of several picornaviruses (FMDV, foot-and-mouth disease virus; EMCV, encephalomyocarditis virus) and EV types, including EV-A71, PV (poliovirus), CVB3 (coxsackievirus B3), and HRV (human rhinovirus). As a consequence, the autophagosome with its unaltered content can fuse its membrane with the cell plasma membrane. This mechanism triggers the release within a single-membrane vesicle, of virus particles inside a single-membrane vesicle. Figure from Sun et al., 2019.

During this process, double-membrane autophagosome englobing virion particles are formed, which inhibit the fusion to lysosomes and the degradation of infectious virus (Giansanti et al., 2020). The knowledge of mediators of non-lytic cycle is scarce. Carbohydrate residues, such as Galectin-1 can be related with fusion of autophagosome to plasma membrane and the virion is released within a single-membrane vesicle (Lee et al., 2015).

VIII. Pathogenicity of severe HFMD caused by EV-A71

a. Brainstem encephalitis

During brainstem encephalitis associated with EV-A71 infection, the CNS autonomic functions are impaired and this is associated with pulmonary edema mediated by pro-inflammatory cytokines (Wang et al., 2008; Finsterer, 2019; and Liao et al., 2019). At

the initial stages of infection, the IL-6 production orchestrates a protective inflammatory response (Wang et al., 2017). Then with disease progression, the systemic response intensifies and the plasma levels of IL-6 are elevated, as well as other important pro-inflammatory cytokines, such as IL-1β, TNF-α, and IL-10 (Wang et al., 2003; Wang et al., 2006; Zheng et al., 2014; and Zheng et al., 2017). During brainstem encephalitis these cytokines present high concentrations in cerebrospinal fluid (CSF) (Jubelt et al., 2011). Elevated levels of IL-8 in CSF are highly associated with disease severity (Wang et al., 2008 and Wang et al., 2014). In brain parenchyma of infected mice, the pro-inflammatory cytokine IL-12p40 was demonstrated as a key mediator of neuropathogenic process. IL-12p40 activates the microglial response, leading to an excessive activity of inducible nitric oxide synthase (iNOS), in consequence, the production of nitric oxide (NO) cause a serious neural damage (**Fig. 17**) (Lai et al., 2022). However, is important to highlight that the findings in human suggest that the response mediated by IL-12p40 is nonspecific. A study performed by Y. Xu et al., 2019 compared the levels if IL-12 in the CSF of patients with neurological complications caused by EV-A71 infection with patients with febrile convulsion. The respective study did not observe significative difference between the groups.

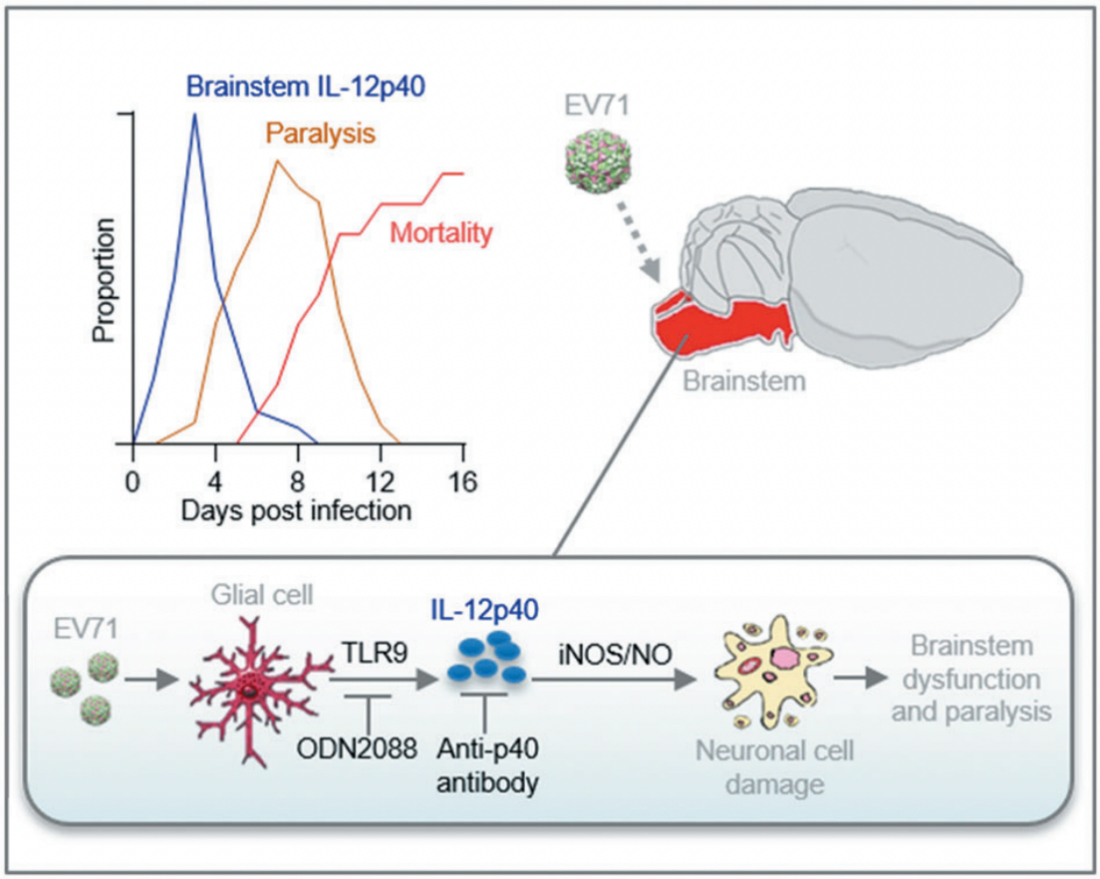

Fig. 17. Neuroinflammatory response associated with EV-A71 infection. This figure shows the progression of neuroinflammatory process in mice experimentally infected with EV-A71 via oral or intraperitoneal. The mice outcomes and infection severity are associated with different inflammatory profiles in the brainstem. The proinflammatory cytokine IL-12p40 is highlighted as an important factor in this process. The presence of sensor proteins in glial cells, such as TLR9 riggers the production of inducible nitric oxide synthase (iNOS) that causes death of neural cells. The authors also observed an impairment on neural damage by targeting TLR9 and IL-12p40 with ODN2088 and Anti-p40 antibody, respectively. Figure from Lai et al., 2022.

b. Genetic background of patients associated with severe EV-A71 infections

The role of genetic polymorphisms in the progression from mild EV-A71 infections to brainstem encephalitis was investigated among Chinese infants due the high incidence of severe HFMD (Li et al., 2017 and Li et al., 2021). Infants carrying certain alleles respond differentially to EV-A71 infections due to possible variations in expressing mediators of inflammatory process (Li et al., 2018 and Chen et al., 2021). Genetic polymorphisms in genes involved in the release of chemokines (CCL2 and CCL10) and cytokines (IL-6, IL-8, IL-4, IL-10, and IL-17) as well as production of NOS are often

reported as a risk factor for development of brainstem encephalitis (Yang et al., 2012; Han et al., 2014; Li et al., 2014; Li et al., 2015; Yuan et al., 2015; and Li et al., 2018). The polymorphisms are associated with the increase of pro-inflammatory mediators in serum and CSF.

However, some polymorphisms may also have a protective effect to EV-A71 infections. Alterations in encoding gene of mitochondrial protein carnitine palmitoyltransferase 2 (CPT2) are frequent in patients manifesting mild disease. This protein participates of β-oxidation of fatty acids, and therefore may affect the efficiency of viral replication (Guo et al., 2019). Interestingly, the IL-17 gene also main present alterations associated with reduced inflammatory response (Lv et al., 2013).

An observational study performed with Chinese infants compared the difference between the immune response of young children with polymorphism in the TLR3 gene (A.-Y. Yuan et al., 2017). Despite the absence of direct correlation between TLR3 polymorphism and brainstem encephalitis, the serum levels of TLR3 in children below 1 year were lower than in children aged ≥1 year. Low levels of TLR3 in serum may be indicative of the development of encephalitis in infants.

c. Evasion of EV-A71 from the host innate immunity

Immune evasion mechanisms rely on virus-encoded proteins that target pattern-recognition receptors (PRRs) and signaling molecules involved in innate immune response. These interactions between viral and host components may lead to clinical and pathological outcomes in the body. EV-A71 evades the host immune defenses by affecting interferon (IFN) signaling at different levels (**Fig. 18**). Viral proteases 2A and 3C are the two main antagonists of type I IFN. These proteases impair functioning of type I IFN cell receptors and the nuclear translocation of transcription factors involved in antiviral signaling (Wang et al., 2015; Rasti et al., 2019; and Dong et al., 2022).

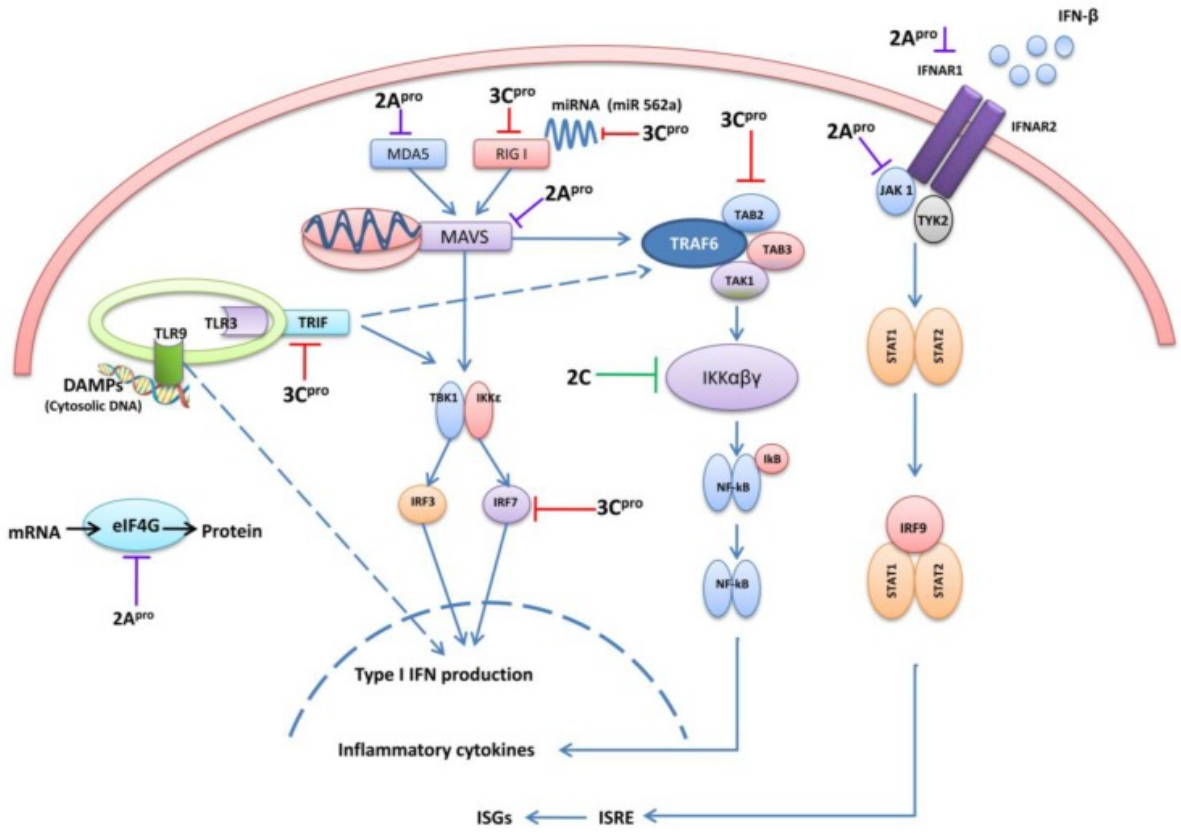

Fig. 18. Evasion of immune system. The viral proteins 2A and 3C interact with several host factors to block the IFN signaling. MDA5: Melanoma-differentiation-associated protein5, RIG-I: Retinoic acid-inducible gene 1, MAVS: Mitochondrial antiviral-signaling protein, TBK1:TANK-binding kinase 1, IRF3/7:Interferon Regulatory Factor 3/7, TRIF: TIR-domain-containing adapter-inducing interferon-β, TLR: Toll-like receptors, DAMPs: Danger associated molecular patterns, eIFG4: eukaryotic translation initiation factor 4G, TRAF6: TNF receptor-associated factor 6, TAK1:Transforming growth factor-β activated kinase 1, TAB2/3: TGF-β Activated Kinase 2/3, IFNAR: Interferon-α/β receptor, TAK1: Janus kinase 1, TYK2: Tyrosine Kinase 2, STAT1/2: Signal transducer and activator of transcription 1/2, ISG: interferon-stimulated genes, ISRE: Interferon-sensitive response element, IFNs: Interferons. Figure from Pathinayake et al., 2015.

Melanoma differentiation-associated protein 5 (MDA5) is a key PRR for detecting single-stranded viral RNAs within the infected cells (Kuo et al., 2013). After binding to viral RNAs, MDA5 interacts with mitochondrial antiviral-signaling protein (MAVS), which induces signaling for the induction of type I IFNs (Blank et al., 2016). The EV-A71 protease 2A disrupts the cytoplasmic signal transduction by targeting the MDA5 receptor. The MDA5 disruption decreases activation of interferon regulatory factor 3 (IRF3) and down-regulates type I IFN production. MAVS protein is also targeted by 2A protease (Wang et al., 2013 and Feng et al., 2014). The EV-A71 2A protease cleaves

MAVS at Gly209, Gly251, and Gly265, generating by-products in the cytosol. The cleavages abolish the IRF3 phosphorylation and type I IFN production, thereby increasing virus replication.

Like MDA5, retinoic acid-inducible gene I (RIG-I) is another intracellular sensing protein involved in the detection of intracellular viral RNAs. During EV-A71 infection, the 3C protease binds to the N terminal domain of RIG-I, which compromises its interaction with MAVS protein and results in decreased activation of IRF3 and low type I IFN production (Chen & Ling, 2019). However, another study showed that RIG-I knockdown using siRNA does not prevent the activation of IRF3 after EV-A71 RNA transfection, suggesting that interaction between 3Cpro and RIG-I plays little role during EV-A71 infection.

TIR-domain-containing adapter-inducing interferon-β (TRIF), interferon regulatory factors 7 (IRF7), and other intracellular proteins (Transforming growth factor-β (TGF-β)-activated kinase 1 (TAK1) and TAK1-binding proteins TAB1, TAB2, and TAB3) are other targets of the EV-A71 protease 3C. The protease cleaves TRIF between amino acid residues Q312-S313, attenuating IRF3 and NF-κB-mediated IFN-β induction (Lei et al., 2011). Cleavage of IRF7 impairs the induction of type I IFNs and the subsequent production of interferon-stimulated genes (ISGs) in a dose-dependent effect. The EV-A71 3C protease directly binds to and cleaves TAK1 and TAB2, thereby impairing activation of NF-κB and induction of inflammatory cytokines (Lei et al., 2016).

In conclusion, cellular proteins targeted by the viral 2A and 3C proteases and micro-RNA molecules are considered key molecules for enhancing viral replication through the inhibition of the IFN pathway (Ho et al., 2014 and Pathinayake et al., 2015).

IX. Mediators of inflammation during the neuro-infection caused by EV-A71

The invasion of the CNS by EV-A71 triggers an acute inflammatory process, which is followed by neurological involvement. The neuroinflammation is characterized by infiltrate of immune cells into the CNS structures, activation of adaptative response, and further neurodegeneration (Nguyen et al., 2022). The EV-A71 neuropathogenesis involve an intense inflammatory response associated with increased levels of several proinflammatory cytokines (Chen et al., 2012 and Suanpan et al., 2022).

a. TNF-α

TNF-α is mainly secreted by macrophages and involved in immune regulation, fever, and inflammation. Patients with severe EV-A71 infections, compared with those with mild infection, present higher levels of TNF-α in the serum. Such features suggest a participation of TNF-α in disease severity (Zheng et al., 2017). Patients with severe complications, including brainstem encephalitis, neurogenic pulmonary edema, and sepsis, have high levels of TNF-α, which then decreased with disease progression (Xie & Duan, 2016). In another study, patients with critical condition (convulsions, coma, brain hernia, pulmonary rales, or circulatory insufficiency) also have higher levels of TNF-α than the severe patient (acute flaccid paralysis or convulsions) and mild groups (Zheng et al, 2017). TNF-α is a crucial cytokine in severe EV-A71-infected HFMD.

b. IFN-γ

For defending the organism against intracellular pathogens or tumoral cells, immune cells generate an adaptative response. Activated T cells, natural killer (NK) cells, and NKT cells produce IFN-γ, a distinctive cytokine of type I helper T cells (Th1 cells), which have antivirus, immune regulation, and antitumor properties (Fenimore & A Young, 2016). Elevated levels of IFN-γ in the serum of patients with brainstem encephalitis and pulmonary edema suggest an involvement of this cytokine in the progression of EV-A71 to neurological complications (Wang et al., 2003). Sun et al., 2018 observed that among patients with severe HFMD, the serum level of IFN-γ was distinctively higher in those who presented neurogenic pulmonary edema. Such clinical findings indicate IFN-γ as factor associated with life-threatening complications of patients infected with EV-A71.

c. Members of the interleukin 1 cytokine family

IL-1β is a proinflammatory cytokine produced in response to infections by cells of the innate immune system, mainly monocytes, endothelial cells, and fibroblasts. IL-1β can stimulate the local antigen-presenting cells, activate T cells, and promote the proliferation of B cells (Wang et al., 2003; Shang et al., 2017; and Griffiths et al., 2012). Patients with brainstem encephalitis and cardiorespiratory abnormalities caused by EV-A71 infections present elevated levels of IL-1β compared with those with aseptic

meningitis and acute flaccid paralysis (Griffiths et al., 2012). A study performed by Ye et al. (2015) correlates the high levels of IL-1β in the plasma of patients with respiratory failure, circulatory collapse, and even coma. Overall, IL-1β may play an important role in severity of infections caused by EV-A71.

In response to infections, several tissues can produce IL-18 that mediates the switch between the innate and adaptative response. IL-18 can induce Th1 cells to secrete cytokines to active NK cells and to promote T cell proliferation. Patients infected with EV-A71 present elevated levels of IL-18 in the serum, especially those with pulmonary edema, gastrointestinal symptoms (vomiting and diarrhea), and myocardial injury (Li et al., 2017).

Finally, a study found a marked increase in the levels of IL-33 in patients with severe (myoclonus, vomiting, ataxia, irritability, and hypersomnia) and critical (acute respiratory failure and PE) symptoms associated with neurological manifestations (Zhang et al., 2013).

d. Members of the interleukin 2 cytokine family

Severe forms of HFMD with encephalitis symptoms are characterised by higher levels of IL-4 than those found in patients with HFMD alone. In addition, the serum level of IL-13 are consistently elevated when patients with severe HFMD manifest pulmonary edema or cardiopulmonary failure (Wang et al., 2003 and Zhang et al., 2020). These cytokines might contribute to the pathogenesis of EV-A71 infection.

e. Interleukin 6 (IL-6)

IL-6 is produced by macrophages, fibroblasts, endothelial cells, and T helper 2 (Th2) cells. This cytokine participates in Th2 and Th1 responses, therefore, IL-6 activates B and T cells, and stimulates the synthesis of acute phase proteins. Due the participation in multiples biological functions, immune responses mediated by IL-6 are unspecific. Several studies reported high levels of IL-6 in patients with severe EV-A71 infection (Zheng et al., 2017 and Chen et al., 2014). Increased levels of IL-6 in CSF is observed in the early stages of neurological manifestations, including encephalitis, poliomyelitis-like syndrome, meningitis, and pulmonary edema. High levels of IL-6 are also observed in patients with cardiopulmonary failure (Chen et al., 2014). Patients with aseptic

meningitis associated with EV-A71 infection were evaluated in a study performed by Lee et al. (2018). These authors suggest a cutoff value of 66 pg/mL for IL-6 as an indicator of severity.

f. Members of IL-12 cytokine family

Macrophages and B cells produces IL-12. This cytokine stimulates the proliferation and activation of T cells, inducing the differentiation of Th0 cells into Th1 cells (Sun et al., 2015). The cytotoxic activity of NK cells are also activated by IL-12, and activated NK cells secretes cytokines, such as TNF-α, IFN-γ, and GM-CSF. The levels of IL-12 in patients with severe EV-A71-associated HFMD (encephalitis and pulmonary edema) were higher than the levels detected in patients with encephalitis alone or with mild HFMD (Shang et al., 2017).

The participation of other members of the IL-12 cytokine family was suggested in the progression of mild HFMD caused by EV-A7 to encephalitis, cardiopulmonary failure, and cardiorespiratory dysfunction. The occurrence of these neurological manifestations correlate to high levels of IL-23, IL-27, and IL-35 in the serum (Zhang et al., 2020 and Huang et al., 2017).

g. Members of IL-10 cytokine family

IL-10 is an anti-inflammatory cytokine produced by macrophages and Th2 cells. IL-10 levels are modulated in acute neuropathological conditions (Wang et al., 2006 and Yang et al., 2012). Patients with pulmonary edema present high plasma levels of IL-10, compared with those detected in patients with nervous system dysregulation and brainstem encephalitis group (Wang et al., 2003). Thus, enhanced IL-10 may have a protective effect in the development of pulmonary edema by influencing the pulmonary capillary permeability.

A large array of immune cells involved in the innate and adaptive immunity produce IL-22, as a response of the synthesis of acute phase proteins (Perusina Lanfranca et al., 2020). Compared with mild EV-A71 infections, the plasma levels of IL-22 are elevated in severe cases (Cui et al., 2017).

h. Chemokines

IL-8, also known as chemokine CXCL8 is produced by macrophages and other cell types, and has the function of attract and activate neutrophils. Patients with brainstem encephalitis or pulmonary edema present elevated levels of IL-8 at the moment of admission (Wang et al., 2014). Elevated concentration of IL-8 in the serum is associated with the most critical manifestations of the EV-A71 infections, such as convulsions, coma, brain hernia, and pulmonary rales.

CXCL10, or interferon gamma-induced protein 10 (IP-10) is a member of C-X-C family cytokine produced by different cell types under IFN-γ stimulation, such as monocytes, dendritic cells, and NK cells. The role of CXCL10 is to mediate inflammatory response Th1. A study performed by Zhang et al. (2013) compared the levels of CXCL10 in healthy individuals with those in HFMD patients, diagnosed with EV-A71 infection. The authors observed a significant increase in the levels of CXCL10 in EV-A71 HFMD patients compared with healthy controls.

Two other chemokines are closely associated with severe forms of EV-A71 infections: CCL2 (also known as monocyte chemoattractant protein (MCP)-1) that is produced by monocytes macrophages, fibroblasts, and CCL5 (also named RANTES, regulated on activation, normal T cell expressed and secreted), a main chemotactic factor for a large array of immune cells. Both CCL2 and CCL5 levels are elevated in children with severe EV-A71 infection associated with neurological manifestations such as encephalitis or paralysis (Shang et al., 2017).

i. Granulocyte colony-stimulating factor (G-CSF)

Monocytes and macrophages activated by endotoxins, TNF-α, and IFN-γ produce G-CSF. G-CSF is a stimulatory blood factor that induces the proliferation, differentiation, and activation of neutrophils. Patients with EV-A71 infection associated with acute respiratory failure present high levels of G-CSF in the plasma (Zhang et al., 2013). The GCSF levels are remarkably higher in the CSF than in the plasma of patients with neurological manifestations. The G-CSF is suggested as a main inflammatory mediator during neurological damage (Griffiths et al., 2012).

X. Viremia

Systemic dissemination into the bloodstream (viremia) and draining lymph nodes is a well-known feature of EV diseases, which results in infection of peripheral tissues including for instance the gastrointestinal tract, skin, oral mucosa. In an earlier study, we showed that viremia occurs early after the onset of symptoms and is of short duration (Lafolie et al., 2018). A prospective investigation of a pediatric population suggests that EV-A71 viremia occurred more frequently in infants (below one year) and viremia detected beyond three days after the onset of disease correlated with more severe disease compared with mild infection cases (Cheng et al., 2014). Beyond this study, data on viremia are lacking in patients infected by EV-A71.

In animal models, systemic spread of EV-A71 (viremia and/or RNAemia) have been detected. In a mouse model, inoculation through the oral route results in viral infection in the intestine, viremia, and EV-A71 spreads to peripheral tissues via blood circulation (Chang et al., 2019). Viremia is also detected in a neonatal rhesus macaque model infected via the respiratory route, EV-A71 infection is observed in the respiratory tract epithelium and the associated lymphoid tissues, and subsequently into a dendritic cell population (Zhao et al., 2017). Evidence suggest that EV-A71 is spread in the blood of another non-human primate model (Cynomolgus Monkey) infected with a virus variant harboring a glutamic acid in the VP1 protein at position 145, suggesting the involvement of amino acid polymorphism in the in vivo viral replication and pathogenesis (Kataoka et al., 2015). To conclude, even though virus and/or viral RNA is detected in the blood or serum, the temporal kinetics of viremia and whether this occurs only during severe disease require further investigations.

XI. Access of EV-A71 to the central nervous system (CNS)

Several receptors contribute for the EV-A71 spread throughout the body (**Table 2**). Structures of extracellular matrix offer initial binding sites that facilitate the attachment of EV-A71 to surface receptors (Pankov & Yamada, 2002; Bae et al., 2004; and Tayyari et al., 2011). These receptors are present in many cell types, and mediates different steps of EV-A71 infectivity (surface attachment, cell entry, uncoating, and replication) (Yamayoshi et al., 2013). In particular, some EV-A71 strains may use P-selectin glycoprotein ligand-1 (PSGL1; CD162) to infect circulating blood leukocytes. Receptor

binding and/or pH alterations in the endosomal vesicles induce virus uncoating and the release into the cytoplasm of the viral genome through the formation of pores in the endosomal membrane (Baggen et al., 2018).

Table 2. Cell surface receptors associated with EV-A71 tropism reported in the literature.

Receptor	Cell type	Cell compartment	Biological function	Role on EV-A71 infection	Target strategy	Source
hSCARB2	Present in gastrointestinal, pulmonary, and brain cells	Expressed at plasma membrane and lysossomes	Participates of endocytosis and directoning of intracellular vesicles to lysossomes	It is involved in viral endocytosis and uncoating	Evaluating subunits of virion capsid by gradient centrifugation analysis	Yamayoshi et al., 2009; Yamayoshi et al., 2013; and Jiao et al., 2014.
PSGL-1	Expressed amog leukocytes	It is found at plasma membrane	Mediates the initial adhesion of leukocytes on inflammed endothelium	Participates of cell entry	Costaining viral particles with early endossomal markers	Somers et al., 2000; Nishimura et al., 2009; and Yamayoshi et al., 2013.
Heparan sulfate	Present in many cell types, including immune and endothelial cells	Present at cell surfaces and extracellular matrix	Gives support to molecular interactions mainly during cell adhesion	Furnish initial binding site to cell surface	Neutralization of electrical charges of cell surface	Lindahl et al., 1998; Tan et al., 2013; and Li & Kusche-Gullberg, 2016.
Vimentin	Present in mesenchymal cells, such as fibroblas as well as endothelial and immune cells	Expresset at cytoplasm and plasma membrane	Constitute the intermediate filaments	Facilitates the cell attachment	Coimmunoprecipitation assays	Du et al., 2014 and Feliksiak et al., 2020.
Annexin II	Expressed by epithelial, endothelial, and immune cells	Present at cell surface	Has an important role in organizing intracellular structures	Interact with viral proteins enhancing the cell entry and viral replication	Blocking receptor with antibodies	S.-L. Yang et al., 2011); Grindheim et al., 2017; Dallacasagrande & Hajjar, 2020); and Q. Zhang et al., 2021.
Sialylated glycans	Present in gastrointestinal and respiratory cells	It is bound to proteins of cell surface	Participates of post-translational modification of proteins, important for recognizing antibodies	It is important for surface attachment	Hamperingthe access to binding sites by using other glycans	Yang et al., 2009 and Ohmi et al., 2021.
CypA	Expressed by smooth muscle, immune, and endothelial cells	Expressed in cytoplasm, but can be excreted	Regulate mitochondrial functions and when secreted act	Mediates the cell entry and viral replication	Using inhibitory compounds	Qing et al., 2014 and Liang et al., 2021.

			as chemokine			
WARS	Higly expressed in intestine, lung, and liver	Expressed as a cytoplasmic factor that can be excreted	Act as a regulator of IFN signaling	Play a role in cell entry	inhibition via siRNA	Yeung et al., 2018 and Lee et al., 2020.
Prohibitin	Higly expressed in progenitor and mature neural cells	Expressed at mitochondria	Mediates mitochondrial biogenesis and degradation	Participates of viral replication	inhibition via siRNA	Hernando-Rodríguez & Artal-Sanz, 2018; Huang et al., 2021; and Too et al., 2018.
Nucleolin	Present in immune and endothelial cells	Distributed in nucleus, cytoplasm, and cell surface	Regulates the metabolism of nucleic acids	Facilitates the cell attachment	Purification by chromatografy followed by immunoprecipitation with EV-A71 particles	Tajrishi et al., 2011; Tayyari et al., 2011; Su et al., 2015; and Fang et al., 2020.
Fibronectin	Produced by many cell types including fibroblasts, hepatocytes, and endothelial cells	Component of extracellular matrix	Participates of extracellular interactions during cell growth, migration and differentiation	Mediates the surface attachment and enhances the cell entry	Hamperingthe access to binding sites by using syntetic peptides	Pankov & Yamada, 2002; Bae et al., 2004; Andrews et al., 2018; and He et al., 2018.

Human scavenger receptor class B member 2 (hSCARB2); P-selectin glycoprotein ligand-1 (PSGL-1); Cyclophilin A (CypA); and tryptophanyl-tRNA synthetase (WARS).

The main transmission route of EV-A71 infections is fecal-oral. Therefore, the virus proliferates initially in the oral cavity and digestive tract, and further invades other tissues and organs, including the CNS (**Fig. 19**) (Ooi et al., 2010).

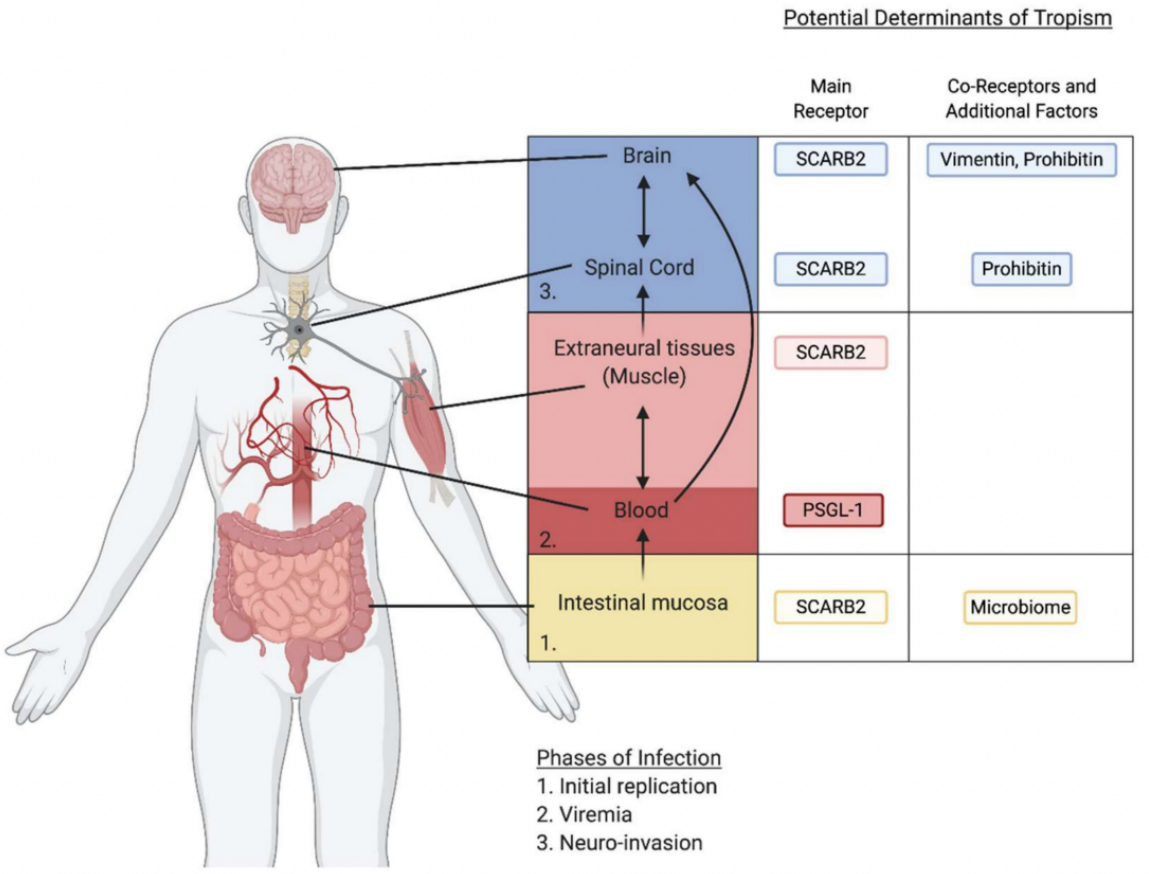

Fig. 19. Entry of EV-A71 into the CNS. Following replication within primary replication sites, such as intestinal mucosa, EV-A71 can spread to different tissues and reach the CNS. EV-A71 can infect terminal nerves and migrate to CNS by retrograde axonal transport. The brain invasion can also occur by hematogenous route. The image shows the possible routes of EV-A71 spreading and the respective cell receptors that may be associated with the tissue tropism. SCARB2 is widely expressed in human tissues, such as intestine, smooth muscule, and neurons. Expression of other receptors is more limited: PSGL-1 is expressed exclusively in blood cells, while vimentin and prohibitin is found in the CNS. Figure adapted from Peters et al., 2015.

EV-A71 may gain access to the CNS through two routes: i) a neural route by using the retrograde axonal transport, and ii) the hematogenous route. The latter may involve crossing of the BBB by infected leukocytes in a mechanism commonly known as “trojan horse’’, or direct crossing of brain microvascular endothelial cells by free virus particles (Huang & Shih, 2015; Chen et al., 2020; and Yang et al., 2022).

a. CNS invasion by retrograde axonal transport

EV-A71 hijack the retrograde axonal transport – the transport of vesicles and substances along microtubules from terminal nerves to the cell body (**Fig. 20**) (Millecamps & Julien, 2013).

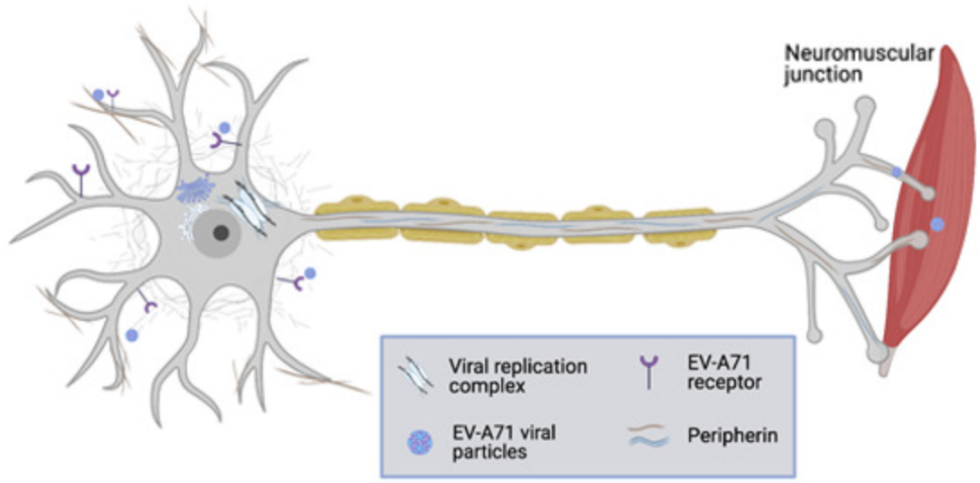

Fig. 20. Retrograde axonal transport. During the retrograde axonal transport, EV-A71 can access the axons terminations and migrate to the cell body of motor neurons into the CNS. The image shows the passage of EV-A71 from muscle to the neuromuscular junction, and the utilization of Peripherin for migrating into the neuron body. In the neuron body, EV-A71 replicates and produces new infectious particles. Figure from Lim et al., 2021.

Retrograde axonal transport is well described as a major mechanism for virus spreading to the CNS during EV-A71 infection (Chen et al., 2007). Sensory, autonomic, and mainly motor nerves are targeted by EV-A71 (Xing et al., 2016). Magnetic resonance imaging (MRI) scans of the nervous system in children with severe HFMD associated with proven EV-A71 show lesions in the brainstem, the spinal nerve roots, the brainstem plus cervical spinal cord, the cervical spinal cord, the brainstem plus spinal nerve root (Li et al., 2019). The data agree with the hypothesis of retrograde axonal transport in EV-A71 pathogenesis involving tropism for pharyngeal branch of the vagus nerve.

A recent study reports that peripherin, a type III intermediate neurofilament, is an attachment factor for EV-A71 at the surface of neuron-like and neuroblastoma cell lines

(Lim et al., 2021). In addition, intracellular peripherin may enhance the replication of viral genome through interactions with structural and non-structural viral components.

b. CNS invasion by hematogenous route

Leukocytes carrying intracellular pathogens can become vehicles for spreading the infection to the CNS (**Fig. 21**) (Constant et al., 2022). During neuroinfection, immune cells coming from the blood and perivascular space of the brain microvasculature or from fenestrated vasculature of the plexus choroid, can migrate to the brain parenchyma (Carson et al., 1999).

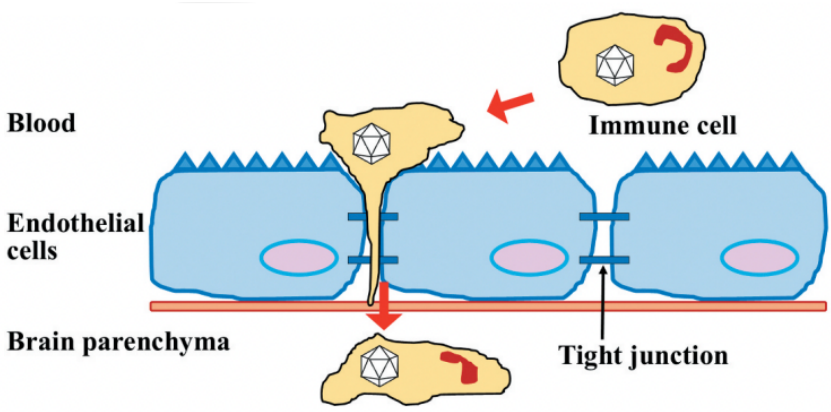

Fig. 21. The Trojan horse pathway. Neurotropic viruses can use leukocytes as vehicles to invade the CNS. During a neuroinflammatory context the cellular infiltrate into the brain parenchyma may carry virus into the CNS through infected leukocytes. The image shows infected leukocytes migrating through the BBB carrying virus into the CNS Figure from Tee et al., 2021.

The release of inflammatory mediators increases the expression of adhesion molecules on vasculature, which facilitates the transmigration of leukocytes through endothelial cells (Stamatovic et al., 2008 and Spindler & Hsu, 2012). EV-A71 may effectively infect leukocytes, binding to the N-terminal region of the PSGL-1 receptor (Miyamura et al., 2011 and Kataoka et al., 2015). This interaction is mediated by VP1 protein, notably the VP1-145 position (see above). Therefore, the data suggest that leukocytic infection occurs in a strain-dependent manner (Nishimura et al., 2009 and Nishimura et al., 2013). In addition, few studies at molecular level show possible involvement of mi-RNAs in mediating trans-endothelial migration during EV-A71 infections (Deng et al., 2012; Tang et al., 2016; and Yang et al., 2022).

Cell-free viruses in the blood, can reach the CNS by simply passing through the brain microvascular endothelial cells (Spudich & González-Scarano, 2012 and Constant et al., 2022). These cells can be equally infected and release viruses to the brain parenchyma (**Fig. 22**) (Dittmar et al., 2008; Papa et al., 2017; Verma et al., 2010). EV-A71 infect endothelial cells without causing macro alterations in functions and cellular structures, however, it was reported that VP1 induces cytoplasmic redistribution of intracellular structures (Jheng et al., 2016 and Luo et al., 2019).

A study conducted by Volle et al. (2015) compared the infectivity potential of different species of enterovirus, including EV-A71. The authors performed investigations in monolayers of endothelial cells and observed that strains of echovirus 6 (E6) are potentially cytolytic, causing disruption of the cell monolayer and inducing considerable levels of cell death by necrosis and apoptosis. In contrast, EV-A71 infection affect a limited number of endothelial cells and the rare presence of necrotic and apoptotic bodies are incapable of affecting the paracellular permeability functions.

The vimentin receptor is targeted by EV-A71 during infections in endothelial cells (Du et al., 2014; Zhu et al., 2019; Kobayashi & Koike, 2020; and Wang et al., 2020). Vimentin is an intermediate filament that mediates a crosstalk with actin microfilaments and microtubules, the main structures of the cellular cytoskeleton (Chang & Goldman, 2004; Patteson et al., 2020; and Ramos et al., 2020).

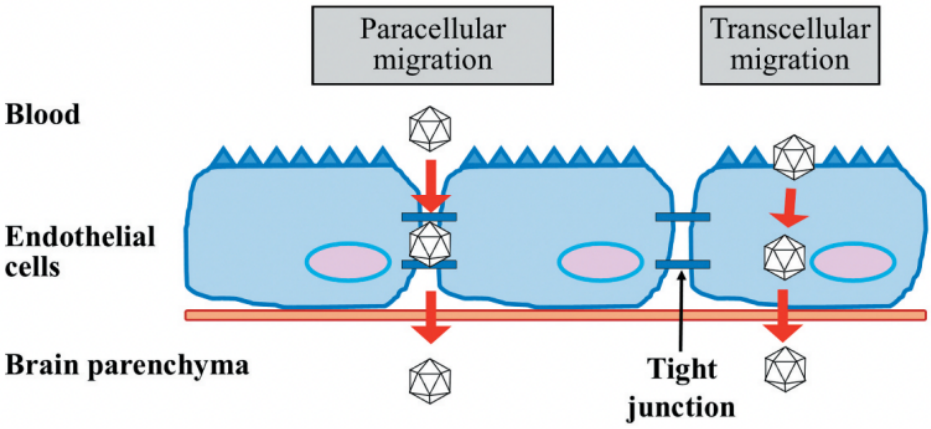

Fig. 22. Crossing through the brain microvasculature. Neurotropic viruses can cross the brain microvasculature through paracellular spaces, a mechanism known as paracellular migration. Neurotropic viruses may also infect endothelial cells and spread into the CNS through the process of transcellular migration. The schematic figure shows virions crossing freely across the paracellular spaces between adjacent cells (at left) or crossing the BBB through endothelial cells (at right). Figure from Tee et al., 2021.

The attachment of EV-A71 on the cell surface vimentin activates the inflammasome and triggers an inflammatory response (Xiao et al., 2018). The inflammasome is a complex of cytosolic proteins and a critical component of the innate immune responses because it mediates the release biologically active interleukin-1β/IL-18 through caspase-1 activation (Wang et al., 2015). Nod-like receptor protein 3 (NLRP3) is the best-characterized inflammasome.

The inflammasome activation depends of phosphorylation of extracellular signal-regulated kinases 1/2 (Shao et al., 2016 and Yu et al., 2017). In response to this signal, NF-κB translocate rapidly into the nucleus and activates the assembly of the multiprotein inflammasome (**Fig. 23**). Overall, the NLRP3 inflammasome is a ring-shape complex composed by the association between NLRP3 with caspase-1, and the adaptor protein apoptosis-associated speck-like protein (ASC), which mediates cleavage of pro-IL-1β into mature IL-1β (Wang et al., 2017).

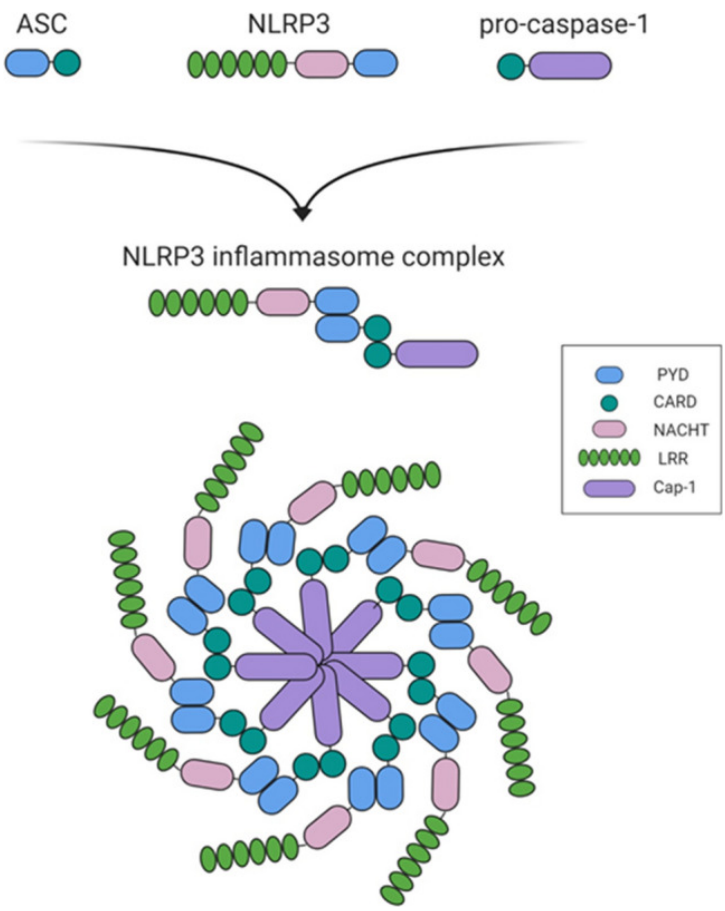

Fig. 23. The structure of NRLP3 inflammasome. The inflammasome is a group of intracellular multimeric protein complexes that activate the inflammatory caspase-1 (Cap-1). A two-domain adaptor protein, apoptosis-associated speck-like protein (ASC) containing a caspase-recruitment domain, facilitates the recruitment of pro-caspase-1 to the inflammasome complex. NLRP3 is a tripartite protein that consists of an amino-terminal pyrin domain (PYD), a central nucleotide-binding and oligomerization domain (NOD or NACHT), and a C-terminal leucine-rich repeat (LRR) domain. CARD, caspase activation and recruitment domain. Figure from Seok et al., 2021.

XII. The blood-brain barrier (BBB)

The BBB is a dynamic interface between the blood and the brain parenchyma that removes xenobiotics and metabolites from the brain interstitial fluid, controls substance exchanges and supplies the brain with essential molecules to ensure homeostasis (Redzic, 2011 and Benz & Liebner, 2022). Brain microvasculature confers the functions to the BBB that has a unique architecture compared to the microvasculature of other organs of the human body (Hayashi et al., 1997 and Langen et al., 2019). The brain endothelial cells in association with astrocytes, pericytes, and glial cells, form together a complex multi-cellular structure, the neurovascular unit (NVU), which

regulates CNS functioning (McConnell et al., 2017; Kugler et al., 2021; Benz & Liebner, 2022). Endothelial cells of the brain microvasculature lay on a basement membrane, in which pericytes are embedded. End feet of astrocytes cover this arrangement and the direct contact with neurons and microglia forms the core functional NVU (**Fig. 24**) (McConnell et al., 2017; Kugler et al., 2021; and Benz & Liebner, 2022).

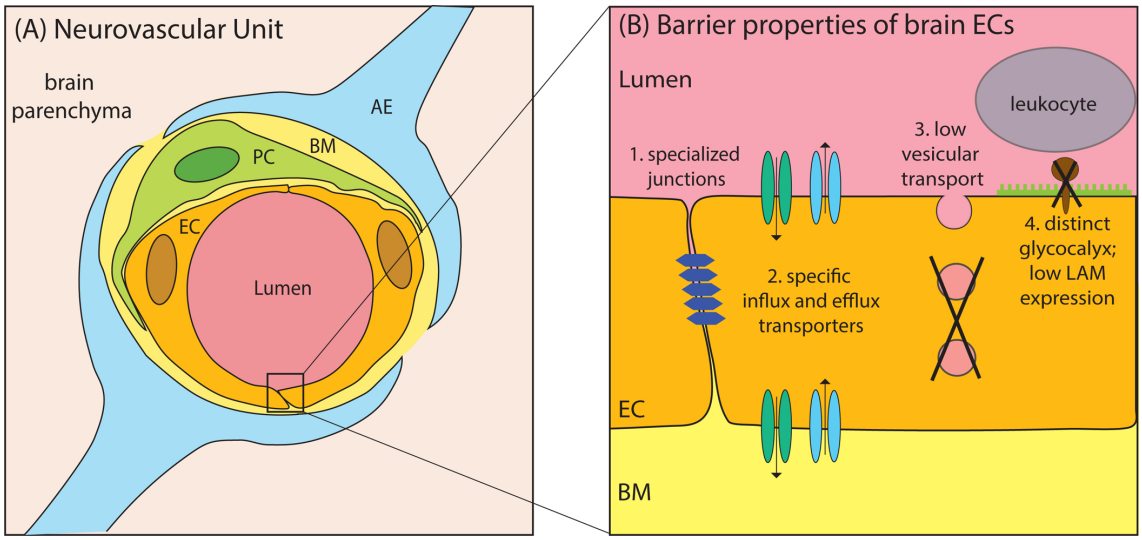

Fig. 24. Structure and function of NVUs. Endothelial cells of NVUs are surrounded by pericytes and maintain close contact with astrocytes end feet and other cell types of brain parenchyma. The unique architecture of NVUs induces the expression of specialized junctions and transporters at endothelial cells, shaping the BBB phenotype. The figure shows the expression of specialized proteins between adjacent cells, expression of transporters in both luminal and abluminal membrane, low vesicular transport, and low expression of leukocyte adhesion molecules in the BBB under physiological conditions. Figure from Langen et al., 2019.

XIII. Molecular components of the human BBB

a. Membrane transporters

Membrane transporters expressed by NVU endothelial cells play an important role in maintaining BBB properties (Suhy et al., 2017). The ATP-binding cassette (ABC) is a superfamily of transporters consisting of the multidrug resistance proteins (MRP, ABCC), breast cancer resistance protein (BCRP, ABCG2), and P-GP (ABCB1) (**Fig. 25**) (Eng et al., 2022). The P-gp efflux pump actively eliminate drug, toxins, and xenobiotics from the brain parenchyma (Balzer et al., 2022).

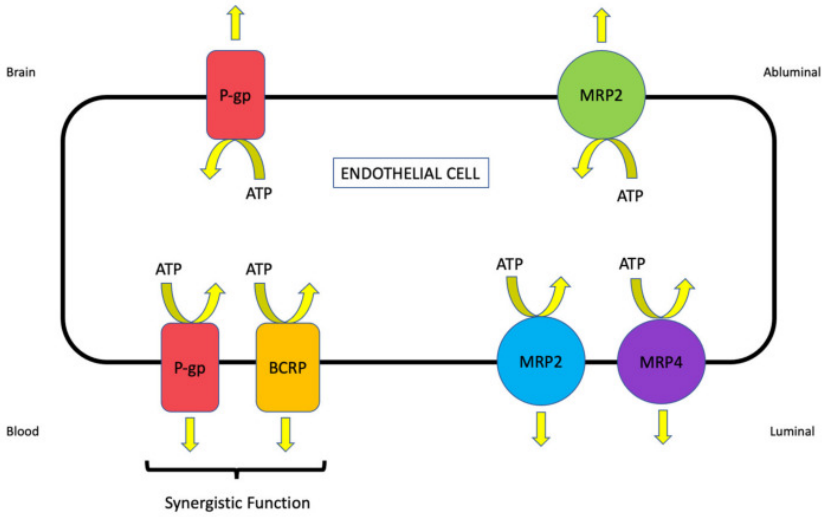

Fig. 25. Localization of the ATP-binding cassette (ABC) transporters. The ABC membrane transporters are expressed differently in the luminal and abluminal sides of the brain microvascular endothelial cells. P-gp and MRP2 is expressed in both luminal and abluminal membrane, other transporters, such as BCRP and MRP4 are expressed exclusively at luminal membrane of endothelial cells. BCRP: Breast cancer resistance protein; MRPs: Multidrug resistance proteins; P-gp: P-glycoprotein. Figure from Nilles et al., 2022.

Solute carriers (SLC) also participate in the transport of a wide range of molecules such as organic and inorganic ions, sugars, and amino acids across the BBB. The delivery of energy sources for the neuronal cells is carried specifically by the glucose transporter 1 (GLUT-1) (Szablewski, 2017 and Koepsell, 2020). This insulin insensitive receptor is expressed in endothelial cells, and enable the passive transport of D-glucose from blood to brain parenchyma (Cornford & Hyman, 2005; Ishida et al., 2006; and Vulturar et al., 2022). The glucose uptake is directly associated with the manutention of the AMP-activated protein kinase (AMPK), an important regulator of metabolic pathways (Veys et al., 2020). Organic anion transporting polypeptides (OATPs) as well as organic cation transporters (OCTs) are other transporter proteins in the BBB (Abdullahi et al., 2017; Kadoguchi et al., 2022; and Nilles et al., 2022). They are differentially expressed at the luminal and abluminal membranes of brain microvascular cells (**Fig. 26**) (Girardin, 2006 and Geier et al., 2013).

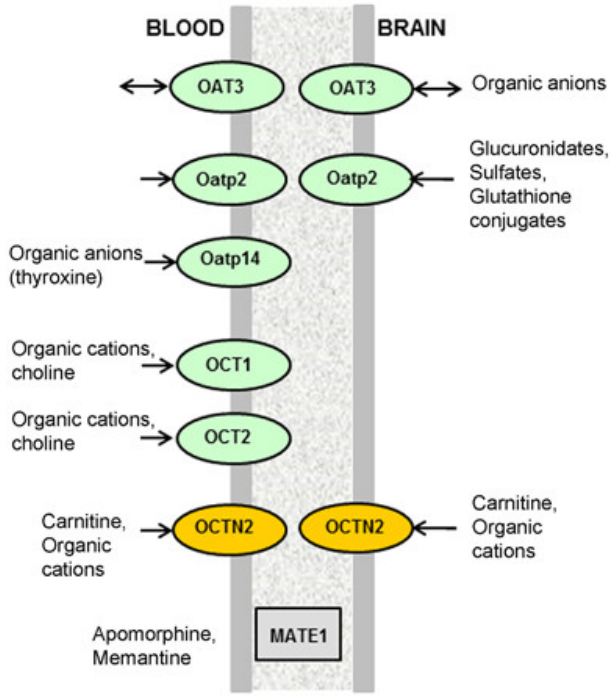

Fig. 26. Localization of proteins transporting organic ions. The image shows the distribution of ion transporters. OAT3 is located in both luminal and abluminal membrane and can transport ions in either direction luminal-abluminal or abluminal-luminal. Oatp2 is located only at the abluminal membrane, and expulses glucoronidates, sulfates, glutathione conjugates from the brain parenchyma into the blood flow. Oatp14 is located in luminal membrane and transport organic anions from blood flow into the brain parenchyma. OCT1 and 2 is located only at the luminal surface, and transport organic cations from blood to the brain parenchyma. OCTN2 is located in luminal and abluminal membrane and transport carnitine and organic cations from the blood to the brain, and from the brain to the blood. Figure from Nałęcz, 2017.

b. Gap junctions

Gap junctions are macromolecular complexes made by the assemblage of connexin proteins (Gaete et al., 2014 and Nalewajska et al., 2020). Gap junctions form poorly selective channels that connects the cytoplasm of two adjacent cells (**Fig. 27**) (Stamatovic et al., 2016). Gap junctions promote ion exchange and circulation of small metabolites between endothelial cells and contribute to tissue homeostasis (Beyer & Berthoud, 2018 and Burboa et al., 2022).

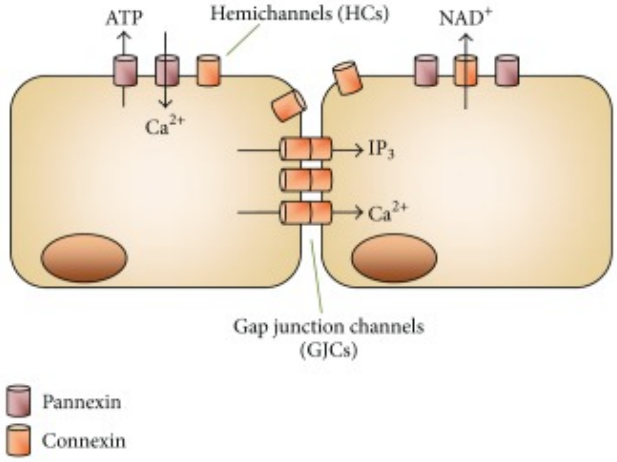

Fig. 27. Localization of connexin proteins and gap junctions. Endothelial cells communicates with theirs pairs. It is important for the cell homeostasis the interchange of electrolytes for performing physiological functions. These cells has hemichannels that allows the entrance of calcium from extracellular environment to cytoplasm the calcium may pass from one cell to other through the gap junctions. The image shows the entrance of calcium from extracellular environement in cytoplasm of endothelial cells by Pannexins and the passage of this ion between adjacent cells through Connexins. IP3, inositol 1,4,5-trisphosphate; NAD, nicotinamide adenine dinucleotide. Figure from Vega et al., 2013.

c. Adherens junctions

Adherens junctions are made of cadherin transmembrane proteins, cadherins, mostly responsible for the adhesion between cells and cytoplasmic/scaffolding proteins, catenins, involved in supporting cadherin association and regulating out-in signaling processes. VE-cadherin is the main protein within the adherens junctions, and plays an important role in maintaining the endothelial integrity (Castro Dias et al., 2019). The cytoplasmic domains of VE-cadherin bind to α-catenin and β-catenin, which acts as a bridge between other cadherins and reorganize structures of actin cytoskeleton (**Fig. 28**) (De Bock et al., 2014). VE-cadherin also regulates the expression of transcription factors, and its stabilization is considered a prerequisite for the formation of tight junctions (Tietz & Engelhardt, 2015).

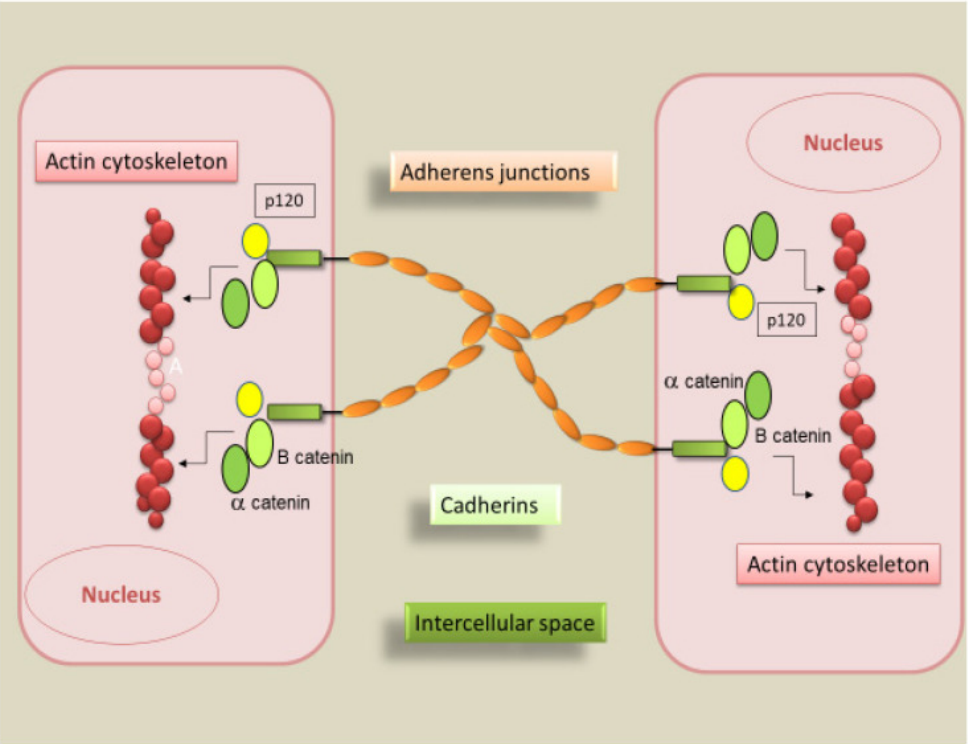

Fig. 28. Cytoskeleton anchorage. At basal level of endothelial cells cadherin proteins project their structures at extracellular spaces. The extracellular domains of cadherins attach to their counterparts to maintain the adherence between adjacent cells. The intracellular domains of cadherins is associated with α and β-catenins, this molecular complexes is anchored in actin cytoskeleton, which is important for maintaining the stability of adherens junctions. Figure from Sisto et al., 2021.

d. Tight junctions

A complex arrangement of cytoskeleton molecules sustains the formation of intercellular tight junctions (Hawkins & Davis, 2005 and Kealy et al., 2020). Zonula occludens (ZO) are intracellular proteins that comprise three isoforms: ZO-1, ZO-2, and ZO-3. These proteins belong to the large family of membrane-associated guanylate kinase (MAGUK)-like proteins (Qiao et al., 2014). The classification of these proteins is based on sequence similarity and characteristic of cytoplasmic domains (Hervé et al., 2014). The first PDZ domain of ZO proteins interacts with the claudin C-terminal domain and their GUK domains to occludin (**Fig. 29**).

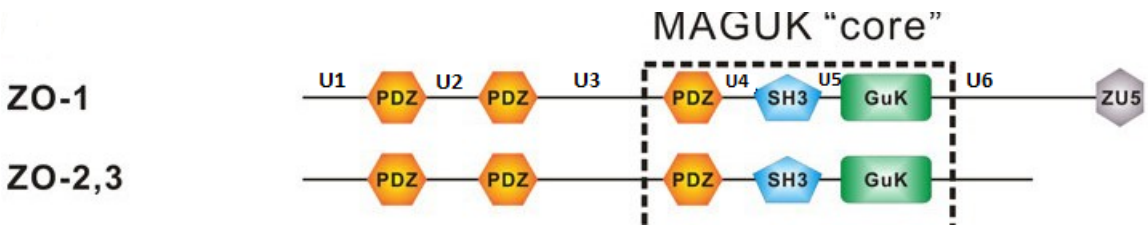

Fig. 29. Domain organization of zonula occludens (ZO) proteins. ZO-1 is considered an important marker of the BBB. This protein is situated at intracellular level and its function is basically furnish physical surface for tight junction proteins. This protein is subdivided in amino acid domains (PDZ, SH3, GuK, and ZU5). The image shows the comparison between ZO-1 and other members of the family of proteins zonula occludens, such as ZO-2 and 3. Basically, The primary structure of ZO-1 protein is composed by three PDZ domains followed by a SH3, GuK, and ZU5 domain. The two first PDZ domains are site of interaction with claudins, while the third PDZ domain in association with SH3 and GuK domains form a ''core'' known as MAGUK, important for interact with occludins. Figure adapted from Pan et al., 2011.

ZO proteins are thus essential for the assembly of claudins and occludin at tight junctions, allowing anchoring of this multimolecular complex to the actin cytoskeleton. During the brain angiogenesis, ZO-1 proteins acts as a signaling transducer that interfere on the gene expression and cell behavior, as well as structural component of cell architecture (Bauer et al., 2010). Some cytoplasmic domains of ZO-1 are associated to Wnt–β-catenin regulation and orientation of centrioles during the cell division (Kuo et al., 2021; Liu et al., 2022; and Ram & Vairappan, 2022). Other domains regulate the gene expression by affecting the cytoplasmic availability of transcription factors that are sequestered to assemble ZO-1 scaffolds, known as perijunctional complexes (González-Mariscal et al., 2000 and Spadaro et al., 2014).

During tight junction formation, cytoplasmic domains of ZO-1, such as ZU5 and U6 domains recruits several cytoskeleton-associated and cytoplasmic proteins (CGN, CGNL1, F-BAR) to perijunctional complexes (Fanning & Anderson, 2009; Ahmed et al., 2010; and Vasileva et al., 2022). Tight junction-associated marvel proteins (TAMPs), such as occludin, MarvelD3 and tricellulin are recruited as well to stabilize the ZO-1 scaffold (Ikenouchi et al., 2008; Günzel & Fromm, 2012; and Saito et al., 2021). This molecular interaction allows the further assembly of tight junction networks (Pulimeno et al., 2011; Van Itallie et al., 2015; and Vasileva et al., 2022).

Claudins and occludin are localized at the lateral membrane of endothelial cells and define the limit between the luminal and abluminal cytoplasmic space (**Fig. 30**). Some

members of claudin family can form paracellular channels that mediates selective flow of ions and solutes between adjacent cells (Fromm et al., 2017 and Rosenthal et al., 2017). In contrast other claudin proteins, such as claudin-5 and claudin-1 prevent the paracellular transport (Günzel & Fromm, 2012 and Tanaka et al., 2017). The extracellular regions of claudin-5 interact with claudin-1 counterparts anchored in the membrane of the adjacent cells. These interactions seal the paracellular spaces and restricts the passive diffusion of small molecules across the BBB (Suzuki et al., 2015 and Sasson et al., 2021).

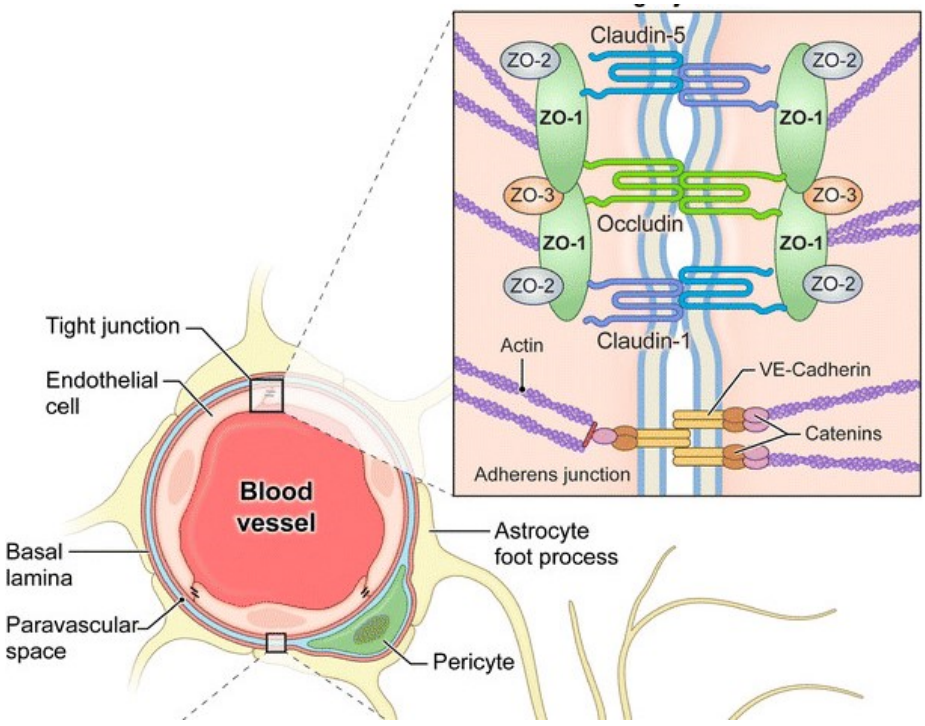

Fig. 30. Junctional complex. The architecture of brain microvasculature exposes endothelial cells to direct contact with pericytes, astrocyte end-feet, and other neuronal cells. This complex microenvironment induces the expression of specialized proteins in endothelial cells. Overall, these proteins associates into cytoskeleton structures. At apical region, the class of proteins ZO-1 forms an intracellular foundation, which Claudin-5 and occludin attaches and forms bridges that connect adjacent cells, this molecular complex is known as tight junction, and seal the paracellular spaces. At basal region, cadherins and catenins form adherens junctions, important for connecting adjacent cells. Figure adapted from Murayi & Chittiboina, 2016.

XIV. BBB dysfunctions

a. Leakage of ATP

Systemic and neuro-inflammatory responses may affect the BBB and lead to the leakage of molecules into the CNS (Coisne & Engelhardt, 2011 and Butsabong et al., 2021). Microglia cells respond to extracellular alterations by releasing TNF-α and IL-1β, potent proinflammatory cytokines implicated in the induction and progression of neuro-inflammation (Rodrigues & Granger, 2015 and Monif et al., 2016). Cytokine stimulation open connexin channels, releasing ATP to extracellular environment (**Fig. 31**) (Bennett et al., 2021 and McDouall et al., 2022). The release of ATP is self-sustained by micro-environment sensors, such as pannexins and P2XR7 receptors, which increases ATP release and induces death signals within brain cells by inflammasome activation (Takenouchi et al., 2011; Dubyak, 2012; Davidson et al., 2015; Yang et al., 2016; Willebrords et al., 2017; and Zhang et al., 2021).

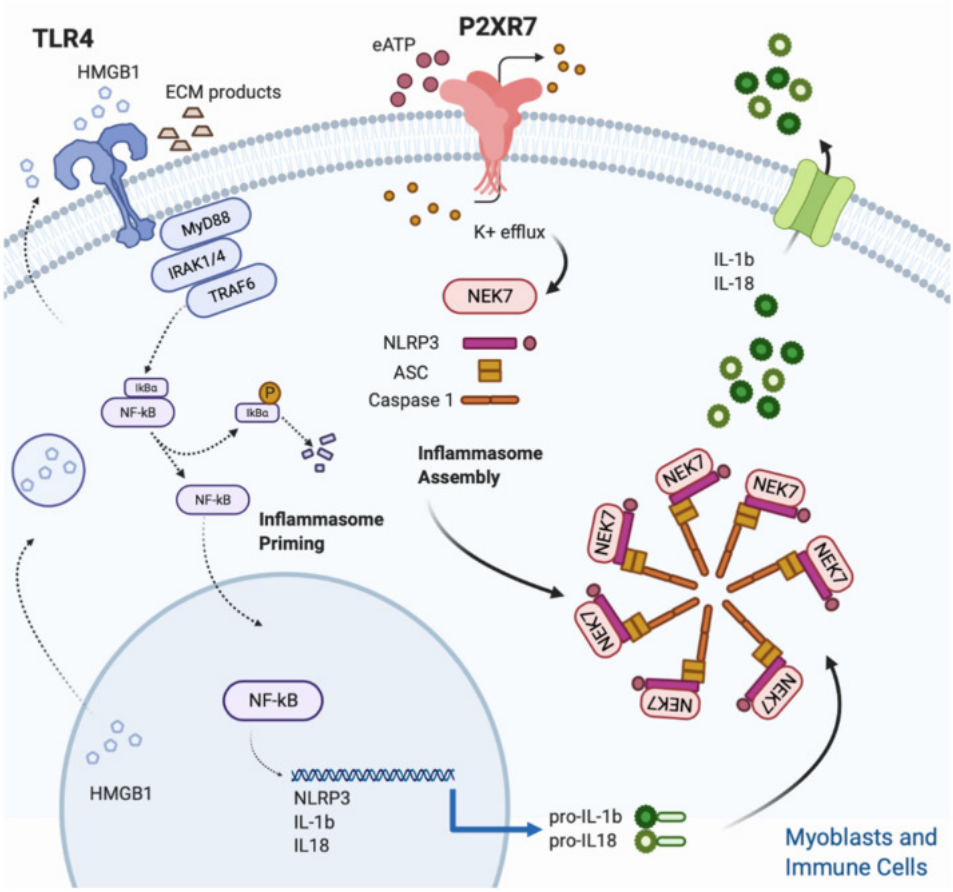

Fig. 31. Activation of inflammatory response. Extracellular ATP is sensed by P2X purinoceptor 7 (P2XR7) and the downstream signal induces the inflammasome assembly that triggers a pro-inflammatory response. Two major receptors are indicated in this schema: P2XR7 that mediates the inflammasome assembly and TLR4 that mediates the production of pro-IL18 and pro-IL-1β. ASC (apoptosis-associated speck-like protein), HMGB1 (high-mobility group protein 1), IkBa (factor kappa light polypeptide gene enhancer in B-cells inhibitor, alpha), IRAK1/4 (interleukin-1 receptor-associated kinase 4), MyD88 (myeloid differentiation primary response 88), NEK7 (NIMA related kinase 7), NF-Kb (factor nuclear kappa B), NLRP3 (NOD-like receptor family, pyrin domain containing 3), TRAF6 (TNF Receptor Associated Factor 6). Figure from Panicucci et al., 2020.

b. Phosphorylation of adherens junctions

Neuro-inflammatory responses increase calcium entry within the endothelial cells, which causes an electrochemical imbalance affecting the endothelial paracellular permeability (Soni et al., 2017; Galinsky et al., 2018; and Panattoni et al., 2021). The increase in cytoplasmic levels of calcium triggers signals that activates the phosphorylation and disassembly of VE-cadherin (**Fig. 32**) (Tiruppathi et al., 2006; Sundivakkam et al., 2013; Rho et al., 2017; and Soni et al., 2017). Several signaling pathways are involved in the phosphorylation of the intercellular junctional proteins. Key mediators, such as protein kinase C-delta (PKCδ) and Rho kinase (RhoK) are involved in the disassembly of adherens junctions (Yamamoto et al., 2008; Kim et al., 2010; and Chun et al., 2021). PKCδ activation is a trigger event within endothelial cells for inducing structural and functional changes in the BBB, vascular alteration, and inflammation-induced tissue damage (Jiao et al., 2011).

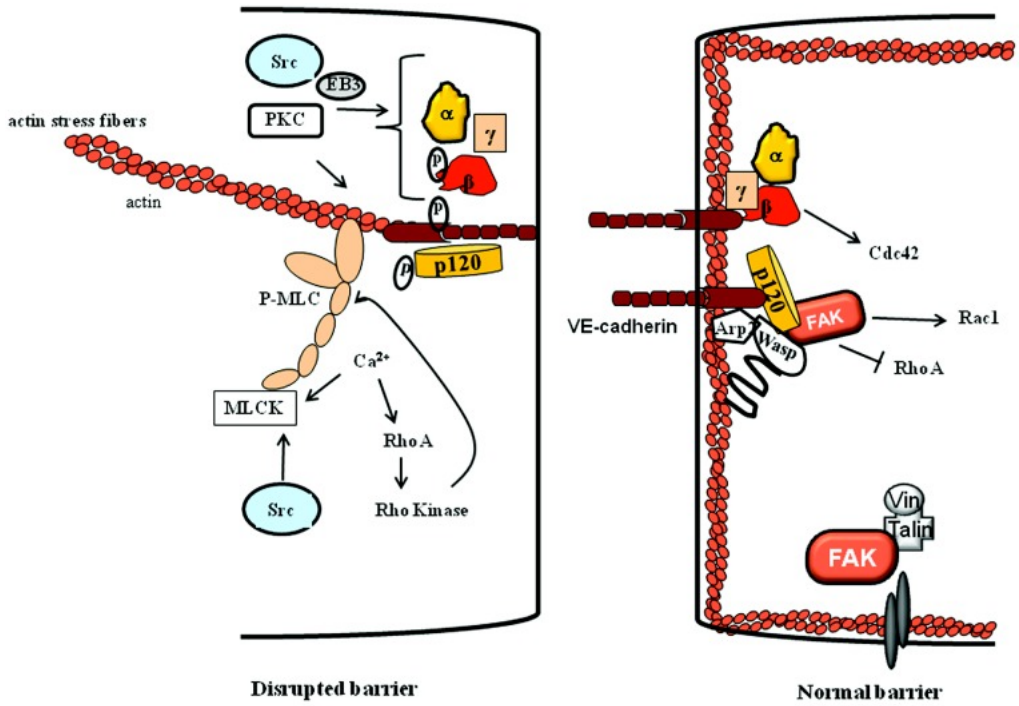

Fig. 32. Cadherin disassembling. The intracellular imbalance of Ca^{+} activates signaling pathways that phosphorylate and disassemble junctional proteins. The increase in intracellular levels of Ca^{+} activates the formation of actin stress fibers through myosin light-chain kinase (MLCK) and RhoA-Rho kinase-dependent pathways. This contributes to VE-cadherin disassembly. In addition, End-binding protein 3 (EBP3), Protein kinase C (PKC), and Src increases the dynamic of microtubules, which also contributes to cadherin disassembly. On the opposite, other intracellular factors block RhoA activity, favoring the reasembly of adherens junctions. The association of actin-related protein 2/3 (Arp2/3), focal adhesion kinase (FAK), neural Wiskott–Aldrich syndrome protein (N-WASP), and p120-catenin induces the formation of cortical actin and may restore the adherens junctions. Figure from Sukriti et al., 2014.

c. Tight junction alteration

In neuroinflammation, pericytes and astrocytes release IL-6 and other factors, such as vascular endothelial growth factor (VEGF), and matrix metalloproteinases (MMPs), which affect the endothelial paracellular permeability (Chen et al., 2014 and Chang et al., 2015). IL-6 and astrocyte-derived VEGF are stressors of endothelial cells, which activate janus kinase-2 (JAK2), a signaling effector inducing the expression of transcription factor STAT3 (**Fig. 33**) (Ozawa et al., 2008 and Babon et al., 2014). This transduction signal promotes ubiquitination and degradation of ZO-1 (Sasaki et al., 2006; Chen et al., 2014; and Chang et al., 2015).

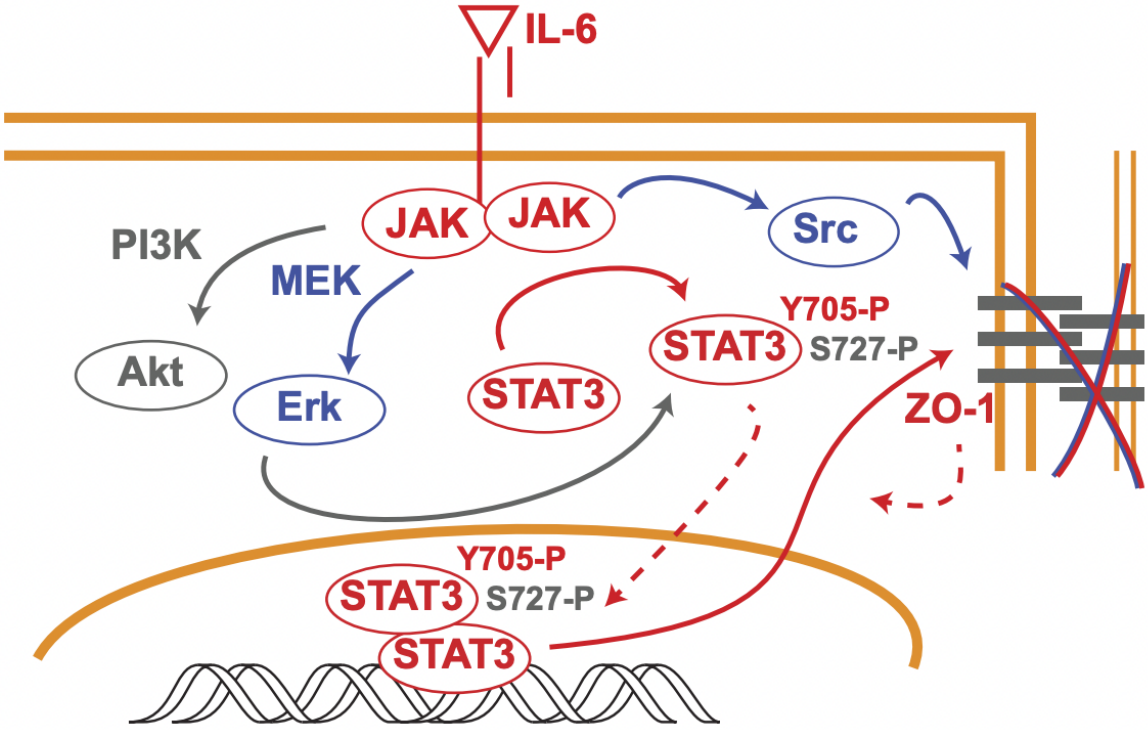

Fig. 33. Tight junction degradation. Pro-inflammatory cytokines, such as IL-6 activates JAK-STAT (Janus kinase 2, signal transducer and activator of transcription 3) signaling that induces a succession of intracellular reactions, which result in the degradation of tight junction proteins. The scheme illustrates the cell signaling triggered by IL-6. Following this stimulation, JAK proteins mediates the activation of intracellular transcription factos, such as Akt, Erk, STAT3, and Src. The activity of STAT3 and Src are determinants for the degradation of ZO-1. Akt, V-akt murine thymoma viral oncogene homolog; Erk, Extracellular signal-regulated kinase; and MEK, Mitogen-activated protein kinase kinase. Figure from Alsaffar et al., 2018.

In vivo and in vitro evidence show that the levels of active MMP-2 and MMP-9, which are extremely low in normal brain tissue, mediate occludin degradation in pathological conditions (Yuan et al., 2020). For instance, the expression of occludin is significantly decreased by the MMP-2/MMP-9 activation in brain microvascular endothelial cells, after stimulation of the mitogen-activated protein kinase pathway (Liu et al., 2012).

d. BBB dysfunction in viral infections

Neurotropic viruses disrupt the BBB by different mechanisms. The interaction between HIV protein such as Tat and endothelial cells increases the expression of IL-6, a potent neuroinflammatory cytokine (Bhargavan & Kanmogne, 2018). The expression of IL-6 involves the activation of STAT pathway that is associated with the decreased

expression of tight junction proteins claudin-5 and ZO-1 (Chaudhuri et al., 2008). More recently, the newly severe acute respiratory syndrome coronavirus 2 (SARS-CoV-2) was also reported as neurotropic virus capable of interact with the human BBB. In patients infected with SARS-CoV-2 and manifesting neurological symptoms, BBB disruption and leakage were reported. In vitro studies associates the interaction between the spike protein, the main protein of SARS-CoV-2 pathogenicity with the downregulation of tight junction proteins of endothelial cells. SARS-CoV-2 may also cause an indirect disruption of the BBB through the hypoxia caused by lung injury, the coagulopathy, and systemic inflammation (Chen et al., 2022). The Japanese Encephalitis Virus invades the CNS by neural routes and the neuroinflammatory process disrupts the BBB (Li et al., 2015). Similarly, the West Nile Virus (WNV) also induces an indirect disruption of the BBB, however WNV crosses directly the BBB (Verma et al., 2010). An in vitro study performed showed that WNV increase the expression of adhesion molecules in endothelial cells, which may facilitate the migration of inflammatory cells in the brain parenchyma (Verma et al., 2009).

XV. Studying the BBB

a. Assessment of the paracellular BBB permeability in animal models

Experimental insults in animals disrupt the BBB and increases passage of molecules into the brain parenchyma (Kaya & Ahishali, 2011). The functional and structural alterations of the BBB can be analyzed by intravascular injection of exogenous tracers (**Fig. 34**) (Ahishali & Kaya, 2021). Evans blue is the most common tracer used to estimate the blood volume, map lymph nodes, localize tumor lesions, and analyze breakdown of the BBB. This dye has high-water solubility, binds tightly to serum albumin, and present a slow excretion (Yao et al., 2018 and Ryu et al., 2018). Other tracers, such as albumin-Alexa fluorine conjugates, cadaverine-Alexa fluorine, sodium fluorescein, horseradish peroxidase, and FITC-dextran can be used solely or even in association to visualize BBB leakage (Xu et al., 2019 and Ahishali & Kaya, 2021). BBB studies were mostly performed in rodents that provided several important physiological BBB features (Roux & Couraud, 2005).

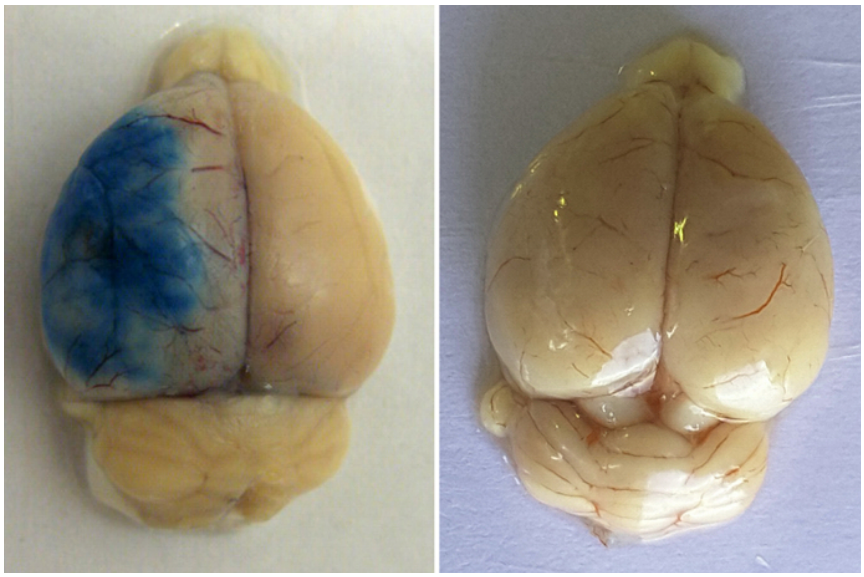

Fig. 34. BBB leakage. The intact BBB limit the massage of molecules from blood to brain parenchyma. The intravenous administration of Evans blue, a tracer that binds to serum albumin is unable to cross the BBB. Further an injury, as an example a ischemic shock, the brain of animals present intense signs of tracer. The image shows the leakage of tracer in the brain of animals with disrupted BBB (left), and the brain of healthy mice (right). Figure adapted from Panahpour et al., 2018.

Animal models can reproduce a number of aspects of neurological syndromes seen in humans, upon infection with EV-A71. The intramuscular infection of vervet monkeys with clinical isolates of EV-A71 induces signs of neurological manifestations with cytologic evidence of lymphocytic and monocytic infiltration in brain parenchyma. The impairment of CNS caused by EV-A71 infections is reproduced by experiments in rats as well (Koroleva et al., 2014). Despite of important insights to elucidate mechanisms associated with EV-A71 spreading, animal models present limitations in demonstrating realistic pathogenicity of EV-A71 infection. A study performed by Zhao et al. (2017), a chimeric fluorescent EV-A71 strain was used to trace the route of infection in neonatal rhesus macaques. The authors demonstrated an efficient viral replication in epithelial cells of the respiratory tract but the model did not present evidence of infection in the alimentary tract, while EV-A71 is considered an enteric pathogen. To solve such limitation, SCARB2 transgenic mice are used to facilitate the EV-A71 infection. However, Shih et al. (2018) reviewed animal models used to study the EV-A71 pathogenesis and indicate that SCARB2 transgenic mice appears to be limited to certain EV-A71 strains.

b. Modeling the BBB in vitro

In vitro models of the BBB are traditionally performed in transwell systems where endothelial cells are cultured on a semi-permeable membrane to form a confluent monolayer (Strazza et al., 2016 and Deligne et al., 2020). These models are well-established and there is a large body of evidence showing their reproducibility (Shayan et al., 2011; Wilhelm et al., 2011; Helms et al., 2016; Guo et al., 2018; Jamieson et al., 2019; Cegarra et al., 2022; Gubern-Mérida et al., 2022; and Rado et al., 2022).

The integrity of in vitro BBB models can be addressed by measuring the trans-endothelial electrical resistance (TEER) (**Fig. 35**) (Cohen-Kashi Malina et al., 2009). Devices, such as cellZscope® and chopstick electrodes of voltohmmeter type (EVOM) are both used to measure the cell membrane capacitance and resistance, determined by transcellular and paracellular ionic transport, respectively (Czupalla et al., 2014).

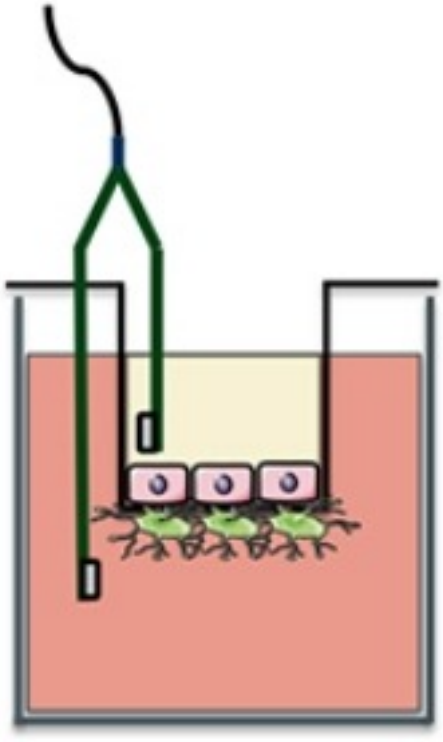

Fig. 35. TEER measurement of in vitro BBB model. The BBB model behaves like a closed system. In consequence of difference (in terms of volume and composition) between the culture medium of the luminal and abluminal side of the model the ionic distribution is not the same in these compartments. The principle of the TEER measurement is to apply a electrical current from luminal to abluminal compartment, that in turn will promote an ordered ionic movement. Confluent cell monolayers are more restrictive to ionic passage, therefore, there will be higher difference of potential (ddp) between the luminal and basolateral compartments. The resistance is calculated according the Ohm law rationing the ddp by the electrical current. In summary, confluent monolayers are restrictive to ionic passage, form higher ddp, and consequently present higher resistance. Figure adapted from Paradis et al., 2016.

The protein transporters are assessed by functional assays based on small drug-like compounds, which demonstrate the uptake and efflux transport of the cell monolayers (**Fig. 36**) (Yusof et al., 2014). Assays based on lipophilic compounds often formation of aqueous boundary layer due inefficient homogenization. This troubleshooting is compensated by associating paracellular permeability assays to calculations and software analysis, which improves the estimation of mechanistic information about the paracellular BBB permeability (Deli et al., 2005 and Yusof et al., 2014).

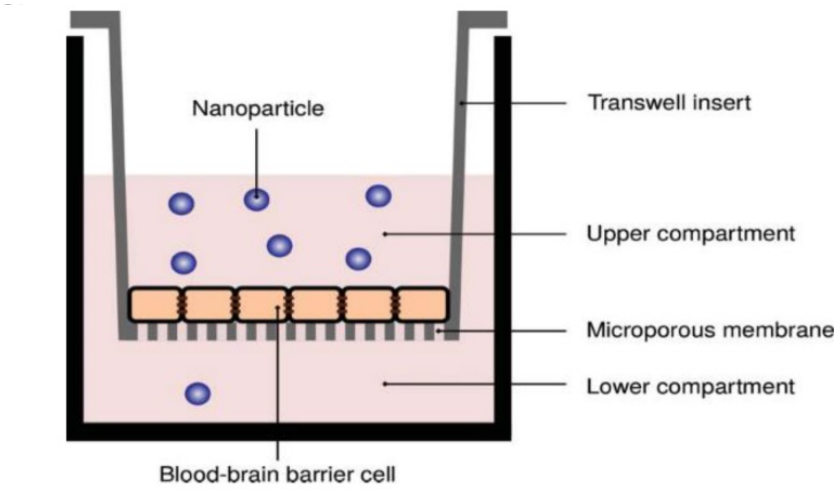

Fig. 36. Investigating the endothelial paracellular permeability in vitro. The endothelial cells are traditionally cultured in semi-permeable membranes for reproducing aspects of the human BBB. The ability of cellular barrier to restrict the passage of molecules may be evaluated by using ‘’drug-like’’ fluorescent compounds. These small molecules cross the barrier slowly when the cell monolayer is confluent. Figure adapted from Hajal et al., 2018.

c. BBB model based on primary cells

Cell isolation from the CNS of humans and animals is a consolidated method that was important to overcome animal testings and establish cellular and molecular mechanisms of BBB function in vitro (Abbott et al., 2012; Bernard-Patrzynski et al., 2019; and Lynch & Gobbo, 2021). However, cell isolation methods frequently result in suboptimal cellular purity. Animal species such as cow and pig are used as high-throughput sources of CNS cells (Thomsen et al., 2015 and Bernard-Patrzynski et al., 2019). The comparisons between in vitro models based on primary cells isolated from mouse, rats, and pigs indicate a wide applicability of these models, which display a number of in vitro differences (TEER values, claudin expression) and some similarities such as the expression and functionality of the P-GP efflux transporter (M. S. Thomsen et al., 2021). Accordingly, the choice of animal primary cells to build an in vitro BBB model will depend on the downstream applications (Perrière et al., 2007; Shayan et al., 2011; and Molino et al., 2014).

d. BBB model based on immortalized cells

Immortalized cell lines have been extensively used to develop in vitro BBB models (Roux & Couraud, 2005; Watanabe et al., 2013; and Guo et al., 2018). However, they lack crucial BBB characteristics and are rarely fully characterized. The hCMEC/D3 cell line is one of the most characterized and well-studied cell lines, and it is widely used as a BBB research tool. hCMEC/D3 was derived from normal human brain endothelial cells transduced by a lentiviral vector containing the telomerase gene, and therefore grows indefinitely without manifest alterations on karyotype or differentiation status. Several important tight junction proteins are expressed but the levels of claudin 5, occludin, and junctional adhesion molecule 2 are low (Weksler et al., 2005). Immortalized cells have the advantage to be low-cost but they display low TEER values and paracellular permeability to small molecules, which indicates that tightness is quite remote from in the vivo BBB (Boveri et al., 2005; Delsing et al., 2020; and Sun et al., 2022).

e. BBB model based on human induced pluripotent stem cells (iPSCs)

Human induced pluripotent stem cell (iPSCs) emerged as an unlimited source of cells, which can differentiate in endothelial cells to form tighter cell layers with superior BBB properties (Hollmann et al., 2017; Delsing et al., 2020; Wellens et al., 2021; and Sun et al., 2022). Differentiation methods were developed from various iPSCs lines in defined culture medium by activating Wnt/β-catenin signaling pathway (Qian et al., 2017). iPSCs are usually cultured onto coating matrices such as Matrigel, a commercial component isolated from mouse sarcoma cells. The iPSCs differentiation is quite laborious and lack the expression of adhesion molecules, in addition the variation among lots of cellular components may impact the efficiency of endothelial differentiation (Aoki et al., 2020). Fully defined substrates were developed to improve cell culture conditions (Patel & Alahmad, 2016) iPSCs-based models display TEER range from 1500 to 4000 Ω cm^2, and resemble a more physiological BBB functions (Qian et al., 2017 and Jamieson et al., 2019).

f. BBB model based on co-culture systems

Several arrangements can be adopted to upgrade an in vitro BBB model, and the selection of each of them can vary according the study aims (Menaceur et al., 2021 and Rice et al., 2022). A major improvement of a BBB model is the co-culture of endothelial cells with other cellular components of the NVU by using different approaches (**Fig. 37**). This can be performed with standard semi-permeable membrane devices (Thomsen et al., 2015 and Mossu et al., 2019), through organoid or spheroid development (Nzou et al., 2018), assembly in hydrogel scaffolds (Weber & Clyne, 2021), and culture in microfluidic systems (Bhalerao et al., 2020). Shear stress can be generated in microfluidic devices allowing the development of improved barrier properties (**Fig. 37**). Each of these approaches are useful to mimic the NVU architecture (Thomsen et al., 2015; Mossu et al., 2019; Nzou et al., 2018; Bhalerao et al., 2020; Weber & Clyne, 2021; Raut et al., 2022; and Wei et al., 2022. Overall, the co-culture systems expose endothelial cells to signals involved in cell communication existing at NVUs (Abbott et al., 2012 and Rizzi et al., 2021). Transwell models provided evidence that endothelial cells are stimulated by the abluminal environment, through secretion of extracellular mediators from astrocytes and pericytes (Siddharthan et al., 2007 and Colgan et al., 2008).

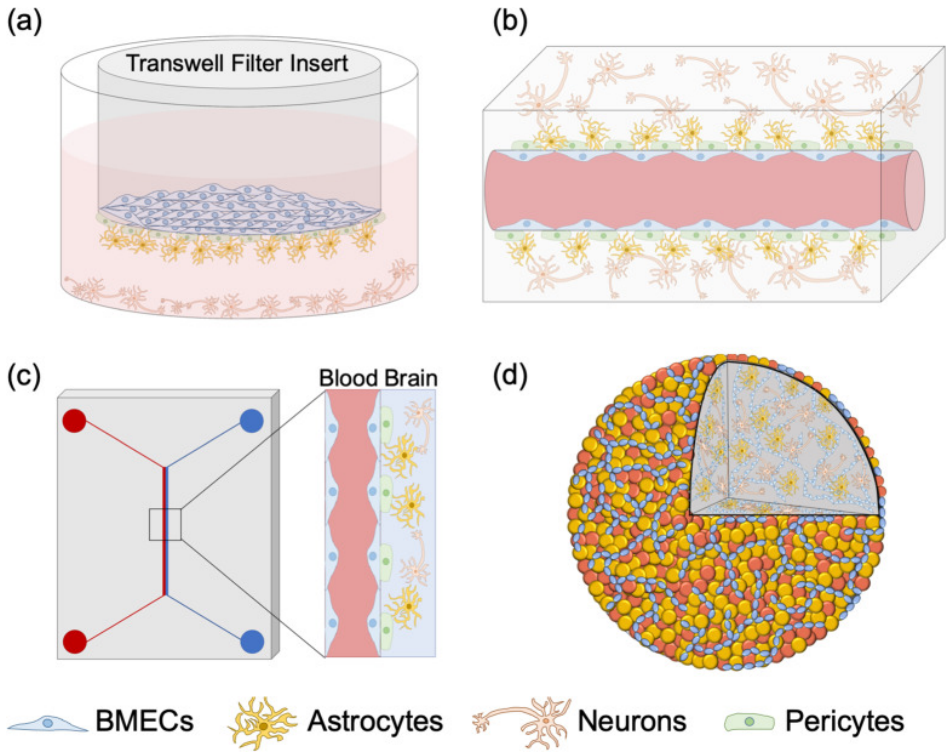

Fig. 37. Co-culture systems. The BBB may be recapitulates by different cellular approaches. The cells that form the NVUs are classically cultured in transwell systems. This method is based on culturing cells in a semi-permeable membrane (**a**). NVU cells may also be immersed onto biocompatible matrices for resemble the structural architecture of the brain microvasculature (**b**). NVU cells may also be cultured in microchips dispositives coupled to fluidic systems in order to evaluate the influence of biophysical forces of blood flow in the wall of brain microvasculature (**c**). NVU cells may simply be culture together in non-adherent environement. As cells harbor a ''biological memory'' of their respective anatomical sites, they self-organize spheroidic structures with pattern similar of that observed in NVUs (**d**). Figure adapted from Weber & Clyne, 2021.

g. Use of hematopoietic progenitors for modeling the BBB

The proper development of an in vitro BBB identity at the functional and transcriptional levels requires the induction of signals that closely resemble those reported during the human development (Motallebnejad & Azarin, 2020; Roudnicky et al., 2020; Lu et al., 2021; and Wellens et al., 2021). Hematopoietic stem and progenitor cells (HSPCs) are characterised in adult tissues like umbilical cord blood by expressing the CD34 surface protein (Pedroso et al., 2011). Blood and ECs have a common ancestor in developmental hierarchy and HPSCs represent a promising source of physiologically relevant ECs (**Fig. 38**) (Tsuji-Tamura & Ogawa, 2018).

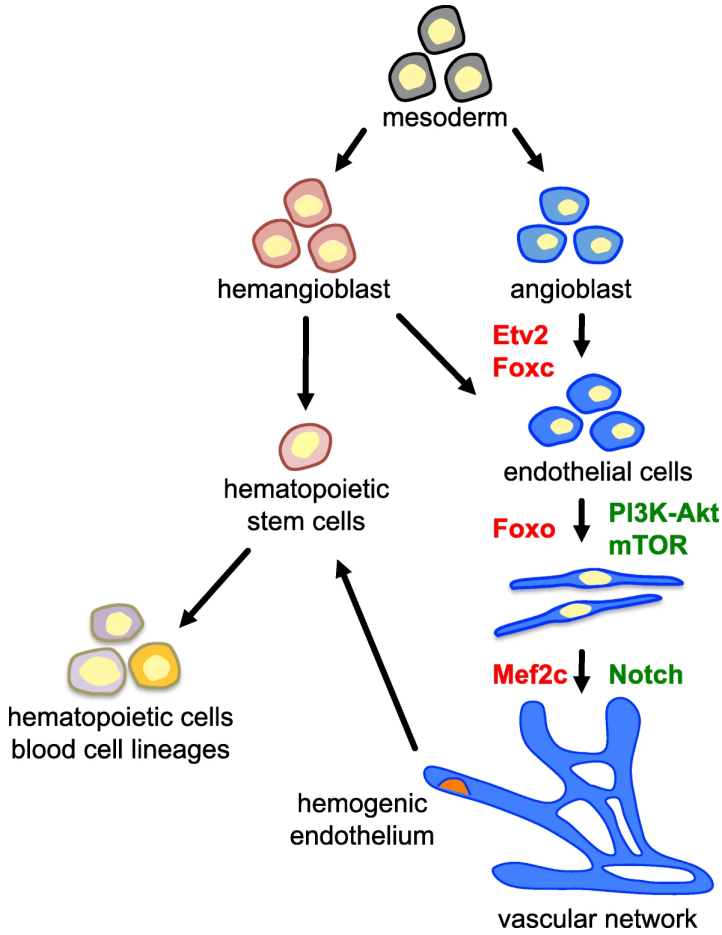

Fig. 38. Ontogeny of endothelial cells. Blood and endothelial cells are originated from a common mesodermal progenitor. The scheme demonstrates the derivation of two different progenitors: hemangioblasts, cells with potential to form hematopoietic and endothelial cells, and angioblasts with potential to form endothelial cells. The expression of transcription factors Etv2 and Foxc is associated to endothelial differentiation. The endothelial maturation and further formation of vascular network are conducted by the activation ow key signaling pathways, such as PI3K-Akt-mTOR and Notch, respectively. During these processes, the transcription factors Foxo and Mef2c play important role in the mediation of cell differentiation. Figure adapted from Tsuji-Tamura & Ogawa, 2018.

The isolation and differentiation of $CD34^+$-derived endothelial cells and the co-culture with pericytes induces the expression of a strong BBB phenotype. For this reason these $CD34^+$-derived ECs are also designated brain-like endothelial cells (BLECs). The co-culture of BLECs with pericytes mediates the expression of BBB markers via Wnt/β-catenin signaling pathway and sustain the BBB phenotype for at least 20 days (**Fig. 39**) (Cecchelli et al., 2014). This model has been applied to a large array of research areas: to investigate the toxicity of potential xenobiotics (Ravid et al., 2018),

explore vascular leakage (Loiola et al., 2021), assess the activity of drug transporters (Versele et al., 2020), study the passage of immune T cells across the BBB (Mossu et al., 2019), and address the issue of endocytosis in endothelial cells (Moya et al., 2022). The co-culture of human BLECs derived from HSPCs with pericytes in a transwell system provides a reproducible in vitro BBB model for validating pre-clinical studies (Cecchelli et al., 2014 and Curtaz et al., 2020).

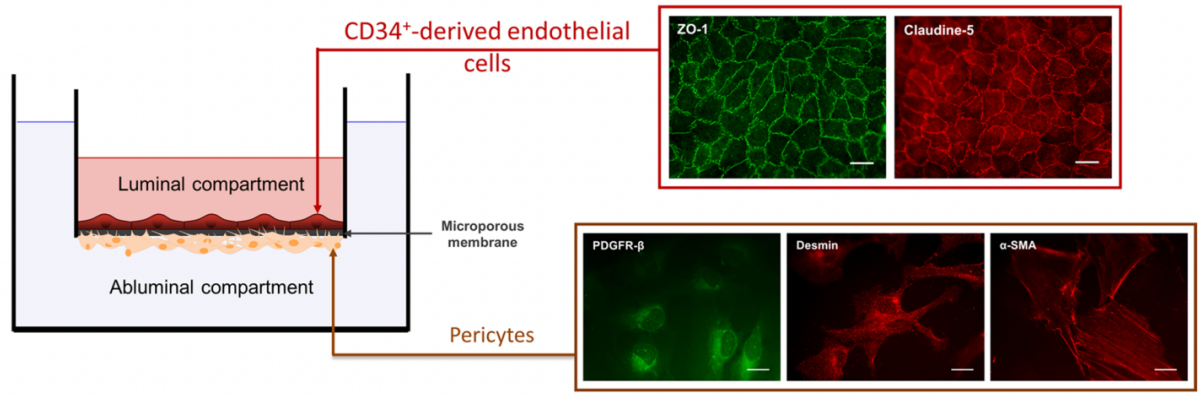

Fig. 39. Co-culture of endothelial cells and pericytes. Hematopoietic progenitors $CD34^+$ are collected from umbilical cord blood and differentiated in endothelial cells. These cells are co-cultured in transwell systems with pericytes for expressing the phenotype of the human BBB, for this reason this model is called brain-like cells (BLECs). The indirect immunofluorescence reveal the protein expression of ZO-1 and Claudin-5 in BLECs. The identity of pericytes was confirmed by the protein expression of platelet-derived growth factor (PDGFR)-β, Desmin, and alpha smooth muscle actin (α-SMA). Figure adapted from Deligne et al., 2020.

OBJECTIVES

3) Objectives

I. Main objective

Determine if EV-A71 could cross the human BBB.

II. Secondaire objectives

- Investigate whether EV-A71 infection is associated with BBB changes,
- Analyze the influence of the inflammatory context on the infectivity of EV-A71,
- Measure the passage of EV-A71 through the BBB.

METHODS

4) Methods

I. Cell culture

The human RD (Rhabdomyossarcoma), an immortalized cell line isolated from smooth muscle, was obtained from European Collection of Authenticated Cell Cultures. These cells were cultured in Dulbecco's Modified Eagle's Medium (DMEM), high glucose (Dutcher, Cat L0103) supplemented with 10% Fœtal Bovine Serum (FBS). The endothelial cells and bovine pericytes were obtained from the Laboratory of Blood-brain barrier (Université D'Artrois, Prof. Fabien Gosselet). The BLECs were cultured in Endothelial Cell Medium (ECM) (ScienCell, Cat 1001) supplemented with 1% ECGS (ScienCell, Cat 1001), 5% FBS, and 50 ug/ml gentamicin (Sigma-Andrich, Cat G1272); while the bovine pericytes were cultured in DMEM GlutaMAX (ThermoFisher, Cat 31966021) supplemented with 20% FBS and 50 ug/mL gentamicin (Sigma-Andrich, Cat G1272). Both EC and pericytes expanded onto 0.2% porcine gelatin (Merck, Cat G2500) in T75 culture flasks.

For cell passages, the cells were washed twice with PBS for two minutes followed by incubation with two mL of a trypsin-EDTA mixture (Dutscher, Cat L0930-100) until most cells adopted a round shape, approximately six minutes (depends on the cell type). The process was stopped by adding six mL of DMEM (Dutcher, Cat L0103). The cells were counted before using the suspension in downstream applications.

II. Viral strains used in this study and preparation of viral stocks

The laboratory is equipped with class 2 biosafety cabinets and authorization for manipulation of infectious agents for research propose. Informed consent was obtained from all subjects involved in the study. The study was approved by the review committee of the University Hospital of Clermont-Ferrand, France 2022/ CE19. A viral stock was prepared to expand each virus isolate in ten T-75 flasks seeded with $3x10^6$ RD cells. After incubation for two days at 37°C, the cell monolayers were inoculated. The flasks were maintained at 37°C until lysis of 90% of the cells. After performing three cycles of freezing/thawing, the cells were scraped and transferred into 50 mL Falcon tubes. Each tube was supplemented with HEPES (Dutscher, cat L0180) (20 uL/mL) and centrifuged at 10,000 $\times$ g 4°C for 10 minutes to eliminate cell debris. Then,

the supernatants were transferred into two ultrafiltration units (Vivaspin 20 mL, Sartorius) to carry out successive two-hour centrifugation cycles at 6000 × g at 4°C to concentrate the viral particles. The virus stock suspensions were titrated as described in the paragraph below to perform inoculation assays under a defined multiplicity of infection (MOI).

III. Building the blood-brain barrier model

To recapitulate aspects of the BBB we co-cultured endothelial cells previously differentiated from hematopoietic progenitors isolated from umbilical cord blood with bovine pericytes in opposite side of semi-permeable 0.4 μm polyester membranes (Deligne et al., 2020). The inserts were placed upside down at the lid of the culture plate and treated with 100 μL Collagen type I (RD systems, Cat 3440-100-01) for one hour. Next, we dissociated the bovine pericytes with Trypsin-EDTA (Dutscher, Cat L0930-100) for approximately six minutes at 37°C. We tap the flask gently and then observed the cell detachment at the microscope. The trypsinization was neutralized by adding culture medium. We homogenized the cell suspension gently, and after numbering we prepared a cell suspension at 5 x 10^5 cells/mL. A drop of 100 μL of cell suspension was dispensed onto abluminal side of the inserts and the cells were incubated at 37°C for three hours. To avoid the evaporation of culture medium we humidified the lid of the culture plate with a dry paper towel. We observed the cell attachment at the microscope and removed the excess of culture medium. The inserts were transferred for a culture plate containing 1.5 mL Dulbecco's Modified Eagle Medium (DMEM) GlutaMAX (ThermoFisher, Cat 31966021) supplemented with 10% FBS and 50 mg/mL gentamicin (Sigma-Andrich, Cat G1272). We add 500 μL Matrigel® dilution (9 mg/mL) (Corning, Cat 356237) and incubated the inserts at 37°C for one hour. We dissociated the endothelial cells with Trypsin-EDTA (Dutscher, Cat L0930-100) for six minutes at 37°C. We tap the flask and observed the cell detachment on the microscope, and after numbering we prepared a cell suspension at 1.6 x 10^5 cells/mL. Further removing the Matrigel solution and washing the inserts, we dispensed 500 μL cell suspension in luminal side of each insert (**Fig. 40**). The cells were maintained at 37°C and the culture medium was changed every two days.

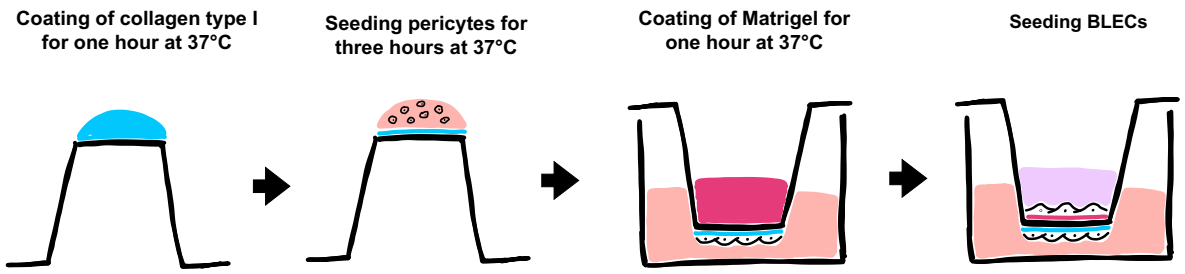

Fig. 40. Co-culturing BLECs and bovine pericytes in close contact. The transwell inserts were initially pre-coated with collagen type I at abluminal side for culturing the bovine pericyes. Next, the luminal side of the same inserts were treated with Matrigel® and cultured with BLECs.

IV. Cell inoculation

Firstly, we dissociated the endothelial cells with Trypsin-EDTA (Dutscher, Cat L0930-100) for eight minutes at 37°C and counted the cells to prepare the inoculum as a proportion of approximately one infectious particle per cell (MOI =1). The in vitro BBB model was infected by inoculating endothelial cells with the inoculum for on e and half hour. To assure the optimal condition of the cell monolayers, we changed the culture medium (without antibiotic) two hours before the experiment.

The cryotubes containing viral stock suspensions were thawed on ice. Each of them had a previous indication of quantity of infectious particles, expressed as: particles/50 μL). Further preparing the inoculum at MOI = 1 in DMEM without FBS and without antibiotics, we rinsed the cells and incubated with it at 37°C for 1h30. The cell monolayers were washed with PBS and incubated with antibiotic-free culture medium at 37°C (**Fig. 41**).

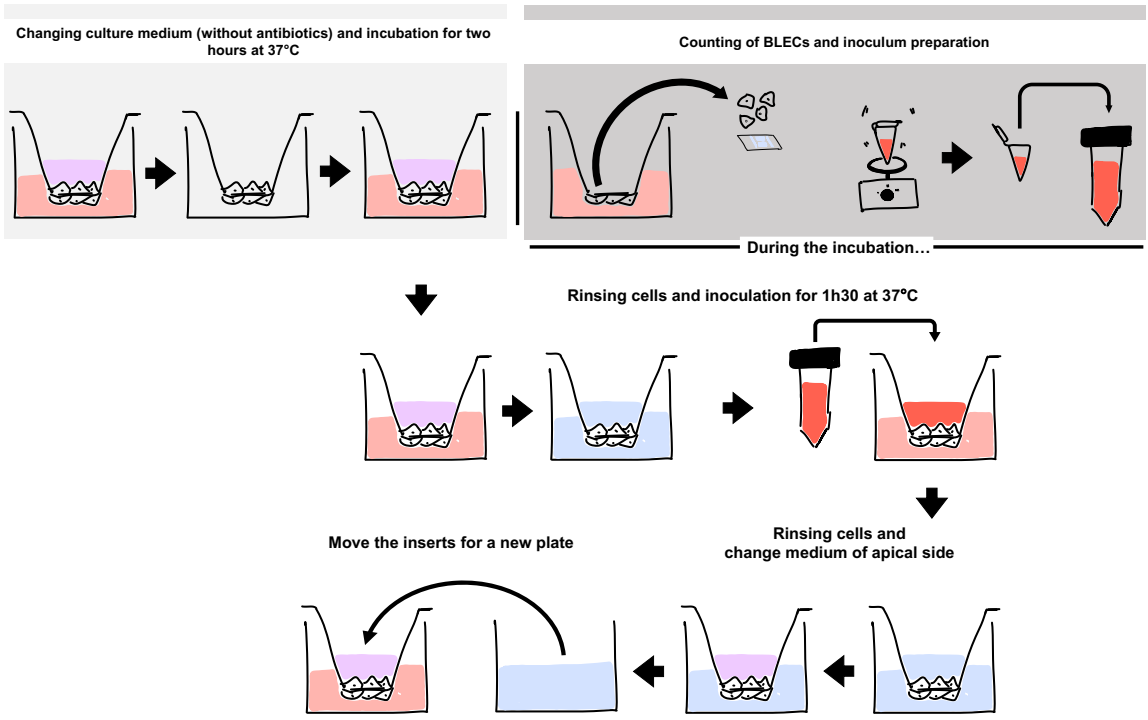

Fig. 41. Infection of the BBB model. The culture medium was changed two hours before starting the inoculation. During this period, the numbering we estimated the number of BLECs for preparing an inoculum of MOI = 1. Further the inoculation of BLECs, we changed the culture medium of luminal compartment and transferred it for a new plate containing fresh medium without antibiotics.

V. Trans-endothelial electrical resistance

The trans-endothelial electrical resistance (TEER) was measured with an EVOM2 epithelial voltammeter (World Precision Instruments, Sarasota, FL). This equipment applies an alternating electrical current across the cell monolayer. The EVOM2 was used with the STX2 chopstick electrode. Each stick of the electrode contains a silver/silver-chloride pellet for measuring voltage and a silver electrode for passing current. The STX2 electrode was used according to the provider's recommendations: cleaning and disinfecting the electrode before positioning it carefully between the cell monolayer. Before the TEER measurement, the EVOM2 was calibrated for 1000 Ω. For TEER measurement, the plate containing inserts was placed on a warming plate (SP SCIENCEWARE, Cat F37015-0000) at 37°C. We measured a firstly a blank (inserts without cells), and then the inserts containing the cell monolayers. For each insert we performed the measurement in triplicate.

Within a circuit composed by an ionic solution, the electrical charge propagates and promotes an organized movement of ions that migrate towards electrical fields of

opposite charges. During the course of electric current, it is possible to have obstacles (called resistors) impairing passage of current and ions. A cell monolayer grown on a semi permeable membrane separating two compartments behaves like resistors in a closed circuit. Each compartment contains ionic solutions (culture medium) and represents different poles of such a circuit. Once ions have an elemental charge, an ionic solution has an electrical potential, which translates into the potential to transport energy through the matter movement. Therefore, according to Ohm's law resistance is the ratio of the potential difference between two circuit poles (expressed in volts) and electric current (expressed in amperes).

$$R = \frac{U}{I}$$

R = Resistance

U = Potential difference

I = Electric current

A discontinuity in the cell monolayer facilitates the ionic movement between the two compartments, so the potential difference between the two poles of the circuit decreases and reflects a resistance weakness. Therefore, a continuous cell monolayer restricts the ionic movement and accentuates the potential difference between the poles, evidencing a greater resistance.

VI. Lucifer Yellow assay

The Lucifer Yellow (LY) assay consist in incubating cell monolayers with a fluorescent compound for performiong a fluorometric-based analysis. LY CH dilithium salt (Merck, Cat L0259-25MG) is a hydrophilic fluorescent dye commonly used to test the barrier efficiency of cell monolayers cultured onto semi-permeable membranes. Cell monolayers retain the LY in the luminal compartment; however, there is minimal passage to the abluminal compartment. It means that tighter monolayers retard the passage of LY, consequently the fluorescence signal detected in the abluminal compartment will be weaker.

The LY compound was diluted in 1 mL water to prepare a stock solution (54.67 mM) and stored at 2°C following provider’s recommendations. All LY assays were performed starting from stock solution.

To perform a LY assay we diluted 10 µL of stock solution in 10 mL Hank's balanced salt solution (HBSS) (Sigma-Aldrich, Cat H8264) supplemented with 1% sodium pyruvate (Sigma-Aldrich, S8636) and 1% HEPES buffer 1M (Dutscher, Cat L0180) pre-heated.

Prior to start the experiment, we prepared a 12-well plate with 1.5 mL HBSS (at 1% sodium pyruvate and 1% HEPES buffer 1M) pre-heated. This plate is used to incubate the inserts treated with LY. Each insert used in the experiment requires three wells with HBSS (at 1% sodium pyruvate and 1% HEPES buffer 1M) pre-heated and one empty well to receive the LY solution from the cell incubation. To test the paracellular permeability, we removed the culture medium of each insert and added 500 µL LY solution. Empty inserts were also used as control. We always worked with a triplicate for each experimental condition.

Before receiving the LY solution, each insert was rapidly transferred to the first well containing HBSS (at 1% sodium pyruvate and 1% HEPES buffer 1M) for an incubation of 20 minutes at 37°C. Every 20 minutes of incubation, the inserts were transferred to the next well. After 60 minutes of incubation, the LY solution from the inserts were transferred to the empty well.

At the end of the incubation step, we prepared a 96-well plate for reading the fluorescence signal. The work volume in this plate was 200 µL. We firstly prepared eight wells with a standard courve with (dilution factor 1/2). We also reserved three wells for the LY solution and three wells for HBSS (at 1% sodium pyruvate and 1% HEPES buffer 1M), our "start'' and our "blank''. Then, we completed this plate with samples of LY incubation every in triplicate. LY fluorescence was measured with a Fluoroskan microplate reader (Thermo Scientific) with an excitation and emission wavelength 428 and 540 nm, respectively.

To calculate the clearance volume, we used a method described by Siflinger-Birnboim et al., 1987. In summary, we divided the amount of LY that crossed the inserts during the incubation time points by its concentration at the beginning of the experiment. To estimate the slope, a linear regression was performed by potting the average cumulative volume cleared versus time. This analysis generated a mean and the standard deviation. In this calculation, we correlate the clearance curve of the area of

empty inserts with the area of the inserts (PSf) with the cell monolayer (PSt). The result of this notation is equivalent to clearance curve of the cell monolayer (PSe), which is expressed in microliters per minute per square centimeters. The PSe value was obtaines as follows:

$$1/PSe = 1/PSt - 1/PSf$$

The endothelial coefficient (Pe) is then calculated by dividing the PSe by the surface area of the insert and the value is expressed in cm per min.

VII. Rhodamine 123 assay

To investigate the functionality of efflux pumps of the BBB model, we washed the BLECs and we added 500 µL of a solution containing 5 mM Rhodamine 123 (Merck, Cat R8004) or a solution containing 5 mM Rhodamine 123 and 0.5 mM Elacridar (Merck, Cat SML0486). The cellular inserts were incubated at 37°C for two hours. Then, we dissociated the cells by using a solution of 650 µL lysis buffer (Ripa) at 4°C for 30 minutes. The lysis buffer was collected from each insert and was subjected to a centrifugation at 14.000 x *g* for 15 minutes. Each supernatant was collected and split into three wells of 96 well plate (200 µL). We measured the luminescence of the supernatants by using an excitation wavelength of 501 nm and emission wavelength of 538 nm.

VIII. Viability assay

We prepared an EC suspension of 100,000 cells/mL. 100 µL of cell the suspension was dispensed in each well of 96 well plate. We cultured the cells until forming a complete monolayer, and then we performed the inoculation with our respective strains, as described above. To check the cell viability, we used the CellTiter-Fluor™ Cell Viability Assay (Promega, Cat G6881) kit. The principle of this assay is to incubate cells with a proteinase K substrate (GF-AFC, Glycyl-phenylalanyl-aminofluorocoumarin). Briefly the viability assay consists in incubating the cells with GF-AFC for 30 minutes at 37°C followed by reading of luminescence by using excitation wavelength of 380-400 nm and emission wavelength of 505 nm.

IX. Sampling of virus-infected BLEC monolayers

The BLEC monolayers were infected at a defined MOI and the infection was followed over three days; the culture medium was not changed during the test period. Four infection time points were analyzed: 6, 24, 48, and 72 hours post-infection (h.p.i). For each time point, three inserts were prepared. The culture medium was collected separately from the luminal and abluminal compartments. All the samples were stored at –20°C for further analyses.

X. Extraction of total nucleic acids

An aliquot of 200 µL of each sample collected in the two compartments at the indicated time points was subjected to total nucleic acids purification. Nucleic acids were extracted using the NucliSens® EasyMAG platform (bioMérieux, Marcy l'Etoile, France) or the Maxwell platform (Promega). The nucleic acids were recovered in a final volume of 50 µL of molecular grade water and stored immediately at –80°C until future applications.

XI. Quantification of the number of enterovirus genome copies

The nucleic acid extracts obtained from the supernatants were tested for the quantitative detection of the EV-A71 genomes by a quantitative real-time RT-PCR. The technique was derived from the one-step real-time RT-qPCR reported earlier (Volle et al., 2012). The forward and reverse primers and the TaqMan probe designed for targeting the EV 5’ UTR were adapted from those described previously. The real-time RT-PCR assay allows an absolute quantification with an external standard. The standard is a recombinant RNA synthesized in vitro from a DNA fragment covering the amplification target, cloned in a plasmid DNA.

A reaction mix containing all enzymes, oligonucleotides, and substrates necessary for one-step reverse transcription, amplification, and detection reactions was prepared with Luna® Probe One-Step RT-qPCR 4X Mix with UDG. In this mix, the primers were set at 20 µM and the probe at 5 µM. Each reaction was performed in a final volume of 20 µL, containing 5 µL of the nucleic acid extract to be analysed.

XII. Viral titration

The limiting dilution method was used to estimate the number of infectious particles in the virus suspensions. A serial dilution (ratio 1/4) of the viral suspensions was performed in eight tubes containing 600 µL of culture medium, then 50 µL from each dilution were transferred to 11 wells in a 96-well plate. Negative control cells (with only culture medium) were included in all titration plates. A RD cell suspension was prepared at 80,000 cells/mL and 150 µL from that placed into each well, and the plates were incubated at 37°C. After seven days, the wells were scored for the presence of lysed cells and the number of infectious particles was calculated using an “in-house algorithm” and expressed as the most probable number of infectious units (MPNCU).

XIII. Confocal analyses

The BLECs were stained and analyzed by indirect immunofluorescence. The inserts were rinsed with PBS twice under manual agitation for two minutes and fixed during 10 minutes with 2% of paraphormaldehyde solution. The cells were rinsed as descried before and permeabilized for 10 min with 0.5 % Triton X (ThermoFisher Scientific, Cat 85111). We rinsed the cells and blocked the cellular epitopes to avoid nonspecific reactions during our staining by incubating the cells for 30 minutes with 5% of goat serum solution (ThermoFisher Scientific, Cat 16210064). Further the blocking step we rinsed the cells and performed a quenching reaction in order to reduce the self-fluorescence of cellular structures and improve the background of the images. The quenching consists in incubation of the cells with a glycine solution (0.1 M) during 15 minutes. Then, we rinsed the cells and incubated with 5% of goat serum solution containing primary antibodies: rabbit anti-ZO-1 (1:400) (Cell Signaling Technology, Danvers, USA, Cat 13663) and mouse anti-dsRNA (1:500) (Sciscons, Szirák, Hungary, Cat 10010200). At the next day, further rinsing the cells we performed an incubation of 40 minutes protected from the light with 5 % of goat serum solution containing the secondary antibodies: goat anti-rabbit AF647Cy5 (1:500) (gently donated by iGReD) and goat anti-mouse Alexa Fluor 488 (1:500) (Thermo Fisher Scientific, Waltham, USA, Cat 11001) and DAPI (for nuclear staining) (STEMCELL technologies, Vancouver, Canada, Cat 75004). At the end of the staining we rinsed the cells carefully for five times. The acquisition of the images was performed by using a confocal microscope Leica (Molecular Devices, California, USA).

XIV. Automatized quantification of immunofluorescence images

We quantified our image set by using the open source platform CellPrifiler® (Broad Institute, Massachusetts, USA). From the confocal acquisition we obtained CZI files. Each image on CZI is a ‘’content’’ composed by grey scale acquisitions obtained from different channels at different focal planes. Therefore, to analyze our image set automatically we elaborated three independent pipelines: i) for extracting the images, ii) for defining the optimal focal plane of each channel, and ii) for perform our analysis (identification and quantification of objects).

We extracted the images referring to each channel by matching the metadata with the stack frame. This allowed obtain from each channel a single image, designated as “Movie/Stack”. Each stack corresponds to synchronization of all focal planes. Next, we set the focal plane of our interest by defining the “Sum” as a selection criterion. This rule sums the intensity of each focal plane of a stack for projecting a single image, as format TIFF. In our third pipeline, we used all our TIFF images for matching the respective channels. From each image we set up rules for delineate the margins of cell nuclei, designated as primary objects. We used modules for expanding the primary objects in three pixels, and them projecting larger objects, designated as secondary objects (used to estimate the perimeter of each cell). The segmentation of dsRNA was also performed (tertiary objects). We them relate the object secondary with the object tertiary to identify: among secondary objects (cell), which of them correlated with the tertiary object (infected cells). The number of cells and infected cells was then achieved from each image during our analysis.

XV. Statistical analysis

The appropriate statistical analysis was applied according to the data set characteristics using the Prism 9 software (GraphPad Software, San Diego,CA, USA). The paired t test was used to compare two groups. For comparisons of three or more groups the one-way ANOVA test was applied. Longitudinal analysis comparing multiple groups, the mean of each time point was bulked and compared among the groups by Kruskal-Wallis analysis.

RESULTS

5) Results

Neurotropic RNA viruses commonly target the human BBB during the invasion of CNS (Miller et al., 2012; Al-Obaidi et al., 2017; and Chen & Li, 2021). Here we used a cellular model based on co-culture of endothelial cells and pericytes to evaluate the interaction between the EV-A71 and the BBB (Stone et al., 2019; Heymans et al., 2020; and Kim et al., 2022).

I. Characterisation of the in vitro BBB model

The close contact co-culture of endothelial cells and pericytes resemble aspects of the human BBB (**Fig. 42**) (Boveri et al., 2005; Colgan et al., 2008; Barar et al., 2010; Wang et al., 2019; and Balzer et al., 2022). We reproduced a cellular model of the BBB, including brain-like endothelial cells (BLECs) and bovine pericytes (Cecchelli et al., 2014; Clé et al., 2020; Curtaz et al., 2020; Versele et al., 2020; and Loiola et al., 2021). The two cell types were co-cultured on the opposite sides of the same membrane of transwell inserts, to maintain a close contact (as described in the section materials and methods) (Kulczar et al., 2017). The restrictive character of the BBB is consolidated due the protein expression of highly specialized proteins that seals the intercellular spaces between adjacent cells (Krause et al., 1991; Cai et al., 2015; and Zeng et al., 2022). The indirect immunofluorescence (IF) staining revealed that BLECs expresses protein F-actin filaments and Zonula occludens 1 (ZO-1). These proteins form the foundations of tight junctional complexes; essential for anchoring of proteins involved in sealing extracellular domains (Watson et al., 1991; Gao & Shivers, 2004; Luo et al., 2006; Liu et al., 2008; Wu et al., 2008; and Helms et al., 2010). The passage of organic molecules electrically charged across the BBB model was measured by applying of electrical charges among the luminal and abluminal compartments (Jurkiewicz et al., 2017 and Meuren et al., 2022).

The difference of electrical potential among the compartments was investigated through transendothelial electrical resistance (TEER). Overall, the BBB model presented TEER values near 40 Ω*cm^2 along 14 days of cell culture. The low permeability of the BBB model to small molecules was evaluated by the lucifer yellow assay (LY) (Zhao et al., 2019). Our analysis showed a low rate of small molecules crossing through the BBB model, represented by a mean of permeability coefficient

near to 0.5 x 10^{-3} cm/min. The monitoring of the permeability coefficient of the BBB model did not present any alteration during 11 and 14 days of cell culture, indicating a considerable stability of the endothelial permeability. The BBB actively expulses exogenous components from the brain thanks to the presence of efflux pumps. We assessed the function of these transporters by providing the labeled substrate Rhodamine 123 (Rho 123) (Ito et al., 2019). After treating the BLECs with an efflux pump inhibitor (Elacridar), we observed a significant intracellular accumulation of Rho 123, showing that the BBB model displays functional P-gp.

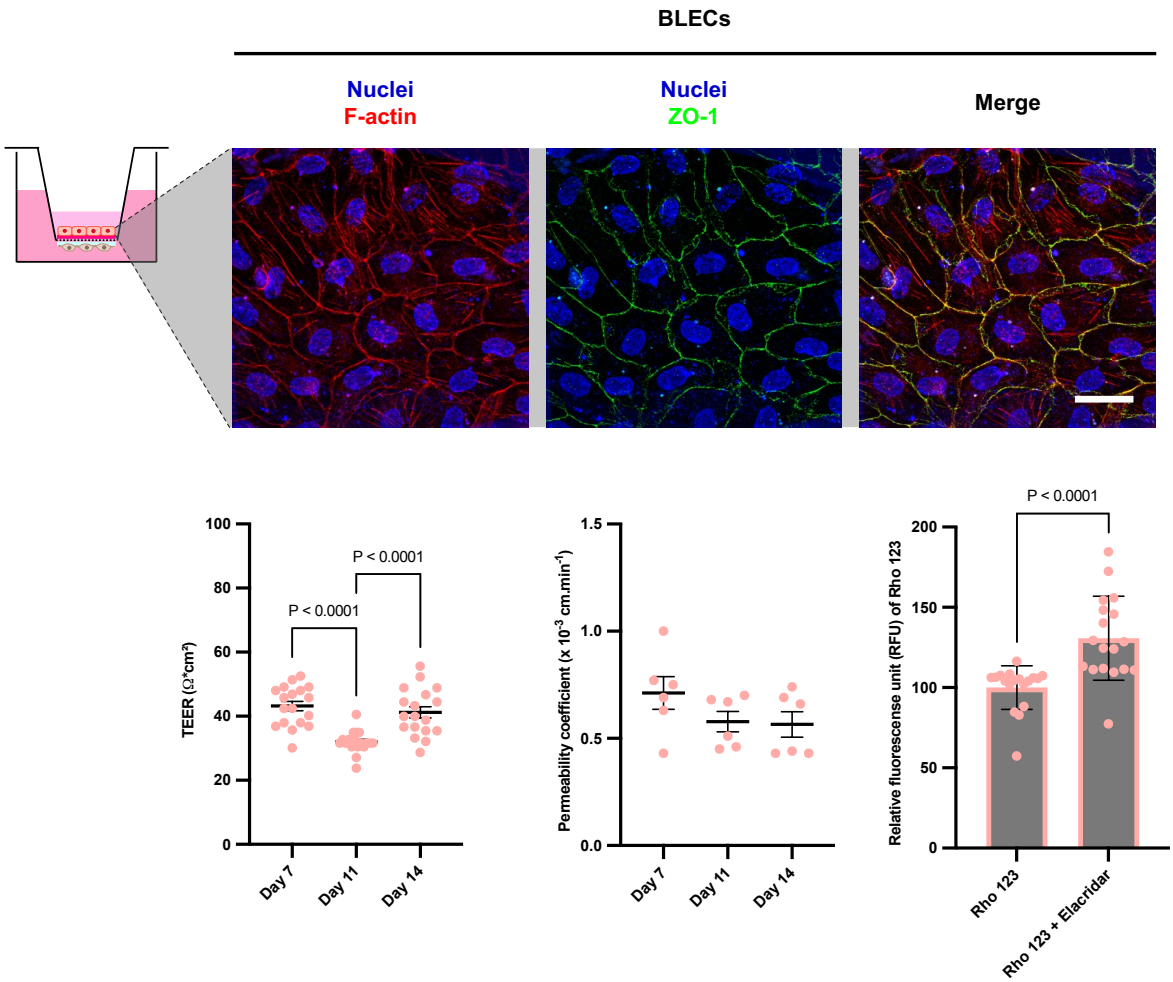

Fig. 42. Close contact co-culture of BLECs and pericytes mimicking aspects of the human BBB. After 14 days of cell culture, BLECs showed protein expression of F-actin filaments and tight junction ZO-1. The monitoring of the BBB at the days 7, 11, and 14 showed low variations of TEER (range from 35 to 40 Ω*cm^2). The incubation of luminal cells with fluorescent dye of small molecular weight displayed at day 11 and 14 a low permeability coefficient (0.5 x 10^{-3} cm/min). The BBB model, when treated with transporter protein inhibitor (elacridar) showed intracellular accumulation of Rho 123 substrate, showing functional efflux pumps. The scale barr represent 100 μm. Comparisons between two groups were analyzed by Paired T-student test, while comparisons three or more groups were analysed by using One-way ANOVA.

II. Infectivity of EV-A71 in endothelial cells

EV-A71 has a limited capacity to infect endothelial cells (Volle et al., 2015). The BLECs were cultured for 11 days, and then were infected with the C1-16 strain by using a MOI = 1. As a positive control, we infected the BLECs with a cytolytic strain of echovirus 6 (E6). After 24 hours of infection, the infected BLECs were imaged, and the open source software CellProfiler® was used to estimate the number of infected cells (**Fig. 43**). The indirect IF staining of dsRNA in BLECs confirmed active viral replication. We observed a reduced cell density in the model infected with the E6 and C4-04 strains. Qualitatively the ratio of cells infected by the C1-06 strain were quite higher than other EV-A71 strains. However, the percentage of cells infected by EV-A71 did not exceed 5 % (**Fig. 44a**).

To check the susceptibility of BLECs to EV-A71, we used these cells cultivated as monolayers on glass slide chambers and tested the protease activity of living cells with the GF-AFC compound. The fluorescence levels of GF-AFC emitted by all infected BLECs was elevated and similar to MOCK condition at 24 hours post infection (h.p.i). The infection with E6 caused a drastic reduction on GF-AFC fluorescence at 48 h.p.i. In contrast, BLECs infected with EV-A71 strains decreased reasonably the GF-AFC fluorescence of living cells at 72 h.p.i (**Fig. 44b**).

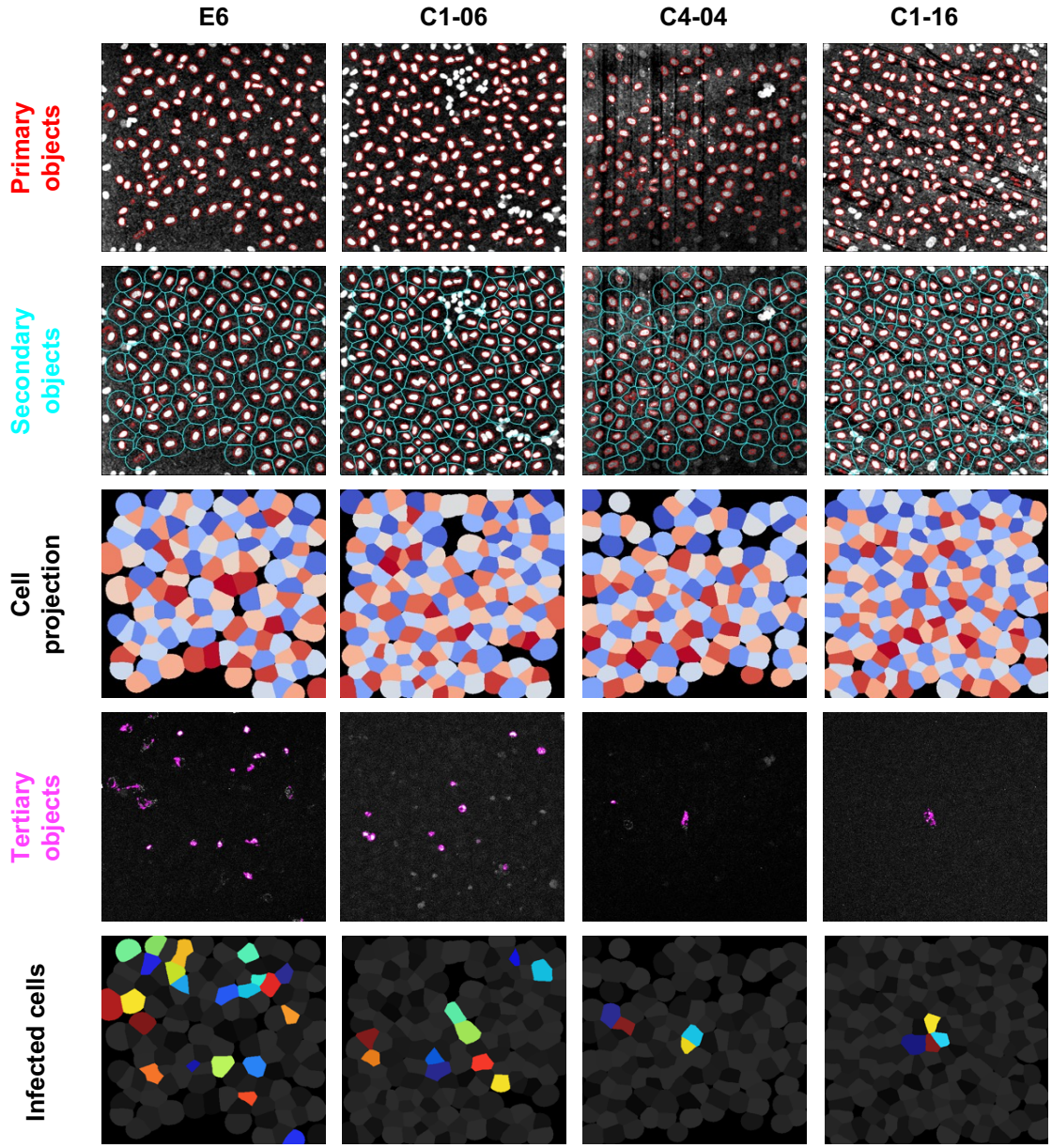
E6
C1-06
C4-04
C1-16
Primary objects
Secondary objects
Cell projection
Tertiary objects
Infected cells

Fig. 43. The number of infected BLECs was estimated from nuclear and dsRNA segmentations. We segmented the nuclei staining (primary objects) of IF image and expanded their limits to secondary objects – used to estimate the number of cells. Tertiary objects also were generated from the segmentation of dsRNA staining. Next, the combination between secondary and tertiary objects evidence cells harbouring dsRNA stain, designated as infected cells.

a)

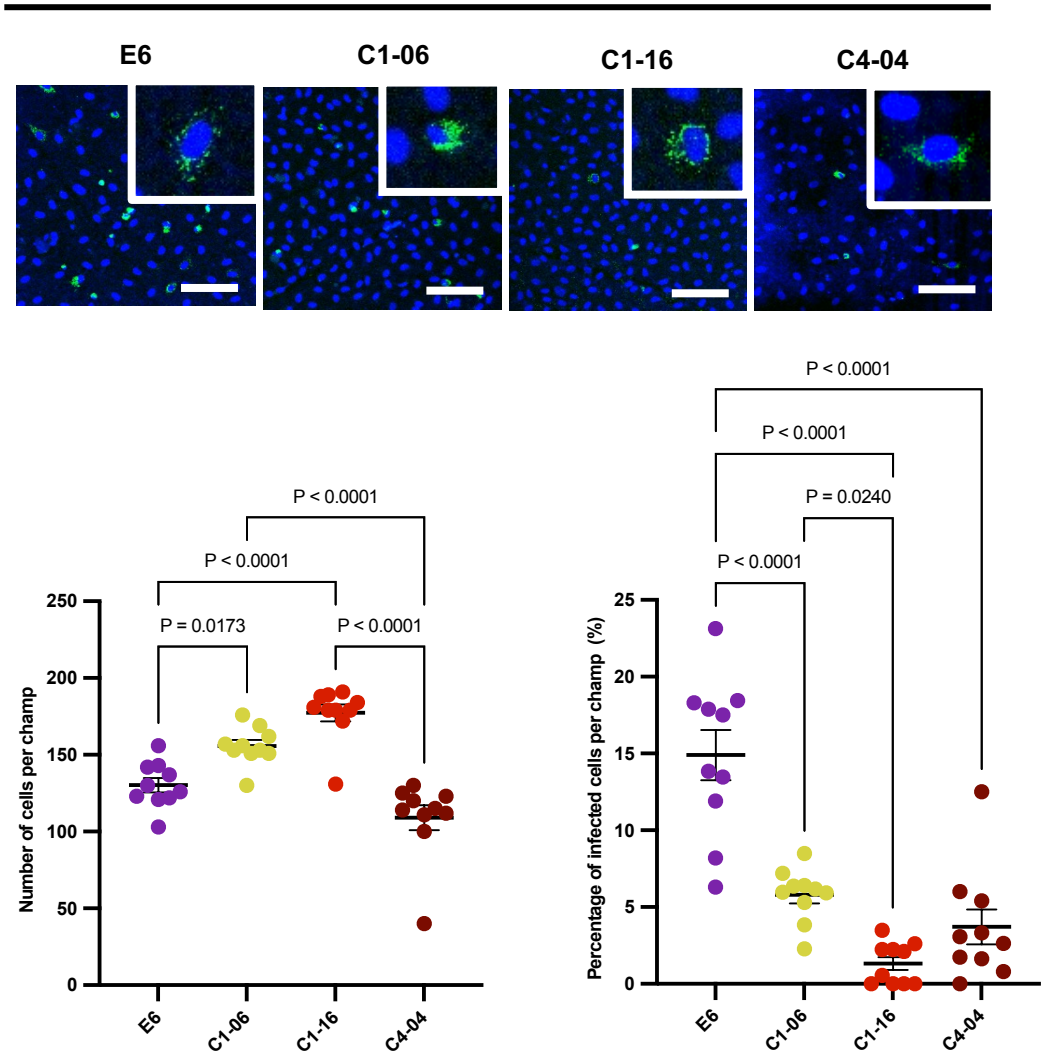
24 h.p.i
E6
C1-06
C1-16
C4-04
Number of cells per champ
P < 0.0001
P < 0.0001
P = 0.0173
P < 0.0001
Percentage of infected cells per champ (%)
P < 0.0001
P < 0.0001
P = 0.0240
P < 0.0001

b)

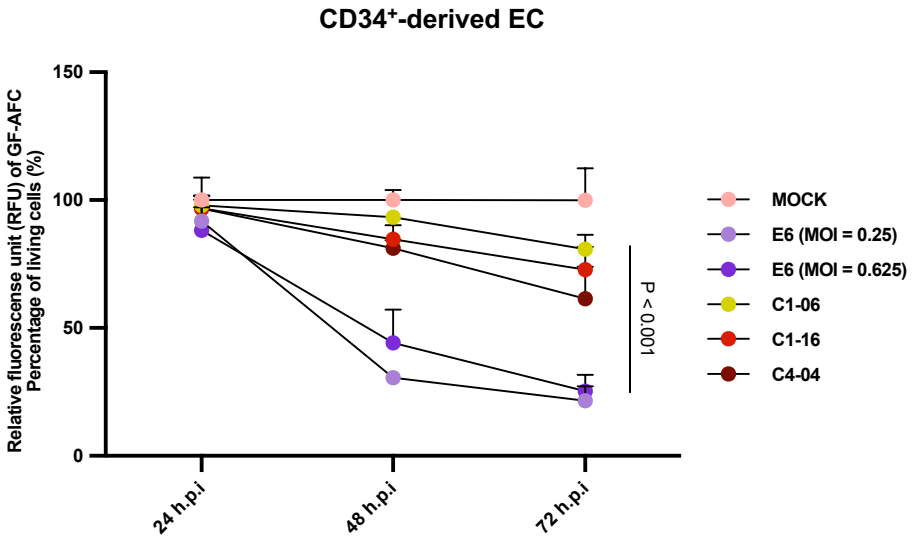
CD34+-derived EC
Relative fluorescense unit (RFU) of GF-AFC
Percentage of living cells (%)
24 h.p.i
48 h.p.i
72 h.p.i
P < 0.001
MOCK
E6 (MOI = 0.25)
E6 (MOI = 0.625)
C1-06
C1-16
C4-04

Fig. 44. EV-A71 presents a limited potential to infect BLECs. At 24 h.p.i, the total number of BLECs from model infected with the E6 and C4-04 strains were significantly lower compared with the models infected with C1-06 and C1-16 strains, but overall, a low number of cells were infected by EV-A71 (below 5%) **(a)**. The scale barr represent 100 μm. Comparisons between two groups were analyzed by One-way ANOVA. A viability assay was performed in the BLECs cultured as monolayer. The BLECs infected with EV-A71 strains displayed high fluorescence of GF-AFC until 48 h.p.i, indicating large number of living cells. At 72 h.p.i the GF-AFC decreased significantly in infected cells compared to MOCK-infected cells **(b)**. The mean values of each experimental group were compared to MOCK and analyzed by Kruskal-Wallis test.

III. Phenotypic evaluation of infected BBB model

EV-A71 does not cause substantial alterations at the BBB. In order to mimic a systemic inflammatory response, we stimulated the BBB model with TNF-α (10 ng/mL) via luminal or abluminal sides during 6 hours followed by infection with the C1-16 (Lu et al., 2020; Voirin et al., 2020; and Versele et al., 2022). The indirect IF staining of BLECs showed a similar pattern of protein expression of ZO-1 between uninfected condition (MOCK) and the E6 infection. However, inserts stimulated with TNF-α presented a visible alteration in protein expression of ZO-1 after 24 hours, mainly those which received TNF-α stimulation at the luminal side (**Fig. 45a**). We observed that TNF-α stimulation causes a slight increase in endothelial permeability of the BBB model that behaves like a wave of 24 hours of action. The stimulation at the abluminal side presents a delay until manifests. Apparently, the infection of the stimulated model with C1-16 strain prolonged the TNF-α effect on Pe of the BBB model. However, the C1-06 infection of the BBB model exclusively, was not sufficient to cause alterations at the endothelial permeability (**Fig. 45b**). A comparative analysis among the EV-A71 strains tested in our experiments showed intact ZO-1 structures of infected BLECs, and Pe values similar to MOCK condition (**Fig. 45c**).

a)

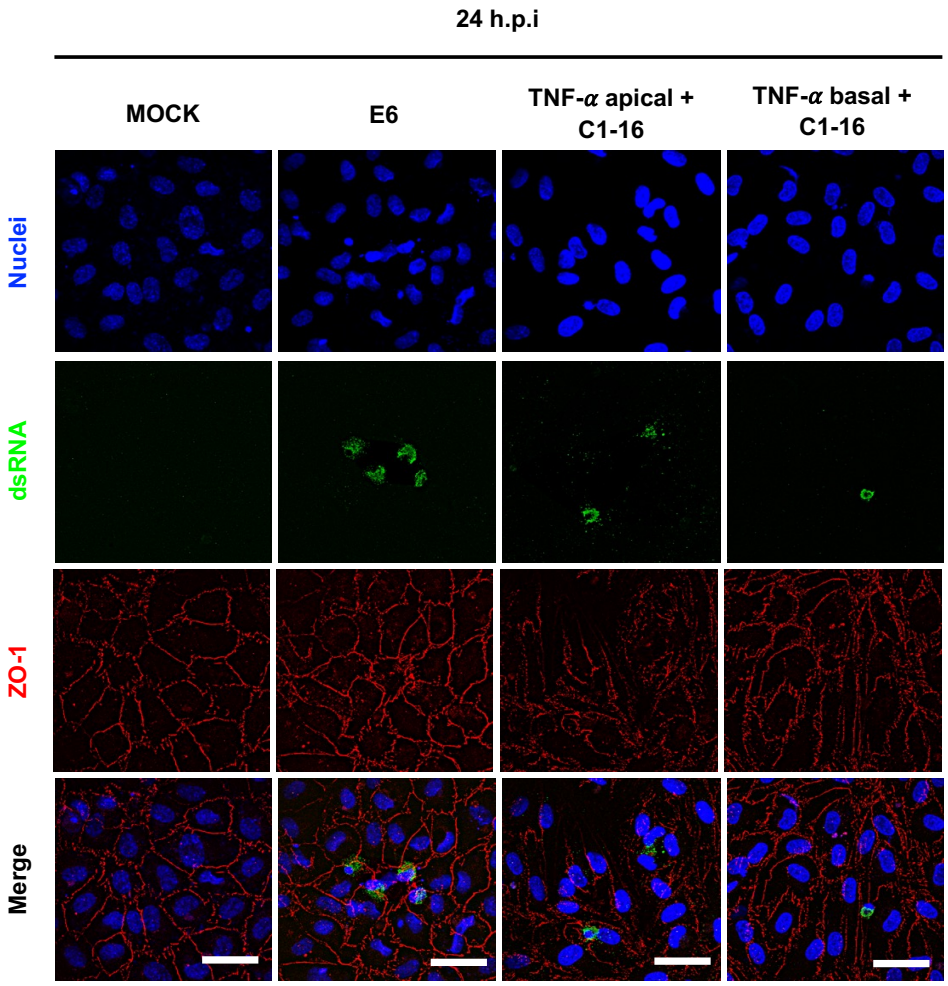
24 h.p.i
MOCK
E6
TNF-α apical + C1-16
TNF-α basal + C1-16
Nuclei
dsRNA
ZO-1
Merge

b)

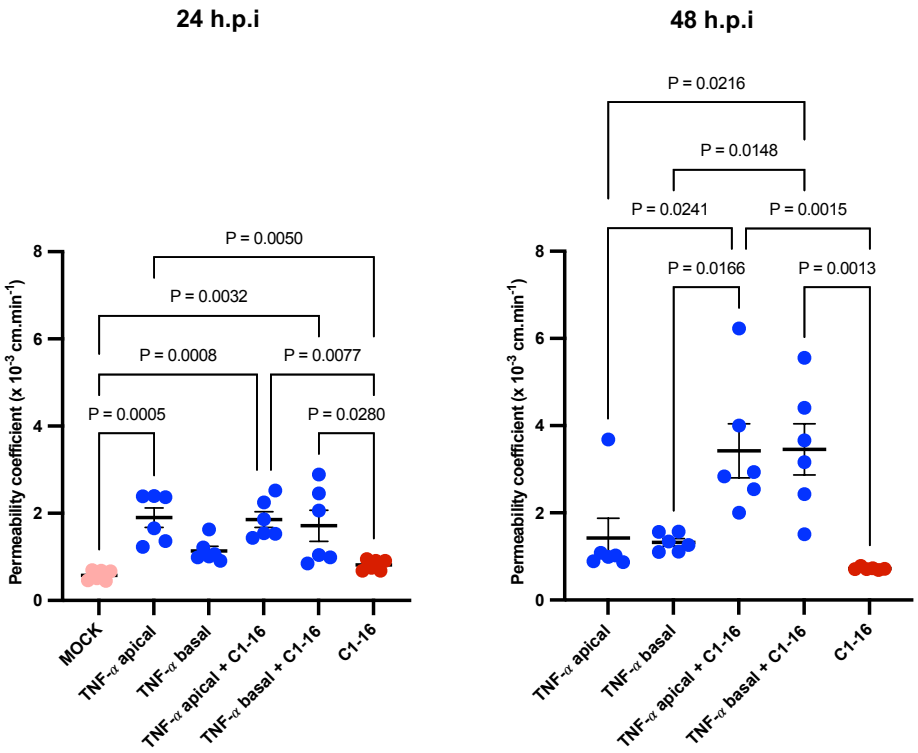
24 h.p.i
48 h.p.i
Permeability coefficient (x 10-3 cm.min-1)
P = 0.0050
P = 0.0032
P = 0.0008
P = 0.0077
P = 0.0005
P = 0.0280
P = 0.0216
P = 0.0148
P = 0.0241
P = 0.0015
P = 0.0166
P = 0.0013
MOCK
TNF-α apical
TNF-α basal
TNF-α apical + C1-16
TNF-α basal + C1-16
C1-16

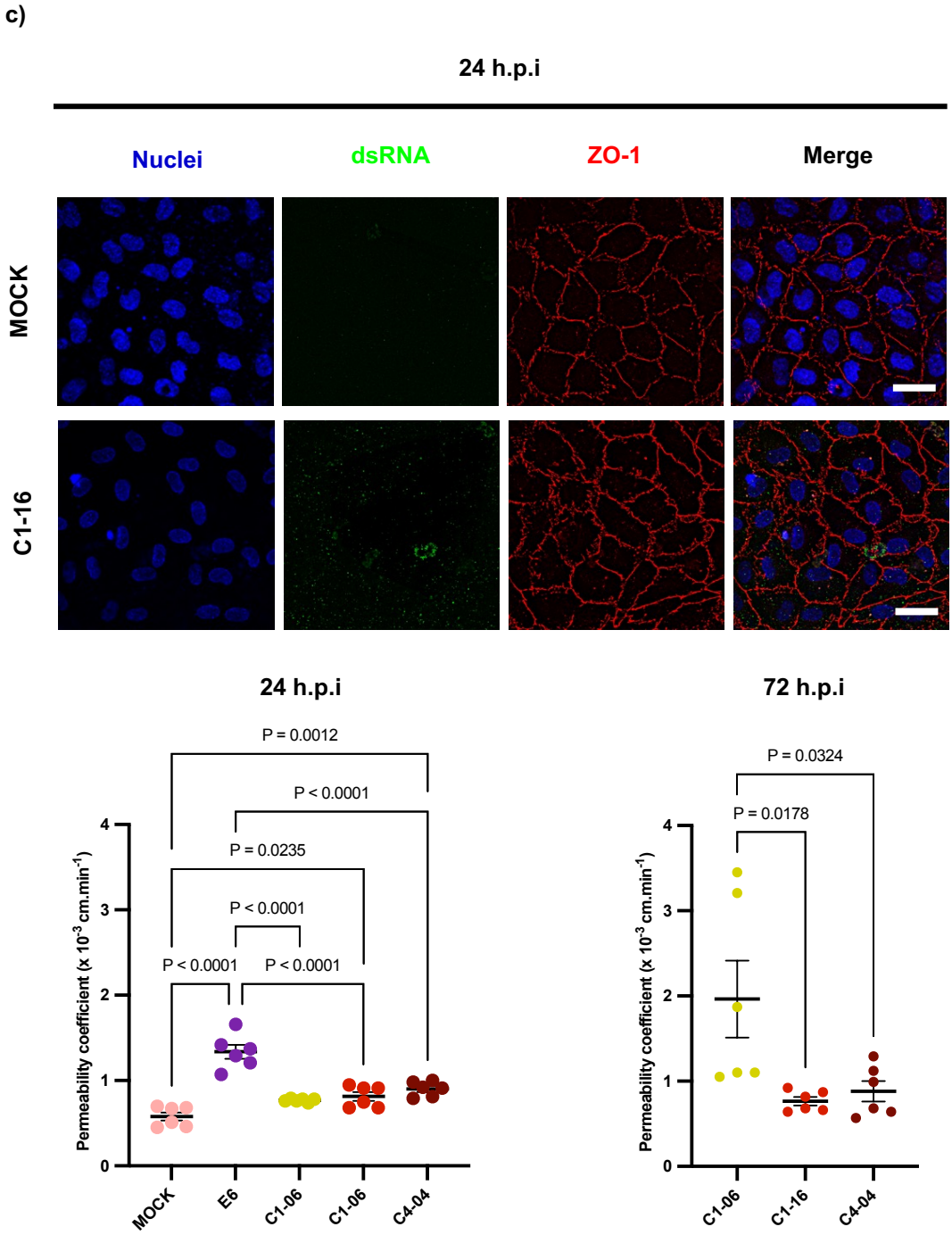

Fig. 45. EV-A71 does not disrupt the in vitro BBB model. The BBB model was treated with TNF-α via luminal or abluminal sides followed by infection with the C1-06 strain. The indirect IF staining of BLECs showed a disruption of protein expression of ZO-1 at 24 h.p.i **(a)**. This effect was accompanied by a slight increase in the endothelial permeability caused by TNF-α stimulation **(b)**. The EV-A71 strains were not capable to produce any expressive alteration on the BBB phenotype **(c)**. The scale barr represent 100 μm. Comparisons among three or more groups were analyzed by One-way ANOVA.

IV. Measurement of the viral replication

The BBB model infected with EV-A71 releases infectious particles rather at the luminal side. The titration assays were performed to evaluate the infectious virus produced by ECs with human rhabdomyosarcoma cells susceptible to EV-A71 infection. The analysis of serial dilutions estimates the virus yields, expressed as most probable number of cytopathogenic units (MPNCU). The titrations of luminal supernatants at 6 h.p.i evidenced low amounts of infectious particles: the MPNCU estimation were near the limit of detection (values below 500 MPNCU). The TNF-α stimulation did not cause any effect on the release of EV-A71 infectious particles in the luminal supernatant during the course of 48 h.p.i. The MPNCU estimation in luminal supernatants of the model infected with EV-A71 strains showed an expressive increasement on infectious particles releasing between 24 h.p.i. and 72 h.p.i (**Fig. 46).** The cell supernatants from abluminal compartment were capable to induce cytopathogenic in a number of units below the limit of detection of titration. Therefore, the viral yield at abluminal supernatant was detected, but not quantifiable (data not shown).

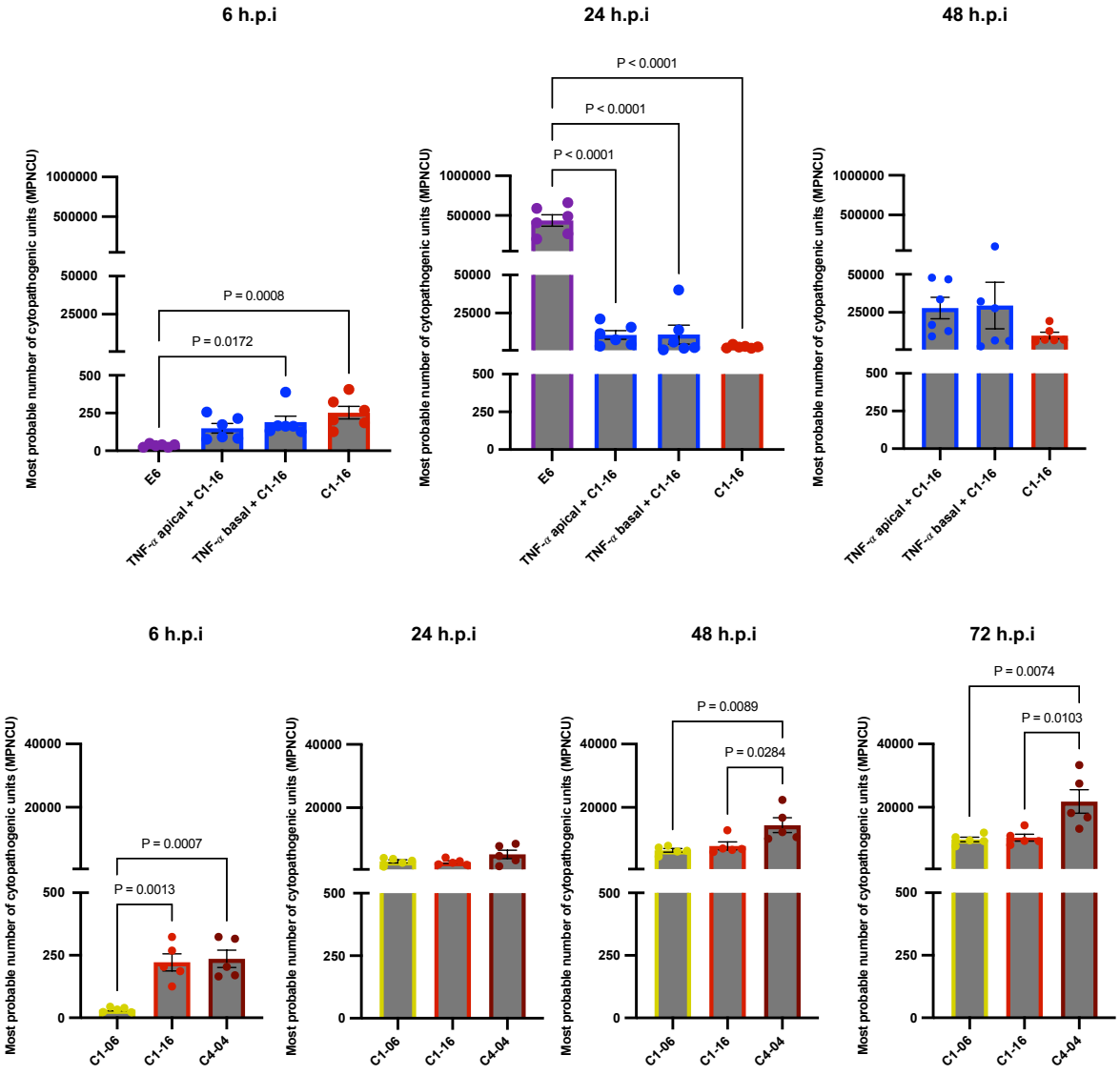

Fig. 46. The infected BBB model releases infectious virus particles into the luminal compartment. Titration analysis from luminal supernatants showed that under TNF-α effect the release of infectious virus particles was not affected, and had an expressive increasement starting from 24 h.p.i, regardless of the EV-A71 strain. Comparisons among three or more groups were analyzed by One-way ANOVA.

The infected BBB model releases EV-A71 genomes at both the luminal and abluminal sides (**Fig. 47**). The BLECs of the BBB model were maintained in a commercial culture medium, which carry a supplementation containing growth factors, and hormones. To investigate if these factors compete with EV-A71 for receptors, we evaluated the performance of the BBB model culturing the BLECs with or without supplementation. Any difference at the endothelial permeability of the BBB model was observed. After collecting cell supernatants of the infected BBB model, we detected the viral genome

by using a RT-qPCR assay. The availability of viral genome particles in the cell supernatants limits the time in which the amplification reaction occurs, expressed by cycles of quantification (CQ). The RT-qPCR analysis showed that availability of viral genome at luminal supernatant limited the amplification reaction to a mean of 20 CQ. In contrast, for the analysis of abluminal supernatants, in which the lower availability of viral genome allowed the extension of amplification reaction until approximately 30 CQ. Both culture conditions: with or without supplementation; showed this same amplification pattern regarding the detection of viral genome at luminal and abluminal supernatants (**Fig. 47a**). The cell supernatants did not evidenced differences related to releasing of viral genome from the BBB model infected with C1-16 strain, independently of presence or absence of TNF-α stimulation (**Fig. 47b**). The comparison of cell supernatants also revealed that the pattern viral genome releasing from the infected BBB model is similar among EV-A71 strains (**Fig. 47c**).

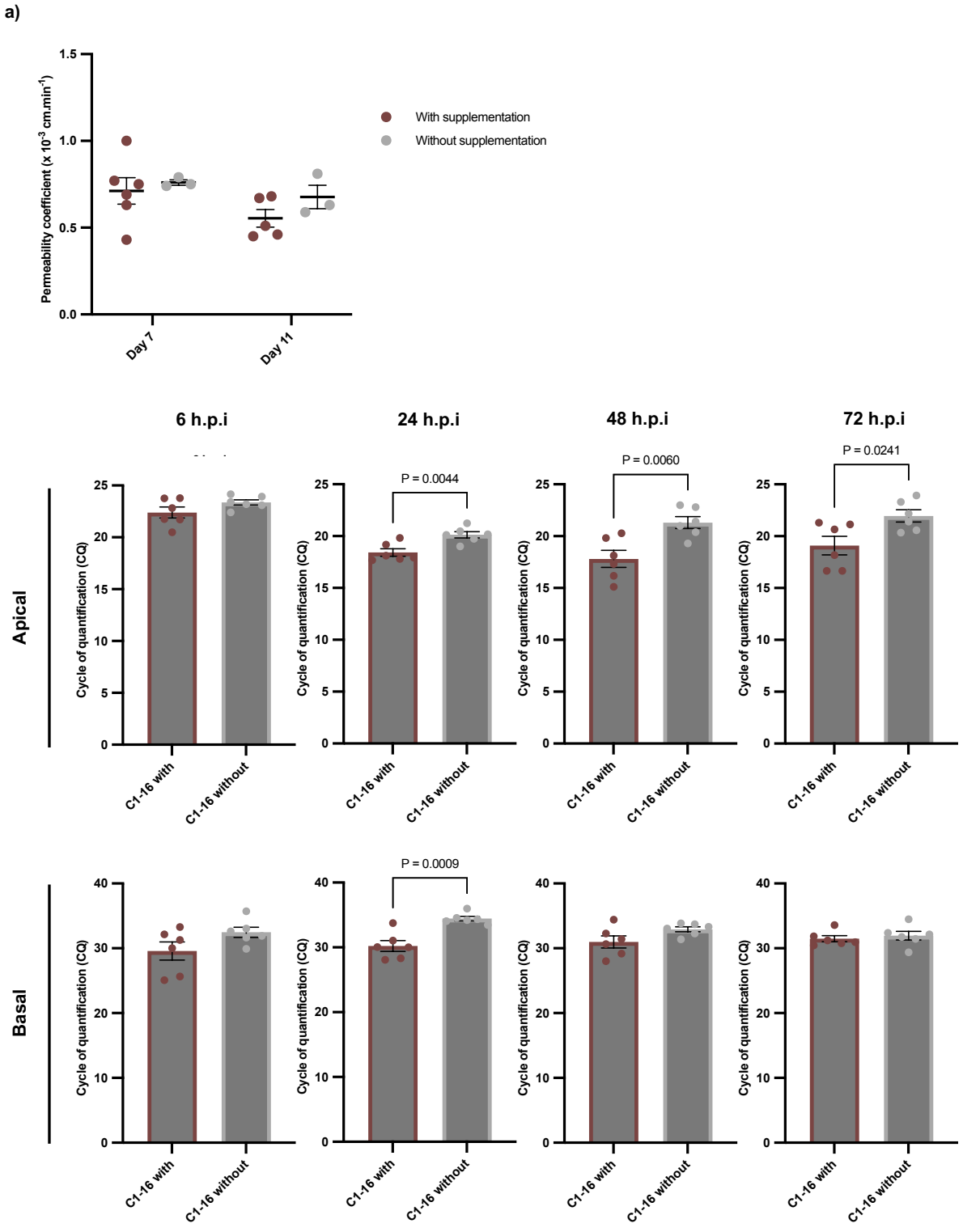
a)
Permeability coefficient (x 10-3 cm.min-1)
1.5
1.0
0.5
0.0
Day 7
Day 11
With supplementation
Without supplementation
6 h.p.i
24 h.p.i
48 h.p.i
72 h.p.i
Apical
Basal
Cycle of quantification (CQ)
P = 0.0044
P = 0.0060
P = 0.0241
P = 0.0009
C1-16 with
C1-16 without

b)

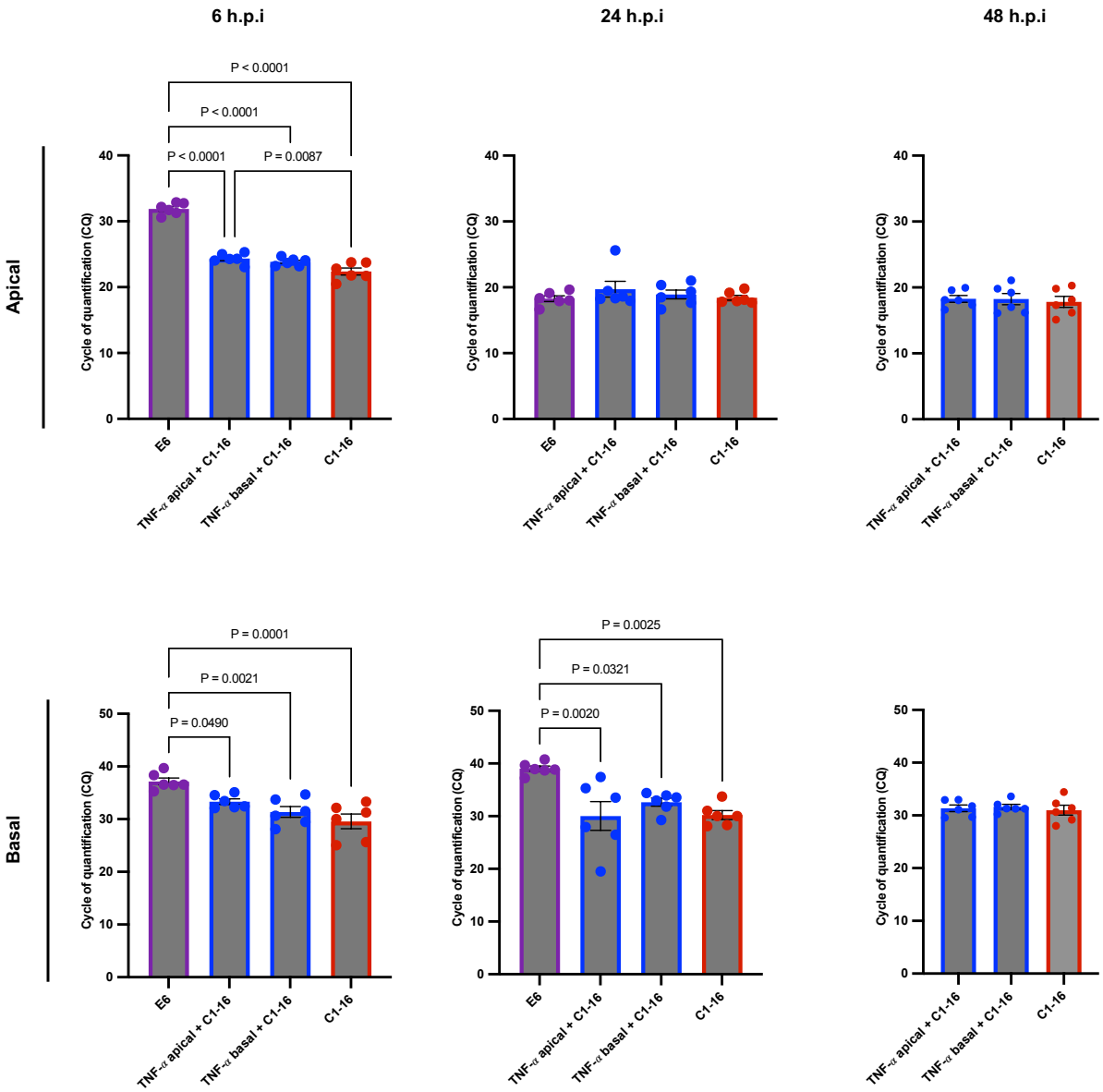
6 h.p.i
24 h.p.i
48 h.p.i
Apical
Basal
Cycle of quantification (CQ)
P < 0.0001
P < 0.0001
P < 0.0001
P = 0.0087
P = 0.0001
P = 0.0021
P = 0.0490
P = 0.0025
P = 0.0321
P = 0.0020
E6
TNF-α apical + C1-16
TNF-α basal + C1-16
C1-16

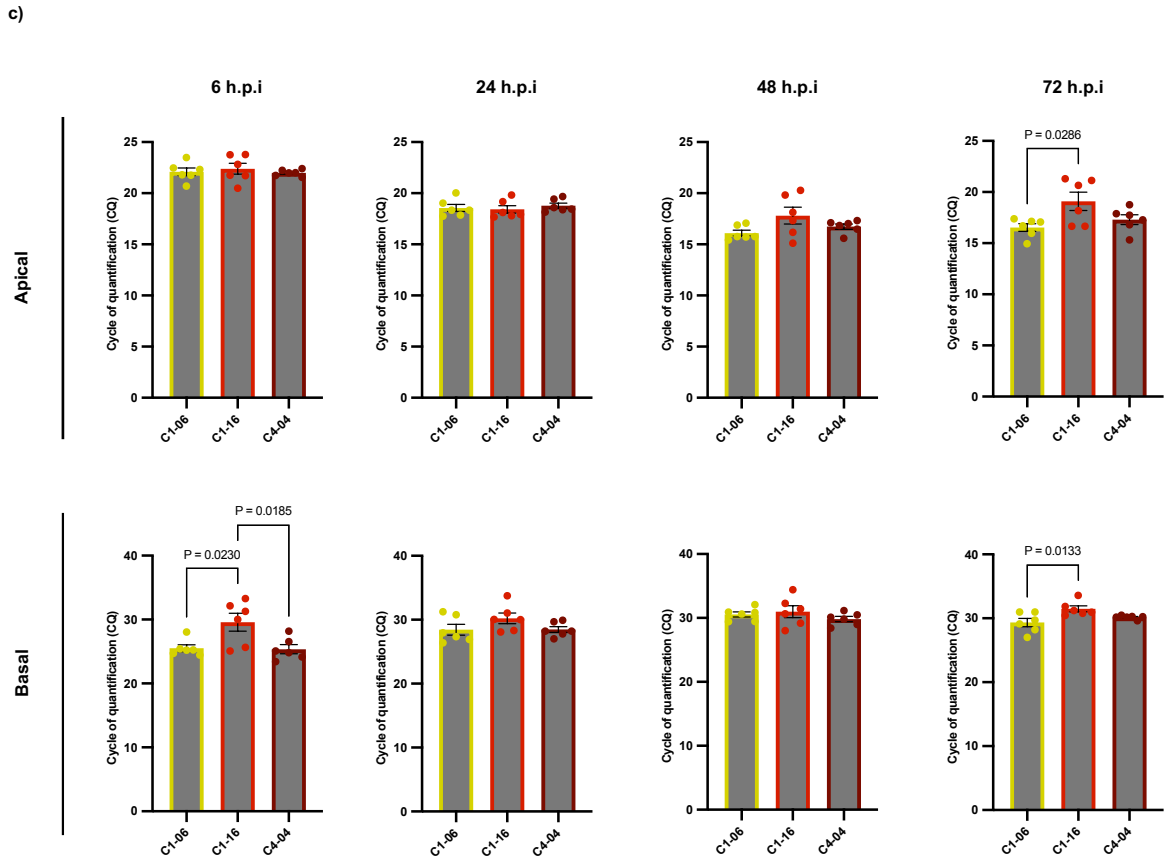

Fig. 47. The BBB model infected with EV-A71 releases viral genome at both luminal and abluminal sides. The supplementation of culture medium was essayed to verify if growth factors competes with EV-A71 for receptors. No significant alteration was observed in the endothelial permeability of the BBB model. Independent of supplementation, the viral genome was detected in both luminal and abluminal supernatants at similar levels **(a)**. The TNF-α stimulation also did not affect the release of viral genomes from the infected BBB model **(b)**. The viral genome releasing occurred in a similar pattern for all EV-A71 analysed **(c).** The scale bar represents 100 μm. Comparisons of three or more groups were analysed by One-way ANOVA.

DISCUSSION

6) Discussion

This study used an in vitro BBB model for studying the pathogenicity of EV-A71. Despite EV-A71 does not alter the expression of ZO-1 protein neither increases the endothelial permeability, the infection of in vitro BBB model lead to the release of viral particles in both luminal and abluminal compartments. Concerning the release of virions, we noticed that infectious particles were mainly released in the luminal compartment. Titration analyses showed an exponential increase of virions in the luminal compartment between 6 and 24 h.p.i followed by a stationary phase. We detected infectious virus in the abluminal compartment as well but the amounts were not quantifiable. The cell supernatants also revealed that the infected BBB model releases viral RNAs in both luminal and abluminal compartments. The release of EV-A71 genome in the luminal compartment entered in the stationary phase at 48 h.p.i; a *plateau* is also observed in the abluminal compartment since 6 h.p.i (**Fig. 48**).

We highlight that the limitations on our study design must be taken in consideration before interpreting the data obtained. Here we adopted only ZO-1 as BBB marker. This protein forms molecular complexes at the intracellular domains of endothelial cells. Tight junction proteins, such as claudin-5 and occludin, anchor to ZO-1 to seal paracellular spaces. We can not affirm what is the effect of EV-A71 directly on tight junction proteins. In our experiments we infected BLEC by using a unique MOI (MOI = 1). This scenario reproduces a viremia with a low viral load of circulating virus in the blood flow, however, the lack of experiments at higher MOIs prevent us from reproducing a scenario of higher viral loads. Moreover, our study does not assess cell receptors that are used by EV-A71 in the present BBB model.

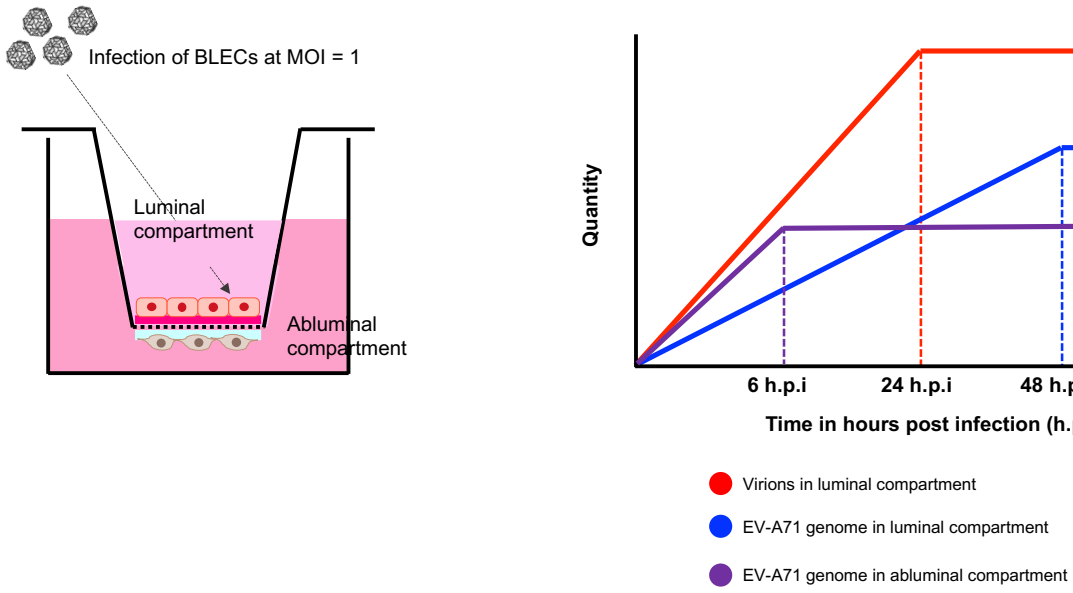

Fig. 48. Schematic representation of the release of viral particles from infected BBB model. The BLECs were infected at MOI = 1 and the releasing of viral particles in both luminal and abluminal compartments was monitored during a course of 72 h.p.i. The releasing of virions in luminal compartment increased exponentially until 24 h.p.i, followed by a stationary phase. The levels of virions released in abluminal compartment were below the limit of detection of titration. A similar standard was observed for the releasing of particles of viral genome. The releasing of EV-A71 genome in luminal compartment entered in a stationary phase at 48 h.p.i. This *plateau* was observed at 6 h.p.i in the abluminal compartment.

The invasion on the CNS is the most critical scenario of severe EV-A71 infections. The main route to access the CNS occurs through retrograde axonal transport due the cellular tropism of EV-A71 for neural cells (Chen et al., 2007; Tan et al., 2014; and Li et al., 2019). EV-A71 also can infect leukocytes, which could carry the virus to the CNS, but this mechanism happens in response to pro-inflammatory stimulus; probably when the brain infection is already established (Nishimura et al., 2013). Therefore, the chance of infected leukocytes to promote a primary brain infection is low. To evaluate the participation of the BBB in the neuropathogenesis of EV-A71, our work focused on direct interaction between EV-A71 and the human BBB.

Our experiments show that EV-A71 infects a limited number of endothelial cells and does not affect the BBB phenotype. EV-A71 infections are capable to induce non-lytic replicative cycles and propagate among cells inside extracellular vesicles (Lee et al., 2014; Mao et al., 2016; Gu et al., 2020; Gu et al., 2020; Lin & Huang, 2020; and Wang

et al., 2020). Experimental conditions near to our study design revealed that EV-A71 can cross the BBB model inside infected extracellular vesicles, and these vesicles are capable to infect astrocytes (J. Gu et al., 2022). Previous transcriptomic analysis of human umbilical vein endothelial cells infected with EV-A71 revealed a differential expression of micro-RNA molecules (miRNA) associated with the regulation of BBB functions (Song et al., 2017 and Song et al., 2019). Among these molecules, miR-126, miR-204-5p, and miR-619-5p distinguishes for participating of extracellular vesicles biogenesis (Schneider et al., 2018; Tapia-Castillo et al., 2019; Kim et al., 2020; Sabo et al., 2020; Yao et al., 2020; Hu et al., 2021; Matsuzaki et al., 2021; Bordin et al., 2022; Ma et al., 2022; Wu et al., 2022; and Xu et al., 2022).

We demonstrated that the in vitro BBB model infected with EV-A71 releases viral RNA genome through both luminal and abluminal cell supernatants. The delivery of viral RNA has been considered as a mechanism of induction of innate immune responses (Kesimer et al., 2009; Schwab et al., 2015; Kouwaki et al., 2016; and Kouwaki et al., 2017). Hence, could the EV-A71 genome induce responses on resident cells of brain parenchyma? We suggest that the traffic of the EV-A71 genome across the BBB may be a possible signaling from the BBB to brain parenchyma, which is related with the neuroinflammation caused by severe EV-A71.

Exogenous extracellular RNA molecules are recognized by Toll Like Receptors (TLRs) expressed by astrocytes and microglia (Scumpia et al., 2005; Yoshida et al., 2007; Kim et al., 2008; Lee et al., 2009; Lehmann et al., 2012; Scumpia et al., 2014). The activation of multiple TLRs contributes to neuroinflammatory processes caused by viral infections (Olson & Miller, 2004; Lee et al., 2007; Lewis et al., 2008; Nazmi et al., 2014; and Dembny et al., 2020). Severe infections caused by EV-A71 are characterized by neuroinflammatory responses, and the low indices of viral antigens into the CNS. These findings suggest the efficiency of neuroinflammation in promoting the viral clearance (P. Yu et al., 2015). However, for reasons still unknown some patients loose fine tune regulation of neuroinflammatory process and develop neurological complications.

Here we suggest that the BBB resist to EV-A71 infections and the viral RNA genome released in the abluminal supernatant may be an evidence of a communication system between the BBB and the brain parenchyma (Martins et al., 2016; Bhowmick et al.,

2019; Yao et al., 2020; and Kriaučiūnaitė et al., 2021). We refuse the hypothesis of that EV-A71 crosses directly the human BBB. However, the interaction between EV-A71 and the BBB may result in a releasing of viral RNA genome into the brain parenchyma. We argue that the viral genome released from the BBB might not be sufficient for triggering a severe neuroinflammation by itself, but it could eventually contribute for enhancing a previously established neuroinflammatory responses. Our interest is to investigate whether implication the viral RNA genome of EV-A71 on the brain parenchyma.

CONCLUSIONS & PERSPECTIVES

7) Conclusions & Perspectives

The development of neurological complications associated with the EV-A71 infections is a multifactorial phenomenon that can be related to innate characteristics, or even strain-dependent factors. In this work, I investigated the role of the BBB in EV-A71 pathogenesis. The BBB functions are essential for maintaining the brain homeostasis. In a context of a neuroinflammatory disease, the BBB mediates the infiltration of inflammatory cells on the brain parenchyma, which contributes for neurodegeneration. I evaluated the interaction of EV-A71 with a cellular model physiologically relevant that resembles key aspects of the human BBB. The study mimics a viremia context, when free virions are circulating within the blood flow. This allowed to investigate if EV-A71 can directly induce some alterations in the human BBB. In the experiments, EV-A71 did not affect significantly this barrier, neither was capable cross the in vitro BBB in large amounts. Curiously, there is a passage of viral RNA genomes across the in vitro BBB. Here, I conclude that EV-A71 within the blood flow does not present a high risk of disrupting the human BBB or crossing it. However, during a context of viremia associated with EV-A71 infections, viral RNA genomes may be released from the BBB into the brain parenchyma.

Neuroinflammation is also associated with the neurological damages caused by severe EV-A71 infections. Most of the information relating to the effects of these infections on the brain come from investigations of post mortem infection cases. However, little is known about how the brain effectively reacts to acute phase of neuroinfections caused by EV-A71. Despite the low ability of EV-A71 to affect or cross the human BBB, the viral RNA genome may be released into the baso-lateral side of the endothelial cells. In vivo, resident cells into the brain parenchyma, such as astrocytes and microglial cells that actively responds to stimulus, therefore, there is a need to understand if this phenomenon could participate in EV-A71 neuropathogenesis.

In the appendix VII (pages 199 – 221), I propose a project that aims to understand cellular and molecular mechanisms existing between the human BBB and the brain parenchyma during EV-A71 neuropathogenesis. In this project, I suggest to characterize how the BBB may release viral RNA genome from the baso-lateral side of endothelial cells, and evaluate if this phenomenon may induce an immune response in the brain parenchyma. To elevate my study to superior levels of physiological

complexity, the key challenge is to integrate the current in vitro BBB model with cerebral organoids.

The project is structured in two axes. Axis 1 aims to evaluate the effect of EV-A71 in the human brain. To investigate the neuropathogenesis of EV-A71, I propose to deliver a study platform with high level of physiological similarity with the human brain: “microglia-enriched cerebral organoids’’. During the human development, hematopoietic progenitors migrate to different sites of the embryo, including the brain. we hypothesize that the transplantation of hematopoietic progenitors into cerebral organoids may enhance the population of microglia and improve the neural development in vitro. The microglia-enriched cerebral organoids could be infected with various EV-A71 strains to trace a parallel with the brain infection. Axis 2 aims to investigate the communication between the BBB and the brain parenchyma during EV-A71 infections. We hypothesize that the BBB release viral RNA genome into the brain parenchyma, and this may induce the production of immune mediators. Thus, we propose to merge the current in vitro BBB model with microglia-enriched cerebral organoids. This will enable investigation of the release of viral RNA genomes inside extracellular vesicles. We also propose to block signaling mechanisms associated to this phenomenon. Moreover, placing inserts of the in vitro BBB under microglia-enriched cerebral organoids will allow to evaluate the impacts of brain infection on the BBB. Such investigations have potential to aid us to better understand the neural damages caused by EV-A71.

REFERENCES

8) References

1. Abbott, N. J., Dolman, D. E. M., Drndarski, S., & Fredriksson, S. M. (2012). An improved in vitro blood-brain barrier model: Rat brain endothelial cells co-cultured with astrocytes. *Methods in Molecular Biology (Clifton, N.J.)*, *814*, 415–430. https://doi.org/10.1007/978-1-61779-452-0_28

2. Abdul Wahid, N. A., Suhaila, J., & Rahman, H. A. (2021). Effect of climate factors on the incidence of hand, foot, and mouth disease in Malaysia: A generalized additive mixed model. *Infectious Disease Modelling*, *6*, 997–1008. https://doi.org/10.1016/j.idm.2021.08.003

3. Abdullahi, W., Davis, T. P., & Ronaldson, P. T. (2017). Functional Expression of P-glycoprotein and Organic Anion Transporting Polypeptides at the Blood-Brain Barrier: Understanding Transport Mechanisms for Improved CNS Drug Delivery? *The AAPS Journal*, *19*(4), 931–939. https://doi.org/10.1208/s12248-017-0081-9

4. Ahishali, B., & Kaya, M. (2021). Evaluation of Blood-Brain Barrier Integrity Using Vascular Permeability Markers: Evans Blue, Sodium Fluorescein, Albumin-Alexa Fluor Conjugates, and Horseradish Peroxidase. *Methods in Molecular Biology (Clifton, N.J.)*, *2367*, 87–103. https://doi.org/10.1007/7651_2020_316

5. Ahmed, S., Bu, W., Lee, R. T. C., Maurer-Stroh, S., & Goh, W. I. (2010). F-BAR domain proteins: Families and function. *Communicative & Integrative Biology*, *3*(2), 116–121. https://doi.org/10.4161/cib.3.2.10808

6. Al-Obaidi, M. M. J., Bahadoran, A., Har, L. S., Mui, W. S., Rajarajeswaran, J., Zandi, K., Manikam, R., & Sekaran, S. D. (2017). Japanese encephalitis virus disrupts blood-brain barrier and modulates apoptosis proteins in THBMEC cells. *Virus Research*, *233*, 17–28. https://doi.org/10.1016/j.virusres.2017.02.012

7. Alsaffar, H., Martino, N., Garrett, J. P., & Adam, A. P. (2018). Interleukin-6 promotes a sustained loss of endothelial barrier function via Janus kinase-mediated STAT3 phosphorylation and de novo protein synthesis. *American Journal of Physiology. Cell Physiology*, *314*(5), C589–C602. https://doi.org/10.1152/ajpcell.00235.2017

8. Andrews, R. N., Caudell, D. L., Metheny-Barlow, L. J., Peiffer, A. M., Tooze, J. A., Bourland, J. D., Hampson, R. E., Deadwyler, S. A., & Cline, J. M. (2018). Fibronectin Produced by Cerebral Endothelial and Vascular Smooth Muscle Cells Contributes to Perivascular Extracellular Matrix in Late-Delayed Radiation-Induced Brain Injury. *Radiation Research*, *190*(4), 361–373. https://doi.org/10.1667/RR14961.1

9. Ang, L. Y. E., Too, H. K. I., Tan, E. L., Chow, T.-K. V., Shek, L. P.-C., Tham, E. H., & Alonso, S. (2016). Antiviral activity of Lactobacillus reuteri Protectis against Coxsackievirus A and Enterovirus 71 infection in human skeletal muscle and colon cell lines. *Virology Journal*, *13*, 111. https://doi.org/10.1186/s12985-016-0567-6

10. Ang, P. Y., Chong, C. W. H., & Alonso, S. (2021a). Viral determinants that drive Enterovirus-A71 fitness and virulence. *Emerging Microbes & Infections*, *10*(1), 713–724. https://doi.org/10.1080/22221751.2021.1906754

11. Ang, P. Y., Chong, C. W. H., & Alonso, S. (2021b). Viral determinants that drive Enterovirus-A71 fitness and virulence. *Emerging Microbes & Infections*, *10*(1), 713–724. https://doi.org/10.1080/22221751.2021.1906754

12. Ansardi, D. C., & Morrow, C. D. (1993). Poliovirus capsid proteins derived from P1 precursors with glutamine-valine cleavage sites have defects in assembly and RNA encapsidation. *Journal of Virology*, *67*(12), 7284–7297. https://doi.org/10.1128/JVI.67.12.7284-7297.1993

13. Aoki, H., Yamashita, M., Hashita, T., Iwao, T., & Matsunaga, T. (2020). Laminin 221 fragment is suitable for the differentiation of human induced pluripotent stem cells into brain microvascular endothelial-like cells with robust barrier integrity. *Fluids and Barriers of the CNS*, *17*(1), 25. https://doi.org/10.1186/s12987-020-00186-4

14. Apostol, L. N., Shimizu, H., Suzuki, A., Umami, R. N., Jiao, M. M. A., Tandoc, A., Saito, M., Lupisan, S., & Oshitani, H. (2019). Molecular characterization of enterovirus-A71 in children with acute flaccid paralysis in the Philippines. *BMC Infectious Diseases*, *19*(1), 370. https://doi.org/10.1186/s12879-019-3955-x

15. Aylward, R. B., Acharya, A., England, S., Agocs, M., & Linkins, J. (2003). Global health goals: Lessons from the worldwide effort to eradicate poliomyelitis. *Lancet (London, England)*, *362*(9387), 909–914. https://doi.org/10.1016/S0140-6736(03)14337-1

16. Babon, J. J., Lucet, I. S., Murphy, J. M., Nicola, N. A., & Varghese, L. N. (2014). The molecular regulation of Janus kinase (JAK) activation. *The Biochemical Journal*, *462*(1), 1–13. https://doi.org/10.1042/BJ20140712

17. Bae, E., Sakai, T., & Mosher, D. F. (2004). Assembly of exogenous fibronectin by fibronectin-null cells is dependent on the adhesive substrate. *The Journal of Biological Chemistry*, *279*(34), 35749–35759. https://doi.org/10.1074/jbc.M406283200

18. Baggen, J., Thibaut, H. J., Strating, J. R. P. M., & van Kuppeveld, F. J. M. (2018). The life cycle of non-polio enteroviruses and how to target it. *Nature Reviews. Microbiology*, *16*(6), 368–381. https://doi.org/10.1038/s41579-018-0005-4

19. Balzer, V., Poc, P., Puris, E., Martin, S., Aliasgari, M., Auriola, S., & Fricker, G. (2022). Re-evaluation of the hCMEC/D3 based in vitro BBB model for ABC transporter studies. *European Journal of Pharmaceutics and Biopharmaceutics: Official Journal of Arbeitsgemeinschaft Fur Pharmazeutische Verfahrenstechnik e.V*, *173*, 12–21. https://doi.org/10.1016/j.ejpb.2022.02.017

20. Barar, J., Gumbleton, M., Asadi, M., & Omidi, Y. (2010). Barrier functionality and transport machineries of human ECV304 cells. *Medical Science Monitor: International Medical Journal of Experimental and Clinical Research*, *16*(1), BR52-60.

21. Bauer, H., Zweimueller-Mayer, J., Steinbacher, P., Lametschwandtner, A., & Bauer, H. C. (2010). The dual role of zonula occludens (ZO) proteins. *Journal of Biomedicine & Biotechnology*, *2010*, 402593. https://doi.org/10.1155/2010/402593

22. Bennett, M. L., Song, H., & Ming, G.-L. (2021). Microglia modulate neurodevelopment in human neuroimmune organoids. *Cell Stem Cell*, *28*(12), 2035–2036. https://doi.org/10.1016/j.stem.2021.11.005

23. Benschop, K. S. M., Broberg, E. K., Hodcroft, E., Schmitz, D., Albert, J., Baicus, A., Bailly, J.-L., Baldvinsdottir, G., Berginc, N., Blomqvist, S., Böttcher, S., Brytting, M., Bujaki, E., Cabrerizo, M., Celma, C., Cinek, O., Claas, E. C. J., Cremer, J., Dean, J., … Simmonds, P. (2021). Molecular Epidemiology and Evolutionary Trajectory of Emerging Echovirus 30, Europe. *Emerging Infectious Diseases*, *27*(6), 1616–1626. https://doi.org/10.3201/eid2706.203096

24. Benz, F., & Liebner, S. (2022). Structure and Function of the Blood-Brain Barrier (BBB). *Handbook of Experimental Pharmacology*, *273*, 3–31. https://doi.org/10.1007/164_2020_404

25. Bernard-Patrzynski, F., Lécuyer, M.-A., Puscas, I., Boukhatem, I., Charabati, M., Bourbonnière, L., Ramassamy, C., Leclair, G., Prat, A., & Roullin, V. G. (2019). Isolation of endothelial cells, pericytes and astrocytes from mouse brain. *PloS One*, *14*(12), e0226302. https://doi.org/10.1371/journal.pone.0226302

26. Beyer, E. C., & Berthoud, V. M. (2018). Gap junction gene and protein families: Connexins, innexins, and pannexins. *Biochimica Et Biophysica Acta. Biomembranes*, *1860*(1), 5–8. https://doi.org/10.1016/j.bbamem.2017.05.016

27. Bhalerao, A., Sivandzade, F., Archie, S. R., Chowdhury, E. A., Noorani, B., & Cucullo, L. (2020). In vitro modeling of the neurovascular unit: Advances in the field. *Fluids and Barriers of the CNS*, *17*(1), 22. https://doi.org/10.1186/s12987-020-00183-7

28. Bhargavan, B., & Kanmogne, G. D. (2018). Differential Mechanisms of Inflammation and Endothelial Dysfunction by HIV-1 Subtype-B and Recombinant CRF02_AG Tat Proteins on Human Brain Microvascular Endothelial Cells: Implications for Viral Neuropathogenesis. *Molecular Neurobiology*, *55*(2), 1352–1363. https://doi.org/10.1007/s12035-017-0382-0

29. Bhowmick, S., D'Mello, V., Caruso, D., Wallerstein, A., & Abdul-Muneer, P. M. (2019). Impairment of pericyte-endothelium crosstalk leads to blood-brain barrier dysfunction following traumatic brain injury. *Experimental Neurology*, *317*, 260–270. https://doi.org/10.1016/j.expneurol.2019.03.014

30. Bible, J. M., Pantelidis, P., Chan, P. K. S., & Tong, C. Y. W. (2007). Genetic evolution of enterovirus 71: Epidemiological and pathological implications. *Reviews in Medical Virology*, *17*(6), 371–379. https://doi.org/10.1002/rmv.538

31. Bitnun, A., & Yeh, E. A. (2018). Acute Flaccid Paralysis and Enteroviral Infections. *Current Infectious Disease Reports*, *20*(9), 34. https://doi.org/10.1007/s11908-018-0641-x

32. Blank, T., Detje, C. N., Spieß, A., Hagemeyer, N., Brendecke, S. M., Wolfart, J., Staszewski, O., Zöller, T., Papageorgiou, I., Schneider, J., Paricio-Montesinos, R., Eisel, U. L. M., Manahan-Vaughan, D., Jansen, S., Lienenklaus, S., Lu, B., Imai, Y., Müller, M., Goelz, S. E., … Prinz, M. (2016). Brain Endothelial- and Epithelial-Specific Interferon Receptor Chain 1 Drives Virus-Induced Sickness Behavior and Cognitive Impairment. *Immunity*, *44*(4), 901–912. https://doi.org/10.1016/j.immuni.2016.04.005

33. Bordin, A., Chirivì, M., Pagano, F., Milan, M., Iuliano, M., Scaccia, E., Fortunato, O., Mangino, G., Dhori, X., De Marinis, E., D'Amico, A., Miglietta, S., Picchio, V., Rizzi, R., Romeo, G., Pulcinelli, F., Chimenti, I., Frati, G., & De Falco, E. (2022). Human platelet lysate-derived extracellular vesicles enhance angiogenesis through miR-126. *Cell Proliferation*, e13312. https://doi.org/10.1111/cpr.13312

34. Boveri, M., Berezowski, V., Price, A., Slupek, S., Lenfant, A.-M., Benaud, C., Hartung, T., Cecchelli, R., Prieto, P., & Dehouck, M.-P. (2005). Induction of blood-brain barrier properties in cultured brain capillary endothelial cells: Comparison between primary glial cells and C6 cell line. *Glia*, *51*(3), 187–198. https://doi.org/10.1002/glia.20189

35. Brouwer, L., Moreni, G., Wolthers, K. C., & Pajkrt, D. (2021). World-Wide Prevalence and Genotype Distribution of Enteroviruses. *Viruses*, *13*(3), 434. https://doi.org/10.3390/v13030434

36. Brown, D. M., Zhang, Y., & Scheuermann, R. H. (2020). Epidemiology and Sequence-Based Evolutionary Analysis of Circulating Non-Polio Enteroviruses. *Microorganisms*, *8*(12), E1856. https://doi.org/10.3390/microorganisms8121856

37. Burboa, P. C., Puebla, M., Gaete, P. S., Durán, W. N., & Lillo, M. A. (2022). Connexin and Pannexin Large-Pore Channels in Microcirculation and Neurovascular Coupling Function. *International Journal of Molecular Sciences*, *23*(13), 7303. https://doi.org/10.3390/ijms23137303

38. Butsabong, T., Felippe, M., Campagnolo, P., & Maringer, K. (2021). The emerging role of perivascular cells (pericytes) in viral pathogenesis. *The Journal of General Virology*, *102*(8). https://doi.org/10.1099/jgv.0.001634

39. Cai, H., Liu, W., Xue, Y., Shang, X., Liu, J., Li, Z., Wang, P., Liu, L., Hu, Y., & Liu, Y. (2015). Roundabout 4 regulates blood-tumor barrier permeability through the modulation of ZO-1, Occludin, and Claudin-5 expression. *Journal of Neuropathology and Experimental Neurology*, *74*(1), 25–37. https://doi.org/10.1097/NEN.0000000000000146

40. Cao, J., Liu, H., Qu, M., Hou, A., Zhou, Y., Sun, B., Cai, L., Gao, F., Su, W., & Jiang, C. (2019). Determination of the cleavage site of enterovirus 71 VP0 and the effect of this cleavage on viral infectivity and assembly. *Microbial Pathogenesis*, *134*, 103568. https://doi.org/10.1016/j.micpath.2019.103568

41. Cao, J., Qu, M., Liu, H., Wan, X., Li, F., Hou, A., Zhou, Y., Sun, B., Cai, L., Su, W., & Jiang, C. (2020). Myristoylation of EV71 VP4 is Essential for Infectivity and Interaction with Membrane Structure. *Virologica Sinica*, *35*(5), 599–613. https://doi.org/10.1007/s12250-020-00226-1

42. Carson, M. J., Reilly, C. R., Sutcliffe, J. G., & Lo, D. (1999). Disproportionate recruitment of CD8+ T cells into the central nervous system by professional antigen-presenting cells. *The American Journal of Pathology*, *154*(2), 481–494. https://doi.org/10.1016/S0002-9440(10)65294-7

43. Casas-Alba, D., de Sevilla, M. F., Valero-Rello, A., Fortuny, C., García-García, J.-J., Ortez, C., Muchart, J., Armangué, T., Jordan, I., Luaces, C., Barrabeig, I., González-Sanz, R., Cabrerizo, M., Muñoz-Almagro, C., & Launes, C. (2017).

Outbreak of brainstem encephalitis associated with enterovirus-A71 in Catalonia, Spain (2016): A clinical observational study in a children's reference centre in Catalonia. *Clinical Microbiology and Infection: The Official Publication of the European Society of Clinical Microbiology and Infectious Diseases*, *23*(11), 874–881. https://doi.org/10.1016/j.cmi.2017.03.016

44. Castro Dias, M., Mapunda, J. A., Vladymyrov, M., & Engelhardt, B. (2019). Structure and Junctional Complexes of Endothelial, Epithelial and Glial Brain Barriers. *International Journal of Molecular Sciences*, *20*(21), E5372. https://doi.org/10.3390/ijms20215372

45. Cecchelli, R., Aday, S., Sevin, E., Almeida, C., Culot, M., Dehouck, L., Coisne, C., Engelhardt, B., Dehouck, M.-P., & Ferreira, L. (2014). A stable and reproducible human blood-brain barrier model derived from hematopoietic stem cells. *PloS One*, *9*(6), e99733. https://doi.org/10.1371/journal.pone.0099733

46. Cegarra, C., Chaves, C., Déon, C., Do, T. M., Dumas, B., Frenzel, A., Kuhn, P., Roudieres, V., Guillemot, J. C., & Lesuisse, D. (2022). Exploring ITM2A as a new potential target for brain delivery. *Fluids and Barriers of the CNS*, *19*(1), 25. https://doi.org/10.1186/s12987-022-00321-3

47. Chang, C.-K., Wu, S.-R., Chen, Y.-C., Lee, K.-J., Chung, N.-H., Lu, Y.-J., Yu, S.-L., Liu, C.-C., & Chow, Y.-H. (2018). Mutations in VP1 and 5'-UTR affect enterovirus 71 virulence. *Scientific Reports*, *8*(1), 6688. https://doi.org/10.1038/s41598-018-25091-7

48. Chang, C.-S., Liao, C.-C., Liou, A.-T., Chang, Y.-S., Chang, Y.-T., Tzeng, B.-H., Chen, C.-C., & Shih, C. (2019). Enterovirus 71 targets the cardiopulmonary

system in a robust oral infection mouse model. *Scientific Reports*, *9*(1), 11108. https://doi.org/10.1038/s41598-019-47455-3

49. Chang, C.-S., Liao, C.-C., Liou, A.-T., Chou, Y.-C., Yu, Y.-Y., Lin, C.-Y., Lin, J.-S., Suen, C.-S., Hwang, M.-J., & Shih, C. (2021). Novel Naturally Occurring Mutations of Enterovirus 71 Associated With Disease Severity. *Frontiers in Microbiology*, *11*, 610568. https://doi.org/10.3389/fmicb.2020.610568

50. Chang, C.-Y., Li, J.-R., Chen, W.-Y., Ou, Y.-C., Lai, C.-Y., Hu, Y.-H., Wu, C.-C., Chang, C.-J., & Chen, C.-J. (2015). Disruption of in vitro endothelial barrier integrity by Japanese encephalitis virus-Infected astrocytes. *Glia*, *63*(11), 1915–1932. https://doi.org/10.1002/glia.22857

51. Chang, L., & Goldman, R. D. (2004). Intermediate filaments mediate cytoskeletal crosstalk. *Nature Reviews. Molecular Cell Biology*, *5*(8), 601–613. https://doi.org/10.1038/nrm1438

52. Chang, L.-Y., Huang, L.-M., Gau, S. S.-F., Wu, Y.-Y., Hsia, S.-H., Fan, T.-Y., Lin, K.-L., Huang, Y.-C., Lu, C.-Y., & Lin, T.-Y. (2007). Neurodevelopment and cognition in children after enterovirus 71 infection. *The New England Journal of Medicine*, *356*(12), 1226–1234. https://doi.org/10.1056/NEJMoa065954

53. Chaudhuri, A., Yang, B., Gendelman, H. E., Persidsky, Y., & Kanmogne, G. D. (2008). STAT1 signaling modulates HIV-1-induced inflammatory responses and leukocyte transmigration across the blood-brain barrier. *Blood*, *111*(4), 2062–2072. https://doi.org/10.1182/blood-2007-05-091207

54. Chen, B., Brinkmann, K., Chen, Z., Pak, C. W., Liao, Y., Shi, S., Henry, L., Grishin, N. V., Bogdan, S., & Rosen, M. K. (2014). The WAVE regulatory complex links diverse receptors to the actin cytoskeleton. *Cell*, *156*(1–2), 195–207. https://doi.org/10.1016/j.cell.2013.11.048

55. Chen, B.-S., Lee, H.-C., Lee, K.-M., Gong, Y.-N., & Shih, S.-R. (2020). Enterovirus and Encephalitis. *Frontiers in Microbiology*, *11*, 261. https://doi.org/10.3389/fmicb.2020.00261

56. Chen, C.-S., Yao, Y.-C., Lin, S.-C., Lee, Y.-P., Wang, Y.-F., Wang, J.-R., Liu, C.-C., Lei, H.-Y., & Yu, C.-K. (2007). Retrograde axonal transport: A major transmission route of enterovirus 71 in mice. *Journal of Virology*, *81*(17), 8996–9003. https://doi.org/10.1128/JVI.00236-07

57. Chen, G.-P., Xiang, K., Sun, L., Shi, Y.-L., Meng, C., Song, L., Liu, R.-S., Li, W.-D., & Pan, H.-F. (2021). TLR3 polymorphisms are associated with the severity of hand, foot, and mouth disease caused by enterovirus A71 in a Chinese children population. *Journal of Medical Virology*, *93*(11), 6172–6179. https://doi.org/10.1002/jmv.27115

58. Chen, H., Zhang, Y., Yang, E., Liu, L., Che, Y., Wang, J., Zhao, H., Tang, D., Dong, C., Yang, L., Shen, D., Wang, X., Liao, Y., Wang, L., Na, R., Liang, Y., & Li, Q. (2012). The effect of enterovirus 71 immunization on neuropathogenesis and protein expression profiles in the thalamus of infected rhesus neonates. *Virology*, *432*(2), 417–426. https://doi.org/10.1016/j.virol.2012.06.026

59. Chen, K.-R., & Ling, P. (2019). Interplays between Enterovirus A71 and the innate immune system. *Journal of Biomedical Science*, *26*, 95. https://doi.org/10.1186/s12929-019-0596-8

60. Chen, S.-L., Liu, Y.-G., Zhou, Y.-T., Zhao, P., Ren, H., Xiao, M., Zhu, Y.-Z., & Qi, Z.-T. (2019). Endophilin-A2-mediated endocytic pathway is critical for enterovirus 71 entry into caco-2 cells. *Emerging Microbes & Infections*, *8*(1), 773–786. https://doi.org/10.1080/22221751.2019.1618686

61. Chen, Y., Yang, W., Chen, F., & Cui, L. (2022). COVID-19 and cognitive impairment: Neuroinvasive and blood–brain barrier dysfunction. *Journal of Neuroinflammation*, *19*(1), 222. https://doi.org/10.1186/s12974-022-02579-8

62. Chen, Z., & Li, G. (2021). Immune response and blood-brain barrier dysfunction during viral neuroinvasion. *Innate Immunity*, *27*(2), 109–117. https://doi.org/10.1177/1753425920954281

63. Chen, Z., Li, R., Xie, Z., Huang, G., Yuan, Q., & Zeng, J. (2014). IL-6, IL-10 and IL-13 are associated with pathogenesis in children with Enterovirus 71 infection. *International Journal of Clinical and Experimental Medicine*, *7*(9), 2718–2723.

64. Cheng, H.-Y., Huang, Y.-C., Yen, T.-Y., Hsia, S.-H., Hsieh, Y.-C., Li, C.-C., Chang, L.-Y., & Huang, L.-M. (2014). The correlation between the presence of viremia and clinical severity in patients with enterovirus 71 infection: A multi-center cohort study. *BMC Infectious Diseases*, *14*, 417. https://doi.org/10.1186/1471-2334-14-417

65. Chiu, M.-L., Luo, S.-T., Chen, Y.-Y., Chung, W. Y., Duong, V., Dussart, P., Chan, Y.-F., Perera, D., Ooi, M. H., Thao, N. T. T., Truong, H. K., & Lee, M.-S. (2020). Establishment of Asia-Pacific Network for Enterovirus Surveillance. *Vaccine*, *38*(1), 1–9. https://doi.org/10.1016/j.vaccine.2019.09.111

66. Chua, K. B., & Kasri, A. R. (2011). Hand foot and mouth disease due to enterovirus 71 in Malaysia. *Virologica Sinica*, *26*(4), 221–228. https://doi.org/10.1007/s12250-011-3195-8

67. Chun, K.-H., Cho, S.-J., Lee, J.-W., Seo, J. H., Kim, K.-W., & Lee, S.-K. (2021). Protein kinase C-δ interacts with and phosphorylates ARD1. *Journal of Cellular Physiology*, *236*(1), 379–391. https://doi.org/10.1002/jcp.29866

68. Chung, Y.-C., Huang, J.-H., Lai, C.-W., Sheng, H.-C., Shih, S.-R., Ho, M.-S., & Hu, Y.-C. (2006). Expression, purification and characterization of enterovirus-71 virus-like particles. *World Journal of Gastroenterology*, *12*(6), 921–927. https://doi.org/10.3748/wjg.v12.i6.921

69. Cifuente, J. O., Lee, H., Yoder, J. D., Shingler, K. L., Carnegie, M. S., Yoder, J. L., Ashley, R. E., Makhov, A. M., Conway, J. F., & Hafenstein, S. (2013). Structures of the procapsid and mature virion of enterovirus 71 strain 1095. *Journal of Virology*, *87*(13), 7637–7645. https://doi.org/10.1128/JVI.03519-12

70. Clé, M., Desmetz, C., Barthelemy, J., Martin, M.-F., Constant, O., Maarifi, G., Foulongne, V., Bolloré, K., Glasson, Y., De Bock, F., Blaquiere, M., Dehouck, L., Pirot, N., Tuaillon, E., Nisole, S., Najioullah, F., Van de Perre, P., Cabié, A., Marchi, N., … Salinas, S. (2020). Zika Virus Infection Promotes Local Inflammation, Cell Adhesion Molecule Upregulation, and Leukocyte

Recruitment at the Blood-Brain Barrier. *MBio*, *11*(4), e01183-20. https://doi.org/10.1128/mBio.01183-20

71. Cohen-Kashi Malina, K., Cooper, I., & Teichberg, V. I. (2009). Closing the gap between the in-vivo and in-vitro blood-brain barrier tightness. *Brain Research*, *1284*, 12–21. https://doi.org/10.1016/j.brainres.2009.05.072

72. Coisne, C., & Engelhardt, B. (2011). Tight junctions in brain barriers during central nervous system inflammation. *Antioxidants & Redox Signaling*, *15*(5), 1285–1303. https://doi.org/10.1089/ars.2011.3929

73. Colgan, O. C., Collins, N. T., Ferguson, G., Murphy, R. P., Birney, Y. A., Cahill, P. A., & Cummins, P. M. (2008). Influence of basolateral condition on the regulation of brain microvascular endothelial tight junction properties and barrier function. *Brain Research*, *1193*, 84–92. https://doi.org/10.1016/j.brainres.2007.11.072

74. Constant, O., Maarifi, G., Blanchet, F. P., Van de Perre, P., Simonin, Y., & Salinas, S. (2022). Role of Dendritic Cells in Viral Brain Infections. *Frontiers in Immunology*, *13*, 862053. https://doi.org/10.3389/fimmu.2022.862053

75. Cornford, E. M., & Hyman, S. (2005). Localization of brain endothelial luminal and abluminal transporters with immunogold electron microscopy. *NeuroRx: The Journal of the American Society for Experimental NeuroTherapeutics*, *2*(1), 27–43. https://doi.org/10.1602/neurorx.2.1.27

76. Coyne, C. B., Kim, K. S., & Bergelson, J. M. (2007). Poliovirus entry into human brain microvascular cells requires receptor-induced activation of SHP-2. *The EMBO Journal*, *26*(17), 4016–4028. https://doi.org/10.1038/sj.emboj.7601831

77. Cui, D., Zhong, F., Lin, J., Wu, Y., Long, Q., Yang, X., Zhu, Q., Huang, L., Mao, Q., Huo, Z., Zhou, Z., Xie, G., Zheng, S., Yu, F., & Chen, Y. (2017). Changes of circulating Th22 cells in children with hand, foot, and mouth disease caused by enterovirus 71 infection. *Oncotarget*, *8*(17), 29370–29382. https://doi.org/10.18632/oncotarget.14083

78. Curry, S., Fry, E., Blakemore, W., Abu-Ghazaleh, R., Jackson, T., King, A., Lea, S., Newman, J., & Stuart, D. (1997). Dissecting the roles of VP0 cleavage and RNA packaging in picornavirus capsid stabilization: The structure of empty capsids of foot-and-mouth disease virus. *Journal of Virology*, *71*(12), 9743–9752. https://doi.org/10.1128/JVI.71.12.9743-9752.1997

79. Curtaz, C. J., Schmitt, C., Herbert, S.-L., Feldheim, J., Schlegel, N., Gosselet, F., Hagemann, C., Roewer, N., Meybohm, P., Wöckel, A., & Burek, M. (2020). Serum-derived factors of breast cancer patients with brain metastases alter permeability of a human blood-brain barrier model. *Fluids and Barriers of the CNS*, *17*(1), 31. https://doi.org/10.1186/s12987-020-00192-6

80. Czupalla, C. J., Liebner, S., & Devraj, K. (2014). In vitro models of the blood-brain barrier. *Methods in Molecular Biology (Clifton, N.J.)*, *1135*, 415–437. https://doi.org/10.1007/978-1-4939-0320-7_34

81. D'Acremont, V., Kilowoko, M., Kyungu, E., Philipina, S., Sangu, W., Kahama-Maro, J., Lengeler, C., Cherpillod, P., Kaiser, L., & Genton, B. (2014). Beyond

malaria—Causes of fever in outpatient Tanzanian children. *The New England Journal of Medicine*, *370*(9), 809–817. https://doi.org/10.1056/NEJMoa1214482

82. Dallacasagrande, V., & Hajjar, K. A. (2020). Annexin A2 in Inflammation and Host Defense. *Cells*, *9*(6), E1499. https://doi.org/10.3390/cells9061499

83. Dan, X., Wan, Q., Yi, L., Lu, J., Jiao, Y., Li, H., Song, D., Chen, Y., Xu, H., & He, M.-L. (2019). Hsp27 Responds to and Facilitates Enterovirus A71 Replication by Enhancing Viral Internal Ribosome Entry Site-Mediated Translation. *Journal of Virology*, *93*(9), e02322-18. https://doi.org/10.1128/JVI.02322-18

84. Dang, M., Wang, X., Wang, Q., Wang, Y., Lin, J., Sun, Y., Li, X., Zhang, L., Lou, Z., Wang, J., & Rao, Z. (2014). Molecular mechanism of SCARB2-mediated attachment and uncoating of EV71. *Protein & Cell*, *5*(9), 692–703. https://doi.org/10.1007/s13238-014-0087-3

85. Davidson, J. O., Green, C. R., Bennet, L., & Gunn, A. J. (2015). Battle of the hemichannels—Connexins and Pannexins in ischemic brain injury. *International Journal of Developmental Neuroscience: The Official Journal of the International Society for Developmental Neuroscience*, *45*, 66–74. https://doi.org/10.1016/j.ijdevneu.2014.12.007

86. De Bock, M., Vandenbroucke, R. E., Decrock, E., Culot, M., Cecchelli, R., & Leybaert, L. (2014). A new angle on blood-CNS interfaces: A role for connexins? *FEBS Letters*, *588*(8), 1259–1270. https://doi.org/10.1016/j.febslet.2014.02.060

87. Deli, M. A., Abrahám, C. S., Kataoka, Y., & Niwa, M. (2005). Permeability studies on in vitro blood-brain barrier models: Physiology, pathology, and pharmacology. *Cellular and Molecular Neurobiology*, *25*(1), 59–127. https://doi.org/10.1007/s10571-004-1377-8

88. Deligne, C., Hachani, J., Duban-Deweer, S., Meignan, S., Leblond, P., Carcaboso, A. M., Sano, Y., Shimizu, F., Kanda, T., Gosselet, F., Dehouck, M.-P., & Mysiorek, C. (2020). Development of a human in vitro blood-brain tumor barrier model of diffuse intrinsic pontine glioma to better understand the chemoresistance. *Fluids and Barriers of the CNS*, *17*(1), 37. https://doi.org/10.1186/s12987-020-00198-0

89. Delsing, L., Herland, A., Falk, A., Hicks, R., Synnergren, J., & Zetterberg, H. (2020). Models of the blood-brain barrier using iPSC-derived cells. *Molecular and Cellular Neurosciences*, *107*, 103533. https://doi.org/10.1016/j.mcn.2020.103533

90. Dembny, P., Newman, A. G., Singh, M., Hinz, M., Szczepek, M., Krüger, C., Adalbert, R., Dzaye, O., Trimbuch, T., Wallach, T., Kleinau, G., Derkow, K., Richard, B. C., Schipke, C., Scheidereit, C., Stachelscheid, H., Golenbock, D., Peters, O., Coleman, M., … Lehnardt, S. (2020). Human endogenous retrovirus HERV-K(HML-2) RNA causes neurodegeneration through Toll-like receptors. *JCI Insight*, *5*(7), 131093. https://doi.org/10.1172/jci.insight.131093

91. Deng, J.-X., Nie, X.-J., Lei, Y.-F., Ma, C.-F., Xu, D.-L., Li, B., Xu, Z.-K., & Zhang, G.-C. (2012). The highly conserved 5’ untranslated region as an effective target towards the inhibition of Enterovirus 71 replication by unmodified and

appropriate 2'-modified siRNAs. *Journal of Biomedical Science*, *19*, 73. https://doi.org/10.1186/1423-0127-19-73

92. Ding, L., Zhang, N., Zhu, B., Liu, J., Wang, X., Liu, F., & Mao, Y. (2021). Spatiotemporal characteristics and meteorological determinants of hand, foot and mouth disease in Shaanxi Province, China: A county-level analysis. *BMC Public Health*, *21*(1), 374. https://doi.org/10.1186/s12889-021-10385-9

93. Dittmar, S., Harms, H., Runkler, N., Maisner, A., Kim, K. S., & Schneider-Schaulies, J. (2008). Measles virus-induced block of transendothelial migration of T lymphocytes and infection-mediated virus spread across endothelial cell barriers. *Journal of Virology*, *82*(22), 11273–11282. https://doi.org/10.1128/JVI.00775-08

94. Dong, Q., Men, R., Dan, X., Chen, Y., Li, H., Chen, G., Zee, B., Wang, M. H. T., & He, M.-L. (2018). Hsc70 regulates the IRES activity and serves as an antiviral target of enterovirus A71 infection. *Antiviral Research*, *150*, 39–46. https://doi.org/10.1016/j.antiviral.2017.11.020

95. Dong, Y., Liu, J., Lu, N., & Zhang, C. (2022). Enterovirus 71 Antagonizes Antiviral Effects of Type III Interferon and Evades the Clearance of Intestinal Intraepithelial Lymphocytes. *Frontiers in Microbiology*, *12*, 806084. https://doi.org/10.3389/fmicb.2021.806084

96. Dong, Z., Liu, Z.-W., Chen, R., Wen, X.-J., Ji, J., Zheng, X.-X., Zhao, L., Wang, Z.-Y., & Wen, H.-L. (2019). The untranslated regions of EV-A71 contribute to its pathogenicity and virulence. *Virus Research*, *263*, 55–63. https://doi.org/10.1016/j.virusres.2018.12.019

97. Du, N., Cong, H., Tian, H., Zhang, H., Zhang, W., Song, L., & Tien, P. (2014). Cell surface vimentin is an attachment receptor for enterovirus 71. *Journal of Virology*, *88*(10), 5816–5833. https://doi.org/10.1128/JVI.03826-13

98. Dubyak, G. R. (2012). P2X7 receptor regulation of non-classical secretion from immune effector cells. *Cellular Microbiology*, *14*(11), 1697–1706. https://doi.org/10.1111/cmi.12001

99. Duncan, I. B. (1961). An outbreak of aseptic meningitis associated with a previously unrecognized virus. *The Journal of Hygiene*, *59*, 181–189. https://doi.org/10.1017/s0022172400038845

100. Earley, D. F., Bailly, B., Maggioni, A., Kundur, A. R., Thomson, R. J., Chang, C.-W., & von Itzstein, M. (2019). Efficient Blocking of Enterovirus 71 Infection by Heparan Sulfate Analogues Acting as Decoy Receptors. *ACS Infectious Diseases*, *5*(10), 1708–1717. https://doi.org/10.1021/acsinfecdis.9b00070

101. Eng, M. E., Imperio, G. E., Bloise, E., & Matthews, S. G. (2022). ATP-binding cassette (ABC) drug transporters in the developing blood-brain barrier: Role in fetal brain protection. *Cellular and Molecular Life Sciences: CMLS*, *79*(8), 415. https://doi.org/10.1007/s00018-022-04432-w

102. Fan, S., Xu, Z., Liu, P., Qin, Y., & Chen, M. (2021). Enterovirus 71 2A Protease Inhibits P-Body Formation To Promote Viral RNA Synthesis. *Journal of Virology*, *95*(19), e0092221. https://doi.org/10.1128/JVI.00922-21

103. Fang, L., Wang, K.-K., Huang, Q., Cheng, F., Huang, F., & Liu, W.-W. (2020). Nucleolin Mediates LPS-induced Expression of Inflammatory Mediators and

Activation of Signaling Pathways. *Current Medical Science*, *40*(4), 646–653. https://doi.org/10.1007/s11596-020-2229-6

104. Fanning, A. S., & Anderson, J. M. (2009). Zonula occludens-1 and -2 are cytosolic scaffolds that regulate the assembly of cellular junctions. *Annals of the New York Academy of Sciences*, *1165*, 113–120. https://doi.org/10.1111/j.1749-6632.2009.04440.x

105. Feliksiak, K., Witko, T., Solarz, D., Guzik, M., & Rajfur, Z. (2020). Vimentin Association with Nuclear Grooves in Normal MEF 3T3 Cells. *International Journal of Molecular Sciences*, *21*(20), E7478. https://doi.org/10.3390/ijms21207478

106. Feng, Q., Langereis, M. A., Lork, M., Nguyen, M., Hato, S. V., Lanke, K., Emdad, L., Bhoopathi, P., Fisher, P. B., Lloyd, R. E., & van Kuppeveld, F. J. M. (2014). Enterovirus 2Apro targets MDA5 and MAVS in infected cells. *Journal of Virology*, *88*(6), 3369–3378. https://doi.org/10.1128/JVI.02712-13

107. Fenimore, J., & A Young, H. (2016). Regulation of IFN-γ Expression. *Advances in Experimental Medicine and Biology*, *941*, 1–19. https://doi.org/10.1007/978-94-024-0921-5_1

108. Finsterer, J. (2019). Neurological Perspectives of Neurogenic Pulmonary Edema. *European Neurology*, *81*(1–2), 94–102. https://doi.org/10.1159/000500139

109. Flewett, T. H., Warin, R. P., & Clarke, S. K. (1963). “Hand, foot, and mouth disease” associated with Coxsackie A5 virus. *Journal of Clinical Pathology*, *16*, 53–55. https://doi.org/10.1136/jcp.16.1.53

110. Foli-Andersen, P. J., Munkholm, A., Rønde, G., Børresen, M. L., Nielsen, J. E. K., Midgley, S., & Bang, D. (2022). Acute flaccid rhombencephalomyelitis with radiculitis in a child with an enterovirus A71 infection seen for the first time in Denmark: A case report. *Journal of Medical Case Reports*, *16*(1), 32. https://doi.org/10.1186/s13256-021-03246-x

111. Fromm, M., Piontek, J., Rosenthal, R., Günzel, D., & Krug, S. M. (2017). Tight junctions of the proximal tubule and their channel proteins. *Pflugers Archiv: European Journal of Physiology*, *469*(7–8), 877–887. https://doi.org/10.1007/s00424-017-2001-3

112. Fujii, K., Sudaka, Y., Takashino, A., Kobayashi, K., Kataoka, C., Suzuki, T., Iwata-Yoshikawa, N., Kotani, O., Ami, Y., Shimizu, H., Nagata, N., Mizuta, K., Matsuzaki, Y., & Koike, S. (2018). VP1 Amino Acid Residue 145 of Enterovirus 71 Is a Key Residue for Its Receptor Attachment and Resistance to Neutralizing Antibody during Cynomolgus Monkey Infection. *Journal of Virology*, *92*(15), e00682-18. https://doi.org/10.1128/JVI.00682-18

113. Gaete, P. S., Lillo, M. A., & Figueroa, X. F. (2014). Functional role of connexins and pannexins in the interaction between vascular and nervous system. *Journal of Cellular Physiology*, *229*(10), 1336–1345. https://doi.org/10.1002/jcp.24563

114. Galinsky, R., Davidson, J. O., Dean, J. M., Green, C. R., Bennet, L., & Gunn, A. J. (2018). Glia and hemichannels: Key mediators of perinatal encephalopathy.

Neural Regeneration Research, *13*(2), 181–189. https://doi.org/10.4103/1673-5374.226378

115. Gao, P., & Shivers, R. R. (2004). Correlation of the presence of blood-brain barrier tight junctions and expression of zonula occludens protein ZO-1 in vitro: A freeze-fracture and immunofluorescence study. *Journal of Submicroscopic Cytology and Pathology*, *36*(1), 7–15.

116. Geier, E. G., Chen, E. C., Webb, A., Papp, A. C., Yee, S. W., Sadee, W., & Giacomini, K. M. (2013). Profiling solute carrier transporters in the human blood-brain barrier. *Clinical Pharmacology and Therapeutics*, *94*(6), 636–639. https://doi.org/10.1038/clpt.2013.175

117. Giansanti, P., Strating, J. R. P. M., Defourny, K. A. Y., Cesonyte, I., Bottino, A. M. S., Post, H., Viktorova, E. G., Ho, V. Q. T., Langereis, M. A., Belov, G. A., Nolte-'t Hoen, E. N. M., Heck, A. J. R., & van Kuppeveld, F. J. M. (2020). Dynamic remodelling of the human host cell proteome and phosphoproteome upon enterovirus infection. *Nature Communications*, *11*(1), 4332. https://doi.org/10.1038/s41467-020-18168-3

118. Gilsdorf, J. R. (2019). Acute Flaccid Myelitis: Lessons From Polio. *Journal of the Pediatric Infectious Diseases Society*, *8*(6), 550–553. https://doi.org/10.1093/jpids/piz017

119. Girardin, F. (2006). Membrane transporter proteins: A challenge for CNS drug development. *Dialogues in Clinical Neuroscience*, *8*(3), 311–321.

120. Goksugur, N., & Goksugur, S. (2010). Images in clinical medicine. Hand, foot, and mouth disease. *The New England Journal of Medicine*, *362*(14), e49. https://doi.org/10.1056/NEJMicm0910628

121. González-Mariscal, L., Betanzos, A., & Avila-Flores, A. (2000). MAGUK proteins: Structure and role in the tight junction. *Seminars in Cell & Developmental Biology*, *11*(4), 315–324. https://doi.org/10.1006/scdb.2000.0178

122. Griffiths, M. J., Ooi, M. H., Wong, S. C., Mohan, A., Podin, Y., Perera, D., Chieng, C. H., Tio, P. H., Cardosa, M. J., & Solomon, T. (2012). In enterovirus 71 encephalitis with cardio-respiratory compromise, elevated interleukin 1β, interleukin 1 receptor antagonist, and granulocyte colony-stimulating factor levels are markers of poor prognosis. *The Journal of Infectious Diseases*, *206*(6), 881–892. https://doi.org/10.1093/infdis/jis446

123. Grindheim, A. K., Saraste, J., & Vedeler, A. (2017). Protein phosphorylation and its role in the regulation of Annexin A2 function. *Biochimica Et Biophysica Acta. General Subjects*, *1861*(11 Pt A), 2515–2529. https://doi.org/10.1016/j.bbagen.2017.08.024

124. Gu, J., Wu, J., Cao, Y., Zou, X., Jia, X., Yin, Y., Shen, L., Fang, D., & Mao, L. (2020). A Mouse Model for Infection with Enterovirus A71 in Small Extracellular Vesicles. *MSphere*, *5*(4), e00377-20. https://doi.org/10.1128/mSphere.00377-20

125. Gu, J., Wu, J., Fang, D., Qiu, Y., Zou, X., Jia, X., Yin, Y., Shen, L., & Mao, L. (2020). Exosomes cloak the virion to transmit Enterovirus 71 non-lytically. *Virulence*, *11*(1), 32–38. https://doi.org/10.1080/21505594.2019.1705022

126. Gu, J., Zhao, Y., Wu, J., Chen, Y., Yin, Y., Jia, X., & Mao, L. (2022). Enterovirus-71 utilizes small extracellular vesicles to cross the blood-brain barrier for infecting the central nervous system via transcytosis. *Journal of Medical Virology*. https://doi.org/10.1002/jmv.28120

127. Gu, Y.-Y., Shi, K., Yao, S., Yang, X., Liu, Y.-H., Tang, L., Dang, Y.-W., Chen, G., Feng, Z.-B., & Pan, H.-B. (2017). Morphological characteristics of fatal pediatric hand, foot and mouth disease: A clinicopathological study with related receptors of EV71. *Pathology, Research and Practice*, *213*(9), 1144–1151. https://doi.org/10.1016/j.prp.2017.07.004

128. Gubern-Mérida, C., Comajoan, P., Huguet, G., García-Yebenes, I., Lizasoain, I., Moro, M. A., Puig-Parnau, I., Sánchez, J. M., Serena, J., Kádár, E., & Castellanos, M. (2022). Cav-1 Protein Levels in Serum and Infarcted Brain Correlate with Hemorrhagic Volume in a Mouse Model of Thromboembolic Stroke, Independently of rt-PA Administration. *Molecular Neurobiology*, *59*(2), 1320–1332. https://doi.org/10.1007/s12035-021-02644-y

129. Gunaseelan, S., Wong, K. Z., Min, N., Sun, J., Ismail, N. K. B. M., Tan, Y. J., Lee, R. C. H., & Chu, J. J. H. (2019). Prunin suppresses viral IRES activity and is a potential candidate for treating enterovirus A71 infection. *Science Translational Medicine*, *11*(516), eaar5759. https://doi.org/10.1126/scitranslmed.aar5759

130. Günzel, D., & Fromm, M. (2012). Claudins and other tight junction proteins. *Comprehensive Physiology*, *2*(3), 1819–1852. https://doi.org/10.1002/cphy.c110045

131. Guo, H., Li, Y., Liu, G., Jiang, Y., Shen, S., Bi, R., Huang, H., Cheng, T., Wang, C., & Wei, W. (2019). A second open reading frame in human enterovirus determines viral replication in intestinal epithelial cells. *Nature Communications*, *10*(1), 4066. https://doi.org/10.1038/s41467-019-12040-9

132. Guo, M. Z., Zhu, C. D., Cai, Q., Xu, Y. L., & Huang, M. (2018). [The regulation of tight junction protein via PKCα/β for abnormal permeability of brain microvascular endothelial cells exposed to paraquat]. *Zhonghua Lao Dong Wei Sheng Zhi Ye Bing Za Zhi = Zhonghua Laodong Weisheng Zhiyebing Zazhi = Chinese Journal of Industrial Hygiene and Occupational Diseases*, *36*(12), 881–889. https://doi.org/10.3760/cma.j.issn.1001-9391.2018.12.001

133. Guo, Y., Zhang, Y., Liu, P., Li, F., Xin, D., He, H., Liu, Y., Yang, C., & Chen, Z. (2019). Association of the Polymorphism of rs1799822 on Carnitine Palmitoyltransferase II Gene with Severe Enterovirus 71 Encephalitis in Chinese Children. *Journal of Molecular Neuroscience: MN*, *69*(2), 188–196. https://doi.org/10.1007/s12031-019-01348-2

134. Hafenstein, S., Bowman, V. D., Chipman, P. R., Bator Kelly, C. M., Lin, F., Medof, M. E., & Rossmann, M. G. (2007). Interaction of decay-accelerating factor with coxsackievirus B3. *Journal of Virology*, *81*(23), 12927–12935. https://doi.org/10.1128/JVI.00931-07

135. Hajal, C., Campisi, M., Mattu, C., Chiono, V., & Kamm, R. D. (2018). In vitro models of molecular and nano-particle transport across the blood-brain barrier. *Biomicrofluidics*, *12*(4), 042213. https://doi.org/10.1063/1.5027118

136. Han, J.-F., Cao, R.-Y., Tian, X., Yu, M., Qin, E.-D., & Qin, C.-F. (2010). Producing infectious enterovirus type 71 in a rapid strategy. *Virology Journal*, *7*, 116. https://doi.org/10.1186/1743-422X-7-116

137. Han, Z., Li, J., & Chen, Z. (2014). Genetic polymorphism of CCL2-2510 and susceptibility to enterovirus 71 encephalitis in a Chinese population. *Archives of Virology*, *159*(9), 2503–2507. https://doi.org/10.1007/s00705-014-2082-7

138. Harvala, H., Benschop, K. S. M., Berginc, N., Midgley, S., Wolthers, K., Simmonds, P., Feeney, S., Bailly, J.-L., Mirand, A., Fischer, T. K., & On Behalf Of The Enpen Hospital-Based Surveillance Network, null. (2021). European Non-Polio Enterovirus Network: Introduction of Hospital-Based Surveillance Network to Understand the True Disease Burden of Non-Polio Enterovirus and Parechovirus Infections in Europe. *Microorganisms*, *9*(9), 1827. https://doi.org/10.3390/microorganisms9091827

139. Hassel, C., Mirand, A., Lukashev, A., TerletskaiaLadwig, E., Farkas, A., Schuffenecker, I., Diedrich, S., Huemer, H. P., Archimbaud, C., Peigue-Lafeuille, H., Henquell, C., & Bailly, J.-L. (2015). Transmission patterns of human enterovirus 71 to, from and among European countries, 2003 to 2013. *Euro Surveillance: Bulletin Europeen Sur Les Maladies Transmissibles = European Communicable Disease Bulletin*, *20*(34), 30005. https://doi.org/10.2807/1560-7917.ES.2015.20.34.30005

140. Hawkins, B. T., & Davis, T. P. (2005). The blood-brain barrier/neurovascular unit in health and disease. *Pharmacological Reviews*, *57*(2), 173–185. https://doi.org/10.1124/pr.57.2.4

141. Hayashi, Y., Nomura, M., Yamagishi, S., Harada, S., Yamashita, J., & Yamamoto, H. (1997). Induction of various blood-brain barrier properties in non-neural endothelial cells by close apposition to co-cultured astrocytes. *Glia*, *19*(1), 13–26.

142. He, F., Rui, J., Deng, Z., Zhang, Y., Qian, K., Zhu, C., Yu, S., Tu, J., Xia, W., Zhu, Q., Chen, S., Chen, T., & Zhou, X. (2022). Surveillance, Epidemiology and Impact of EV-A71 Vaccination on Hand, Foot, and Mouth Disease in Nanchang, China, 2010-2019. *Frontiers in Microbiology*, *12*, 811553. https://doi.org/10.3389/fmicb.2021.811553

143. He, Q.-Q., Ren, S., Xia, Z.-C., Cheng, Z.-K., Peng, N.-F., & Zhu, Y. (2018). Fibronectin Facilitates Enterovirus 71 Infection by Mediating Viral Entry. *Journal of Virology*, *92*(9), e02251-17. https://doi.org/10.1128/JVI.02251-17

144. He, X., Dong, S., Li, L., Liu, X., Wu, Y., Zhang, Z., & Mei, S. (2020). Using a Bayesian spatiotemporal model to identify the influencing factors and high-risk areas of hand, foot and mouth disease (HFMD) in Shenzhen. *PLoS Neglected Tropical Diseases*, *14*(3), e0008085. https://doi.org/10.1371/journal.pntd.0008085

145. He, Y., Zou, L., Chong, M. K. C., Men, R., Xu, W., Yang, H., Yao, X., Chen, L., Xian, H., Zhang, H., Luo, M., Cheng, J., Ma, H., Feng, Q., Huang, Y., Wang, Y., Yeoh, E.-K., Zee, B. C.-Y., Zhou, Y., … Wang, M. H. (2016). Genetic evolution

of Human Enterovirus A71 subgenotype C4 in Shenzhen, China, 1998-2013. *The Journal of Infection*, *72*(6), 731–737. https://doi.org/10.1016/j.jinf.2016.03.014

146. Helms, H. C., Abbott, N. J., Burek, M., Cecchelli, R., Couraud, P.-O., Deli, M. A., Förster, C., Galla, H. J., Romero, I. A., Shusta, E. V., Stebbins, M. J., Vandenhaute, E., Weksler, B., & Brodin, B. (2016). In vitro models of the blood-brain barrier: An overview of commonly used brain endothelial cell culture models and guidelines for their use. *Journal of Cerebral Blood Flow and Metabolism: Official Journal of the International Society of Cerebral Blood Flow and Metabolism*, *36*(5), 862–890. https://doi.org/10.1177/0271678X16630991

147. Helms, H. C., Waagepetersen, H. S., Nielsen, C. U., & Brodin, B. (2010). Paracellular tightness and claudin-5 expression is increased in the BCEC/astrocyte blood-brain barrier model by increasing media buffer capacity during growth. *The AAPS Journal*, *12*(4), 759–770. https://doi.org/10.1208/s12248-010-9237-6

148. Hernando-Rodríguez, B., & Artal-Sanz, M. (2018). Mitochondrial Quality Control Mechanisms and the PHB (Prohibitin) Complex. *Cells*, *7*(12), E238. https://doi.org/10.3390/cells7120238

149. Hervé, J.-C., Derangeon, M., Sarrouilhe, D., & Bourmeyster, N. (2014). Influence of the scaffolding protein Zonula Occludens (ZOs) on membrane channels. *Biochimica Et Biophysica Acta*, *1838*(2), 595–604. https://doi.org/10.1016/j.bbamem.2013.07.006

150. Heymans, M., Figueiredo, R., Dehouck, L., Francisco, D., Sano, Y., Shimizu, F., Kanda, T., Bruggmann, R., Engelhardt, B., Winter, P., Gosselet, F., & Culot, M. (2020). Contribution of brain pericytes in blood-brain barrier formation and maintenance: A transcriptomic study of cocultured human endothelial cells derived from hematopoietic stem cells. *Fluids and Barriers of the CNS*, *17*(1), 48. https://doi.org/10.1186/s12987-020-00208-1

151. Ho, B.-C., Yu, I.-S., Lu, L.-F., Rudensky, A., Chen, H.-Y., Tsai, C.-W., Chang, Y.-L., Wu, C.-T., Chang, L.-Y., Shih, S.-R., Lin, S.-W., Lee, C.-N., Yang, P.-C., & Yu, S.-L. (2014). Inhibition of miR-146a prevents enterovirus-induced death by restoring the production of type I interferon. *Nature Communications*, *5*, 3344. https://doi.org/10.1038/ncomms4344

152. Hohmann, E. L., & Kim, J. (2012). Case records of the Massachusetts General Hospital. Case 8-2012. A 53-year-old man with Crohn's disease, diarrhea, fever, and bacteremia. *The New England Journal of Medicine*, *366*(11), 1039–1045. https://doi.org/10.1056/NEJMcpc1110054

153. Hollander, H., Schaefer, P. W., & Hedley-Whyte, E. T. (2005). Case records of the Massachusetts General Hospital. Case 22-2005. An 81-year-old man with cough, fever, and altered mental status. *The New England Journal of Medicine*, *353*(3), 287–295. https://doi.org/10.1056/NEJMcpc059017

154. Hollmann, E. K., Bailey, A. K., Potharazu, A. V., Neely, M. D., Bowman, A. B., & Lippmann, E. S. (2017). Accelerated differentiation of human induced pluripotent stem cells to blood-brain barrier endothelial cells. *Fluids and Barriers of the CNS*, *14*(1), 9. https://doi.org/10.1186/s12987-017-0059-0

155. Horstmann, D. M. (1965). ENTEROVIRUS INFECTIONS: ETIOLOGIC, EPIDEMIOLOGIC AND CLINICAL ASPECTS. *California Medicine*, *103*, 1–8.

156. Hu, Y., Zai, H., Jiang, W., Yao, Y., Ou, Z., & Zhu, Q. (2021). MiR-126 in Extracellular Vesicles Derived from Hepatoblastoma Cells Promotes the Tumorigenesis of Hepatoblastoma through Inducing the Differentiation of BMSCs into Cancer Stem Cells. *Journal of Immunology Research*, *2021*, 6744715. https://doi.org/10.1155/2021/6744715

157. Huang, C. C., Liu, C. C., Chang, Y. C., Chen, C. Y., Wang, S. T., & Yeh, T. F. (1999). Neurologic complications in children with enterovirus 71 infection. *The New England Journal of Medicine*, *341*(13), 936–942. https://doi.org/10.1056/NEJM199909233411302

158. Huang, H., Zhang, S., Li, Y., Liu, Z., Mi, L., Cai, Y., Wang, X., Chen, L., Ran, H., Xiao, D., Li, F., Wu, J., Li, T., Han, Q., Chen, L., Pan, X., Li, H., Li, T., He, K., … Man, J. (2021). Suppression of mitochondrial ROS by prohibitin drives glioblastoma progression and therapeutic resistance. *Nature Communications*, *12*(1), 3720. https://doi.org/10.1038/s41467-021-24108-6

159. Huang, H.-I., & Shih, S.-R. (2015). Neurotropic Enterovirus Infections in the Central Nervous System. *Viruses*, *7*(11), 6051–6066. https://doi.org/10.3390/v7112920

160. Huang, L., Wang, T., Liu, X., Fu, Y., Zhang, S., Chu, Q., Nie, T., Tu, H., Cheng, J., & Fan, Y. (2022). Spatial-temporal-demographic and virological changes of hand, foot and mouth disease incidence after vaccination in a vulnerable region

of China. *BMC Public Health*, *22*(1), 1468. https://doi.org/10.1186/s12889-022-13860-z

161. Huang, Q., Wang, Y., Si, C., Zhao, D., Wang, Y., & Duan, Y. (2017). Interleukin-35 Modulates the Imbalance Between Regulatory T Cells and T Helper 17 Cells in Enterovirus 71-Induced Hand, Foot, and Mouth Disease. *Journal of Interferon & Cytokine Research: The Official Journal of the International Society for Interferon and Cytokine Research*, *37*(12), 522–530. https://doi.org/10.1089/jir.2017.0080

162. Huang, S.-W., Cheng, D., & Wang, J.-R. (2019). Enterovirus A71: Virulence, antigenicity, and genetic evolution over the years. *Journal of Biomedical Science*, *26*(1), 81. https://doi.org/10.1186/s12929-019-0574-1

163. Huang, S.-W., Hsu, Y.-W., Smith, D. J., Kiang, D., Tsai, H.-P., Lin, K.-H., Wang, S.-M., Liu, C.-C., Su, I.-J., & Wang, J.-R. (2009). Reemergence of enterovirus 71 in 2008 in taiwan: Dynamics of genetic and antigenic evolution from 1998 to 2008. *Journal of Clinical Microbiology*, *47*(11), 3653–3662. https://doi.org/10.1128/JCM.00630-09

164. Hung, C.-T., Kung, Y.-A., Li, M.-L., Brewer, G., Lee, K.-M., Liu, S.-T., & Shih, S.-R. (2016). Additive Promotion of Viral Internal Ribosome Entry Site-Mediated Translation by Far Upstream Element-Binding Protein 1 and an Enterovirus 71-Induced Cleavage Product. *PLoS Pathogens*, *12*(10), e1005959. https://doi.org/10.1371/journal.ppat.1005959

165. Ikenouchi, J., Sasaki, H., Tsukita, S., Furuse, M., & Tsukita, S. (2008). Loss of occludin affects tricellular localization of tricellulin. *Molecular Biology of the Cell*, *19*(11), 4687–4693. https://doi.org/10.1091/mbc.e08-05-0530

166. Ishida, H., Takemori, K., Dote, K., & Ito, H. (2006). Expression of glucose transporter-1 and aquaporin-4 in the cerebral cortex of stroke-prone spontaneously hypertensive rats in relation to the blood-brain barrier function. *American Journal of Hypertension*, *19*(1), 33–39. https://doi.org/10.1016/j.amjhyper.2005.06.023

167. Ito, R., Umehara, K., Suzuki, S., Kitamura, K., Nunoya, K.-I., Yamaura, Y., Imawaka, H., Izumi, S., Wakayama, N., Komori, T., Anzai, N., Akita, H., & Furihata, T. (2019). A Human Immortalized Cell-Based Blood-Brain Barrier Triculture Model: Development and Characterization as a Promising Tool for Drug-Brain Permeability Studies. *Molecular Pharmaceutics*, *16*(11), 4461–4471. https://doi.org/10.1021/acs.molpharmaceut.9b00519

168. Jamieson, J. J., Linville, R. M., Ding, Y. Y., Gerecht, S., & Searson, P. C. (2019). Role of iPSC-derived pericytes on barrier function of iPSC-derived brain microvascular endothelial cells in 2D and 3D. *Fluids and Barriers of the CNS*, *16*(1), 15. https://doi.org/10.1186/s12987-019-0136-7

169. Jheng, J.-R., Wang, S.-C., Jheng, C.-R., & Horng, J.-T. (2016). Enterovirus 71 induces dsRNA/PKR-dependent cytoplasmic redistribution of GRP78/BiP to promote viral replication. *Emerging Microbes & Infections*, *5*, e23. https://doi.org/10.1038/emi.2016.20

170. Jiang, M., Wei, D., Ou, W.-L., Li, K.-X., Luo, D.-Z., Li, Y.-Q., Chen, E., & Nong, G.-M. (2012). Autopsy findings in children with hand, foot, and mouth disease. *The New England Journal of Medicine*, *367*(1), 91–92. https://doi.org/10.1056/NEJMc1110981

171. Jiang, Y., Xu, J., Lai, H., & Lin, H. (2021). Association between Meteorological Parameters and Hand, Foot and Mouth Disease in Mainland China: A Systematic Review and Meta-Analysis. *Iranian Journal of Public Health*, *50*(9), 1757–1765. https://doi.org/10.18502/ijph.v50i9.7046

172. Jiao, H., Wang, Z., Liu, Y., Wang, P., & Xue, Y. (2011). Specific role of tight junction proteins claudin-5, occludin, and ZO-1 of the blood-brain barrier in a focal cerebral ischemic insult. *Journal of Molecular Neuroscience: MN*, *44*(2), 130–139. https://doi.org/10.1007/s12031-011-9496-4

173. Jiao, X.-Y., Guo, L., Huang, D.-Y., Chang, X.-L., & Qiu, Q.-C. (2014). Distribution of EV71 receptors SCARB2 and PSGL-1 in human tissues. *Virus Research*, *190*, 40–52. https://doi.org/10.1016/j.virusres.2014.05.007

174. Jin, Y., Zhang, R., Wu, W., & Duan, G. (2018). Antiviral and Inflammatory Cellular Signaling Associated with Enterovirus 71 Infection. *Viruses*, *10*(4), E155. https://doi.org/10.3390/v10040155

175. Johnson, R. T., Shuey, H. E., & Buescher, E. L. (1960). Epidemic central nervous system disease of mixed enterovirus etiology. I. Clinical and epidemiologic description. *American Journal of Hygiene*, *71*, 321–330. https://doi.org/10.1093/oxfordjournals.aje.a120116

176. Jubelt, B., Mihai, C., Li, T. M., & Veerapaneni, P. (2011). Rhombencephalitis / brainstem encephalitis. *Current Neurology and Neuroscience Reports*, *11*(6), 543–552. https://doi.org/10.1007/s11910-011-0228-5

177. Jurkiewicz, D., Michalec, K., Skowronek, K., & Nałęcz, K. A. (2017). Tight junction protein ZO-1 controls organic cation/carnitine transporter OCTN2 (SLC22A5) in a protein kinase C-dependent way. *Biochimica Et Biophysica Acta. Molecular Cell Research*, *1864*(5), 797–805. https://doi.org/10.1016/j.bbamcr.2017.02.014

178. Kadoguchi, M., Arakawa, H., Honda, R., Hotta, K., Shirasaka, Y., Deguchi, Y., & Tamai, I. (2022). Characterization of Aripiprazole Uptake Transporter in the Blood-Brain Barrier Model hCMEC/D3 Cells by Targeted siRNA Screening. *Pharmaceutical Research*, *39*(7), 1549–1559. https://doi.org/10.1007/s11095-022-03223-z

179. Kamau, E., Nguyen, D., Celma, C., Blomqvist, S., Horby, P., Simmonds, P., & Harvala, H. (2021). Seroprevalence and Virologic Surveillance of Enterovirus 71 and Coxsackievirus A6, United Kingdom, 2006-2017. *Emerging Infectious Diseases*, *27*(9), 2261–2268. https://doi.org/10.3201/eid2709.204915

180. Karrasch, M., Fischer, E., Scholten, M., Sauerbrei, A., Henke, A., Renz, D. M., Mentzel, H.-J., Böer, K., Böttcher, S., Diedrich, S., Krumbholz, A., & Zell, R. (2016). A severe pediatric infection with a novel enterovirus A71 strain, Thuringia, Germany. *Journal of Clinical Virology: The Official Publication of the Pan American Society for Clinical Virology*, *84*, 90–95. https://doi.org/10.1016/j.jcv.2016.09.007

181. Kataoka, C., Suzuki, T., Kotani, O., Iwata-Yoshikawa, N., Nagata, N., Ami, Y., Wakita, T., Nishimura, Y., & Shimizu, H. (2015). The Role of VP1 Amino Acid Residue 145 of Enterovirus 71 in Viral Fitness and Pathogenesis in a Cynomolgus Monkey Model. *PLoS Pathogens*, *11*(7), e1005033. https://doi.org/10.1371/journal.ppat.1005033

182. Kaya, M., & Ahishali, B. (2011). Assessment of permeability in barrier type of endothelium in brain using tracers: Evans blue, sodium fluorescein, and horseradish peroxidase. *Methods in Molecular Biology (Clifton, N.J.)*, *763*, 369–382. https://doi.org/10.1007/978-1-61779-191-8_25

183. Ke, Y.-Y., Chen, Y.-C., & Lin, T.-H. (2006). Structure of the virus capsid protein VP1 of enterovirus 71 predicted by some homology modeling and molecular docking studies. *Journal of Computational Chemistry*, *27*(13), 1556–1570. https://doi.org/10.1002/jcc.20460

184. Kealy, J., Greene, C., & Campbell, M. (2020). Blood-brain barrier regulation in psychiatric disorders. *Neuroscience Letters*, *726*, 133664. https://doi.org/10.1016/j.neulet.2018.06.033

185. Kean, K. M., Teterina, N., & Girard, M. (1990). Cleavage specificity of the poliovirus 3C protease is not restricted to Gln-Gly at the 3C/3D junction. *The Journal of General Virology*, *71 (Pt 11)*, 2553–2563. https://doi.org/10.1099/0022-1317-71-11-2553

186. Kesimer, M., Scull, M., Brighton, B., DeMaria, G., Burns, K., O'Neal, W., Pickles, R. J., & Sheehan, J. K. (2009). Characterization of exosome-like vesicles released from human tracheobronchial ciliated epithelium: A possible role in

innate defense. *FASEB Journal: Official Publication of the Federation of American Societies for Experimental Biology*, *23*(6), 1858–1868. https://doi.org/10.1096/fj.08-119131

187. Kim, D. H., Park, S., Kim, H., Choi, Y. J., Kim, S. Y., Sung, K. J., Sung, Y. H., Choi, C.-M., Yun, M., Yi, Y.-S., Lee, C. W., Kim, S.-Y., Lee, J. C., & Rho, J. K. (2020). Tumor-derived exosomal miR-619-5p promotes tumor angiogenesis and metastasis through the inhibition of RCAN1.4. *Cancer Letters*, *475*, 2–13. https://doi.org/10.1016/j.canlet.2020.01.023

188. Kim, H., Yang, E., Lee, J., Kim, S.-H., Shin, J.-S., Park, J. Y., Choi, S. J., Kim, S. J., & Choi, I.-H. (2008). Double-stranded RNA mediates interferon regulatory factor 3 activation and interleukin-6 production by engaging Toll-like receptor 3 in human brain astrocytes. *Immunology*, *124*(4), 480–488. https://doi.org/10.1111/j.1365-2567.2007.02799.x

189. Kim, H.-J., Son, H. S., Lee, S. W., Yoon, Y., Hyeon, J.-Y., Chung, G. T., Lee, J.-W., & Yoo, J. S. (2019). Efficient expression of enterovirus 71 based on virus-like particles vaccine. *PloS One*, *14*(3), e0210477. https://doi.org/10.1371/journal.pone.0210477

190. Kim, W., Kim, J., Lee, S.-Y., Kim, H.-M., Joo, K. M., & Nam, D.-H. (2022). Simplified in vitro 3D co-culture-based blood-brain barrier model using transwell. *Biochemical and Biophysical Research Communications*, *620*, 63–68. https://doi.org/10.1016/j.bbrc.2022.06.083

191. Kim, Y.-A., Park, S. L., Kim, M.-Y., Lee, S. H., Baik, E. J., Moon, C.-H., & Jung, Y.-S. (2010). Role of PKCbetaII and PKCdelta in blood-brain barrier

permeability during aglycemic hypoxia. *Neuroscience Letters*, *468*(3), 254–258. https://doi.org/10.1016/j.neulet.2009.11.007

192. Kobayashi, K., & Koike, S. (2020). Cellular receptors for enterovirus A71. *Journal of Biomedical Science*, *27*(1), 23. https://doi.org/10.1186/s12929-020-0615-9

193. Kobayashi, K., Nishimura, H., Mizuta, K., Nishizawa, T., Chu, S. T., Ichimura, H., & Koike, S. (2021). Virulence of Enterovirus A71 Fluctuates Depending on the Phylogenetic Clade Formed in the Epidemic Year and Epidemic Region. *Journal of Virology*, *95*(23), e0151521. https://doi.org/10.1128/JVI.01515-21

194. Kobayashi, K., Sudaka, Y., Takashino, A., Imura, A., Fujii, K., & Koike, S. (2018). Amino Acid Variation at VP1-145 of Enterovirus 71 Determines Attachment Receptor Usage and Neurovirulence in Human Scavenger Receptor B2 Transgenic Mice. *Journal of Virology*, *92*(15), e00681-18. https://doi.org/10.1128/JVI.00681-18

195. Koepsell, H. (2020). Glucose transporters in brain in health and disease. *Pflugers Archiv: European Journal of Physiology*, *472*(9), 1299–1343. https://doi.org/10.1007/s00424-020-02441-x

196. Koh, W. M., Badaruddin, H., La, H., Chen, M. I.-C., & Cook, A. R. (2018). Severity and burden of hand, foot and mouth disease in Asia: A modelling study. *BMJ Global Health*, *3*(1), e000442. https://doi.org/10.1136/bmjgh-2017-000442

197. Koh, W. M., Bogich, T., Siegel, K., Jin, J., Chong, E. Y., Tan, C. Y., Chen, M. I., Horby, P., & Cook, A. R. (2016). The Epidemiology of Hand, Foot and Mouth

Disease in Asia: A Systematic Review and Analysis. *The Pediatric Infectious Disease Journal*, *35*(10), e285-300. https://doi.org/10.1097/INF.0000000000001242

198. Koroleva, G. A., Karmysheva, V. Y., & Lukashev, A. N. (2014). Enterovirus 71 pathogenicity in monkeys and cotton rats. *Archives of Virology*, *159*(5), 1133–1138. https://doi.org/10.1007/s00705-013-1895-0

199. Kouwaki, T., Fukushima, Y., Daito, T., Sanada, T., Yamamoto, N., Mifsud, E. J., Leong, C. R., Tsukiyama-Kohara, K., Kohara, M., Matsumoto, M., Seya, T., & Oshiumi, H. (2016). Extracellular Vesicles Including Exosomes Regulate Innate Immune Responses to Hepatitis B Virus Infection. *Frontiers in Immunology*, *7*, 335. https://doi.org/10.3389/fimmu.2016.00335

200. Kouwaki, T., Okamoto, M., Tsukamoto, H., Fukushima, Y., & Oshiumi, H. (2017). Extracellular Vesicles Deliver Host and Virus RNA and Regulate Innate Immune Response. *International Journal of Molecular Sciences*, *18*(3), E666. https://doi.org/10.3390/ijms18030666

201. Kovacs, A., Wasserman, S. S., Burns, D., Wright, D. J., Cohn, J., Landay, A., Weber, K., Cohen, M., Levine, A., Minkoff, H., Miotti, P., Palefsky, J., Young, M., Reichelderfer, P., DATRI Study Group, & WIHS Study Group. (2001). Determinants of HIV-1 shedding in the genital tract of women. *Lancet (London, England)*, *358*(9293), 1593–1601. https://doi.org/10.1016/S0140-6736(01)06653-3

202. Krause, D., Mischeck, U., Galla, H. J., & Dermietzel, R. (1991). Correlation of zonula occludens ZO-1 antigen expression and transendothelial resistance in

porcine and rat cultured cerebral endothelial cells. *Neuroscience Letters*, *128*(2), 301–304. https://doi.org/10.1016/0304-3940(91)90284-z

203. Kriaučiūnaitė, K., Kaušylė, A., Pajarskienė, J., Tunaitis, V., Lim, D., Verkhratsky, A., & Pivoriūnas, A. (2021). Immortalised Hippocampal Astrocytes from 3xTG-AD Mice Fail to Support BBB Integrity In Vitro: Role of Extracellular Vesicles in Glial-Endothelial Communication. *Cellular and Molecular Neurobiology*, *41*(3), 551–562. https://doi.org/10.1007/s10571-020-00871-w

204. Kristensen, T., & Belsham, G. J. (2019). Identification of a short, highly conserved, motif required for picornavirus capsid precursor processing at distal sites. *PLoS Pathogens*, *15*(1), e1007509. https://doi.org/10.1371/journal.ppat.1007509

205. Kristensen, T., Normann, P., & Belsham, G. J. (2022). The N-terminal region (VP4) of the foot-and-mouth disease capsid precursor (P1-2A) is not required during its synthesis to allow subsequent processing by the 3C protease. *Virology*, *570*, 29–34. https://doi.org/10.1016/j.virol.2022.03.006

206. Kugler, E. C., Greenwood, J., & MacDonald, R. B. (2021). The “Neuro-Glial-Vascular” Unit: The Role of Glia in Neurovascular Unit Formation and Dysfunction. *Frontiers in Cell and Developmental Biology*, *9*, 732820. https://doi.org/10.3389/fcell.2021.732820

207. Kulczar, C., Lubin, K. E., Lefebvre, S., Miller, D. W., & Knipp, G. T. (2017). Development of a direct contact astrocyte-human cerebral microvessel endothelial cells blood-brain barrier coculture model. *The Journal of Pharmacy and Pharmacology*, *69*(12), 1684–1696. https://doi.org/10.1111/jphp.12803

208. Kuo, F.-L., Khanh, T. H., Chung, W.-Y., Hung, N. T., Luo, S.-T., Chang, W.-C., Nhan, L. N. T., Thinh, L. Q., & Lee, M.-S. (2020). Seroprevalence of EV-A71 neutralizing antibodies following the 2011 epidemic in HCMC, Vietnam. *PLoS Neglected Tropical Diseases*, *14*(3), e0008124. https://doi.org/10.1371/journal.pntd.0008124

209. Kuo, R.-L., Kao, L.-T., Lin, S.-J., Wang, R. Y.-L., & Shih, S.-R. (2013). MDA5 Plays a Crucial Role in Enterovirus 71 RNA-Mediated IRF3 Activation. *PLoS ONE*, *8*(5), e63431. https://doi.org/10.1371/journal.pone.0063431

210. Kuo, W.-T., Zuo, L., Odenwald, M. A., Madha, S., Singh, G., Gurniak, C. B., Abraham, C., & Turner, J. R. (2021). The Tight Junction Protein ZO-1 Is Dispensable for Barrier Function but Critical for Effective Mucosal Repair. *Gastroenterology*, *161*(6), 1924–1939. https://doi.org/10.1053/j.gastro.2021.08.047

211. Lafolie, J., Labbé, A., L'Honneur, A. S., Madhi, F., Pereira, B., Decobert, M., Adam, M. N., Gouraud, F., Faibis, F., Arditty, F., Marque-Juillet, S., Guitteny, M. A., Lagathu, G., Verdan, M., Rozenberg, F., Mirand, A., Peigue-Lafeuille, H., Henquell, C., Bailly, J.-L., … Blood Enterovirus Diagnosis Infection (BLEDI) in paediatric population study team. (2018). Assessment of blood enterovirus PCR testing in paediatric populations with fever without source, sepsis-like disease, or suspected meningitis: A prospective, multicentre, observational cohort study. *The Lancet. Infectious Diseases*, *18*(12), 1385–1396. https://doi.org/10.1016/S1473-3099(18)30479-1

212. Lai, J. K. F., Sam, I.-C., Verlhac, P., Baguet, J., Eskelinen, E.-L., Faure, M., & Chan, Y. F. (2017). 2BC Non-Structural Protein of Enterovirus A71 Interacts with SNARE Proteins to Trigger Autolysosome Formation. *Viruses*, *9*(7), E169. https://doi.org/10.3390/v9070169

213. Lai, M.-C., Chen, H.-H., Xu, P., & Wang, R. Y. L. (2020a). Translation control of Enterovirus A71 gene expression. *Journal of Biomedical Science*, *27*(1), 22. https://doi.org/10.1186/s12929-019-0607-9

214. Lai, M.-C., Chen, H.-H., Xu, P., & Wang, R. Y. L. (2020b). Translation control of Enterovirus A71 gene expression. *Journal of Biomedical Science*, *27*(1), 22. https://doi.org/10.1186/s12929-019-0607-9

215. Lai, R.-H., Chow, Y.-H., Chung, N.-H., Chen, T.-C., Shie, F.-S., & Juang, J.-L. (2022). Neurotropic EV71 causes encephalitis by engaging intracellular TLR9 to elicit neurotoxic IL12-p40-iNOS signaling. *Cell Death & Disease*, *13*(4), 328. https://doi.org/10.1038/s41419-022-04771-3

216. Langen, U. H., Ayloo, S., & Gu, C. (2019). Development and Cell Biology of the Blood-Brain Barrier. *Annual Review of Cell and Developmental Biology*, *35*, 591–613. https://doi.org/10.1146/annurev-cellbio-100617-062608

217. Lee, C. S., Won, C., Yoo, H., Yi, E. H., Cho, Y., Maeng, J. W., Sung, S. H., Ye, S.-K., & Chung, M.-H. (2009). Inhibition of double-stranded RNA-induced inducible nitric oxide synthase expression by fraxinellone and sauchinone in murine microglia. *Biological & Pharmaceutical Bulletin*, *32*(11), 1870–1874. https://doi.org/10.1248/bpb.32.1870

218. Lee, H. J., Kong, P.-J., Lee, S.-H., Kwon, O.-Y., Chun, W.-J., & Kim, S.-S. (2007). Differences between lipopolysaccharide and double-stranded RNA in innate immune responses of BV2 microglial cells. *The International Journal of Neuroscience*, *117*(7), 885–894. https://doi.org/10.1080/00207450600592156

219. Lee, J. Y., Son, M., Kang, J. H., & Choi, U. Y. (2018). Serum interleukin-6 levels as an indicator of aseptic meningitis among children with enterovirus 71-induced hand, foot and mouth disease. *Postgraduate Medicine*, *130*(2), 258–263. https://doi.org/10.1080/00325481.2018.1416257

220. Lee, K.-M., Chen, C.-J., & Shih, S.-R. (2017). Regulation Mechanisms of Viral IRES-Driven Translation. *Trends in Microbiology*, *25*(7), 546–561. https://doi.org/10.1016/j.tim.2017.01.010

221. Lee, K.-M., Wu, C.-C., Wu, S.-E., Lin, Y.-H., Wang, L.-T., Chang, C.-R., Huang, P.-N., Shih, S.-R., & Kuo, R.-L. (2020). The RNA-dependent RNA polymerase of enterovirus A71 associates with ribosomal proteins and positively regulates protein translation. *RNA Biology*, *17*(4), 608–622. https://doi.org/10.1080/15476286.2020.1722448

222. Lee, P.-H., Liu, C.-M., Ho, T.-S., Tsai, Y.-C., Lin, C.-C., Wang, Y.-F., Chen, Y.-L., Yu, C.-K., Wang, S.-M., Liu, C.-C., Shiau, A.-L., Lei, H.-Y., & Chang, C.-P. (2015). Enterovirus 71 virion-associated galectin-1 facilitates viral replication and stability. *PloS One*, *10*(2), e0116278. https://doi.org/10.1371/journal.pone.0116278

223. Lee, Y.-R., Wang, P.-S., Wang, J.-R., & Liu, H.-S. (2014). Enterovirus 71-induced autophagy increases viral replication and pathogenesis in a suckling

mouse model. *Journal of Biomedical Science*, *21*, 80. https://doi.org/10.1186/s12929-014-0080-4

224. Lehmann, S. M., Rosenberger, K., Krüger, C., Habbel, P., Derkow, K., Kaul, D., Rybak, A., Brandt, C., Schott, E., Wulczyn, F. G., & Lehnardt, S. (2012). Extracellularly delivered single-stranded viral RNA causes neurodegeneration dependent on TLR7. *Journal of Immunology (Baltimore, Md.: 1950)*, *189*(3), 1448–1458. https://doi.org/10.4049/jimmunol.1201078

225. Lei, X., Sun, Z., Liu, X., Jin, Q., He, B., & Wang, J. (2011). Cleavage of the adaptor protein TRIF by enterovirus 71 3C inhibits antiviral responses mediated by Toll-like receptor 3. *Journal of Virology*, *85*(17), 8811–8818. https://doi.org/10.1128/JVI.00447-11

226. Lei, X., Xiao, X., & Wang, J. (2016). Innate Immunity Evasion by Enteroviruses: Insights into Virus-Host Interaction. *Viruses*, *8*(1), 22. https://doi.org/10.3390/v8010022

227. Lei, X., Xiao, X., Zhang, Z., Ma, Y., Qi, J., Wu, C., Xiao, Y., Zhou, Z., He, B., & Wang, J. (2017). The Golgi protein ACBD3 facilitates Enterovirus 71 replication by interacting with 3A. *Scientific Reports*, *7*, 44592. https://doi.org/10.1038/srep44592

228. Lewis, S. D., Butchi, N. B., Khaleduzzaman, M., Morgan, T. W., Du, M., Pourciau, S., Baker, D. G., Akira, S., & Peterson, K. E. (2008). Toll-like receptor 7 is not necessary for retroviral neuropathogenesis but does contribute to virus-induced neuroinflammation. *Journal of Neurovirology*, *14*(6), 492–502. https://doi.org/10.1080/13550280802345723

229. Li, C., Qiao, Q., Hao, S.-B., Dong, Z., Zhao, L., Ji, J., Wang, Z.-Y., & Wen, H.-L. (2018). Nonstructural protein 2A modulates replication and virulence of enterovirus 71. *Virus Research*, *244*, 262–269. https://doi.org/10.1016/j.virusres.2017.11.023

230. Li, F., Liu, P., Guo, Y., Han, Z., Liu, Y., Wang, Y., Song, L., Cheng, J., & Chen, Z. (2018). Association of Interleukin-17F gene polymorphisms with susceptibility to severe enterovirus 71 infection in Chinese children. *Archives of Virology*, *163*(7), 1933–1939. https://doi.org/10.1007/s00705-018-3807-9

231. Li, F., Liu, X.-P., Li, J.-A., Han, Z.-L., Liu, P.-P., Wang, Y.-Y., Song, L., & Chen, Z.-B. (2015). Correlation of an interleukin-4 gene polymorphism with susceptibility to severe enterovirus 71 infection in Chinese children. *Archives of Virology*, *160*(4), 1035–1042. https://doi.org/10.1007/s00705-015-2356-8

232. Li, F., Wang, Y., Yu, L., Cao, S., Wang, K., Yuan, J., Wang, C., Wang, K., Cui, M., & Fu, Z. F. (2015). Viral Infection of the Central Nervous System and Neuroinflammation Precede Blood-Brain Barrier Disruption during Japanese Encephalitis Virus Infection. *Journal of Virology*, *89*(10), 5602–5614. https://doi.org/10.1128/JVI.00143-15

233. Li, H., Su, L., Zhang, T., He, F., & Yin, Y. (2019). MRI reveals segmental distribution of enterovirus lesions in the central nervous system: A probable clinical evidence of retrograde axonal transport of EV-A71. *Journal of Neurovirology*, *25*(3), 354–362. https://doi.org/10.1007/s13365-019-00724-3

234. Li, J., Chen, Z., Lv, T., & Han, Z. (2014). Genetic polymorphism of CCL2-2518, CXCL10-201, IL8+781 and susceptibility to severity of Enterovirus-71 infection

in a Chinese population. *Inflammation Research: Official Journal of the European Histamine Research Society ... [et Al.]*, *63*(7), 549–556. https://doi.org/10.1007/s00011-014-0724-6

235. Li, J.-P., & Kusche-Gullberg, M. (2016). Heparan Sulfate: Biosynthesis, Structure, and Function. *International Review of Cell and Molecular Biology*, *325*, 215–273. https://doi.org/10.1016/bs.ircmb.2016.02.009

236. Li, R., Liu, L., Mo, Z., Wang, X., Xia, J., Liang, Z., Zhang, Y., Li, Y., Mao, Q., Wang, J., Jiang, L., Dong, C., Che, Y., Huang, T., Jiang, Z., Xie, Z., Wang, L., Liao, Y., Liang, Y., … Li, Q. (2014). An inactivated enterovirus 71 vaccine in healthy children. *The New England Journal of Medicine*, *370*(9), 829–837. https://doi.org/10.1056/NEJMoa1303224

237. Li, Y., Gao, F., Wang, Y., Li, J., Zhang, Y., Lv, H., Wang, S., Yang, H., Liu, X., Li, K., Wang, H., Yin, Z., Liang, Z., An, Z., Mao, Q., & Feng, Z. (2021). Immunogenicity and safety of inactivated enterovirus A71 vaccines in children aged 6-35 months in China: A non-inferiority, randomised controlled trial. *The Lancet Regional Health. Western Pacific*, *16*, 100284. https://doi.org/10.1016/j.lanwpc.2021.100284

238. Li, Y., Zhai, S., Li, M., Wang, Y., Lu, T., Deng, H., Zhang, X., & Dang, S. (2017). [Polymorphisms of TLR7 rs3853839 and rs179010 are associated with susceptibility to and severity of hand, foot and mouth disease caused by enterovirus 71 in male children]. *Xi Bao Yu Fen Zi Mian Yi Xue Za Zhi = Chinese Journal of Cellular and Molecular Immunology*, *33*(7), 953–958.

239. Li, Y., Zhu, R., Qian, Y., Deng, J., Sun, Y., Liu, L., Wang, F., & Zhao, L. (2011). Comparing Enterovirus 71 with Coxsackievirus A16 by analyzing nucleotide sequences and antigenicity of recombinant proteins of VP1s and VP4s. *BMC Microbiology*, *11*, 246. https://doi.org/10.1186/1471-2180-11-246

240. Li, Y.-P., Li, M., Jia, X.-L., Deng, H.-L., Wang, W.-J., Wu, F.-P., Wang, J., & Dang, S.-S. (2018). Association of gene polymorphisms of pattern-recognition receptor signaling pathway with the risk and severity of hand, foot, and mouth disease caused by enterovirus 71 in Chinese Han population. *Journal of Medical Virology*, *90*(4), 692–698. https://doi.org/10.1002/jmv.25000

241. Li, Y.-P., Wang, M.-Q., Liu, C.-R., Deng, H.-L., Wu, Y., Dang, S.-S., & Xu, L.-H. (2021). Polymorphisms in the DC-SIGN gene and their association with the severity of hand, foot, and mouth disease caused by enterovirus 71. *Archives of Virology*, *166*(4), 1133–1140. https://doi.org/10.1007/s00705-021-04991-6

242. Li, Z., Wang, H., Chen, Y., Niu, J., Guo, Q., Leng, Q., Huang, Z., Deng, Z., & Meng, G. (2017). Interleukin-18 protects mice from Enterovirus 71 infection. *Cytokine*, *96*, 132–137. https://doi.org/10.1016/j.cyto.2017.04.002

243. Liang, L., Lin, R., Xie, Y., Lin, H., Shao, F., Rui, W., & Chen, H. (2021). The Role of Cyclophilins in Inflammatory Bowel Disease and Colorectal Cancer. *International Journal of Biological Sciences*, *17*(10), 2548–2560. https://doi.org/10.7150/ijbs.58671

244. Liao, Y.-T., Wang, S.-M., & Chen, S.-H. (2019). Anti-inflammatory and antiviral effects of minocycline in enterovirus 71 infections. *Biomedicine &*

Pharmacotherapy = Biomedecine & Pharmacotherapie, *118*, 109271. https://doi.org/10.1016/j.biopha.2019.109271

245. Lim, Z. Q., Ng, Q. Y., Oo, Y., Chu, J. J. H., Ng, S. Y., Sze, S. K., & Alonso, S. (2021). Enterovirus-A71 exploits peripherin and Rac1 to invade the central nervous system. *EMBO Reports*, *22*(6), e51777. https://doi.org/10.15252/embr.202051777

246. Lin, J.-Y., & Huang, H.-I. (2020). Autophagy is induced and supports virus replication in Enterovirus A71-infected human primary neuronal cells. *Scientific Reports*, *10*(1), 15234. https://doi.org/10.1038/s41598-020-71970-3

247. Lin, J.-Y., & Shih, S.-R. (2014). Cell and tissue tropism of enterovirus 71 and other enteroviruses infections. *Journal of Biomedical Science*, *21*, 18. https://doi.org/10.1186/1423-0127-21-18

248. Lin, J.-Y., Weng, K.-F., Chang, C.-K., Gong, Y.-N., Huang, G.-J., Lee, H.-L., Chen, Y.-C., Huang, C.-C., Lu, J.-Y., Huang, P.-N., Chiang, H.-J., Chen, C.-M., & Shih, S.-R. (2021). Enterovirus A71 Induces Neurological Diseases and Dynamic Variants in Oral Infection of Human SCARB2-Transgenic Weaned Mice. *Journal of Virology*, *95*(21), e0089721. https://doi.org/10.1128/JVI.00897-21

249. Lin, S.-Y., Chiu, H.-Y., Chiang, B.-L., & Hu, Y.-C. (2015). Development of EV71 virus-like particle purification processes. *Vaccine*, *33*(44), 5966–5973. https://doi.org/10.1016/j.vaccine.2015.04.077

250. Lindahl, U., Kusche-Gullberg, M., & Kjellén, L. (1998). Regulated diversity of heparan sulfate. *The Journal of Biological Chemistry*, *273*(39), 24979–24982. https://doi.org/10.1074/jbc.273.39.24979

251. Liu, J., Gao, R., Gu, X., Yu, B., Wu, Y., Li, Q., Xiang, P., & Xu, H. (2022). A New Insight into Toxicity of Colchicine Analogues by Molecular Docking Analysis Based on Intestinal Tight Junction Protein ZO-1. *Molecules (Basel, Switzerland)*, *27*(6), 1797. https://doi.org/10.3390/molecules27061797

252. Liu, J., Jin, X., Liu, K. J., & Liu, W. (2012). Matrix metalloproteinase-2-mediated occludin degradation and caveolin-1-mediated claudin-5 redistribution contribute to blood-brain barrier damage in early ischemic stroke stage. *The Journal of Neuroscience: The Official Journal of the Society for Neuroscience*, *32*(9), 3044–3057. https://doi.org/10.1523/JNEUROSCI.6409-11.2012

253. Liu, J., Li, X., Fan, X., Ma, C., Qin, C., & Zhang, L. (2013). Adoptive transfer of macrophages from adult mice reduces mortality in mice infected with human enterovirus 71. *Archives of Virology*, *158*(2), 387–397. https://doi.org/10.1007/s00705-012-1495-4

254. Liu, L.-B., Xue, Y.-X., Liu, Y.-H., & Wang, Y.-B. (2008). Bradykinin increases blood-tumor barrier permeability by down-regulating the expression levels of ZO-1, occludin, and claudin-5 and rearranging actin cytoskeleton. *Journal of Neuroscience Research*, *86*(5), 1153–1168. https://doi.org/10.1002/jnr.21558

255. Liu, M. Y., Liu, W., Luo, J., Liu, Y., Zhu, Y., Berman, H., & Wu, J. (2011). Characterization of an outbreak of hand, foot, and mouth disease in Nanchang,

China in 2010. *PloS One*, *6*(9), e25287. https://doi.org/10.1371/journal.pone.0025287

256. Liu, Y., Zhang, F., Fu, C., Wu, S., Chen, X., Shi, Y., Zhou, B., Zhang, L., Zhang, Y., Han, S., Yin, J., Peng, B., He, X., & Liu, W. (2015). Combination of intratypic and intertypic recombinant events in EV71: A novel evidence for the "triple-recombinant" strains of genotype A viruses in Mainland China from 2008 to 2010. *Virus Genes*, *50*(3), 365–374. https://doi.org/10.1007/s11262-015-1170-4

257. Liu, Y., Zhou, J., Ji, G., Gao, Y., Zhang, C., Zhang, T., Huo, J., Liang, W., Yang, J., Shi, Y., & Zhao, S. (2022). A novel subgenotype C6 Enterovirus A71 originating from the recombination between subgenotypes C4 and C2 strains in mainland China. *Scientific Reports*, *12*(1), 593. https://doi.org/10.1038/s41598-021-04604-x

258. Liu, Z.-W., Zhuang, Z.-C., Chen, R., Wang, X.-R., Zhang, H.-L., Li, S.-H., Wang, Z.-Y., & Wen, H.-L. (2019). Enterovirus 71 VP1 Protein Regulates Viral Replication in SH-SY5Y Cells via the mTOR Autophagy Signaling Pathway. *Viruses*, *12*(1), E11. https://doi.org/10.3390/v12010011

259. Loiola, R. A., García-Gabilondo, M., Grayston, A., Bugno, P., Kowalska, A., Duban-Deweer, S., Rizzi, E., Hachani, J., Sano, Y., Shimizu, F., Kanda, T., Mysiorek, C., Mazurek, M. P., Rosell, A., & Gosselet, F. (2021). Secretome of endothelial progenitor cells from stroke patients promotes endothelial barrier tightness and protects against hypoxia-induced vascular leakage. *Stem Cell Research & Therapy*, *12*(1), 552. https://doi.org/10.1186/s13287-021-02608-y

260. Long, L., Xu, L., Xiao, Z., Hu, S., Luo, R., Wang, H., Lu, X., Xu, Z., Yao, X., Zhou, L., Long, H., Gong, J., Song, Y., Zhao, L., Luo, K., Zhang, M., Feng, L., Yang, L., Sheng, X., … Xiao, B. (2016). Neurological complications and risk factors of cardiopulmonary failure of EV-A71-related hand, foot and mouth disease. *Scientific Reports*, *6*, 23444. https://doi.org/10.1038/srep23444

261. Lu, J.-Y., Brewer, G., Li, M.-L., Lin, K.-Z., Huang, C.-C., Yen, L.-C., & Lin, J.-Y. (2021). Secretory Carrier Membrane Protein 3 Interacts with 3A Viral Protein of Enterovirus and Participates in Viral Replication. *Microbiology Spectrum*, *9*(1), e0047521. https://doi.org/10.1128/Spectrum.00475-21

262. Lu, T. M., Barcia Durán, J. G., Houghton, S., Rafii, S., Redmond, D., & Lis, R. (2021). Human Induced Pluripotent Stem Cell-Derived Brain Endothelial Cells: Current Controversies. *Frontiers in Physiology*, *12*, 642812. https://doi.org/10.3389/fphys.2021.642812

263. Lu, Y., Xu, Z., Shen, F., Lin, R., Li, H., Lv, X., & Liu, Z. (2020). Propofol Protects Against TNF-α-induced Blood-brain Barrier Disruption via the PIM-1/eNOS/NO Pathway. *Current Neurovascular Research*, *17*(4), 471–479. https://doi.org/10.2174/1567202617999200819142021

264. Ludlam, C. A., Powderly, W. G., Bozzette, S., Diamond, M., Koerper, M. A., Kulkarni, R., Ritchie, B., Siegel, J., Simmonds, P., Stanley, S., Tapper, M. L., & von Depka, M. (2006). Clinical perspectives of emerging pathogens in bleeding disorders. *Lancet (London, England)*, *367*(9506), 252–261. https://doi.org/10.1016/S0140-6736(06)68036-7

265. Luo, W., Liang, P., Puthiyakunnon, S., Yang, L., & Hong, C. (2019). VP1-binding protein glucose-regulated protein 78 as an important mediator for enterovirus 71 infecting human brain microvascular endothelial cells. *Indian Journal of Medical Microbiology*, *37*(3), 406–414. https://doi.org/10.4103/ijmm.IJMM_19_194

266. Luo, W., Yang, L., Pan, Q., & Qiu, L. (2020). [Enterovirus 71 can induce autophagy and apoptosis of THP-1 macrophages]. *Nan Fang Yi Ke Da Xue Xue Bao = Journal of Southern Medical University*, *40*(6), 828–836. https://doi.org/10.12122/j.issn.1673-4254.2020.06.09

267. Luo, Y., Fukuhara, M., Weitzman, M., & Rizzolo, L. J. (2006). Expression of JAM-A, AF-6, PAR-3 and PAR-6 during the assembly and remodeling of RPE tight junctions. *Brain Research*, *1110*(1), 55–63. https://doi.org/10.1016/j.brainres.2006.06.059

268. Lv, T., Li, J., Han, Z., & Chen, Z. (2013). Association of interleukin-17F gene polymorphism with enterovirus 71 encephalitis in patients with hand, foot, and mouth disease. *Inflammation*, *36*(4), 977–981. https://doi.org/10.1007/s10753-013-9629-8

269. Lynch, M. J., & Gobbo, O. L. (2021). Advances in Non-Animal Testing Approaches towards Accelerated Clinical Translation of Novel Nanotheranostic Therapeutics for Central Nervous System Disorders. *Nanomaterials (Basel, Switzerland)*, *11*(10), 2632. https://doi.org/10.3390/nano11102632

270. Lyu, K., Ding, J., Han, J.-F., Zhang, Y., Wu, X.-Y., He, Y.-L., Qin, C.-F., & Chen, R. (2014). Human enterovirus 71 uncoating captured at atomic resolution. *Journal of Virology*, *88*(6), 3114–3126. https://doi.org/10.1128/JVI.03029-13

271. Ma, Y., He, X., Liu, X., Long, Y., & Chen, Y. (2022). Endothelial Microparticles Derived from Primary Pulmonary Microvascular Endothelial Cells Mediate Lung Inflammation in Chronic Obstructive Pulmonary Disease by Transferring microRNA-126. *Journal of Inflammation Research*, *15*, 1399–1411. https://doi.org/10.2147/JIR.S349818

272. Mandary, M. B., & Poh, C. L. (2018). Changes in the EV-A71 Genome through Recombination and Spontaneous Mutations: Impact on Virulence. *Viruses*, *10*(6), E320. https://doi.org/10.3390/v10060320

273. Mao, L., Wu, J., Shen, L., Yang, J., Chen, J., & Xu, H. (2016). Enterovirus 71 transmission by exosomes establishes a productive infection in human neuroblastoma cells. *Virus Genes*, *52*(2), 189–194. https://doi.org/10.1007/s11262-016-1292-3

274. Mao, Q., Wang, Y., Bian, L., Xu, M., & Liang, Z. (2016). EV-A71 vaccine licensure: A first step for multivalent enterovirus vaccine to control HFMD and other severe diseases. *Emerging Microbes & Infections*, *5*(7), e75. https://doi.org/10.1038/emi.2016.73

275. Martins, J. P., Alves, C. J., Neto, E., & Lamghari, M. (2016). Communication from the periphery to the hypothalamus through the blood-brain barrier: An in vitro platform. *International Journal of Pharmaceutics*, *499*(1–2), 119–130. https://doi.org/10.1016/j.ijpharm.2015.12.058

276. Matsuzaki, K., Fujita, K., Tomiyama, E., Hatano, K., Hayashi, Y., Wang, C., Ishizuya, Y., Yamamoto, Y., Hayashi, T., Kato, T., Jingushi, K., Kawashima, A., Ujike, T., Nagahara, A., Uemura, M., Tsujikawa, K., & Nonomura, N. (2021). MiR-30b-3p and miR-126-3p of urinary extracellular vesicles could be new biomarkers for prostate cancer. *Translational Andrology and Urology*, *10*(4), 1918–1927. https://doi.org/10.21037/tau-20-421

277. McConnell, H. L., Kersch, C. N., Woltjer, R. L., & Neuwelt, E. A. (2017). The Translational Significance of the Neurovascular Unit. *The Journal of Biological Chemistry*, *292*(3), 762–770. https://doi.org/10.1074/jbc.R116.760215

278. McDouall, A., Zhou, K. Q., Bennet, L., Green, C. R., Gunn, A. J., & Davidson, J. O. (2022). Connexins, Pannexins and Gap Junctions in Perinatal Brain Injury. *Biomedicines*, *10*(6), 1445. https://doi.org/10.3390/biomedicines10061445

279. McMinn, P. C. (2014). Enterovirus vaccines for an emerging cause of brain-stem encephalitis. *The New England Journal of Medicine*, *370*(9), 792–794. https://doi.org/10.1056/NEJMp1400601

280. McPhail, J. A., Lyoo, H., Pemberton, J. G., Hoffmann, R. M., van Elst, W., Strating, J. R. P. M., Jenkins, M. L., Stariha, J. T. B., Powell, C. J., Boulanger, M. J., Balla, T., van Kuppeveld, F. J. M., & Burke, J. E. (2020). Characterization of the c10orf76-PI4KB complex and its necessity for Golgi PI4P levels and enterovirus replication. *EMBO Reports*, *21*(2), e48441. https://doi.org/10.15252/embr.201948441

281. McWilliam Leitch, E. C., Cabrerizo, M., Cardosa, J., Harvala, H., Ivanova, O. E., Koike, S., Kroes, A. C. M., Lukashev, A., Perera, D., Roivainen, M., Susi, P.,

Trallero, G., Evans, D. J., & Simmonds, P. (2012). The association of recombination events in the founding and emergence of subgenogroup evolutionary lineages of human enterovirus 71. *Journal of Virology*, *86*(5), 2676–2685. https://doi.org/10.1128/JVI.06065-11

282. Melnick, J. L., Tagaya, I., & von Magnus, H. (1974). Enteroviruses 69, 70, and 71. *Intervirology*, *4*(6), 369–370. https://doi.org/10.1159/000149872

283. Menaceur, C., Gosselet, F., Fenart, L., & Saint-Pol, J. (2021). The Blood-Brain Barrier, an Evolving Concept Based on Technological Advances and Cell-Cell Communications. *Cells*, *11*(1), 133. https://doi.org/10.3390/cells11010133

284. Meng, T., Jia, Q., Wong, S.-M., & Chua, K.-B. (2019). In Vitro and In Vivo Inhibition of the Infectivity of Human Enterovirus 71 by a Sulfonated Food Azo Dye, Brilliant Black BN. *Journal of Virology*, *93*(17), e00061-19. https://doi.org/10.1128/JVI.00061-19

285. Meuren, L. M., Coelho, S. V. A., & de Arruda, L. B. (2022). Evaluation of DENV-Induced Endothelial Cell Permeability by Measurements of Transendothelial Electrical Resistance (TEER) and Extravasation of Proteins and Virus. *Methods in Molecular Biology (Clifton, N.J.)*, *2409*, 207–222. https://doi.org/10.1007/978-1-0716-1879-0_14

286. Millecamps, S., & Julien, J.-P. (2013). Axonal transport deficits and neurodegenerative diseases. *Nature Reviews. Neuroscience*, *14*(3), 161–176. https://doi.org/10.1038/nrn3380

287. Miller, F., Afonso, P. V., Gessain, A., & Ceccaldi, P.-E. (2012). Blood-brain barrier and retroviral infections. *Virulence*, *3*(2), 222–229. https://doi.org/10.4161/viru.19697

288. Mirand, A., Molet, L., Hassel, C., Peigue-Lafeuille, H. C. lA N., Rozenberg, F., Bailly, J.-L., & Henquell, C. C. C. (2015). Enterovirus A71 subgenotype B5, France, 2013. *Emerging Infectious Diseases*, *21*(4), 707–709. https://doi.org/10.3201/eid2104.141093

289. Miyamura, K., Nishimura, Y., Abo, M., Wakita, T., & Shimizu, H. (2011). Adaptive mutations in the genomes of enterovirus 71 strains following infection of mouse cells expressing human P-selectin glycoprotein ligand-1. *The Journal of General Virology*, *92*(Pt 2), 287–291. https://doi.org/10.1099/vir.0.022418-0

290. Mizutani, T., Ishizaka, A., & Nihei, C.-I. (2016). Transferrin Receptor 1 Facilitates Poliovirus Permeation of Mouse Brain Capillary Endothelial Cells. *The Journal of Biological Chemistry*, *291*(6), 2829–2836. https://doi.org/10.1074/jbc.M115.690941

291. Molino, Y., Jabès, F., Lacassagne, E., Gaudin, N., & Khrestchatisky, M. (2014). Setting-up an in vitro model of rat blood-brain barrier (BBB): A focus on BBB impermeability and receptor-mediated transport. *Journal of Visualized Experiments: JoVE*, *88*, e51278. https://doi.org/10.3791/51278

292. Monif, M., Reid, C. A., Powell, K. L., Drummond, K. J., O'Brien, T. J., & Williams, D. A. (2016). Interleukin-1β has trophic effects in microglia and its release is mediated by P2X7R pore. *Journal of Neuroinflammation*, *13*(1), 173. https://doi.org/10.1186/s12974-016-0621-8

293. Morosky, S., Lennemann, N. J., & Coyne, C. B. (2016). BPIFB6 Regulates Secretory Pathway Trafficking and Enterovirus Replication. *Journal of Virology*, *90*(10), 5098–5107. https://doi.org/10.1128/JVI.00170-16

294. Mossu, A., Rosito, M., Khire, T., Li Chung, H., Nishihara, H., Gruber, I., Luke, E., Dehouck, L., Sallusto, F., Gosselet, F., McGrath, J. L., & Engelhardt, B. (2019). A silicon nanomembrane platform for the visualization of immune cell trafficking across the human blood-brain barrier under flow. *Journal of Cerebral Blood Flow and Metabolism: Official Journal of the International Society of Cerebral Blood Flow and Metabolism*, *39*(3), 395–410. https://doi.org/10.1177/0271678X18820584

295. Motallebnejad, P., & Azarin, S. M. (2020). Chemically defined human vascular laminins for biologically relevant culture of hiPSC-derived brain microvascular endothelial cells. *Fluids and Barriers of the CNS*, *17*(1), 54. https://doi.org/10.1186/s12987-020-00215-2

296. Moya, E. L. J., Lombardo, S. M., Vandenhaute, E., Schneider, M., Mysiorek, C., Türeli, A. E., Kanda, T., Shimizu, F., Sano, Y., Maubon, N., Gosselet, F., Günday-Türeli, N., & Dehouck, M.-P. (2022). Interaction of surfactant coated PLGA nanoparticles with in vitro human brain-like endothelial cells. *International Journal of Pharmaceutics*, *621*, 121780. https://doi.org/10.1016/j.ijpharm.2022.121780

297. Murayi, R., & Chittiboina, P. (2016). Glucocorticoids in the management of peritumoral brain edema: A review of molecular mechanisms. *Child's Nervous*

System: ChNS: Official Journal of the International Society for Pediatric Neurosurgery, *32*(12), 2293–2302. https://doi.org/10.1007/s00381-016-3240-x

298. Nałęcz, K. A. (2017). Solute Carriers in the Blood-Brain Barier: Safety in Abundance. *Neurochemical Research*, *42*(3), 795–809. https://doi.org/10.1007/s11064-016-2030-x

299. Nalewajska, M., Marchelek-Myśliwiec, M., Opara-Bajerowicz, M., Dziedziejko, V., & Pawlik, A. (2020). Connexins-Therapeutic Targets in Cancers. *International Journal of Molecular Sciences*, *21*(23), E9119. https://doi.org/10.3390/ijms21239119

300. Nayak, G., Bhuyan, S. K., Bhuyan, R., Sahu, A., Kar, D., & Kuanar, A. (2022). Global emergence of Enterovirus 71: A systematic review. *Beni-Suef University Journal of Basic and Applied Sciences*, *11*(1), 78. https://doi.org/10.1186/s43088-022-00258-4

301. Nazmi, A., Mukherjee, S., Kundu, K., Dutta, K., Mahadevan, A., Shankar, S. K., & Basu, A. (2014). TLR7 is a key regulator of innate immunity against Japanese encephalitis virus infection. *Neurobiology of Disease*, *69*, 235–247. https://doi.org/10.1016/j.nbd.2014.05.036

302. Ngangas, S. T., Lukashev, A., Jugie, G., Ivanova, O., Mansuy, J.-M., Mengelle, C., Izopet, J., L'honneur, A.-S., Rozenberg, F., Leyssene, D., Hecquet, D., Marque-Juillet, S., Boutolleau, D., Burrel, S., Peigue-Lafeuille, H., Archimbaud, C., Benschop, K., Henquell, C., Mirand, A., & Bailly, J.-L. (2019). Multirecombinant Enterovirus A71 Subgenogroup C1 Isolates Associated with

Neurologic Disease, France, 2016-2017. *Emerging Infectious Diseases*, *25*(6), 1204–1208. https://doi.org/10.3201/eid2506.181460

303. Nguyen, T. T., Chiu, C.-H., Lin, C.-Y., Chiu, N.-C., Chen, P.-Y., Le, T. T. V., Le, D. N., Duong, A. H., Nguyen, V. L., Huynh, T. N., Truong, H. K., Phan, T. L., Nguyen, T. T. T., Shih, S.-R., Huang, C.-G., Weng, Y.-J., Hsieh, E.-F., Chang, S., Chen, C., … Huang, L.-M. (2022). Efficacy, safety, and immunogenicity of an inactivated, adjuvanted enterovirus 71 vaccine in infants and children: A multiregion, double-blind, randomised, placebo-controlled, phase 3 trial. *Lancet (London, England)*, *399*(10336), 1708–1717. https://doi.org/10.1016/S0140-6736(22)00313-0

304. Nhu, L. N. T., Nhan, L. N. T., Anh, N. T., Hong, N. T. T., Van, H. M. T., Thanh, T. T., Hang, V. T. T., Han, D. D. K., Ny, N. T. H., Nguyet, L. A., Quy, D. T., Qui, P. T., Khanh, T. H., Hung, N. T., Tuan, H. M., Chau, N. V. V., Thwaites, G., van Doorn, H. R., & Tan, L. V. (2021). Coxsackievirus A16 in Southern Vietnam. *Frontiers in Microbiology*, *12*, 689658. https://doi.org/10.3389/fmicb.2021.689658

305. Nilles, K. L., Williams, E. I., Betterton, R. D., Davis, T. P., & Ronaldson, P. T. (2022). Blood-Brain Barrier Transporters: Opportunities for Therapeutic Development in Ischemic Stroke. *International Journal of Molecular Sciences*, *23*(3), 1898. https://doi.org/10.3390/ijms23031898

306. Nishimura, Y., Lee, H., Hafenstein, S., Kataoka, C., Wakita, T., Bergelson, J. M., & Shimizu, H. (2013). Enterovirus 71 binding to PSGL-1 on leukocytes: VP1-

145 acts as a molecular switch to control receptor interaction. *PLoS Pathogens*, *9*(7), e1003511. https://doi.org/10.1371/journal.ppat.1003511

307. Nishimura, Y., Shimojima, M., Tano, Y., Miyamura, T., Wakita, T., & Shimizu, H. (2009). Human P-selectin glycoprotein ligand-1 is a functional receptor for enterovirus 71. *Nature Medicine*, *15*(7), 794–797. https://doi.org/10.1038/nm.1961

308. Nzou, G., Wicks, R. T., Wicks, E. E., Seale, S. A., Sane, C. H., Chen, A., Murphy, S. V., Jackson, J. D., & Atala, A. J. (2018). Human Cortex Spheroid with a Functional Blood Brain Barrier for High-Throughput Neurotoxicity Screening and Disease Modeling. *Scientific Reports*, *8*(1), 7413. https://doi.org/10.1038/s41598-018-25603-5

309. Oberste, M. S., Peñaranda, S., Maher, K., & Pallansch, M. A. (2004). Complete genome sequences of all members of the species Human enterovirus A. *The Journal of General Virology*, *85*(Pt 6), 1597–1607. https://doi.org/10.1099/vir.0.79789-0

310. Ohka, S., Tan, S. H., Ishiyama, E., Ogasawara, K., Hanasaka, T., Ishida, K., Hagiwara, K., Liu, C.-C., Chong, P. C.-S., Hanaki, K.-I., & Schiavo, G. (2022). The uncoating of EV71 in mature late endosomes requires CD-M6PR. *Biology Open*, *11*(9), bio059469. https://doi.org/10.1242/bio.059469

311. Ohmi, Y., Nishikaze, T., Kitaura, Y., Ito, T., Yamamoto, S., Sugiyama, F., Matsuyama, M., Takahashi, Y., Takeda, A., Kawahara, T., Okajima, T., Furukawa, K., & Furukawa, K. (2021). Majority of alpha2,6-sialylated glycans in the adult mouse brain exist in O-glycans: SALSA-MS analysis for knockout mice

of alpha2,6-sialyltransferase genes. *Glycobiology*, *31*(5), 557–570. https://doi.org/10.1093/glycob/cwaa105

312. Olson, J. K., & Miller, S. D. (2004). Microglia initiate central nervous system innate and adaptive immune responses through multiple TLRs. *Journal of Immunology (Baltimore, Md.: 1950)*, *173*(6), 3916–3924. https://doi.org/10.4049/jimmunol.173.6.3916

313. Ooi, M. H., Wong, S. C., Lewthwaite, P., Cardosa, M. J., & Solomon, T. (2010). Clinical features, diagnosis, and management of enterovirus 71. *The Lancet. Neurology*, *9*(11), 1097–1105. https://doi.org/10.1016/S1474-4422(10)70209-X

314. Owino, C. O., & Chu, J. J. H. (2019). Recent advances on the role of host factors during non-poliovirus enteroviral infections. *Journal of Biomedical Science*, *26*(1), 47. https://doi.org/10.1186/s12929-019-0540-y

315. Ozawa, Y., Nakao, K., Kurihara, T., Shimazaki, T., Shimmura, S., Ishida, S., Yoshimura, A., Tsubota, K., & Okano, H. (2008). Roles of STAT3/SOCS3 pathway in regulating the visual function and ubiquitin-proteasome-dependent degradation of rhodopsin during retinal inflammation. *The Journal of Biological Chemistry*, *283*(36), 24561–24570. https://doi.org/10.1074/jbc.M802238200

316. Pan, L., Chen, J., Yu, J., Yu, H., & Zhang, M. (2011). The structure of the PDZ3-SH3-GuK tandem of ZO-1 protein suggests a supramodular organization of the membrane-associated guanylate kinase (MAGUK) family scaffold protein core. *The Journal of Biological Chemistry*, *286*(46), 40069–40074. https://doi.org/10.1074/jbc.C111.293084

317. Panahpour, H., Farhoudi, M., Omidi, Y., & Mahmoudi, J. (2018). An In Vivo Assessment of Blood-Brain Barrier Disruption in a Rat Model of Ischemic Stroke. *Journal of Visualized Experiments: JoVE*, *133*. https://doi.org/10.3791/57156

318. Panattoni, G., Amoriello, R., Memo, C., Thalhammer, A., Ballerini, C., & Ballerini, L. (2021). Diverse inflammatory threats modulate astrocytes Ca2+ signaling via connexin43 hemichannels in organotypic spinal slices. *Molecular Brain*, *14*(1), 159. https://doi.org/10.1186/s13041-021-00868-6

319. Panicucci, C., Raffaghello, L., Bruzzone, S., Baratto, S., Principi, E., Minetti, C., Gazzerro, E., & Bruno, C. (2020). eATP/P2X7R Axis: An Orchestrated Pathway Triggering Inflammasome Activation in Muscle Diseases. *International Journal of Molecular Sciences*, *21*(17), E5963. https://doi.org/10.3390/ijms21175963

320. Pankov, R., & Yamada, K. M. (2002). Fibronectin at a glance. *Journal of Cell Science*, *115*(Pt 20), 3861–3863. https://doi.org/10.1242/jcs.00059

321. Papa, M. P., Meuren, L. M., Coelho, S. V. A., Lucas, C. G. de O., Mustafá, Y. M., Lemos Matassoli, F., Silveira, P. P., Frost, P. S., Pezzuto, P., Ribeiro, M. R., Tanuri, A., Nogueira, M. L., Campanati, L., Bozza, M. T., Paula Neto, H. A., Pimentel-Coelho, P. M., Figueiredo, C. P., de Aguiar, R. S., & de Arruda, L. B. (2017). Zika Virus Infects, Activates, and Crosses Brain Microvascular Endothelial Cells, without Barrier Disruption. *Frontiers in Microbiology*, *8*, 2557. https://doi.org/10.3389/fmicb.2017.02557

322. Paradis, A., Leblanc, D., & Dumais, N. (2016). Optimization of an in vitro human blood-brain barrier model: Application to blood monocyte transmigration assays. *MethodsX*, *3*, 25–34. https://doi.org/10.1016/j.mex.2015.11.009

323. Patel, R., & Alahmad, A. J. (2016). Growth-factor reduced Matrigel source influences stem cell derived brain microvascular endothelial cell barrier properties. *Fluids and Barriers of the CNS*, *13*, 6. https://doi.org/10.1186/s12987-016-0030-5

324. Pathinayake, P. S., Hsu, A. C.-Y., & Wark, P. A. B. (2015). Innate Immunity and Immune Evasion by Enterovirus 71. *Viruses*, *7*(12), 6613–6630. https://doi.org/10.3390/v7122961

325. Patteson, A. E., Vahabikashi, A., Goldman, R. D., & Janmey, P. A. (2020). Mechanical and Non-Mechanical Functions of Filamentous and Non-Filamentous Vimentin. *BioEssays: News and Reviews in Molecular, Cellular and Developmental Biology*, *42*(11), e2000078. https://doi.org/10.1002/bies.202000078

326. Pedroso, D. C. S., Tellechea, A., Moura, L., Fidalgo-Carvalho, I., Duarte, J., Carvalho, E., & Ferreira, L. (2011). Improved survival, vascular differentiation and wound healing potential of stem cells co-cultured with endothelial cells. *PloS One*, *6*(1), e16114. https://doi.org/10.1371/journal.pone.0016114

327. Perrière, N., Yousif, S., Cazaubon, S., Chaverot, N., Bourasset, F., Cisternino, S., Declèves, X., Hori, S., Terasaki, T., Deli, M., Scherrmann, J.-M., Temsamani, J., Roux, F., & Couraud, P.-O. (2007). A functional in vitro model

of rat blood-brain barrier for molecular analysis of efflux transporters. *Brain Research*, *1150*, 1–13. https://doi.org/10.1016/j.brainres.2007.02.091

328. Perusina Lanfranca, M., Zhang, Y., Girgis, A., Kasselman, S., Lazarus, J., Kryczek, I., Delrosario, L., Rhim, A., Koneva, L., Sartor, M., Sun, L., Halbrook, C., Nathan, H., Shi, J., Crawford, H. C., Pasca di Magliano, M., Zou, W., & Frankel, T. L. (2020). Interleukin 22 Signaling Regulates Acinar Cell Plasticity to Promote Pancreatic Tumor Development in Mice. *Gastroenterology*, *158*(5), 1417-1432.e11. https://doi.org/10.1053/j.gastro.2019.12.010

329. Peters, J., Rittger, A., Weisner, R., Knabbe, J., Zunke, F., Rothaug, M., Damme, M., Berkovic, S. F., Blanz, J., Saftig, P., & Schwake, M. (2015). Lysosomal integral membrane protein type-2 (LIMP-2/SCARB2) is a substrate of cathepsin-F, a cysteine protease mutated in type-B-Kufs-disease. *Biochemical and Biophysical Research Communications*, *457*(3), 334–340. https://doi.org/10.1016/j.bbrc.2014.12.111

330. Phan, Q. T., Phung, L. K., Truong, K. H., Huynh, T. T., Phạm, G. T., Nguyen, B. N., Tran, Q. T., Huynh, V. N. T., Nguyen, T. T. M., Le, T. P. K., Le, N. N. T., Sabanathan, S., van Doorn, H. R., Van Le, T., Nguyen, T. D., Merson, L., Nguyen, D. T. P., Geskus, R., Nguyen, H. T., … Wills, B. (2019). Assessing the efficacy and safety of magnesium sulfate for management of autonomic nervous system dysregulation in Vietnamese children with severe hand foot and mouth disease. *BMC Infectious Diseases*, *19*(1), 737. https://doi.org/10.1186/s12879-019-4356-x

331. Plevka, P., Perera, R., Cardosa, J., Kuhn, R. J., & Rossmann, M. G. (2012). Crystal structure of human enterovirus 71. *Science (New York, N.Y.)*, *336*(6086), 1274. https://doi.org/10.1126/science.1218713

332. Podin, Y., Gias, E. L. M., Ong, F., Leong, Y.-W., Yee, S.-F., Yusof, M. A., Perera, D., Teo, B., Wee, T.-Y., Yao, S.-C., Yao, S.-K., Kiyu, A., Arif, M. T., & Cardosa, M. J. (2006). Sentinel surveillance for human enterovirus 71 in Sarawak, Malaysia: Lessons from the first 7 years. *BMC Public Health*, *6*, 180. https://doi.org/10.1186/1471-2458-6-180

333. Portnoy, B., Hanes, B., Pierce, N. F., Leedom, J. M., Kunzman, E. E., & Wehrle, P. F. (1965). ASEPTIC MENINGITIS ASSOCIATED WITH ECHO VIRUS TYPE 9 INFECTION. WITH SPECIAL REFERENCE TO VARIABILITY BY SEX AND INCIDENCE OF PARALYTIC SEQUELAE. *California Medicine*, *102*, 261–267.

334. Puenpa, J., Wanlapakorn, N., Vongpunsawad, S., & Poovorawan, Y. (2019). The History of Enterovirus A71 Outbreaks and Molecular Epidemiology in the Asia-Pacific Region. *Journal of Biomedical Science*, *26*(1), 75. https://doi.org/10.1186/s12929-019-0573-2

335. Pulimeno, P., Paschoud, S., & Citi, S. (2011). A role for ZO-1 and PLEKHA7 in recruiting paracingulin to tight and adherens junctions of epithelial cells. *The Journal of Biological Chemistry*, *286*(19), 16743–16750. https://doi.org/10.1074/jbc.M111.230862

336. Qian, T., Maguire, S. E., Canfield, S. G., Bao, X., Olson, W. R., Shusta, E. V., & Palecek, S. P. (2017). Directed differentiation of human pluripotent stem cells

to blood-brain barrier endothelial cells. *Science Advances*, *3*(11), e1701679. https://doi.org/10.1126/sciadv.1701679

337. Qiao, X., Roth, I., Féraille, E., & Hasler, U. (2014). Different effects of ZO-1, ZO-2 and ZO-3 silencing on kidney collecting duct principal cell proliferation and adhesion. *Cell Cycle (Georgetown, Tex.)*, *13*(19), 3059–3075. https://doi.org/10.4161/15384101.2014.949091

338. Qing, J., Wang, Y., Sun, Y., Huang, J., Yan, W., Wang, J., Su, D., Ni, C., Li, J., Rao, Z., Liu, L., & Lou, Z. (2014). Cyclophilin A associates with enterovirus-71 virus capsid and plays an essential role in viral infection as an uncoating regulator. *PLoS Pathogens*, *10*(10), e1004422. https://doi.org/10.1371/journal.ppat.1004422

339. Rado, M., Flepisi, B., & Fisher, D. (2022). The Effect of Normoxic and Hypoxic U-87 Glioblastoma Paracrine Secretion on the Modulation of Brain Endothelial Cells. *Cells*, *11*(2), 276. https://doi.org/10.3390/cells11020276

340. Ram, A. K., & Vairappan, B. (2022). Role of zonula occludens in gastrointestinal and liver cancers. *World Journal of Clinical Cases*, *10*(12), 3647–3661. https://doi.org/10.12998/wjcc.v10.i12.3647

341. Ramos, I., Stamatakis, K., Oeste, C. L., & Pérez-Sala, D. (2020). Vimentin as a Multifaceted Player and Potential Therapeutic Target in Viral Infections. *International Journal of Molecular Sciences*, *21*(13), E4675. https://doi.org/10.3390/ijms21134675

342. Ranganathan, S., Singh, S., Poh, C. L., & Chow, V. T. K. (2002). The hand, foot and mouth disease virus capsid: Sequence analysis and prediction of antigenic sites from homology modelling. *Applied Bioinformatics*, *1*(1), 43–52.

343. Rasti, M., Khanbabaei, H., & Teimoori, A. (2019). An update on enterovirus 71 infection and interferon type I response. *Reviews in Medical Virology*, *29*(1), e2016. https://doi.org/10.1002/rmv.2016

344. Rattanakomol, P., Srimanote, P., Tongtawe, P., Khantisitthiporn, O., Supasorn, O., & Thanongsaksrikul, J. (2022). Host neuronal PRSS3 interacts with enterovirus A71 3A protein and its role in viral replication. *Scientific Reports*, *12*(1), 12846. https://doi.org/10.1038/s41598-022-17272-2

345. Raut, S., Bhalerao, A., Noorani, B., & Cucullo, L. (2022). In Vitro Models of the Blood-Brain Barrier. *Methods in Molecular Biology (Clifton, N.J.)*, *2492*, 25–49. https://doi.org/10.1007/978-1-0716-2289-6_2

346. Ravid, O., Elhaik Goldman, S., Macheto, D., Bresler, Y., De Oliveira, R. I., Liraz-Zaltsman, S., Gosselet, F., Dehouck, L., Beeri, M. S., & Cooper, I. (2018). Blood-Brain Barrier Cellular Responses Toward Organophosphates: Natural Compensatory Processes and Exogenous Interventions to Rescue Barrier Properties. *Frontiers in Cellular Neuroscience*, *12*, 359. https://doi.org/10.3389/fncel.2018.00359

347. Redzic, Z. (2011). Molecular biology of the blood-brain and the blood-cerebrospinal fluid barriers: Similarities and differences. *Fluids and Barriers of the CNS*, *8*(1), 3. https://doi.org/10.1186/2045-8118-8-3

348. Rho, S.-S., Ando, K., & Fukuhara, S. (2017). Dynamic Regulation of Vascular Permeability by Vascular Endothelial Cadherin-Mediated Endothelial Cell-Cell Junctions. *Journal of Nippon Medical School = Nippon Ika Daigaku Zasshi*, *84*(4), 148–159. https://doi.org/10.1272/jnms.84.148

349. Rice, O., Surian, A., & Chen, Y. (2022). Modeling the blood-brain barrier for treatment of central nervous system (CNS) diseases. *Journal of Tissue Engineering*, *13*, 20417314221095996. https://doi.org/10.1177/20417314221095997

350. Rizzi, E., Deligne, C., Dehouck, L., Bilardo, R., Sano, Y., Shimizu, F., Kanda, T., Resmini, M., Gosselet, F., Dehouck, M.-P., & Mysiorek, C. (2021). A Triple Culture Cell System Modeling the Human Blood-Brain Barrier. *Journal of Visualized Experiments: JoVE*, *177*. https://doi.org/10.3791/63134

351. Robinson, C. R., Doane, F. W., & Rhodes, A. J. (1958). Report of an outbreak of febrile illness with pharyngeal lesions and exanthem: Toronto, summer 1957; isolation of group A Coxsackie virus. *Canadian Medical Association Journal*, *79*(8), 615–621.

352. Rodrigues, S. F., & Granger, D. N. (2015). Blood cells and endothelial barrier function. *Tissue Barriers*, *3*(1–2), e978720. https://doi.org/10.4161/21688370.2014.978720

353. Rosenthal, R., Günzel, D., Theune, D., Czichos, C., Schulzke, J.-D., & Fromm, M. (2017). Water channels and barriers formed by claudins. *Annals of the New York Academy of Sciences*, *1397*(1), 100–109. https://doi.org/10.1111/nyas.13383

354. Ross, C. J., Atilgan, A. R., Tastan Bishop, Ö., & Atilgan, C. (2018). Unraveling the Motions behind Enterovirus 71 Uncoating. *Biophysical Journal*, *114*(4), 822–838. https://doi.org/10.1016/j.bpj.2017.12.021

355. Roudnicky, F., Zhang, J. D., Kim, B. K., Pandya, N. J., Lan, Y., Sach-Peltason, L., Ragelle, H., Strassburger, P., Gruener, S., Lazendic, M., Uhles, S., Revelant, F., Eidam, O., Sturm, G., Kueppers, V., Christensen, K., Goldstein, L. D., Tzouros, M., Banfai, B., … Cowan, C. A. (2020). Inducers of the endothelial cell barrier identified through chemogenomic screening in genome-edited hPSC-endothelial cells. *Proceedings of the National Academy of Sciences of the United States of America*, *117*(33), 19854–19865. https://doi.org/10.1073/pnas.1911532117

356. Roux, F., & Couraud, P.-O. (2005). Rat brain endothelial cell lines for the study of blood-brain barrier permeability and transport functions. *Cellular and Molecular Neurobiology*, *25*(1), 41–58. https://doi.org/10.1007/s10571-004-1376-9

357. Ryu, H.-W., Lim, W., Jo, D., Kim, S., Park, J. T., Min, J.-J., Hyun, H., & Kim, H.-S. (2018). Low-Dose Evans Blue Dye for Near-Infrared Fluorescence Imaging in Photothrombotic Stroke Model. *International Journal of Medical Sciences*, *15*(7), 696–702. https://doi.org/10.7150/ijms.24257

358. Sabo, A. A., Birolo, G., Naccarati, A., Dragomir, M. P., Aneli, S., Allione, A., Oderda, M., Allasia, M., Gontero, P., Sacerdote, C., Vineis, P., Matullo, G., & Pardini, B. (2020). Small Non-Coding RNA Profiling in Plasma Extracellular Vesicles of Bladder Cancer Patients by Next-Generation Sequencing:

Expression Levels of miR-126-3p and piR-5936 Increase with Higher Histologic Grades. *Cancers*, *12*(6), E1507. https://doi.org/10.3390/cancers12061507

359. Saha, S. K., Schrag, S. J., El Arifeen, S., Mullany, L. C., Shahidul Islam, M., Shang, N., Qazi, S. A., Zaidi, A. K. M., Bhutta, Z. A., Bose, A., Panigrahi, P., Soofi, S. B., Connor, N. E., Mitra, D. K., Isaac, R., Winchell, J. M., Arvay, M. L., Islam, M., Shafiq, Y., … Baqui, A. H. (2018). Causes and incidence of community-acquired serious infections among young children in south Asia (ANISA): An observational cohort study. *Lancet (London, England)*, *392*(10142), 145–159. https://doi.org/10.1016/S0140-6736(18)31127-9

360. Saito, A. C., Higashi, T., Fukazawa, Y., Otani, T., Tauchi, M., Higashi, A. Y., Furuse, M., & Chiba, H. (2021). Occludin and tricellulin facilitate formation of anastomosing tight-junction strand network to improve barrier function. *Molecular Biology of the Cell*, *32*(8), 722–738. https://doi.org/10.1091/mbc.E20-07-0464

361. Sasaki, T., Kojima, H., Kishimoto, R., Ikeda, A., Kunimoto, H., & Nakajima, K. (2006). Spatiotemporal regulation of c-Fos by ERK5 and the E3 ubiquitin ligase UBR1, and its biological role. *Molecular Cell*, *24*(1), 63–75. https://doi.org/10.1016/j.molcel.2006.08.005

362. Sasson, E., Anzi, S., Bell, B., Yakovian, O., Zorsky, M., Deutsch, U., Engelhardt, B., Sherman, E., Vatine, G., Dzikowski, R., & Ben-Zvi, A. (2021). Nano-scale architecture of blood-brain barrier tight-junctions. *ELife*, *10*, e63253. https://doi.org/10.7554/eLife.63253

363. Schmidt, N. J., Lennette, E. H., & Ho, H. H. (1974). An apparently new enterovirus isolated from patients with disease of the central nervous system. *The Journal of Infectious Diseases*, *129*(3), 304–309. https://doi.org/10.1093/infdis/129.3.304

364. Schneider, R., McKeever, P., Kim, T., Graff, C., van Swieten, J. C., Karydas, A., Boxer, A., Rosen, H., Miller, B. L., Laforce, R., Galimberti, D., Masellis, M., Borroni, B., Zhang, Z., Zinman, L., Rohrer, J. D., Tartaglia, M. C., Robertson, J., & Genetic FTD Initiative (GENFI). (2018). Downregulation of exosomal miR-204-5p and miR-632 as a biomarker for FTD: A GENFI study. *Journal of Neurology, Neurosurgery, and Psychiatry*, *89*(8), 851–858. https://doi.org/10.1136/jnnp-2017-317492

365. Schwab, A., Meyering, S. S., Lepene, B., Iordanskiy, S., van Hoek, M. L., Hakami, R. M., & Kashanchi, F. (2015). Extracellular vesicles from infected cells: Potential for direct pathogenesis. *Frontiers in Microbiology*, *6*, 1132. https://doi.org/10.3389/fmicb.2015.01132

366. Scumpia, P. O., Kelly, K. M., Reeves, W. H., & Stevens, B. R. (2005). Double-stranded RNA signals antiviral and inflammatory programs and dysfunctional glutamate transport in TLR3-expressing astrocytes. *Glia*, *52*(2), 153–162. https://doi.org/10.1002/glia.20234

367. Scumpia, P. O., Kelly-Scumpia, K., & Stevens, B. R. (2014). Alpha-lipoic acid effects on brain glial functions accompanying double-stranded RNA antiviral and inflammatory signaling. *Neurochemistry International*, *64*, 55–63. https://doi.org/10.1016/j.neuint.2013.11.006

368. Seok, J. K., Kang, H. C., Cho, Y.-Y., Lee, H. S., & Lee, J. Y. (2021). Therapeutic regulation of the NLRP3 inflammasome in chronic inflammatory diseases. *Archives of Pharmacal Research*, *44*(1), 16–35. https://doi.org/10.1007/s12272-021-01307-9

369. Shang, W., Qian, S., Fang, L., Han, Y., & Zheng, C. (2017). Association study of inflammatory cytokine and chemokine expression in hand foot and mouth disease. *Oncotarget*, *8*(45), 79425–79432. https://doi.org/10.18632/oncotarget.18341

370. Shao, A., Wu, H., Hong, Y., Tu, S., Sun, X., Wu, Q., Zhao, Q., Zhang, J., & Sheng, J. (2016). Hydrogen-Rich Saline Attenuated Subarachnoid Hemorrhage-Induced Early Brain Injury in Rats by Suppressing Inflammatory Response: Possible Involvement of NF-κB Pathway and NLRP3 Inflammasome. *Molecular Neurobiology*, *53*(5), 3462–3476. https://doi.org/10.1007/s12035-015-9242-y

371. Shayan, G., Choi, Y. S., Shusta, E. V., Shuler, M. L., & Lee, K. H. (2011). Murine in vitro model of the blood-brain barrier for evaluating drug transport. *European Journal of Pharmaceutical Sciences: Official Journal of the European Federation for Pharmaceutical Sciences*, *42*(1–2), 148–155. https://doi.org/10.1016/j.ejps.2010.11.005

372. Shen, W. C., Chiu, H. H., Chow, K. C., & Tsai, C. H. (1999). MR imaging findings of enteroviral encephaloymelitis: An outbreak in Taiwan. *AJNR. American Journal of Neuroradiology*, *20*(10), 1889–1895.

373. Shih, C., Liao, C.-C., Chang, Y.-S., Wu, S.-Y., Chang, C.-S., & Liou, A.-T. (2018). Immunocompetent and Immunodeficient Mouse Models for Enterovirus 71 Pathogenesis and Therapy. *Viruses*, *10*(12), E674. https://doi.org/10.3390/v10120674

374. Shingler, K. L., Yoder, J. L., Carnegie, M. S., Ashley, R. E., Makhov, A. M., Conway, J. F., & Hafenstein, S. (2013). The enterovirus 71 A-particle forms a gateway to allow genome release: A cryoEM study of picornavirus uncoating. *PLoS Pathogens*, *9*(3), e1003240. https://doi.org/10.1371/journal.ppat.1003240

375. Siddharthan, V., Kim, Y. V., Liu, S., & Kim, K. S. (2007). Human astrocytes/astrocyte-conditioned medium and shear stress enhance the barrier properties of human brain microvascular endothelial cells. *Brain Research*, *1147*, 39–50. https://doi.org/10.1016/j.brainres.2007.02.029

376. Simmonds, P., Gorbalenya, A. E., Harvala, H., Hovi, T., Knowles, N. J., Lindberg, A. M., Oberste, M. S., Palmenberg, A. C., Reuter, G., Skern, T., Tapparel, C., Wolthers, K. C., Woo, P. C. Y., & Zell, R. (2020). Recommendations for the nomenclature of enteroviruses and rhinoviruses. *Archives of Virology*, *165*(3), 793–797. https://doi.org/10.1007/s00705-019-04520-6

377. Sisto, M., Ribatti, D., & Lisi, S. (2021). Cadherin Signaling in Cancer and Autoimmune Diseases. *International Journal of Molecular Sciences*, *22*(24), 13358. https://doi.org/10.3390/ijms222413358

378. Ślebioda, Z., & Dorocka-Bobkowska, B. (2018). Hand, foot and mouth disease as an emerging public health problem: Case report of familial child-to-adult

transmission. *Dental and Medical Problems*, *55*(1), 99–104. https://doi.org/10.17219/dmp/80995

379. Somers, W. S., Tang, J., Shaw, G. D., & Camphausen, R. T. (2000). Insights into the molecular basis of leukocyte tethering and rolling revealed by structures of P- and E-selectin bound to SLe(X) and PSGL-1. *Cell*, *103*(3), 467–479. https://doi.org/10.1016/s0092-8674(00)00138-0

380. Song, C., He, Y., Bo, Y., Wang, J., Ren, Z., & Yang, H. (2018). Risk Assessment and Mapping of Hand, Foot, and Mouth Disease at the County Level in Mainland China Using Spatiotemporal Zero-Inflated Bayesian Hierarchical Models. *International Journal of Environmental Research and Public Health*, *15*(7), E1476. https://doi.org/10.3390/ijerph15071476

381. Song, J., Hu, Y., Li, J., Zheng, H., Wang, J., Guo, L., Ning, R., Li, H., Yang, Z., Fan, H., & Liu, L. (2017). Different microRNA profiles reveal the diverse outcomes induced by EV71 and CA16 infection in human umbilical vein endothelial cells using high-throughput sequencing. *PloS One*, *12*(5), e0177657. https://doi.org/10.1371/journal.pone.0177657

382. Song, J., Hu, Y., Zheng, H., Guo, L., Huang, X., Jiang, X., Li, W., Li, J., Yang, Z., Dong, S., & Liu, L. (2019). Comparative analysis of putative novel microRNA expression profiles induced by enterovirus 71 and coxsackievirus A16 infections in human umbilical vein endothelial cells using high-throughput sequencing. *Infection, Genetics and Evolution: Journal of Molecular Epidemiology and Evolutionary Genetics in Infectious Diseases*, *73*, 401–410. https://doi.org/10.1016/j.meegid.2019.06.007

383. Soni, D., Regmi, S. C., Wang, D.-M., DebRoy, A., Zhao, Y.-Y., Vogel, S. M., Malik, A. B., & Tiruppathi, C. (2017). Pyk2 phosphorylation of VE-PTP downstream of STIM1-induced Ca2+ entry regulates disassembly of adherens junctions. *American Journal of Physiology. Lung Cellular and Molecular Physiology*, *312*(6), L1003–L1017. https://doi.org/10.1152/ajplung.00008.2017

384. Spadaro, D., Tapia, R., Jond, L., Sudol, M., Fanning, A. S., & Citi, S. (2014). ZO proteins redundantly regulate the transcription factor DbpA/ZONAB. *The Journal of Biological Chemistry*, *289*(32), 22500–22511. https://doi.org/10.1074/jbc.M114.556449

385. Spindler, K. R., & Hsu, T.-H. (2012). Viral disruption of the blood-brain barrier. *Trends in Microbiology*, *20*(6), 282–290. https://doi.org/10.1016/j.tim.2012.03.009

386. Spudich, S., & González-Scarano, F. (2012). HIV-1-related central nervous system disease: Current issues in pathogenesis, diagnosis, and treatment. *Cold Spring Harbor Perspectives in Medicine*, *2*(6), a007120. https://doi.org/10.1101/cshperspect.a007120

387. Stamatovic, S. M., Johnson, A. M., Keep, R. F., & Andjelkovic, A. V. (2016). Junctional proteins of the blood-brain barrier: New insights into function and dysfunction. *Tissue Barriers*, *4*(1), e1154641. https://doi.org/10.1080/21688370.2016.1154641

388. Stamatovic, S. M., Keep, R. F., & Andjelkovic, A. V. (2008). Brain endothelial cell-cell junctions: How to “open” the blood brain barrier. *Current*

Neuropharmacology, *6*(3), 179–192. https://doi.org/10.2174/157015908785777210

389. Stone, N. L., England, T. J., & O'Sullivan, S. E. (2019). A Novel Transwell Blood Brain Barrier Model Using Primary Human Cells. *Frontiers in Cellular Neuroscience*, *13*, 230. https://doi.org/10.3389/fncel.2019.00230

390. Strazza, M., Maubert, M. E., Pirrone, V., Wigdahl, B., & Nonnemacher, M. R. (2016). Co-culture model consisting of human brain microvascular endothelial and peripheral blood mononuclear cells. *Journal of Neuroscience Methods*, *269*, 39–45. https://doi.org/10.1016/j.jneumeth.2016.05.016

391. Su, P.-Y., Wang, Y.-F., Huang, S.-W., Lo, Y.-C., Wang, Y.-H., Wu, S.-R., Shieh, D.-B., Chen, S.-H., Wang, J.-R., Lai, M.-D., & Chang, C.-F. (2015). Cell surface nucleolin facilitates enterovirus 71 binding and infection. *Journal of Virology*, *89*(8), 4527–4538. https://doi.org/10.1128/JVI.03498-14

392. Suanpan, K., Srimanote, P., Tongtawe, P., Khantisitthiporn, O., Supasorn, O., Rattanakomol, P., & Thanongsaksrikul, J. (2022). Transcriptome of human neuroblastoma SH-SY5Y cells in response to 2B protein of enterovirus-A71. *Scientific Reports*, *12*(1), 1765. https://doi.org/10.1038/s41598-022-05904-6

393. Suhy, A. M., Webb, A., Papp, A. C., Geier, E. G., & Sadee, W. (2017). Expression and splicing of ABC and SLC transporters in the human blood-brain barrier measured with RNAseq. *European Journal of Pharmaceutical Sciences: Official Journal of the European Federation for Pharmaceutical Sciences*, *103*, 47–51. https://doi.org/10.1016/j.ejps.2017.02.010

394. Sukriti, S., Tauseef, M., Yazbeck, P., & Mehta, D. (2014). Mechanisms regulating endothelial permeability. *Pulmonary Circulation*, *4*(4), 535–551. https://doi.org/10.1086/677356

395. Sun, D., Wen, X., Wang, M., Mao, S., Cheng, A., Yang, X., Jia, R., Chen, S., Yang, Q., Wu, Y., Zhu, D., Liu, M., Zhao, X., Zhang, S., Wang, Y., Xu, Z., Chen, Z., Zhu, L., Luo, Q., … Chen, X. (2019). Apoptosis and Autophagy in Picornavirus Infection. *Frontiers in Microbiology*, *10*, 2032. https://doi.org/10.3389/fmicb.2019.02032

396. Sun, H., Gao, M., & Cui, D. (2020). Molecular characteristics of the VP1 region of enterovirus 71 strains in China. *Gut Pathogens*, *12*, 38. https://doi.org/10.1186/s13099-020-00377-2

397. Sun, J., Ou, W., Han, D., Paganini-Hill, A., Fisher, M. J., & Sumbria, R. K. (2022). Comparative studies between the murine immortalized brain endothelial cell line (bEnd.3) and induced pluripotent stem cell-derived human brain endothelial cells for paracellular transport. *PloS One*, *17*(5), e0268860. https://doi.org/10.1371/journal.pone.0268860

398. Sun, L., He, C., Nair, L., Yeung, J., & Egwuagu, C. E. (2015). Interleukin 12 (IL-12) family cytokines: Role in immune pathogenesis and treatment of CNS autoimmune disease. *Cytokine*, *75*(2), 249–255. https://doi.org/10.1016/j.cyto.2015.01.030

399. Sun, S., Li, Z., Hu, X., & Huang, R. (2021). Spatiotemporal characters and influence factors of hand, foot and mouth epidemic in Xinjiang, China. *PloS One*, *16*(8), e0254223. https://doi.org/10.1371/journal.pone.0254223

400. Sundivakkam, P. C., Natarajan, V., Malik, A. B., & Tiruppathi, C. (2013). Store-operated Ca2+ entry (SOCE) induced by protease-activated receptor-1 mediates STIM1 protein phosphorylation to inhibit SOCE in endothelial cells through AMP-activated protein kinase and p38β mitogen-activated protein kinase. *The Journal of Biological Chemistry*, *288*(23), 17030–17041. https://doi.org/10.1074/jbc.M112.411272

401. Suzuki, H., Tani, K., Tamura, A., Tsukita, S., & Fujiyoshi, Y. (2015). Model for the architecture of claudin-based paracellular ion channels through tight junctions. *Journal of Molecular Biology*, *427*(2), 291–297. https://doi.org/10.1016/j.jmb.2014.10.020

402. Swain, S. P., & Mohanty, S. (2019). Imidazolidinones and Imidazolidine-2,4-diones as Antiviral Agents. *ChemMedChem*, *14*(3), 291–302. https://doi.org/10.1002/cmdc.201800686

403. Szablewski, L. (2017). Glucose Transporters in Brain: In Health and in Alzheimer's Disease. *Journal of Alzheimer's Disease: JAD*, *55*(4), 1307–1320. https://doi.org/10.3233/JAD-160841

404. Tajrishi, M. M., Tuteja, R., & Tuteja, N. (2011). Nucleolin: The most abundant multifunctional phosphoprotein of nucleolus. *Communicative & Integrative Biology*, *4*(3), 267–275. https://doi.org/10.4161/cib.4.3.14884

405. Takahashi, S., Liao, Q., Van Boeckel, T. P., Xing, W., Sun, J., Hsiao, V. Y., Metcalf, C. J. E., Chang, Z., Liu, F., Zhang, J., Wu, J. T., Cowling, B. J., Leung, G. M., Farrar, J. J., van Doorn, H. R., Grenfell, B. T., & Yu, H. (2016). Hand, Foot, and Mouth Disease in China: Modeling Epidemic Dynamics of Enterovirus

Serotypes and Implications for Vaccination. *PLoS Medicine*, *13*(2), e1001958. https://doi.org/10.1371/journal.pmed.1001958

406. Takenouchi, T., Iwamaru, Y., Sugama, S., Tsukimoto, M., Fujita, M., Sekigawa, A., Sekiyama, K., Sato, M., Kojima, S., Conti, B., Hashimoto, M., & Kitani, H. (2011). The activation of P2X7 receptor induces cathepsin D-dependent production of a 20-kDa form of IL-1β under acidic extracellular pH in LPS-primed microglial cells. *Journal of Neurochemistry*, *117*(4), 712–723. https://doi.org/10.1111/j.1471-4159.2011.07240.x

407. Tan, S. H., Ong, K. C., & Wong, K. T. (2014). Enterovirus 71 can directly infect the brainstem via cranial nerves and infection can be ameliorated by passive immunization. *Journal of Neuropathology and Experimental Neurology*, *73*(11), 999–1008. https://doi.org/10.1097/NEN.0000000000000122

408. Tan, Y. W., Hong, W. J., & Chu, J. J. H. (2016). Inhibition of enterovirus VP4 myristoylation is a potential antiviral strategy for hand, foot and mouth disease. *Antiviral Research*, *133*, 191–195. https://doi.org/10.1016/j.antiviral.2016.08.009

409. Tanaka, H., Tamura, A., Suzuki, K., & Tsukita, S. (2017). Site-specific distribution of claudin-based paracellular channels with roles in biological fluid flow and metabolism. *Annals of the New York Academy of Sciences*, *1405*(1), 44–52. https://doi.org/10.1111/nyas.13438

410. Tang, W.-F., Huang, R.-T., Chien, K.-Y., Huang, J.-Y., Lau, K.-S., Jheng, J.-R., Chiu, C.-H., Wu, T.-Y., Chen, C.-Y., & Horng, J.-T. (2016). Host MicroRNA miR-197 Plays a Negative Regulatory Role in the Enterovirus 71 Infectious Cycle by

Targeting the RAN Protein. *Journal of Virology*, *90*(3), 1424–1438. https://doi.org/10.1128/JVI.02143-15

411. Tapia-Castillo, A., Guanzon, D., Palma, C., Lai, A., Barros, E., Allende, F., Vecchiola, A., Fardella, C. E., Salomón, C., & Carvajal, C. A. (2019). Downregulation of exosomal miR-192-5p and miR-204-5p in subjects with nonclassic apparent mineralocorticoid excess. *Journal of Translational Medicine*, *17*(1), 392. https://doi.org/10.1186/s12967-019-02143-8

412. Tapparel, C., Siegrist, F., Petty, T. J., & Kaiser, L. (2013). Picornavirus and enterovirus diversity with associated human diseases. *Infection, Genetics and Evolution: Journal of Molecular Epidemiology and Evolutionary Genetics in Infectious Diseases*, *14*, 282–293. https://doi.org/10.1016/j.meegid.2012.10.016

413. Tayyari, F., Marchant, D., Moraes, T. J., Duan, W., Mastrangelo, P., & Hegele, R. G. (2011). Identification of nucleolin as a cellular receptor for human respiratory syncytial virus. *Nature Medicine*, *17*(9), 1132–1135. https://doi.org/10.1038/nm.2444

414. Tee, H. K., Tan, C. W., Yogarajah, T., Lee, M. H. P., Chai, H. J., Hanapi, N. A., Yusof, S. R., Ong, K. C., Lee, V. S., Sam, I.-C., & Chan, Y. F. (2019). Electrostatic interactions at the five-fold axis alter heparin-binding phenotype and drive enterovirus A71 virulence in mice. *PLoS Pathogens*, *15*(11), e1007863. https://doi.org/10.1371/journal.ppat.1007863

415. Tee, H. K., Zainol, M. I., Sam, I.-C., & Chan, Y. F. (2021). Recent advances in the understanding of enterovirus A71 infection: A focus on neuropathogenesis.

Expert Review of Anti-Infective Therapy, *19*(6), 733–747. https://doi.org/10.1080/14787210.2021.1851194

416. Tee, K. K., Lam, T. T.-Y., Chan, Y. F., Bible, J. M., Kamarulzaman, A., Tong, C. Y. W., Takebe, Y., & Pybus, O. G. (2010). Evolutionary genetics of human enterovirus 71: Origin, population dynamics, natural selection, and seasonal periodicity of the VP1 gene. *Journal of Virology*, *84*(7), 3339–3350. https://doi.org/10.1128/JVI.01019-09

417. Thomsen, L. B., Burkhart, A., & Moos, T. (2015). A Triple Culture Model of the Blood-Brain Barrier Using Porcine Brain Endothelial cells, Astrocytes and Pericytes. *PloS One*, *10*(8), e0134765. https://doi.org/10.1371/journal.pone.0134765

418. Thomsen, M. S., Humle, N., Hede, E., Moos, T., Burkhart, A., & Thomsen, L. B. (2021). The blood-brain barrier studied in vitro across species. *PloS One*, *16*(3), e0236770. https://doi.org/10.1371/journal.pone.0236770

419. Tietz, S., & Engelhardt, B. (2015). Brain barriers: Crosstalk between complex tight junctions and adherens junctions. *The Journal of Cell Biology*, *209*(4), 493–506. https://doi.org/10.1083/jcb.201412147

420. Tiruppathi, C., Ahmmed, G. U., Vogel, S. M., & Malik, A. B. (2006). Ca2+ signaling, TRP channels, and endothelial permeability. *Microcirculation (New York, N.Y.: 1994)*, *13*(8), 693–708. https://doi.org/10.1080/10739680600930347

421. Tolbert, M., Morgan, C. E., Pollum, M., Crespo-Hernández, C. E., Li, M.-L., Brewer, G., & Tolbert, B. S. (2017). HnRNP A1 Alters the Structure of a Conserved Enterovirus IRES Domain to Stimulate Viral Translation. *Journal of Molecular Biology*, *429*(19), 2841–2858. https://doi.org/10.1016/j.jmb.2017.06.007

422. Tong, W.-B., Wu, X.-Q., He, M., Yang, F.-J., Jiang, Y., Zhang, G., & Zeng, P.-B. (2021). Epidemiological and etiological characteristics of hand, foot, and mouth disease before and after introducing enterovirus 71 vaccines in Sichuan, China: A 6-year retrospective study. *Chinese Medical Journal*, *134*(24), 3017–3019. https://doi.org/10.1097/CM9.0000000000001632

423. Too, I. H. K., Bonne, I., Tan, E. L., Chu, J. J. H., & Alonso, S. (2018). Prohibitin plays a critical role in Enterovirus 71 neuropathogenesis. *PLoS Pathogens*, *14*(1), e1006778. https://doi.org/10.1371/journal.ppat.1006778

424. Tseligka, E. D., Sobo, K., Stoppini, L., Cagno, V., Abdul, F., Piuz, I., Meylan, P., Huang, S., Constant, S., & Tapparel, C. (2018). A VP1 mutation acquired during an enterovirus 71 disseminated infection confers heparan sulfate binding ability and modulates ex vivo tropism. *PLoS Pathogens*, *14*(8), e1007190. https://doi.org/10.1371/journal.ppat.1007190

425. Tsuji-Tamura, K., & Ogawa, M. (2018). Morphology regulation in vascular endothelial cells. *Inflammation and Regeneration*, *38*, 25. https://doi.org/10.1186/s41232-018-0083-8

426. Tu, Y.-F., Lin, C.-H., Lee, H.-T., Yan, J.-J., Sze, C.-I., Chou, Y.-P., Ho, C.-J., & Huang, C.-C. (2015). Elevated cerebrospinal fluid endothelin 1 associated with

neurogenic pulmonary edema in children with enterovirus 71 encephalitis. *International Journal of Infectious Diseases: IJID: Official Publication of the International Society for Infectious Diseases*, *34*, 105–111. https://doi.org/10.1016/j.ijid.2015.03.017

427. van der Sanden, S., van der Avoort, H., Lemey, P., Uslu, G., & Koopmans, M. (2010). Evolutionary trajectory of the VP1 gene of human enterovirus 71 genogroup B and C viruses. *The Journal of General Virology*, *91*(Pt 8), 1949–1958. https://doi.org/10.1099/vir.0.019695-0

428. van Hinsbergh, T. M. T., Elbers, R. G., Hans Ket, J. C. F., van Furth, A. M., & Obihara, C. C. (2020). Neurological and neurodevelopmental outcomes after human parechovirus CNS infection in neonates and young children: A systematic review and meta-analysis. *The Lancet. Child & Adolescent Health*, *4*(8), 592–605. https://doi.org/10.1016/S2352-4642(20)30181-4

429. Van Itallie, C. M., Tietgens, A. J., Krystofiak, E., Kachar, B., & Anderson, J. M. (2015). A complex of ZO-1 and the BAR-domain protein TOCA-1 regulates actin assembly at the tight junction. *Molecular Biology of the Cell*, *26*(15), 2769–2787. https://doi.org/10.1091/mbc.E15-04-0232

430. Vance, L. M., Moscufo, N., Chow, M., & Heinz, B. A. (1997). Poliovirus 2C region functions during encapsidation of viral RNA. *Journal of Virology*, *71*(11), 8759–8765. https://doi.org/10.1128/JVI.71.11.8759-8765.1997

431. Vasileva, E., Spadaro, D., Rouaud, F., King, J. M., Flinois, A., Shah, J., Sluysmans, S., Méan, I., Jond, L., Turner, J. R., & Citi, S. (2022). Cingulin binds to the ZU5 domain of scaffolding protein ZO-1 to promote its extended

conformation, stabilization, and tight junction accumulation. *The Journal of Biological Chemistry*, *298*(4), 101797. https://doi.org/10.1016/j.jbc.2022.101797

432. Vega, J. L., Subiabre, M., Figueroa, F., Schalper, K. A., Osorio, L., González, J., & Sáez, J. C. (2013). Role of gap junctions and hemichannels in parasitic infections. *BioMed Research International*, *2013*, 589130. https://doi.org/10.1155/2013/589130

433. Verma, S., Kumar, M., Gurjav, U., Lum, S., & Nerurkar, V. R. (2010). Reversal of West Nile virus-induced blood-brain barrier disruption and tight junction proteins degradation by matrix metalloproteinases inhibitor. *Virology*, *397*(1), 130–138. https://doi.org/10.1016/j.virol.2009.10.036

434. Verma, S., Lo, Y., Chapagain, M., Lum, S., Kumar, M., Gurjav, U., Luo, H., Nakatsuka, A., & Nerurkar, V. R. (2009). West Nile virus infection modulates human brain microvascular endothelial cells tight junction proteins and cell adhesion molecules: Transmigration across the in vitro blood-brain barrier. *Virology*, *385*(2), 425–433. https://doi.org/10.1016/j.virol.2008.11.047

435. Versele, R., Corsi, M., Fuso, A., Sevin, E., Businaro, R., Gosselet, F., Fenart, L., & Candela, P. (2020). Ketone Bodies Promote Amyloid-β1-40 Clearance in a Human in Vitro Blood-Brain Barrier Model. *International Journal of Molecular Sciences*, *21*(3), E934. https://doi.org/10.3390/ijms21030934

436. Versele, R., Sevin, E., Gosselet, F., Fenart, L., & Candela, P. (2022). TNF-α and IL-1β Modulate Blood-Brain Barrier Permeability and Decrease Amyloid-β

Peptide Efflux in a Human Blood-Brain Barrier Model. *International Journal of Molecular Sciences*, *23*(18), 10235. https://doi.org/10.3390/ijms231810235

437. Veys, K., Fan, Z., Ghobrial, M., Bouché, A., García-Caballero, M., Vriens, K., Conchinha, N. V., Seuwen, A., Schlegel, F., Gorski, T., Crabbé, M., Gilardoni, P., Ardicoglu, R., Schaffenrath, J., Casteels, C., De Smet, G., Smolders, I., Van Laere, K., Abel, E. D., … De Bock, K. (2020). Role of the GLUT1 Glucose Transporter in Postnatal CNS Angiogenesis and Blood-Brain Barrier Integrity. *Circulation Research*, *127*(4), 466–482. https://doi.org/10.1161/CIRCRESAHA.119.316463

438. Visser, L. J., Langereis, M. A., Rabouw, H. H., Wahedi, M., Muntjewerff, E. M., de Groot, R. J., & van Kuppeveld, F. J. M. (2019). Essential Role of Enterovirus 2A Protease in Counteracting Stress Granule Formation and the Induction of Type I Interferon. *Journal of Virology*, *93*(10), e00222-19. https://doi.org/10.1128/JVI.00222-19

439. Voirin, A.-C., Perek, N., & Roche, F. (2020). Inflammatory stress induced by a combination of cytokines (IL-6, IL-17, TNF-α) leads to a loss of integrity on bEnd.3 endothelial cells in vitro BBB model. *Brain Research*, *1730*, 146647. https://doi.org/10.1016/j.brainres.2020.146647

440. Volle, R., Archimbaud, C., Couraud, P.-O., Romero, I. A., Weksler, B., Mirand, A., Pereira, B., Henquell, C., Peigue-Lafeuille, H., & Bailly, J.-L. (2015). Differential permissivity of human cerebrovascular endothelial cells to enterovirus infection and specificities of serotype EV-A71 in crossing an in vitro

model of the human blood-brain barrier. *The Journal of General Virology*, *96*(Pt 7), 1682–1695. https://doi.org/10.1099/vir.0.000103

441. Volle, R., Joffret, M.-L., Ndiaye, K., Fernandez-Garcia, M. D., Razafindratsimandresy, R., Heraud, J.-M., Rezig, D., Sadeuh-Mba, S. A., Boulahbal-Anes, L., Seghier, M., Deshpandeh, J. M., Bessaud, M., & Delpeyroux, F. (2020). Development of a New Internally Controlled One-Step Real-Time RT-PCR for the Molecular Detection of Enterovirus A71 in Africa and Madagascar. *Frontiers in Microbiology*, *11*, 1907. https://doi.org/10.3389/fmicb.2020.01907

442. Volle, R., Nourrisson, C., Mirand, A., Regagnon, C., Chambon, M., Henquell, C., Bailly, J.-L., Peigue-Lafeuille, H., & Archimbaud, C. (2012). Quantitative real-time RT-PCR assay for research studies on enterovirus infections in the central nervous system. *Journal of Virological Methods*, *185*(1), 142–148. https://doi.org/10.1016/j.jviromet.2012.06.019

443. Vulturar, R., Chiș, A., Pintilie, S., Farcaș, I. M., Botezatu, A., Login, C. C., Sitar-Taut, A.-V., Orasan, O. H., Stan, A., Lazea, C., Al-Khzouz, C., Mager, M., Vințan, M. A., Manole, S., & Damian, L. (2022). One Molecule for Mental Nourishment and More: Glucose Transporter Type 1-Biology and Deficiency Syndrome. *Biomedicines*, *10*(6), 1249. https://doi.org/10.3390/biomedicines10061249

444. Wang, B., Xi, X., Lei, X., Zhang, X., Cui, S., Wang, J., Jin, Q., & Zhao, Z. (2013). Enterovirus 71 Protease 2Apro Targets MAVS to Inhibit Anti-Viral Type I

Interferon Responses. *PLOS Pathogens*, *9*(3), e1003231. https://doi.org/10.1371/journal.ppat.1003231

445. Wang, H., Lei, X., Xiao, X., Yang, C., Lu, W., Huang, Z., Leng, Q., Jin, Q., He, B., Meng, G., & Wang, J. (2015). Reciprocal Regulation between Enterovirus 71 and the NLRP3 Inflammasome. *Cell Reports*, *12*(1), 42–48. https://doi.org/10.1016/j.celrep.2015.05.047

446. Wang, J., Hu, Y., & Zheng, M. (2022). Enterovirus A71 antivirals: Past, present, and future. *Acta Pharmaceutica Sinica. B*, *12*(4), 1542–1566. https://doi.org/10.1016/j.apsb.2021.08.017

447. Wang, L.-C., Chen, S.-O., Chang, S.-P., Lee, Y.-P., Yu, C.-K., Chen, C.-L., Tseng, P.-C., Hsieh, C.-Y., Chen, S.-H., & Lin, C.-F. (2015). Enterovirus 71 Proteins 2A and 3D Antagonize the Antiviral Activity of Gamma Interferon via Signaling Attenuation. *Journal of Virology*, *89*(14), 7028–7037. https://doi.org/10.1128/JVI.00205-15

448. Wang, L.-C., Yao, H.-W., Chang, C.-F., Wang, S.-W., Wang, S.-M., & Chen, S.-H. (2017). Suppression of interleukin-6 increases enterovirus A71 lethality in mice. *Journal of Biomedical Science*, *24*(1), 94. https://doi.org/10.1186/s12929-017-0401-5

449. Wang, S.-M., Ho, T.-S., Shen, C.-F., & Liu, C.-C. (2008). Enterovirus 71, one virus and many stories. *Pediatrics and Neonatology*, *49*(4), 113–115. https://doi.org/10.1016/S1875-9572(08)60024-8

450. Wang, S.-M., Lei, H.-Y., Huang, K.-J., Wu, J.-M., Wang, J.-R., Yu, C.-K., Su, I.-J., & Liu, C.-C. (2003). Pathogenesis of enterovirus 71 brainstem encephalitis in pediatric patients: Roles of cytokines and cellular immune activation in patients with pulmonary edema. *The Journal of Infectious Diseases*, *188*(4), 564–570. https://doi.org/10.1086/376998

451. Wang, S.-M., Lei, H.-Y., Huang, M.-C., Su, L.-Y., Lin, H.-C., Yu, C.-K., Wang, J.-L., & Liu, C.-C. (2006). Modulation of cytokine production by intravenous immunoglobulin in patients with enterovirus 71-associated brainstem encephalitis. *Journal of Clinical Virology: The Official Publication of the Pan American Society for Clinical Virology*, *37*(1), 47–52. https://doi.org/10.1016/j.jcv.2006.05.009

452. Wang, S.-M., Lei, H.-Y., Yu, C.-K., Wang, J.-R., Su, I.-J., & Liu, C.-C. (2008). Acute chemokine response in the blood and cerebrospinal fluid of children with enterovirus 71-associated brainstem encephalitis. *The Journal of Infectious Diseases*, *198*(7), 1002–1006. https://doi.org/10.1086/591462

453. Wang, T., Wang, B., Huang, H., Zhang, C., Zhu, Y., Pei, B., Cheng, C., Sun, L., Wang, J., Jin, Q., & Zhao, Z. (2017). Enterovirus 71 protease 2Apro and 3Cpro differentially inhibit the cellular endoplasmic reticulum-associated degradation (ERAD) pathway via distinct mechanisms, and enterovirus 71 hijacks ERAD component p97 to promote its replication. *PLoS Pathogens*, *13*(10), e1006674. https://doi.org/10.1371/journal.ppat.1006674

454. Wang, W., Li, W., Yang, X., Zhang, T., Wang, Y., Zhong, R., Jiao, Y., Li, T., Jiang, T., Tian, Y., & Wu, H. (2014). Interleukin-8 is elevated in severe hand,

foot, and mouth disease. *Journal of Infection in Developing Countries*, *8*(1), 94–100. https://doi.org/10.3855/jidc.3542

455. Wang, W., Sun, J., Wang, N., Sun, Z., Ma, Q., Li, J., Zhang, M., & Xu, J. (2020). Enterovirus A71 capsid protein VP1 increases blood-brain barrier permeability and virus receptor vimentin on the brain endothelial cells. *Journal of Neurovirology*, *26*(1), 84–94. https://doi.org/10.1007/s13365-019-00800-8

456. Wang, W., Xiao, F., Wan, P., Pan, P., Zhang, Y., Liu, F., Wu, K., Liu, Y., & Wu, J. (2017). EV71 3D Protein Binds with NLRP3 and Enhances the Assembly of Inflammasome Complex. *PLoS Pathogens*, *13*(1), e1006123. https://doi.org/10.1371/journal.ppat.1006123

457. Wang, Y., Gallagher, E., Jorgensen, C., Troendle, E. P., Hu, D., Searson, P. C., & Ulmschneider, M. B. (2019). An experimentally validated approach to calculate the blood-brain barrier permeability of small molecules. *Scientific Reports*, *9*(1), 6117. https://doi.org/10.1038/s41598-019-42272-0

458. Wang, Y., Zhang, S., Song, W., Zhang, W., Li, J., Li, C., Qiu, Y., Fang, Y., Jiang, Q., Li, X., & Yan, B. (2020). Exosomes from EV71-infected oral epithelial cells can transfer miR-30a to promote EV71 infection. *Oral Diseases*, *26*(4), 778–788. https://doi.org/10.1111/odi.13283

459. Watanabe, T., Dohgu, S., Takata, F., Nishioku, T., Nakashima, A., Futagami, K., Yamauchi, A., & Kataoka, Y. (2013). Paracellular barrier and tight junction protein expression in the immortalized brain endothelial cell lines bEND.3, bEND.5 and mouse brain endothelial cell 4. *Biological & Pharmaceutical Bulletin*, *36*(3), 492–495. https://doi.org/10.1248/bpb.b12-00915

460. Watson, P. M., Anderson, J. M., Vanltallie, C. M., & Doctrow, S. R. (1991). The tight-junction-specific protein ZO-1 is a component of the human and rat blood-brain barriers. *Neuroscience Letters*, *129*(1), 6–10. https://doi.org/10.1016/0304-3940(91)90708-2

461. Weber, C. M., & Clyne, A. M. (2021). Sex differences in the blood-brain barrier and neurodegenerative diseases. *APL Bioengineering*, *5*(1), 011509. https://doi.org/10.1063/5.0035610

462. Wei, W.-J., Wang, Y.-C., Guan, X., Chen, W.-G., & Liu, J. (2022). A neurovascular unit-on-a-chip: Culture and differentiation of human neural stem cells in a three-dimensional microfluidic environment. *Neural Regeneration Research*, *17*(10), 2260–2266. https://doi.org/10.4103/1673-5374.337050

463. Weksler, B. B., Subileau, E. A., Perrière, N., Charneau, P., Holloway, K., Leveque, M., Tricoire-Leignel, H., Nicotra, A., Bourdoulous, S., Turowski, P., Male, D. K., Roux, F., Greenwood, J., Romero, I. A., & Couraud, P. O. (2005). Blood-brain barrier-specific properties of a human adult brain endothelial cell line. *FASEB Journal: Official Publication of the Federation of American Societies for Experimental Biology*, *19*(13), 1872–1874. https://doi.org/10.1096/fj.04-3458fje

464. Wellens, S., Dehouck, L., Chandrasekaran, V., Singh, P., Loiola, R. A., Sevin, E., Exner, T., Jennings, P., Gosselet, F., & Culot, M. (2021). Evaluation of a human iPSC-derived BBB model for repeated dose toxicity testing with cyclosporine A as model compound. *Toxicology in Vitro: An International*

Journal Published in Association with BIBRA, *73*, 105112. https://doi.org/10.1016/j.tiv.2021.105112

465. Wenner, H. A. (1982). The enteroviruses: Recent advances. *The Yale Journal of Biology and Medicine*, *55*(3–4), 277–282.

466. Wiatr, M., Stump-Guthier, C., Latorre, D., Uhlig, S., Weiss, C., Ilonen, J., Engelhardt, B., Ishikawa, H., Schwerk, C., Schroten, H., Tenenbaum, T., & Rudolph, H. (2019). Distinct migratory pattern of naive and effector T cells through the blood-CSF barrier following Echovirus 30 infection. *Journal of Neuroinflammation*, *16*(1), 232. https://doi.org/10.1186/s12974-019-1626-x

467. Wilhelm, I., Fazakas, C., & Krizbai, I. A. (2011). In vitro models of the blood-brain barrier. *Acta Neurobiologiae Experimentalis*, *71*(1), 113–128.

468. Willebrords, J., Maes, M., Crespo Yanguas, S., & Vinken, M. (2017). Inhibitors of connexin and pannexin channels as potential therapeutics. *Pharmacology & Therapeutics*, *180*, 144–160. https://doi.org/10.1016/j.pharmthera.2017.07.001

469. Wu, L.-F., Zhang, Q., Mo, X.-B., Lin, J., Wu, Y.-L., Lu, X., He, P., Wu, J., Guo, Y.-F., Wang, M.-J., Ren, W.-Y., Deng, H.-W., Lei, S.-F., & Deng, F.-Y. (2022). Identification of novel rheumatoid arthritis-associated MiRNA-204-5p from plasma exosomes. *Experimental & Molecular Medicine*, *54*(3), 334–345. https://doi.org/10.1038/s12276-022-00751-x

470. Wu, L.-W., Yin, F., Peng, J., Wang, W.-D., & Gan, N. (2008). [The tight junction proteins ZO-1, occludin and actin participate in the permeability increasing of

blood-brain barrier induced by hypoxia-ischemia]. *Zhongguo Dang Dai Er Ke Za Zhi = Chinese Journal of Contemporary Pediatrics*, *10*(4), 513–516.

471. Xiao, H.-S., Xie, Q., Zhong, J.-Y., Gerald Rukundo, B., He, X.-L., Qu, Y.-L., & Cao, H. (2018). [Effect of vimentin on activation of NLRP3 inflammasome in the brain of mice with EV71 infection]. *Nan Fang Yi Ke Da Xue Xue Bao = Journal of Southern Medical University*, *38*(6), 704–710.

472. Xie, G., & Duan, Z. (2016). [EV71 Infection and Innate Antiviral Innate Immunity]. *Bing Du Xue Bao = Chinese Journal of Virology*, *32*(4), 501–508.

473. Xing, J., Liu, D., Shen, S., Su, Z., Zhang, L., Duan, Y., Tong, F., Liang, Y., Wang, H., Deng, F., Hu, Z., & Zhou, Y. (2016). Pathologic Studies of Fatal Encephalomyelitis in Children Caused by Enterovirus 71. *American Journal of Clinical Pathology*, *146*(1), 95–106. https://doi.org/10.1093/ajcp/aqw089

474. Xu, J., Qian, Y., Wang, S., Serrano, J. M. G., Li, W., Huang, Z., & Lu, S. (2010). EV71: An emerging infectious disease vaccine target in the Far East? *Vaccine*, *28*(20), 3516–3521. https://doi.org/10.1016/j.vaccine.2010.03.003

475. Xu, Y., Li, S., Cai, C., Liu, J., Wang, Y., Jiang, Y., Du, L., & Chen, Z. (2019). Characterization of inflammatory cytokine profiles in cerebrospinal fluid of hand, foot, and mouth disease children with enterovirus 71-related encephalitis in Hangzhou, Zhejiang, China. *Medicine*, *98*(52), e18464. https://doi.org/10.1097/MD.0000000000018464

476. Xu, Y., Qiu, Y., Lin, Q., Huang, C., Li, J., Chen, L., Xue, Z., Wu, Q., & Wang, Y. (2022). MiR-126-3p-loaded small extracellular vesicles secreted by urine-

derived stem cells released from a phototriggered imine crosslink hydrogel could enhance vaginal epithelization after vaginoplasty. *Stem Cell Research & Therapy*, *13*(1), 331. https://doi.org/10.1186/s13287-022-03003-x

477. Yamamoto, M., Ramirez, S. H., Sato, S., Kiyota, T., Cerny, R. L., Kaibuchi, K., Persidsky, Y., & Ikezu, T. (2008). Phosphorylation of claudin-5 and occludin by rho kinase in brain endothelial cells. *The American Journal of Pathology*, *172*(2), 521–533. https://doi.org/10.2353/ajpath.2008.070076

478. Yamayoshi, S., Fujii, K., & Koike, S. (2012). Scavenger receptor b2 as a receptor for hand, foot, and mouth disease and severe neurological diseases. *Frontiers in Microbiology*, *3*, 32. https://doi.org/10.3389/fmicb.2012.00032

479. Yamayoshi, S., Ohka, S., Fujii, K., & Koike, S. (2013). Functional comparison of SCARB2 and PSGL1 as receptors for enterovirus 71. *Journal of Virology*, *87*(6), 3335–3347. https://doi.org/10.1128/JVI.02070-12

480. Yamayoshi, S., Yamashita, Y., Li, J., Hanagata, N., Minowa, T., Takemura, T., & Koike, S. (2009). Scavenger receptor B2 is a cellular receptor for enterovirus 71. *Nature Medicine*, *15*(7), 798–801. https://doi.org/10.1038/nm.1992

481. Yang, B., Chuang, H., & Yang, K. D. (2009). Sialylated glycans as receptor and inhibitor of enterovirus 71 infection to DLD-1 intestinal cells. *Virology Journal*, *6*, 141. https://doi.org/10.1186/1743-422X-6-141

482. Yang, F., Zhang, N., Chen, Y., Yin, J., Xu, M., Cheng, X., Ma, R., Meng, J., & Du, Y. (2022). Role of Non-Coding RNA in Neurological Complications

Associated With Enterovirus 71. *Frontiers in Cellular and Infection Microbiology*, *12*, 873304. https://doi.org/10.3389/fcimb.2022.873304

483. Yang, F., Zhao, K., Zhang, X., Zhang, J., & Xu, B. (2016). ATP Induces Disruption of Tight Junction Proteins via IL-1 Beta-Dependent MMP-9 Activation of Human Blood-Brain Barrier In Vitro. *Neural Plasticity*, *2016*, 8928530. https://doi.org/10.1155/2016/8928530

484. Yang, J., Zhao, N., Su, N.-L., Sun, J.-L., Lv, T.-G., & Chen, Z.-B. (2012). Association of interleukin 10 and interferon gamma gene polymorphisms with enterovirus 71 encephalitis in patients with hand, foot and mouth disease. *Scandinavian Journal of Infectious Diseases*, *44*(6), 465–469. https://doi.org/10.3109/00365548.2011.649490

485. Yang, S.-L., Chou, Y.-T., Wu, C.-N., & Ho, M.-S. (2011). Annexin II binds to capsid protein VP1 of enterovirus 71 and enhances viral infectivity. *Journal of Virology*, *85*(22), 11809–11820. https://doi.org/10.1128/JVI.00297-11

486. Yang, T. O., Arthur Huang, K.-Y., Chen, M.-H., Chen, P.-C., & Huang, W.-T. (2019). Comparison of Nonpolio Enteroviruses in Children With Herpangina and Hand, Foot and Mouth Disease in Taiwan. *The Pediatric Infectious Disease Journal*, *38*(9), 887–893. https://doi.org/10.1097/INF.0000000000002351

487. Yang, Y., Cong, H., Du, N., Han, X., Song, L., Zhang, W., Li, C., & Tien, P. (2019). Mitochondria Redistribution in Enterovirus A71 Infected Cells and Its Effect on Virus Replication. *Virologica Sinica*, *34*(4), 397–411. https://doi.org/10.1007/s12250-019-00120-5

488. Yao, L., Xue, X., Yu, P., Ni, Y., & Chen, F. (2018). Evans Blue Dye: A Revisit of Its Applications in Biomedicine. *Contrast Media & Molecular Imaging*, *2018*, 7628037. https://doi.org/10.1155/2018/7628037

489. Yao, S., Yin, Y., Jin, G., Li, D., Li, M., Hu, Y., Feng, Y., Liu, Y., Bian, Z., Wang, X., Mao, Y., Zhang, J., Wu, Z., & Huang, Z. (2020). Exosome-mediated delivery of miR-204-5p inhibits tumor growth and chemoresistance. *Cancer Medicine*, *9*(16), 5989–5998. https://doi.org/10.1002/cam4.3248

490. Yee, P. T. I., & Poh, C. L. (2015). Development of Novel Vaccines against Enterovirus-71. *Viruses*, *8*(1), E1. https://doi.org/10.3390/v8010001

491. Yeung, M. L., Jia, L., Yip, C. C. Y., Chan, J. F. W., Teng, J. L. L., Chan, K.-H., Cai, J.-P., Zhang, C., Zhang, A. J., Wong, W.-M., Kok, K.-H., Lau, S. K. P., Woo, P. C. Y., Lo, J. Y. C., Jin, D.-Y., Shih, S.-R., & Yuen, K.-Y. (2018). Human tryptophanyl-tRNA synthetase is an IFN-γ-inducible entry factor for Enterovirus. *The Journal of Clinical Investigation*, *128*(11), 5163–5177. https://doi.org/10.1172/JCI99411

492. Yoshida, H., Imaizumi, T., Lee, S. J., Tanji, K., Sakaki, H., Matsumiya, T., Ishikawa, A., Taima, K., Yuzawa, E., Mori, F., Wakabayashi, K., Kimura, H., & Satoh, K. (2007). Retinoic acid-inducible gene-I mediates RANTES/CCL5 expression in U373MG human astrocytoma cells stimulated with double-stranded RNA. *Neuroscience Research*, *58*(2), 199–206. https://doi.org/10.1016/j.neures.2007.02.017

493. Yu, P., Gao, Z., Zong, Y., Bao, L., Xu, L., Deng, W., Xu, Y., Gao, Z., Yao, Y., Li, F., Lv, Q., & Qin, C. (2015). Distribution of enterovirus 71 RNA in inflammatory

cells infiltrating different tissues in fatal cases of hand, foot, and mouth disease. *Archives of Virology*, *160*(1), 81–90. https://doi.org/10.1007/s00705-014-2233-x

494. Yu, X., Lan, P., Hou, X., Han, Q., Lu, N., Li, T., Jiao, C., Zhang, J., Zhang, C., & Tian, Z. (2017). HBV inhibits LPS-induced NLRP3 inflammasome activation and IL-1β production via suppressing the NF-κB pathway and ROS production. *Journal of Hepatology*, *66*(4), 693–702. https://doi.org/10.1016/j.jhep.2016.12.018

495. Yuan, A., Li, J., Liu, P., Chen, Z., Hou, M., Wang, J., & Han, Z. (2015). Association of interleukin-6-572C/G gene polymorphism and serum or cerebrospinal fluid interleukin-6 level with enterovirus 71 encephalitis in Chinese Han patients with hand, foot, and mouth disease. *Inflammation*, *38*(2), 728–735. https://doi.org/10.1007/s10753-014-9983-1

496. Yuan, A.-Y., He, H.-F., Lyu, F.-Y., Liu, P.-P., Hu, J.-F., & Chen, Z.-B. (2017). [Association of TLR3-1377C/T gene polymorphisms and expression with susceptibility to enterovirus 71 encephalitis in children]. *Zhongguo Dang Dai Er Ke Za Zhi = Chinese Journal of Contemporary Pediatrics*, *19*(1), 39–43.

497. Yuan, J., Shen, L., Wu, J., Zou, X., Gu, J., Chen, J., & Mao, L. (2018). Enterovirus A71 Proteins: Structure and Function. *Frontiers in Microbiology*, *9*, 286. https://doi.org/10.3389/fmicb.2018.00286

498. Yuan, S., Liu, K. J., & Qi, Z. (2020). Occludin regulation of blood-brain barrier and potential therapeutic target in ischemic stroke. *Brain Circulation*, *6*(3), 152–162. https://doi.org/10.4103/bc.bc_29_20

499. Yusof, S. R., Avdeef, A., & Abbott, N. J. (2014). In vitro porcine blood-brain barrier model for permeability studies: PCEL-X software pKa(FLUX) method for aqueous boundary layer correction and detailed data analysis. *European Journal of Pharmaceutical Sciences: Official Journal of the European Federation for Pharmaceutical Sciences*, *65*, 98–111. https://doi.org/10.1016/j.ejps.2014.09.009

500. Zell, R. (2018). Picornaviridae-the ever-growing virus family. *Archives of Virology*, *163*(2), 299–317. https://doi.org/10.1007/s00705-017-3614-8

501. Zeng, X., He, G., Yang, X., Xu, G., Tang, Y., Li, H., Yu, B., Wang, Z., Xu, W., & Song, K. (2022). Zebularine protects against blood-brain-barrier (BBB) disruption through increasing the expression of zona occludens-1 (ZO-1) and vascular endothelial (VE)-cadherin. *Bioengineered*, *13*(2), 4441–4454. https://doi.org/10.1080/21655979.2021.2024323

502. Zhang, H., Wang, X., Wang, Y., Pei, X., Wang, C., Niu, Y., Xu, P., & Peng, Y. (2018). Substituted 3-benzylcoumarins 13 and 14 suppress enterovirus A71 replication by impairing viral 2Apro dependent IRES-driven translation. *Antiviral Research*, *160*, 10–16. https://doi.org/10.1016/j.antiviral.2018.10.012

503. Zhang, Q., Li, S., Lei, P., Li, Z., Chen, F., Chen, Q., Wang, Y., Gong, J., Tang, Q., Liu, X., Lan, K., & Wu, S. (2021). ANXA2 Facilitates Enterovirus 71 Infection by Interacting with 3D Polymerase and PI4KB to Assist the Assembly of Replication Organelles. *Virologica Sinica*, *36*(6), 1387–1399. https://doi.org/10.1007/s12250-021-00417-4

504. Zhang, Q., Zhao, B., Chen, X., Song, N., Wu, J., Li, G., Yu, P., Han, Y., Liu, J., & Qin, C. (2018). GS-9620 inhibits enterovirus 71 replication mainly through the NF-κB and PI3K-AKT signaling pathways. *Antiviral Research*, *153*, 39–48. https://doi.org/10.1016/j.antiviral.2018.02.002

505. Zhang, W., Huang, Z., Huang, M., & Zeng, J. (2020). Predicting Severe Enterovirus 71-Infected Hand, Foot, and Mouth Disease: Cytokines and Chemokines. *Mediators of Inflammation*, *2020*, 9273241. https://doi.org/10.1155/2020/9273241

506. Zhang, Y., Khan, S., Liu, Y., Siddique, R., Zhang, R., Yong, V. W., & Xue, M. (2021). Gap Junctions and Hemichannels Composed of Connexins and Pannexins Mediate the Secondary Brain Injury Following Intracerebral Hemorrhage. *Biology*, *11*(1), 27. https://doi.org/10.3390/biology11010027

507. Zhang, Y., Liu, H., Wang, L., Yang, F., Hu, Y., Ren, X., Li, G., Yang, Y., Sun, S., Li, Y., Chen, X., Li, X., & Jin, Q. (2013). Comparative study of the cytokine/chemokine response in children with differing disease severity in enterovirus 71-induced hand, foot, and mouth disease. *PloS One*, *8*(6), e67430. https://doi.org/10.1371/journal.pone.0067430

508. Zhang, Y., Wang, J., Guo, W., Wang, H., Zhu, S., Wang, D., Bai, R., Li, X., Yan, D., Wang, H., Zhang, Y., Zhu, Z., Tan, X., An, H., Xu, A., & Xu, W. (2011). Emergence and transmission pathways of rapidly evolving evolutionary branch C4a strains of human enterovirus 71 in the Central Plain of China. *PloS One*, *6*(11), e27895. https://doi.org/10.1371/journal.pone.0027895

509. Zhang, Y.-X., Huang, Y.-M., Li, Q.-J., Li, X.-Y., Zhou, Y.-D., Guo, F., Zhou, J.-M., & Cen, S. (2017). A highly conserved amino acid in VP1 regulates maturation of enterovirus 71. *PLoS Pathogens*, *13*(9), e1006625. https://doi.org/10.1371/journal.ppat.1006625

510. Zhao, T., Zhang, Z., Zhang, Y., Feng, M., Fan, S., Wang, L., Liu, L., Wang, X., Wang, Q., Zhang, X., Wang, J., Liao, Y., He, Z., Lu, S., Yang, H., & Li, Q. (2017). Dynamic Interaction of Enterovirus 71 and Dendritic Cells in Infected Neonatal Rhesus Macaques. *Frontiers in Cellular and Infection Microbiology*, *7*, 171. https://doi.org/10.3389/fcimb.2017.00171

511. Zhao, W., Han, L., Bae, Y., & Manickam, D. S. (2019). Lucifer Yellow—A Robust Paracellular Permeability Marker in a Cell Model of the Human Blood-brain Barrier. *Journal of Visualized Experiments: JoVE*, *150*. https://doi.org/10.3791/58900

512. Zhao, Z., Li, Z., Huan, C., Liu, X., & Zhang, W. (2021). SAMHD1 Inhibits Multiple Enteroviruses by Interfering with the Interaction between VP1 and VP2 Proteins. *Journal of Virology*, *95*(13), e0062021. https://doi.org/10.1128/JVI.00620-21

513. Zheng, W., Shi, H., Chen, Y., Xu, Z., Chen, J., & Jin, L. (2017). Alteration of serum high-mobility group protein 1 (HMGB1) levels in children with enterovirus 71-induced hand, foot, and mouth disease. *Medicine*, *96*(17), e6764. https://doi.org/10.1097/MD.0000000000006764

514. Zheng, X.-Q., Chen, X.-Q., Gao, Y., Fu, M., Chen, Y.-P., Xu, D.-P., Lin, A., & Yan, W.-H. (2014). Elevation of human leukocyte antigen-G expression is associated with the severe encephalitis associated with neurogenic pulmonary

edema caused by Enterovirus 71. *Clinical and Experimental Medicine*, *14*(2), 161–167. https://doi.org/10.1007/s10238-013-0237-6

515. Zhou, D., Zhao, Y., Kotecha, A., Fry, E. E., Kelly, J. T., Wang, X., Rao, Z., Rowlands, D. J., Ren, J., & Stuart, D. I. (2019a). Unexpected mode of engagement between enterovirus 71 and its receptor SCARB2. *Nature Microbiology*, *4*(3), 414–419. https://doi.org/10.1038/s41564-018-0319-z

516. Zhou, D., Zhao, Y., Kotecha, A., Fry, E. E., Kelly, J. T., Wang, X., Rao, Z., Rowlands, D. J., Ren, J., & Stuart, D. I. (2019b). Unexpected mode of engagement between enterovirus 71 and its receptor SCARB2. *Nature Microbiology*, *4*(3), 414–419. https://doi.org/10.1038/s41564-018-0319-z

517. Zhou, J., Shi, Y., Miao, L., Zhang, C., & Liu, Y. (2021). Molecular epidemiology and recombination of Enterovirus A71 in mainland China from 1987 to 2017. *International Microbiology: The Official Journal of the Spanish Society for Microbiology*, *24*(3), 291–299. https://doi.org/10.1007/s10123-021-00164-2

518. Zhu, F., Xu, W., Xia, J., Liang, Z., Liu, Y., Zhang, X., Tan, X., Wang, L., Mao, Q., Wu, J., Hu, Y., Ji, T., Song, L., Liang, Q., Zhang, B., Gao, Q., Li, J., Wang, S., Hu, Y., … Wang, N. (2014). Efficacy, safety, and immunogenicity of an enterovirus 71 vaccine in China. *The New England Journal of Medicine*, *370*(9), 818–828. https://doi.org/10.1056/NEJMoa1304923

519. Zhu, H., Cao, Y., Su, W., Huang, S., Lu, W., Zhou, Y., Gao, J., Zhao, W., Zhang, B., & Wu, X. (2019). Enterovirus A71 VP1 Variation A289T Decreases the Central Nervous System Infectivity via Attenuation of Interactions between VP1

and Vimentin In Vitro and In Vivo. *Viruses*, *11*(5), E467. https://doi.org/10.3390/v11050467

520. Zhu, J., Chen, N., Zhou, S., Zheng, K., Sun, L., Zhang, Y., Cao, L., Zhang, X., Xiang, Q., Chen, Z., Wang, C., Fan, C., & He, Q. (2018). Severity of enterovirus A71 infection in a human SCARB2 knock-in mouse model is dependent on infectious strain and route. *Emerging Microbes & Infections*, *7*(1), 205. https://doi.org/10.1038/s41426-018-0201-3

521. Zoll, J., Heus, H. A., van Kuppeveld, F. J. M., & Melchers, W. J. G. (2009). The structure-function relationship of the enterovirus 3'-UTR. *Virus Research*, *139*(2), 209–216. https://doi.org/10.1016/j.virusres.2008.07.014

ANNEXES

9) Annexes

I. Source of data: Fig. 46

TEER		
Day 7	**Day 11**	**Day 14**
45,79556	31,60889	52,26667
48,03556	31,60889	46,66667
42,43556	30,48889	38,82667
48,03556	32,72889	36,58667
37,95556	32,72889	48,90667
51,39556	34,96889	44,42667
49,15556	31,60889	44,42667
45,79556	32,72889	55,62667
52,51556	30,48889	35,46667
42,43556	34,96889	35,46667
30,11556	30,48889	39,94667
35,71556	31,60889	32,10667
49,15556	23,76889	28,74667
36,83556	34,96889	33,22667
36,83556	31,60889	36,58667
46,91556	27,12889	39,94667
37,95556	31,60889	48,90667
40,19556	40,56889	43,30667

Pe

Day 7	Day 11	Day 14
0,43	0,67	0,44
0,75	0,68	0,43
1	0,51	0,43
0,69	0,46	0,74
0,63	0,45	0,66
0,77	0,7	0,69

Rho 123	Rho 123 + Elacridar
82,89001	113,2901
106,202	129,4558
105,793	110,9572
88,23253	111,8512
106,1313	124,6507
105,3792	111,2577
84,82108	111,3941
116,4282	128,6167
104,1228	109,5096
108,3591	154,392
106,3425	155,9162
102,0727	145,8333
104,6556	148,1699
107,3693	140,2002
102,177	77,35893

107,6037	172,3746
104,0424	184,6304
57,37772	124,0756

II. Source of data : Fig. 47

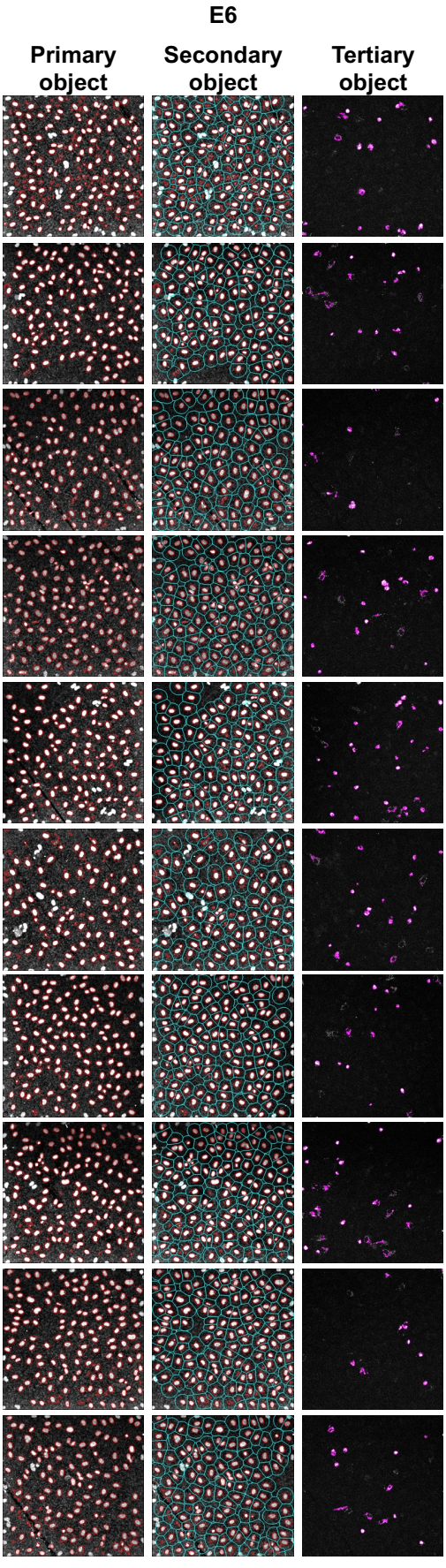
E6
Primary object
Secondary object
Tertiary object

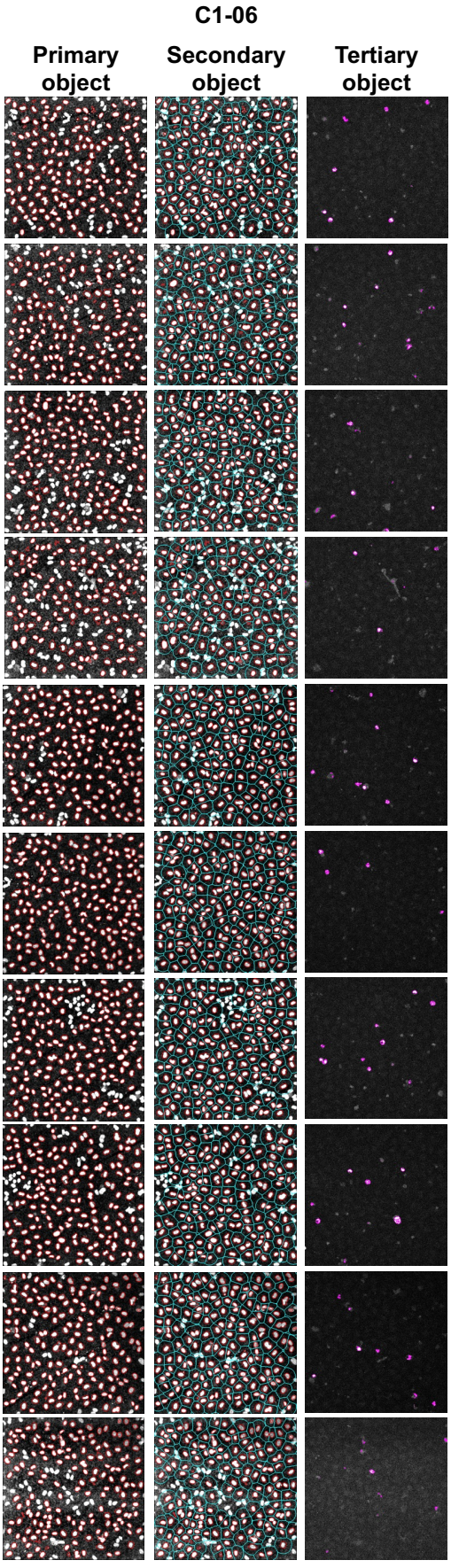
C1-06
Primary object
Secondary object
Tertiary object

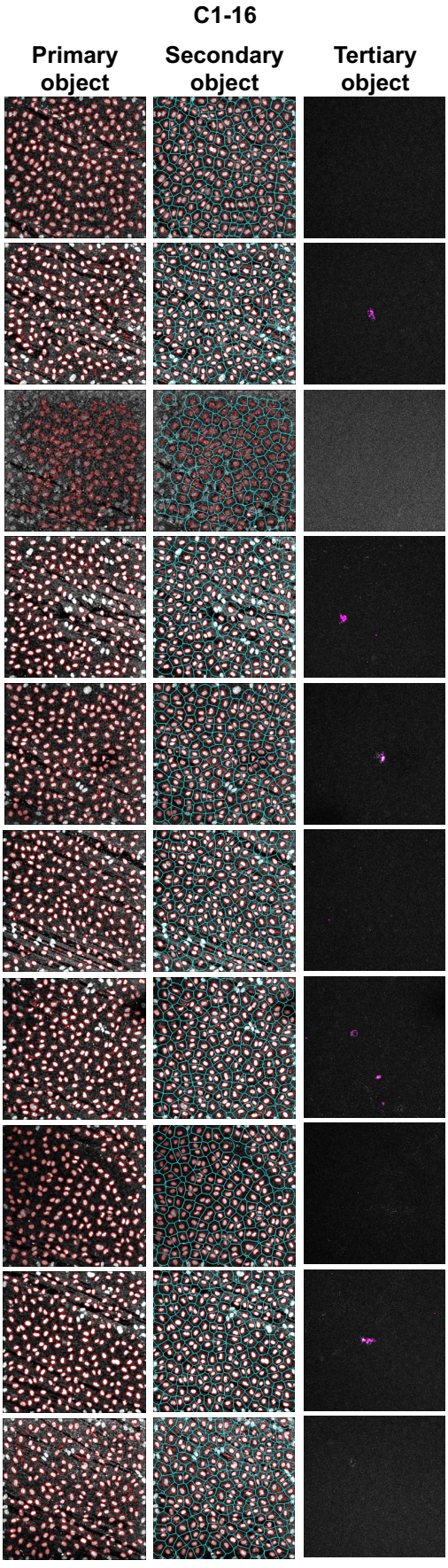
C1-16
Primary object
Secondary object
Tertiary object

C1-04

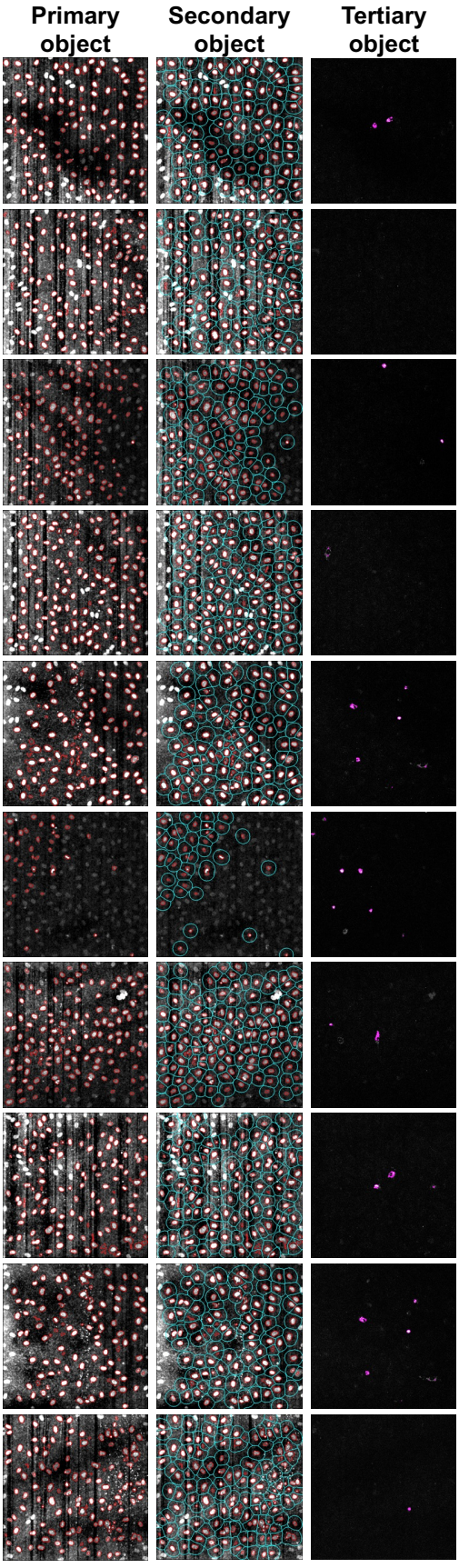

III. Source of data: Fig. 48

Cell counting			
24 h.p.i			
E6	**C1-06**	**C1-16**	**C4-04**
122	151	131	114
137	153	172	123
123	156	189	112
156	130	188	115
121	157	179	111
103	176	184	40
130	162	179	130
142	151	179	120
143	169	191	100
126	153	181	125

Percentage of infected cells			
24 h.p.i			
E6	**C1-06**	**C1-16**	**C4-04**
8,19672131	5,9602649	0	2,63157895
17,5182482	7,18954248	3,48837209	1,62601626
17,8861789	6,41025641	2,11640212	0
13,4615385	3,84615385	0	1,73913044

23,1404959	6,36942675	2,23463687	5,40540541
18,4466019	2,27272727	0,54347826	12,5
13,8461539	6,17283951	2,23463687	3,07692308
18,3098592	5,29801325	0	3,33333333
6,29370629	5,91715976	2,61780105	6
11,9047619	8,49673203	0	0,8

GF-AFC					
24 h.p.i					
MOCK	**E6 (MOI = 0.25)**	**E6 (MOI = 0.625)**	**C1-06**	**C1-16**	**C4-04**
94,05229	85,82492	93,38064	95,54083	94,2582	105,3633
92,79787	83,68687	93,58405	93,03452	89,76831	101,7748
90,77868	83,48652	89,59128	95,81157	96,02218	100,0039
102,0048	97,77163	95,75617	94,5466	103,603	100,0707
92,48392	100,5349	85,4554	98,25073	87,35906	90,50855
123,6928	99,74034	71,68597	94,92026	101,4167	93,11245
101,4154			102,3673	99,44625	94,39285
95,64376			103,601	98,1784	99,23613

98,65123			99,81094	98,88901	95,28793
102,2483			98,18054	100,9282	87,99257
101,9616			94,6562	93,86757	91,63926
104,2694			103,9719	97,63275	100,1189

GF-AFC					
48 h.p.i					
MOCK	**E6 (MOI = 0.25)**	**E6 (MOI = 0.625)**	**C1-06**	**C1-16**	**C4-04**
105,461	32,14043	35,98144	97,60886	89,11664	81,88005
94,97463	31,21847	35,81258	96,18316	87,32582	87,22499
103,7811	31,01564	34,17476	92,74221	83,01186	83,85274
100,7389	28,12497	56,73373	90,44689	90,8743	79,97198
100,0267	33,28742	38,25028	94,10768	95,02625	79,72502
106,3765	27,59218	64,29977	93,8095	87,0423	79,33718
96,85578			95,63461	85,24036	82,97675

95,01418			90,93368	80,26758	82,66233
99,10264			89,69112	83,18177	82,50178
95,17029			91,6749	80,26837	74,51421
102,4961			94,50483	76,74817	79,54124
100,0023			92,885	78,64347	79,45298

GF-AFC					
72 h.p.i					
MOCK	**E6 (MOI = 0.25)**	**E6 (MOI = 0.625)**	**C1-06**	**C1-16**	**C4-04**
110,4761	23,29674	27,94464	91,28218	82,6175	67,76555
106,3631	26,20621	31,71628	86,53858	84,83362	77,85591
108,4293	29,2632	31,92564	81,23538	76,59178	68,71039
115,8323	17,2491	17,0046	83,88694	86,45916	68,46096
116,1802	18,71165	18,85892	87,59396	71,52853	78,38561
111,9583	14,95225	24,76085	82,71501	80,0715	71,22897

88,68599			76,02081	65,81566	59,04411
86,64038			74,5454	68,5703	59,47415
88,40452			76,18829	63,92529	50,59396
90,301			74,82634	66,44009	44,51641
89,81691			75,231	64,24619	47,85986
86,91179			79,623467	62,7632	43,52036

IV. Source of data: Fig 49

Pe				
24 h.p.i				
TNF-α luminal	**TNF-α abluminal**	**TNF-α luminal + C1-16**	**TNF-α abluminal + C1-16**	**C1-16**
2,4	1,01	2,52	1,04	0,91
2,37	0,99	2,25	0,85	0,95
1,66	0,91	1,53	0,99	0,91
1,36	1,22	1,86	2,89	0,68
1,23	1,06	1,44	2,06	0,68
2,39	1,63	1,54	2,46	0,75

Pe				
48 h.p.i				
TNF-α luminal	**TNF-α abluminal**	**TNF-α luminal + C1-16**	**TNF-α abluminal + C1-16**	**C1-16**
0,99	1,57	2,94	3,16	0,71
1,08	1,56	2,54	4,41	0,73
0,89	1,11	4	3,66	0,71
0,87	1,26	2,84	2,43	0,78
1,02	1,1	2	5,56	0,69
3,68	1,34	6,23	1,51	0,72

Pe			
24 h.p.i			
E6	**C1-06**	**C1-16**	**C4-04**
1,29	0,76	0,91	0,98
1,07	0,78	0,95	0,91
1,37	0,76	0,91	0,92
1,21	0,78	0,68	1
1,42	0,74	0,68	0,79
1,66	0,79	0,75	0,81

Pe
72 h.p.i

C1-06	C1-16	C4-04
1,1	0,68	1,29
1,1	0,64	1,12
1,05	0,66	0,99
3,21	0,87	0,68
1,87	0,92	0,57
3,45	0,82	0,64

V. Source of data: Fig 50

MNCPU			
Luminal			
6 h.p.i			
E6	**TNF-α luminal + C1-16**	**TNF-α abluminal + C1-16**	**C1-16**
39,81072	91,20108	165,9587	186,2087
23,98833	75,85776	125,8925	125,8925
34,67369	173,7801	131,8257	407,3803
39,81072	83,17638	162,181	204,1738
48,97788	213,7962	389,0451	323,5937
22,90868	257,0396	162,181	269,1535

MNCPU
Luminal

24 h.p.i			
E6	**TNF-α luminal + C1-16**	**TNF-α abluminal + C1-16**	**C1-16**
407420,1	4365,158	2187,762	1819,701
660717,4	3235,937	724,436	3019,952
588878,3	7244,36	1778,279	4073,803
269193,3	11481,54	13803,84	1778,279
489827,8	20892,96	39810,72	2344,229
204196,7	15488,17	5754,399	2511,886

MNCPU		
Luminal		
48 h.p.i		
TNF-α luminal + C1-16	**TNF-α abluminal + C1-16**	**C1-16**
8317,638	4265,795	5011,872
5888,437	1778,279	2818,383
9332,543	4365,158	2570,396
36307,81	18197,01	10715,19
25703,96	61659,5	16595,87
17782,79	21877,62	3981,072

MNCPU		
Luminal		
6 h.p.i		
C1-06	**C1-16**	**C4-04**
22,90868	186,2087	169,8244
22,38721	125,8925	204,1738
39,81072	204,1738	165,9587
33,11311	323,5937	316,2278
44,66836	269,1535	323,5937

MNCPU		
Luminal		
24 h.p.i		
C1-06	**C1-16**	**C4-04**
3801,894	1819,701	3235,937
1348,963	3019,952	4570,882
2570,396	4073,803	1412,538
4073,803	1778,279	8317,638
3235,937	2344,229	7585,776

MNCPU		
Luminal		
48 h.p.i		
C1-06	**C1-16**	**C4-04**

4073,803	5011,872	7244,36
3162,278	2818,383	7413,102
3467,369	2570,396	8511,38
3235,937	10715,19	8128,305
3019,952	3981,072	14454,4

MNCPU		
Luminal		
72 h.p.i		
C1-06	**C1-16**	**C4-04**
4073,803	2290,868	6165,95
3162,278	2137,962	6025,596
3467,369	2570,396	3162,278
3235,937	1513,561	10715,19
3019,952	4365,158	10964,78

VI. Source of data: Fig 51

Pe			
C1-16 with	**C1-16 without**	**C1-16 with**	**C1-16 without**
Day 7	**Day 7**	**Day 11**	**Day 11**
0,43	0,79	0,67	0,81
0,75	0,75	0,68	0,59
1	0,74	0,51	0,63

0,69		0,46	
0,63		0,45	
0,77			

Cycle of quantification (CQ)	
Luminal	
6 h.p.i	
C1-16 with	**C1-16 without**
20,49	23,4132615
21,77	22,3997466
23,75	23,9304961
23,79	24,1631755
21,72	23,1907897
22,83	23,0868496

Cycle of quantification (CQ)	
Luminal	
24 h.p.i	
C1-16 with	**C1-16 without**
19,17	21,2494954
17,67	19,0207156
19,82	19,7425548
17,8	20,1686501
17,93	20,4681451

18,12	20,1098475

Cycle of quantification (CQ)	
Luminal	
48 h.p.i	
C1-16 with	**C1-16 without**
19,83	22,9798041
20,29	21,4101305
18,13	20,390002
17,32	19,3056627
15,12	22,8010239
16,18	20,9825043

Cycle of quantification (CQ)	
Luminal	
72 h.p.i	
C1-16 with	**C1-16 without**
21,13	23,9354751
20,65	22,1777812
21,31	20,5731024
16,66	20,3477745
16,65	23,2994298
18,17	21,402791

Cycle of quantification (CQ)	
Abluminal	
6 h.p.i	
C1-16 with	**C1-16 without**
33,3	31,9029037
30,02	32,6049635
31,29	31,6486487
32,15	33,0467397
25,08	29,9107273
25,64	35,7210619

Cycle of quantification (CQ)	
Abluminal	
24 h.p.i	
C1-16 with	**C1-16 without**
30,03	33,4583594
28,33	34,3564518
28,09	34,2190228
33,74	34,536208
30,04	34,0589093
31,04	35,9738811

Cycle of quantification (CQ)
Abluminal

48 h.p.i	
C1-16 with	**C1-16 without**
34,43	33,7236504
30,65	32,2794381
28,01	33,0338693
32,27	31,3959402
29,19	33,3090929
31,4	33,8343133

Cycle of quantification (CQ)	
Abluminal	
72 h.p.i	
C1-16 with	**C1-16 without**
33,58	31,7490162
31,84	31,4629417
30,45	32,3983217
30,79	29,3949262
30,95	32,1366809
31,23	34,4845085

Cycle of quantification (CQ)
Luminal
6 h.p.i

E6	TNF-α luminal + C1-16	TNF-α abluminal + C1-16	C1-16
32,89	24,06	24,09	20,49
32,74	24,27	24,71	21,77
32,19	23,04	23,23	23,75
31,71	25,32	23,67	23,79
30,58	24,3	23,19	21,72
31,27	25,01	24,19	22,83

Cycle of quantification (CQ)			
Luminal			
24 h.p.i			
E6	TNF-α luminal + C1-16	TNF-α abluminal + C1-16	C1-16
18,35	17,94	17,64	19,17
17,91	18,35	16,64	17,67
18,01	18,26	18,49	19,82
16,65	18,63	20,36	17,8
19,65	25,6	21,03	17,93
19,12	19,46	19,34	18,12

Cycle of quantification (CQ)

Luminal		
48 h.p.i		
TNF-α luminal + C1-16	**TNF-α abluminal + C1-16**	**C1-16**
17,34	16,17	19,83
18,11	16,13	20,29
16,6	17,03	18,13
18,06	19,22	17,32
19,94	21,07	15,12
19,59	19,8	16,18

Cycle of quantification (CQ)			
Abluminal			
6 h.p.i			
E6	**TNF-α luminal + C1-16**	**TNF-α abluminal + C1-16**	**C1-16**
36,46	33,45	31,52	33,3
39,67	32,27	33,74	30,02
36,57	35,1	34,69	31,29
36,57	32,44	29,48	32,15
38,37	32,12	28,1	25,08
35,26	34,56	30,65	25,64

Cycle of quantification (CQ)			
Abluminal			
24 h.p.i			
E6	**TNF-α luminal + C1-16**	**TNF-α abluminal + C1-16**	**C1-16**
39,69	35,31	34,39	30,03
40,77	37,43	32,97	28,33
38,95	33,53	33,92	28,09
38,68	26,47	31,83	33,74
38,87	19,5	33,57	30,04
37,24	27,93	29,28	31,04

Cycle of quantification (CQ)		
Abluminal		
48 h.p.i		
TNF-α luminal + C1-16	**TNF-α abluminal + C1-16**	**C1-16**
32,97	31,27	34,43
32,95	32,07	30,65
31,77	31,32	28,01
29,7	33,6	32,27

29,55	30,23	29,19
31,12	31,29	31,4

Cycle of quantification (CQ)		
Luminal		
6 h.p.i		
C1-06	**C1-16**	**C4-04**
21,8	20,49	22,41
23,49	21,77	21,55
22,46	23,75	22,23
22,32	23,79	21,98
21,75	21,72	22,01
20,7	22,83	21,74

Cycle of quantification (CQ)		
Luminal		
24 h.p.i		
C1-06	**C1-16**	**C4-04**
17,75	19,17	18,59
19,03	17,67	18,39
18,34	19,82	18,44
17,86	17,8	19,68
20,04	17,93	19,43
18,35	18,12	18,15

Cycle of quantification (CQ)		
Luminal		
48 h.p.i		
C1-06	**C1-16**	**C4-04**
17,07	19,83	17,12
16,88	20,29	16,49
15,76	18,13	17,03
15,72	17,32	17,33
15,75	15,12	16,84
15,43	16,18	15,59

Cycle of quantification (CQ)		
Luminal		
72 h.p.i		
C1-06	**C1-16**	**C4-04**
17,39	21,13	17,73
17,14	20,65	18,77
16,7	21,31	17,89
17,07	16,66	16,8
14,95	16,65	15,32
15,96	18,17	17,28

Cycle of quantification (CQ)

Abluminal		
6 h.p.i		
C1-06	**C1-16**	**C4-04**
24,7	33,3	25,08
25,41	30,02	26,54
28,06	31,29	24,8
25,21	32,15	28,18
25,25	25,08	24,14
24,44	25,64	23,42

Cycle of quantification (CQ)		
Abluminal		
24 h.p.i		
C1-06	**C1-16**	**C4-04**
26,91	30,03	27,77
27,96	28,33	29,68
26,39	28,09	27,03
30,78	33,74	29,92
27,35	30,04	28,21
31,26	31,04	28,2

Cycle of quantification (CQ)
Abluminal
48 h.p.i

C1-06	C1-16	C4-04
30,92	34,43	28,99
29,41	30,65	30,11
29,44	28,01	28,42
30,84	32,27	30,49
32,07	29,19	31,15
30,63	31,4	29,81

Cycle of quantification (CQ)		
Abluminal		
72 h.p.i		
C1-06	**C1-16**	**C4-04**
29,11	33,58	30,27
30,99	31,84	30,18
28,22	30,45	30,19
29,7	30,79	29,6
30,99	30,95	30,24
27,02	31,23	30,49

VII. Neuropathogenesis of Enterovirus 71: Business plan for a biomedical reseach

Igor Lopes Coqueiro

Neuropathogenesis of Enterovirus 71:
Business plan for a biomedical research

Clermont-Ferrand
2022

A pathogenicity study

The comprehension of cellular and molecular mechanisms that underlies the human diseases is fundamental for building solid pillars, in which scientific community can solve questions and inspire the development of appropriate clinical interventions. The box 1 summarize the main study platform that can be adopted for performing biomedical researches. These approaches complement themselves, and their respective choice depends on the addressed questions.

In vitro studies

***Primary cells*:** cells isolated from primary tissues of animals or human biopsies

***Immortalized cell lines*:** cell lines originated from tumors or genetic modification to allows the in vitro long-term propagation

***Embryonic stem cells (ESCs)*:** undifferentiated cells isolated from inner cell mas of blastocist (cellular structure that precedes the implantation). ESCs are able to perform long-term replication without lose their phenotype, and differentiate in whether cell type of human body under appropriate stimulation. This property is known as pluripotency.

***Multipotent stem cells and progenitor cells*:** undifferentiated cells isolated from adult tissues with potential of differentiation tissue-specific.

***Induced pluripotent stem cells (iPSC)*:** reprogramed cells that achieved pluripotent status by cytoplasmic introduction of factors without any genetic manipulation.

***Organoids*:** tridimensional cellular structures originated from primary tissues or iPSC. Organoids resemble organizational patterns and physiological functions of embryony organs.

In vivo studies

***Animal models*:** several species of animals are widely used to validate information from in vitro observations in a complex living organism.

Box 1. Summary of strategies for biomedical investigations

Research background

During the last three years I performed my PhD stage at Université Clermont Auvergne (UCA), in Clermont-Ferrand, in the center of France. UCA is a young University created in 2017 further the fusion of two ancient universities - Université d'Auvergne (Clermont-

I) and Blaise-Pascal (Clermont-II). Currently I am associated to the Laboratoire Microorganismes: Génome Environnement (LMGE), which has a particular interest in microbial interactions. The Epidemiology and Physiopathology of Enterovirus Diseases (EPIE) group is responsible for an expressive surveillance of enteroviruses, a group of pathogens close-related to the polio virus.

My PhD project was part of a consortium (OrganoVIR) created in 2019 by Marie Skłodowska-Curie Actions with an objective of moving the viral research forward through advanced cellular studies with organoids. Such experience gave me opportunity to immerse in the field of virology research and reflect about the complexity of cortical brain microvasculature, as well as it role in regulating neural functions through the blood-brain barrier (BBB) (**Fig. 48**).

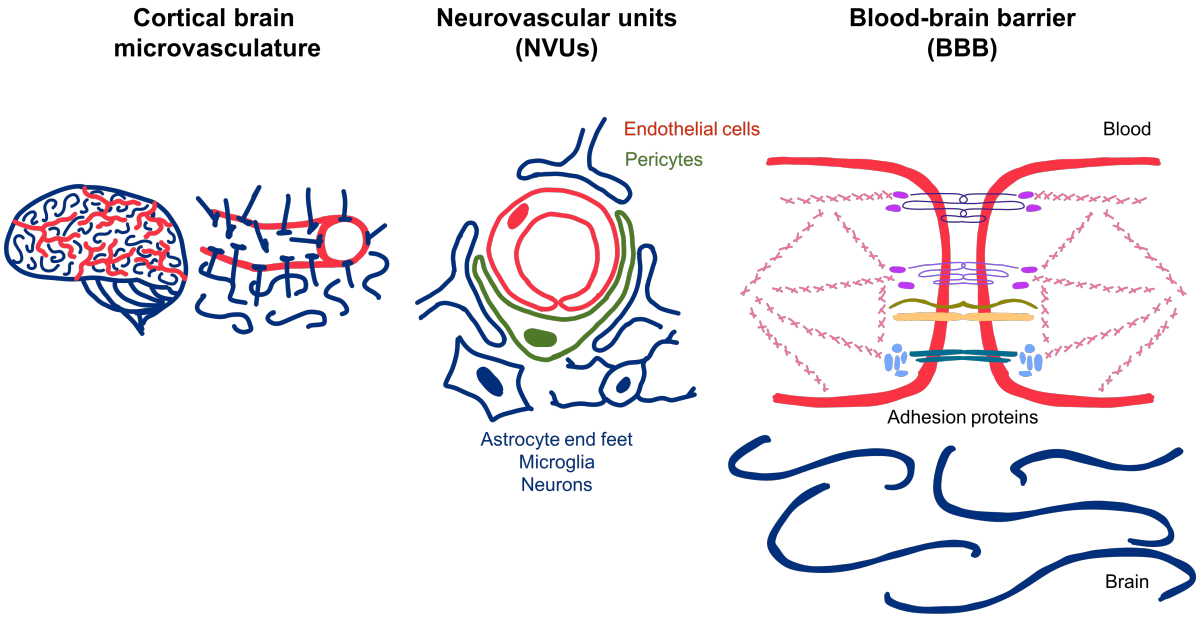

Fig. 49. Anatomy of cortical brain microvasculature. The brain cortex is perfused by microvessels that tailor a unique configuration. The endothelial cells that form the blood vessel walls are hanged by pericytes. This vascular circuit embedded on neural environment exposes the endothelium to astrocyte end feet, microglia and neurons; defined as neurovascular units (NVUs), which induces the expression of highly specialized proteins on endothelial cells. This complex phenotype limits the passage of cells, molecules and pathogens from blood to brain; regulating neural functions through the establishment of the blood-brain barrier (BBB). Author image.

An in vitro BBB model was used in previous experiments to investigate the its interaction with the EV-A71. The cell supernatants of both luminal and abluminal compartments were exposed to cells susceptible to EV-A71, Rhabdomyosarcoma (RD) cells. We performed serial analysis to check if the cell supernatant could induce

the death of RD cells. This analysis indicated the minimal number of cytopathogenic units (MNCPU), which is used as a parameter for estimate the number of infectious particles present in a sample. We could able to observe cytopathogenic units only in cells exposed to luminal supernatant. The assays performed with the abluminal supernatant presented a MNCPU below the levels of detection. The cell supernatants were also summited to molecular analysis based on amplification of viral genome by the technic of reverse transcription of polymerase chain reaction, or simply RT-qPCR. Surprisingly, we detected viral genome in cell supernatants from both luminal and abluminal compartment. Therefore, our results suggest that EV-A71 does not cross freely the BBB, but during this infectious context the human BBB may releases viral genome in the brain parenchyma.

Gap

Some investigations show that EV-A71 may cross the BBB inside extracellular vesicles, and these vesicles may be capable to infect cells of CNS, such astrocytes. We do not know if the detection of the viral RNA genome on the abluminal supernatant may be an indirect evidence of extracellular vesicles, or if endothelial cells are actually releasing viral genome into the extracellular environment by some other mechanism. Moreover, the implications of this phenomenon on the brain parenchyma is poorly understood.

Hypothesis

Endothelial cells may affect the viral life cycle by a mechanism of premature viral genome releasing. During a viremia context, endothelial cells that form the BBB may be infected by EV-A71 and activates a polarized flux of content directed to the brain parenchyma. We hypothesize that endothelial cells may harbor mechanisms so far unknown that may affect the viral life cycle of EV-A71 and cause a premature viral genome releasing. Among intracellular mechanisms that may participate of this phenomenon we suggest signaling pathways that converge in apoptotic processes, mitochondrial mobilization, lysosomal metabolism, as well as activation of endoplasmic reticulum, and Golgi complex. Thus, we suggest that during a context of EV-A71 infection the BBB may releases viral RNA molecules inside extracellular vesicles.

Moreover, we suggest that this phenomenon may induce cellular responses on the brain parenchyma, such as production of immune mediators (**Fig. 49**).

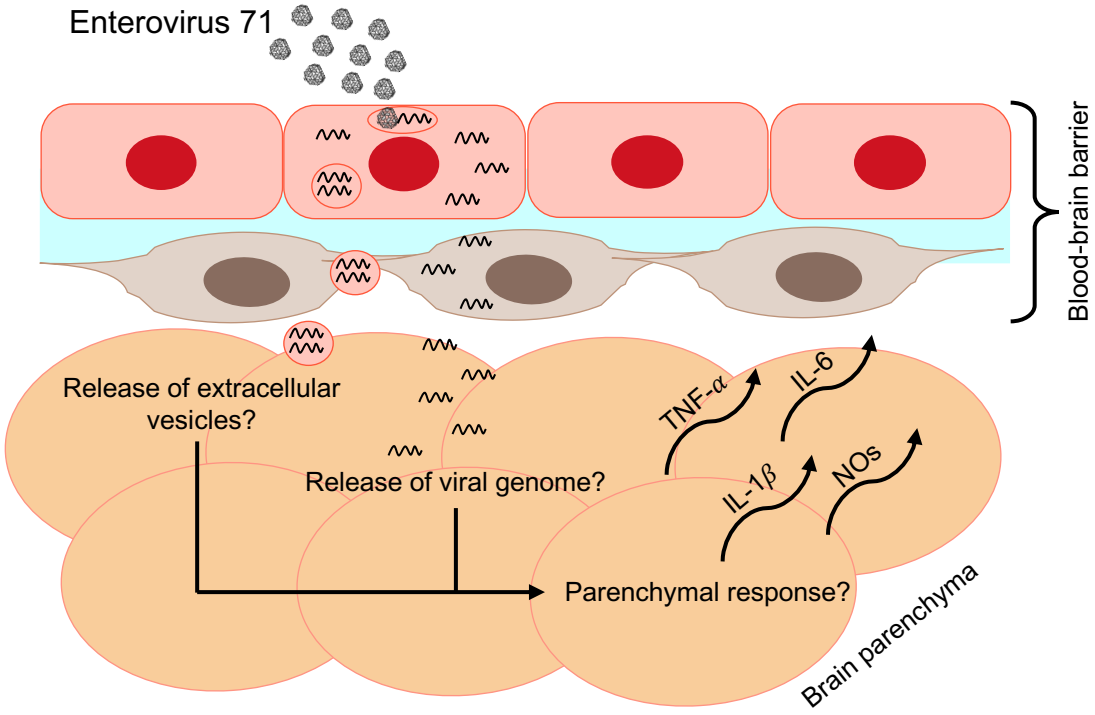

Fig. 50. Hypothesis of premature viral genome release. When EV-A71 infections progress to a viremia the BBB trigger a flux of content that can release viral genome without encapsidation into the brain parenchyma. We are interested on investigating if it may induce parenchymal response, and eventually participate of EV-A71 neuropathogenesis. Copyright image.

Goal

Main goal: Understand cellular and molecular mechanisms existing between the human BBB and the brain parenchyma associated with the neuropathogenesis of EV-A71.

- **Goal #1:** Evaluate how the BBB releases viral genome of EV-A71;
- **Goal #2:** Exploring the communication between the blood-brain barrier and the brain parenchyma;
- **Goal #3:** Integrate an in vitro model of the human BBB to cerebral organoids;
- **Goal #4:** Implement in our laboratory a protocol of cerebral organoid manufacturing for studying aspects of neuropathogenesis of EV-A71.

The proposition

We propose to use a cell-based system as platform for studying neuropathogenesis of EV-A71. To validate our hypothesis, ascertain the neuropathogenesis of EV-A71, our study design consists in integrate a cellular model of the human BBB already established in our laboratory to cerebral organoids (**Fig. 1**).

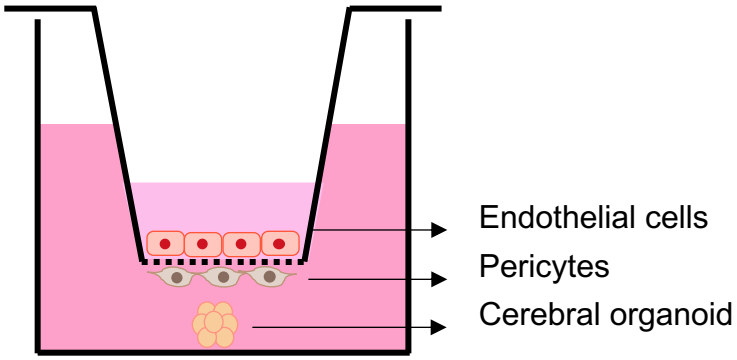

Fig. 51. Interaction of BBB model to cerebral organoid. The respective study design purpose to co-culture endothelial cells and pericytes in opposite sides of semi permeable membranes placed above cerebral organoids. Copyright image.

We subdivided this project in two axes. The **Axis I** will produce and characterize cerebral organoids while, and the **Axis II** will focus on the integration of cerebral organoids into BBB model. This project is designed as a Post-doc training that will be responsible for advising two Ph.D students. Each Ph.D student will conduct one of the axis of this project, and transfer their technical expertise for a master student.

Axis I: Evaluate the effect of Enterovirus 71 on the human brain	**Axis II: Investigate the communication between the blood-brain barrier and the brain parenchyma during Enterovirus 71**
Goal 1: Elaboration of microglia-enriched cerebral organoid;	**Goal 5:** Merge in vitro blood-brain barrier with microglia-enriched cerebral organoids;
Goal 2: Evaluate the influence of hematopoietic progenitors in cerebral organoids;	**Goal 6:** Investigate how the viral RNA genome is released from the BBB;

Goal 3: Standardize an infection assay in microglia-enriched cerebral organoids;	**Goal 7:** Analyze if infection of the BBB affects microglia-enriched cerebral organoids;
Goal 4: Characterize the immune response of microglia-enriched cerebral organoids.	**Goal 8:** Evaluate the if response of microglia enriched cerebral organoid affects the BBB.

The flowchart below summarizes the main strategies for achieving our milestones.

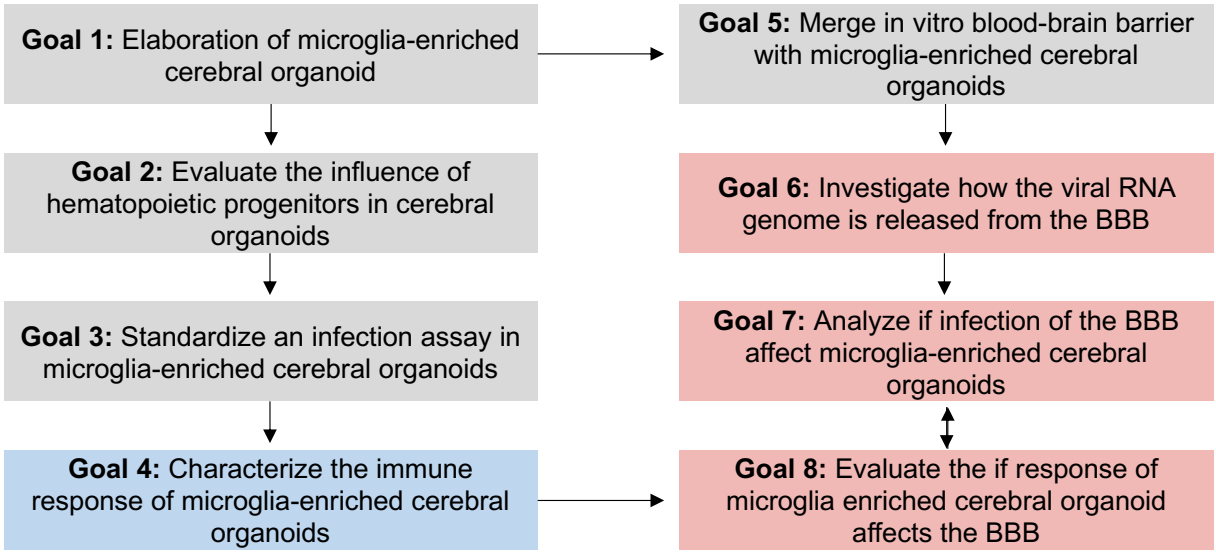

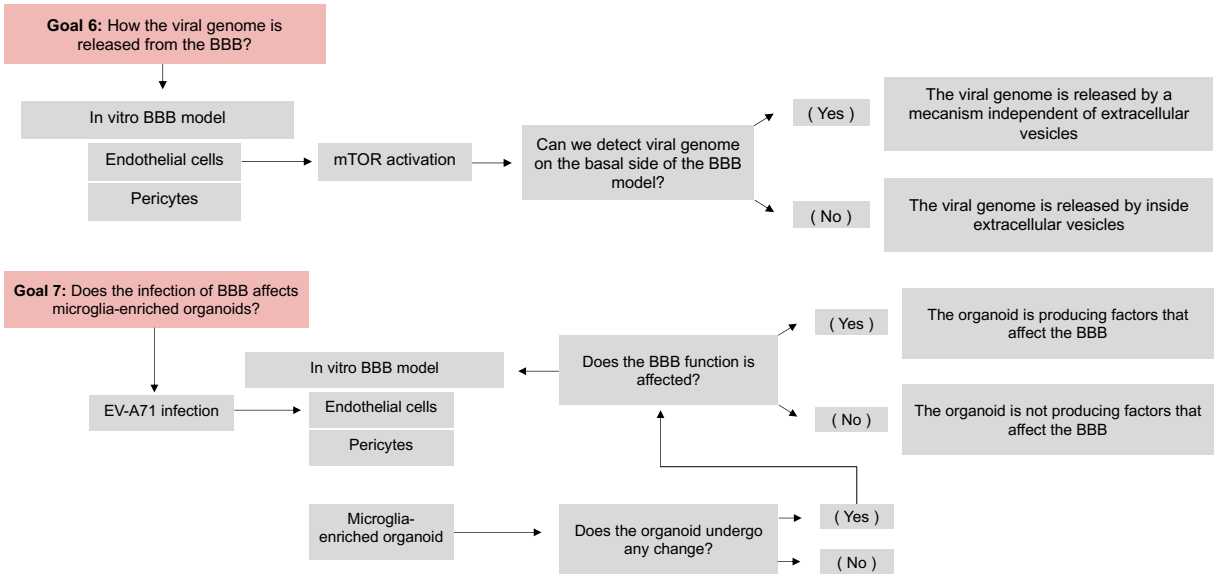

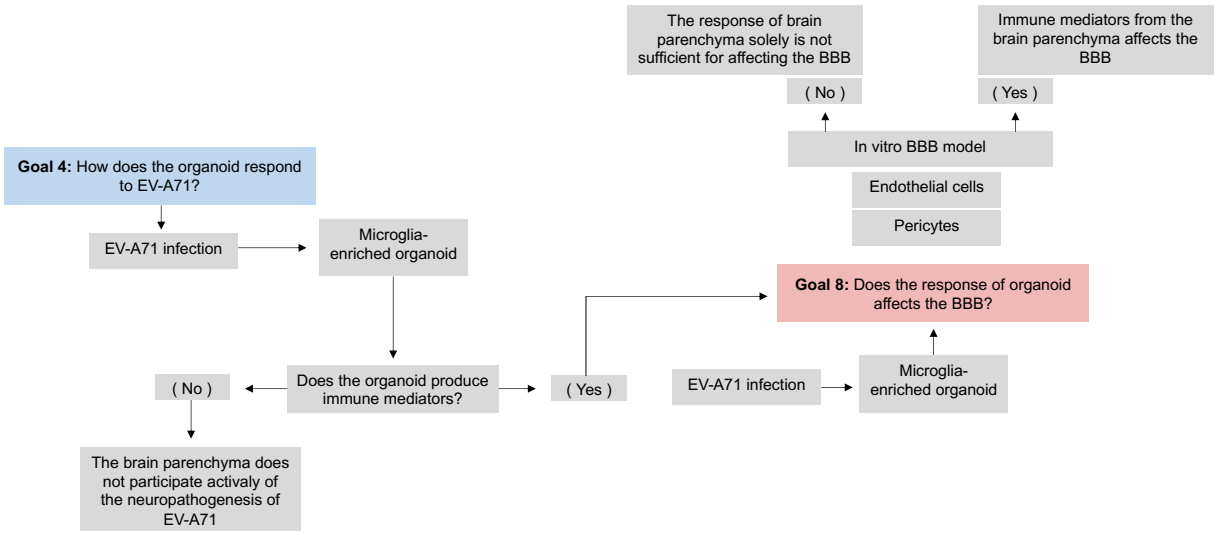

Value proposition (Canvas model)

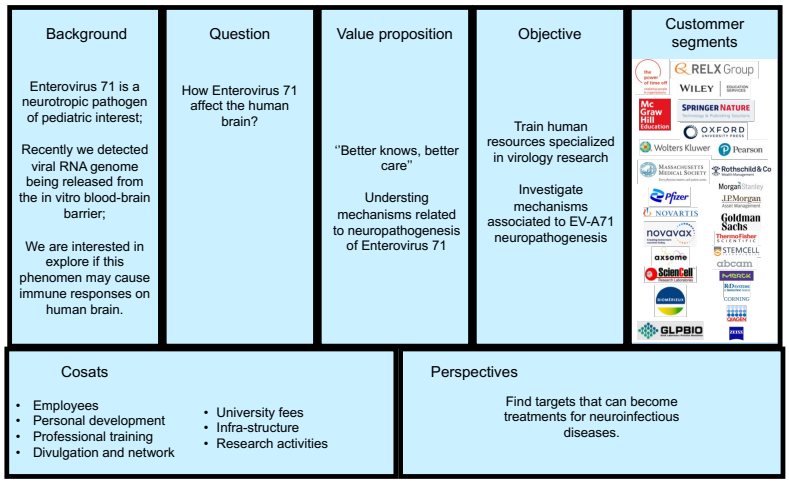

Budget

Detailed budget

Category	Subject	Company	Reference	Unitary price	Quantity	Total price
Employee	Post-doc/five years	Université Clermont Auvergne		260 000,00 €	1	260 000,00 €
Employee	PhD/three and half years	Université Clermont Auvergne		140 000,00 €	2	280 000,00 €
Employee	Master/two years	Université Clermont Auvergne		60 000,00 €	2	120 000,00 €
Personal development	Rewild yourself	The power of time off		275,00 €	6	1 650,00 €

Personal development	Stress less with yin	The power of time off		275,00 €	6	1 650,00 €
Personal development	Eat well: be well	The power of time off		275,00 €	6	1 650,00 €
Personal development	Master your mind	The power of time off		275,00 €	6	1 650,00 €
Professional training	Pluripotent Stem Cell Maintenance & Cell Quality	STEMCELL technologies, Vancouver, Canada	# 500-0171	365,00 €	2	730,00 €
Professional training	Pluripotent Stem Cell Training	STEMCELL technologies, Vancouver, Canada	# 00223NL.2	1 468,00 €	1	1 468,00 €
Professional training	Hematopoietic Colony-Forming Unit Assay Set-up & Enumeration	STEMCELL technologies, Vancouver, Canada	# 500-0223	315,00 €	3	945,00 €
Professional training	Human Intestinal Organoid Maintenance & Downstream Applications	STEMCELL technologies, Vancouver, Canada	# 500-0224	450,00 €	3	1 350,00 €
Professional training	Stage of 90 days for technical training (Hosting)			13 500,00 €	2	27 000,00 €
Professional training	Stage of 90 days for technical training (University fees)			15 000,00 €	2	30 000,00 €
Professional training	Stage of 90 days for technical training (Travel expenses)			7 800,00 €	2	15 600,00 €
Divulgation	International congress (Fees)			700,00 €	3	2 100,00 €
Divulgation	International congress (Hosting)			750,00 €	3	2 250,00 €
Divulgation	International congress (Travel expenses)			1 860,00 €	3	5 580,00 €
Divulgation	Local congress (Fees)			350,00 €	5	1 750,00 €
Divulgation	Local congress (Hosting)			450,00 €	5	2 250,00 €
Divulgation	Local congress (Travel expenses)			660,00 €	5	3 300,00 €

Divulgation	Publication fees			100 000,00 €	1	100 000,00 €
University fees	Tercerized services	Université Clermont Auvergne		20 000,00 €	1	20 000,00 €
Infra-structure	Falcon® Conical Tubes, 50 mL	STEMCELL technologies, Vancouver, Canada	# 38010	206,00 €	2	412,00 €
Infra-structure	Falcon® Conical Tubes, 15 mL	STEMCELL technologies, Vancouver, Canada	# 38009	195,00 €	2	390,00 €
Infra-structure	Corning® Cryogenic Vials with Orange Caps	STEMCELL technologies, Vancouver, Canada	# 38053	343,00 €	2	686,00 €
Infra-structure	Corning® Cryogenic Vial Cap Inserts	STEMCELL technologies, Vancouver, Canada	# 38081	82,00 €	2	164,00 €
Infra-structure	Corning® Lambda™ Plus Multi-Channel Pipettor, 8-Channels	STEMCELL technologies, Vancouver, Canada	# 38110	507,00 €	1	507,00 €
Infra-structure	Corning® Lambda™ Plus Multi-Channel Pipettor, 12-Channels	STEMCELL technologies, Vancouver, Canada	# 38064	706,00 €	1	706,00 €
Infra-structure	Corning® Lambda™ Plus Pipettor	STEMCELL technologi	# 38063	942,00 €	1	942,00 €

		es, Vancouver, Canada				
Infra-structure	Corning® Lambda™ Plus Pipettor, 2 uL	STEMCELL technologies, Vancouver, Canada	# 38062	245,00 €	1	245,00 €
Infra-structure	Axygen® Reagent Reservoir	STEMCELL technologies, Vancouver, Canada	# 38080	173,00 €	2	346,00 €
Infra-structure	Corning® Filtered Pipette Tips, 2 uL	STEMCELL technologies, Vancouver, Canada	# 38035	152,00 €	2	304,00 €
Infra-structure	Corning® Filtered Pipette Tips, 10 uL	STEMCELL technologies, Vancouver, Canada	# 38034	147,00 €	2	294,00 €
Infra-structure	Corning® Filtered Pipette Tips, 30 uL	STEMCELL technologies, Vancouver, Canada	# 38033	141,00 €	2	282,00 €
Infra-structure	Corning® Filtered Pipette Tips, 200 uL	STEMCELL technologies, Vancouver, Canada	# 38032	169,00 €	4	676,00 €
Infra-structure	Corning® Filtered Pipette Tips, 1000 uL	STEMCELL technologies,	# 38031	158,00 €	4	632,00 €

		Vancouver, Canada				
Infra-structure	Costar® Microcentrifuge Tubes, 0.65 mL	STEMCELL technologies, Vancouver, Canada	# 38088	119,00 €	3	357,00 €
Infra-structure	Costar® Microcentrifuge Tubes, 1.7 mL	STEMCELL technologies, Vancouver, Canada	# 38038	389,00 €	1	389,00 €
Infra-structure	Axygen® PCR Tube Storage Rack with Lid, Spectrum Pack	STEMCELL technologies, Vancouver, Canada	# 38109	205,00 €	2	410,00 €
Infra-structure	Falcon® Serological Pipettes, 2 mL	STEMCELL technologies, Vancouver, Canada	# 38002	271,00 €	1	271,00 €
Infra-structure	Falcon® Serological Pipettes, 5 mL	STEMCELL technologies, Vancouver, Canada	# 38003	83,00 €	5	415,00 €
Infra-structure	Falcon® Serological Pipettes, 10 mL	STEMCELL technologies, Vancouver, Canada	# 38004	84,00 €	5	420,00 €
Infra-structure	Falcon® Serological Pipettes, 25 mL	STEMCELL technologies, Vancouver, Canada	# 38005	160,00 €	3	480,00 €

Infra-structure	Station MSC Advantage 1.8, 230V, 50HZ, certification EN	Thermo Fisher Scientific, Waltham, USA	23264	12 038,00 €	1	12 038,00 €
iPSCs culture	mTeSR™ Plus	STEMCELL technologies, Vancouver, Canada	# 100-0276	368,00 €	9	3 312,00 €
iPSCs culture	CryoStor® CS10	STEMCELL technologies, Vancouver, Canada	# 100-1061	404,00 €	2	808,00 €
iPSCs culture	Gentle Cell Dissociation Reagent	STEMCELL technologies, Vancouver, Canada	# 100-0485	51,00 €	1	51,00 €
iPSCs culture	Trypan Blue	STEMCELL technologies, Vancouver, Canada	# 07050	86,00 €	1	86,00 €
iPSCs culture	Corning® Matrigel® hESC-Qualified Matrix	Corning, New York, USA	354277	316,47 €	2	632,94 €
Hematopoietic differentiation	STEMdiff™ Hematopoietic Kit	STEMCELL technologies, Vancouver, Canada	# 05310	642,00 €	15	9 630,00 €
Hematopoietic differentiation	MethoCult™ SF H4636	STEMCELL technologies, Vancouver, Canada	# 04636	536,00 €	15	8 040,00 €

Hematopoietic differentiation	STEMdiff™ Microglia Differentiation Kit	STEMCELL technologies, Vancouver, Canada	# 100-0019	711,00 €	15	10 665,00 €
Cerebral organoid	STEMdiff™ Cerebral Organoid Kit	STEMCELL technologies, Vancouver, Canada	# 08570	352,00 €	15	5 280,00 €
Cerebral organoid	D-PBS (Without Ca++ and Mg++)	STEMCELL technologies, Vancouver, Canada	# 37350	40,00 €	10	400,00 €
Cerebral organoid	Y-27632 (Dihydrochloride)	STEMCELL technologies, Vancouver, Canada	# 72302	159,00 €	1	159,00 €
Cerebral organoid	Costar® 24-Well Flat-Bottom Plate, Tissue Culture-Treated	STEMCELL technologies, Vancouver, Canada	# 38017	184,00 €	1	184,00 €
Cerebral organoid	Costar® 24-well Clear Flat Bottom Ultra-Low Attachment	Corning, New York, USA	3473	548,29 €	1	548,29 €
Cerebral organoid	Corning® 96-well round-bottom ultra-low attachment microplate	Merck, Darmstadt, Germany	CLS7007-24EA	633,00 €	1	633,00 €
Cerebral organoid	Ultra-Low Adherent Plate for Suspension Culture	STEMCELL technologies, Vancouver, Canada	# 38071	601,00 €	3	1 803,00 €
Cerebral organoid	Axygen™ 200 µL wide bore universal pipette tips	Fisher Scientific,	14-222-730	675,00 €	2	1 350,00 €

		Hamton, USA				
Cerebral organoid	100 mm Dish, Non-Treated	STEMCELL technologies, Vancouver, Canada	# 38045	203,00 €	2	406,00 €
Cerebral organoid	Fluo-4 Direct™ Calcium Assay Kit	Thermo Fisher Scientific, Waltham, USA	F10471	524,00 €	1	524,00 €
Cerebral organoid	L-Glutamine Solution 200 mM	Merck, Darmstadt, Germany	59202C-100ML	26,00 €	1	26,00 €
Cerebral organoid	Tetanus Toxoid	Merck, Darmstadt, Germany	582231-25UG	302,00 €	1	302,00 €
Cerebral organoid	PARAFILM® M	Merck, Darmstadt, Germany	P7793-1EA	45,90 €	4	183,60 €
Cerebral organoid	Celltron orbital shaker	Infors AG, Bottmingen, Switzerland	69222	4 818,80 €	1	4 818,80 €
In vitro blood-brain barrier	BLECs	LBHE	///	100,00 €	10	1 000,00 €
In vitro blood-brain barrier	Bovine pericytes	LBHE	///	75,00 €	10	750,00 €
In vitro blood-brain barrier	Fœtal bovine serum for BBB model	LBHE	///	73,50 €	2	147,00 €
In vitro blood-brain barrier	Endothelial Cell Medium	ScienCell, Carlsbad, Canada	#1001	126,00 €	3	378,00 €
In vitro blood-brain barrier	Collagen type I	R&D Systems, Minneapolis, USA	3440-005-01	52,00 €	1	52,00 €
In vitro blood-brain barrier	10 X D-PBS (Without Ca++ and Mg++)	STEMCELL technologies,	# 37354	77,00 €	1	77,00 €

		Vancouver, Canada				
In vitro blood-brain barrier	Gibco™ Distilled Water	Fisher Scientific, Hamton, USA	15-230-196	199,00 €	2	398,00 €
In vitro blood-brain barrier	1 N Sodium hydroxide solution	Merck, Darmstadt, Germany	S2770-100ML	38,10 €	1	38,10 €
In vitro blood-brain barrier	DMEM/F-12 with 15 mM HEPES	STEMCELL technologies, Vancouver, Canada	# 36254	47,00 €	9	423,00 €
In vitro blood-brain barrier	Hanks′ Balanced Salt solution (HBSS)	Merck, Darmstadt, Germany	H6648-1L	54,00 €	15	810,00 €
In vitro blood-brain barrier	HEPES Buffer Solution (1 M)	STEMCELL technologies, Vancouver, Canada	# 07200	179,00 €	3	537,00 €
In vitro blood-brain barrier	Pyruvate de sodium (100 mM)	Fisher Scientific, Hamton, USA	11360070	15,58 €	3	46,74 €
In vitro blood-brain barrier	Lucifer Yellow CH dilithium salt	Merck, Darmstadt, Germany	L0259-25MG	220,00 €	1	220,00 €
In vitro blood-brain barrier	Rhodamine 123	Merck, Darmstadt, Germany	83702	210,00 €	1	210,00 €
In vitro blood-brain barrier	Elacridar	Merck, Darmstadt, Germany	SML0486-10MG	146,00 €	1	146,00 €
In vitro blood-brain barrier	Rapamycin	GLPBIO, Montclair, Canada	GC15031	50,00 €	1	50,00 €
In vitro blood-brain barrier	GS-9620	GLPBIO, Montclair, Canada	GC12555	79,00 €	1	79,00 €

In vitro blood-brain barrier	Formoterol Fumarate Dihydrate (FFD)	GLPBIO, Montclair, Canada	GC19858	90,00 €	1	90,00 €
In vitro blood-brain barrier	Corning® Transwell® polyester membrane cell culture inserts	Merck, Darmstadt, Germany	CLS3460-48EA	393,00 €	8	3 144,00 €
In vitro blood-brain barrier	Corning® CellBIND® Multiple Well Plate	Merck, Darmstadt, Germany	CLS3336	238,00 €	4	952,00 €
Viral genome detection	Enterovirus R-GENE®	BioMérieux, Marcy-l'Étoile, France	Réf.69-005B	1 829,00 €	4	7 316,00 €
Viral genome detection	easyMAG® navette cônes	BioMérieux, Marcy-l'Étoile, France	Ref. 280135	1 829,00 €	4	7 316,00 €
Extracellular vesicles research	Extracellular Vesicle SEC Columns	STEMCELL technologies, Vancouver, Canada	# 100-0414	481,00 €	2	962,00 €
Immune response analysis	Human IL-6 Quantikine ELISA Kit	R&D Systems, Minneapolis, USA	D6050	649,00 €	9	5 841,00 €
Immune response analysis	Human IL-1 beta/IL-1F2 Quantikine ELISA Kit	R&D Systems, Minneapolis, USA	DLB50	614,00 €	9	5 526,00 €
Immune response analysis	Quantikine Immunoassay Control Group 1	R&D Systems, Minneapolis, USA	QC01-1	162,00 €	9	1 458,00 €
Immune response analysis	Human TNF-alpha Quantikine ELISA Kit	R&D Systems, Minneapolis, USA	DTA00D	614,00 €	9	5 526,00 €
Immune response analysis	Quantikine Immunoassay Control Set 248 for Human TNF-alpha	R&D Systems, Minneapolis, USA	QC248	162,00 €	9	1 458,00 €

Immune response analysis	Total Nitric Oxide and Nitrate/Nitrite Parameter Assay Kit	R&D Systems, Minneapolis, USA	KGE001	419,00 €	9	3 771,00 €
Immune response analysis	Parameter Immunoassay Control Set 849 for Nitrate	R&D Systems, Minneapolis, USA	QC134	162,00 €	9	1 458,00 €
Immune response analysis	Parameter Immunoassay Control Set 904 for Nitrite	R&D Systems, Minneapolis, USA	QC135	162,00 €	9	1 458,00 €
Gene expression analys	Kit TURBO DNA-free™	Thermo Fisher Scientific, Waltham, USA	AM1907	210,00 €	9	1 890,00 €
Gene expression analys	Réactif TRIzol™	Thermo Fisher Scientific, Waltham, USA	15596026	290,00 €	9	2 610,00 €
Gene expression analys	Transcriptase inverse SuperScript™ III	Thermo Fisher Scientific, Waltham, USA	18080044	434,00 €	9	3 906,00 €
Gene expression analys	RT² SYBR Green Fluor qPCR Mastermix	QIAGEN, Venlo, Holland	330513	1 983,00 €	9	17 847,00 €
Immunofluorescense microscopy	DeadEnd™ Fluorometric TUNEL System	Promega, Madison, USA	G3250	672,00 €	2	1 344,00 €
Immunofluorescense microscopy	Caspase-Glo® 3/7 3D Assay	Promega, Madison, USA	G8981	397,00 €	2	794,00 €
Immunofluorescense microscopy	2N Hydrochloric Acid	Fisher Scientific, Hamton, USA	SA431-500	106,00 €	1	106,00 €
Immunofluorescense microscopy	Paraformaldehyde Solution, 4% in PBS	Thermo Fisher Scientific,	J19943.K2	59,80 €	1	59,80 €

		Waltham, USA				
Immunofluorescense microscopy	15mL Sucrose Standard Solution, Brix 30%	Fisher Scientific, Hamton, USA	12613166	69,55 €	1	69,55 €
Immunofluorescense microscopy	Triton X-100 (1%)	Thermo Fisher Scientific, Waltham, USA	HFH10	96,50 €	1	96,50 €
Immunofluorescense microscopy	Normal Donkey Serum	Fisher Scientific, Hamton, USA	OB003001	57,00 €	1	57,00 €
Immunofluorescense microscopy	Donkey anti-Rabbit, Alexa Fluor™ 647	Thermo Fisher Scientific, Waltham, USA	# A-31573	335,00 €	1	335,00 €
Immunofluorescense microscopy	Donkey anti-Rabbit, Alexa Fluor™ 488	Thermo Fisher Scientific, Waltham, USA	# R37118	180,00 €	1	180,00 €
Immunofluorescense microscopy	Donkey anti-Rabbit, Alexa Fluor™ 568	Thermo Fisher Scientific, Waltham, USA	# A10042	307,00 €	1	307,00 €
Immunofluorescense microscopy	Donkey anti-Goat, Alexa Fluor™ 568	Thermo Fisher Scientific, Waltham, USA	# A-11057	306,00 €	1	306,00 €
Immunofluorescense microscopy	Donkey anti-Mouse, Alexa Fluor™ 488	Thermo Fisher Scientific, Waltham, USA	# R37114	180,00 €	1	180,00 €
Immunofluorescense microscopy	Donkey anti-Mouse, Alexa Fluor™ 647	Thermo Fisher Scientific,	# A-31571	335,00 €	1	335,00 €

		Waltham, USA				
Immunofluorescense microscopy	Hoechst 34580	Thermo Fisher Scientific, Waltham, USA	H21486	309,00 €	1	309,00 €
Immunofluorescense microscopy	SlowFade™ Gold Antifade Mountant	Thermo Fisher Scientific, Waltham, USA	S36940	60,50 €	1	60,50 €
Immunofluorescense microscopy	Corning® cover glasses	Merck, Darmstadt, Germany	CLS284518	137,00 €	1	137,00 €
Immunofluorescense microscopy	BRAND® microscope slide	Merck, Darmstadt, Germany	BR474702	262,00 €	1	262,00 €
Immunofluorescense microscopy	Anti-Sox2 Antibody, Rabbit	Merck, Darmstadt, Germany	AB5603-25UG	144,00 €	1	144,00 €
Immunofluorescense microscopy	Anti-Tubulin β 3 (TUJ1), Mouse	BioLegend, San Diego, USA	801213	142,00 €	1	142,00 €
Immunofluorescense microscopy	Anti-GFAP, Rabbit	Cell Signaling Technology, Danvers, USA	12389S	407,00 €	1	407,00 €
Immunofluorescense microscopy	Anti-Iba1, Goat	Abcam, Cambridge, UK	ab48004	545,00 €	1	545,00 €
Immunofluorescense microscopy	Anti-ZO-1, Goat	Thermo Fisher Scientific, Waltham, USA	# PA5-19090	473,00 €	1	473,00 €
Immunofluorescense microscopy	Anti-MPM-2, Mouse	Abcam, Cambridge, UK	ab14581	465,00 €	1	465,00 €

Immunofluorescense microscopy	Anti-LAMP2, Rabbit	Thermo Fisher Scientific, Waltham, USA	# PA1-655	455,00 €	1	455,00 €
Immunofluorescense microscopy	Anti-LC3B, Rabbit	Abcam, Cambridge, UK	ab192890	640,00 €	1	640,00 €
Immunofluorescense microscopy	Anti-CLDN5, Mouse	Thermo Fisher Scientific, Waltham, USA	# CF500843	492,00 €	1	492,00 €
Immunofluorescense microscopy	Anti-GRP94, Goat	Abcam, Cambridge, UK	ab52031	485,00 €	1	485,00 €
Immunofluorescense microscopy	Anti-SEC23IP, Rabbit	Abcam, Cambridge, UK	ab224546	475,00 €	1	475,00 €
Immunofluorescense microscopy	Anti-GM130, Rabbit	Abcam, Cambridge, UK	ab52649	635,00 €	1	635,00 €
Immunofluorescense microscopy	Anti-ARF1, Mouse	Abcam, Cambridge, UK	ab183576	495,00 €	1	495,00 €
					Total	**1 040 813,82 €**

Summarized budget

Category	**Coast**
Employees	660 000,00 €
Personal development	6 600,00 €
Professional training	77 093,00 €
Divulgation	117 230,00 €
University fees	20 000,00 €
Infra-structure	21 366,00 €
Research activities	138 524,82 €
Total coast	**1 040 813,82 €**

Risks

The production of cerebral organoids requires expertise, and this is the first experience of our laboratory in working with this approach. The main challenge of the Axis I is related to downstream applications of the cerebral organoids, such as the standardization of the infection and the phenotypic characterization; during the first year of this project. Another key point of this project is the evaluation of the mechanism of viral releasing from the BBB during the second year of our activities. The main risk of our investigation is to raise inconclusive informations to the validation of the hypothesis that the BBB releases viral genome inside extracellular vesicles.

Competitors

Here, we list few groups that lead researches on the themes proposed by this project:

Penn Neuroscience

Bennett ML, Song H, Ming GL. Microglia modulate neurodevelopment in human neuroimmune organoids. *Cell Stem Cell*. 2021;28(12):2035-2036. doi:10.1016/j.stem.2021.11.005

OrganoVIR LABS

https://organovirlabs.com/

Depla JA, Mulder LA, de Sá RV, et al. Human Brain Organoids as Models for Central Nervous System Viral Infection. *Viruses*. 2022;14(3):634. doi:10.3390/v14030634

Center for Research and Innovation, Mahidol University

https://mt.mahidol.ac.th/en/departments/center-for-research-and-innovation/

Jintana K, Prasertsopon J, Puthavathana P, Lerdsamran H. Antiviral effect in association with anti-apoptosis and anti-autophagy of repurposing formoterol fumarate dihydrate on enterovirus A71-infected neuronal cells. Virus Res. 2022;311:198692. doi:10.1016/j.virusres.2022.198692

Lancaster Lab

https://www2.mrc-lmb.cam.ac.uk/groups/lancaster/

Lancaster MA, Renner M, Martin CA, et al. Cerebral organoids model human brain development and microcephaly. *Nature*. 2013;501(7467):373-379. doi:10.1038/nature12517

Pasterkamp Lab

www.jeroenpasterkamplab.com

Ormel PR, Vieira de Sá R, van Bodegraven EJ, et al. Microglia innately develop within cerebral organoids. *Nat Commun*. 2018;9(1):4167. doi:10.1038/s41467-018-06684-2

NOW Lab

https://nowakowski-lab.squarespace.com/

Popova G, Soliman SS, Kim CN, et al. Human microglia states are conserved across experimental models and regulate neural stem cell responses in chimeric organoids. *Cell Stem Cell*. 2021;28(12):2153-2166.e6. doi:10.1016/j.stem.2021.08.015

Organo Therapeutics

http://organo-therapeutics.com/

Sabate-Soler S, Nickels SL, Saraiva C, et al. Microglia integration into human midbrain organoids leads to increased neuronal maturation and functionality. *Glia*. 2022;70(7):1267-1288. doi:10.1002/glia.24167

Institute of Laboratory Animal Sciences, Chinese Academy of Medical Sciences

https://cnilas.org/en/TeamDesc/717_4641

Zhang Q, Zhao B, Chen X, et al. GS-9620 inhibits enterovirus 71 replication mainly through the NF-κB and PI3K-AKT signaling pathways. *Antiviral Res*. 2018;153:39-48. doi:10.1016/j.antiviral.2018.02.002

Chronogram

Chronogram for achievement of milestones		
Year	**Category**	**Purpose**
2024	Short-term	Assessment of viral genome particles released from infected BBB barriers
2025	Short-term	Identify a panel of cytokines released by the human blood-brain barrier during EV-A71 infection
2026	Mid-term	Validate the hypothesis that the human blood-brain barrier could release the EV-A71 genome inside extracellular vesicles
2027	Mid-term	Explain the possible roles of human leukocytes in neuroinflammation caused by EV-A71
2028		
2029	Long-terme	Establish a three-dimensional cellular model of the human brain to validate neuropathogenicity studies of EV-A71

Perspectives

- Assess possible involvement of immune mediators in EV-A71 neuropathogenesis;
- Investigate how the BBB releases the EV-A71 genome;
- Analyze how the brain parenchyma react to infected BBB;
- Evaluate if immune mediators originated from brain parenchyma may affect the blood-brain barrier;
- Investigate if infected BBB may intensify cellular responses of pre-established neuroinfections.

Implement in our laboratory a platform physiologically relevant based on cerebral organoids for studying neuroinfectious disease

Résumé

La barrière hémato-encéphalique (BHE) formée par la microvasculature cérébrale peut être contournée lors de l'invasion du système nerveux central (SNC) par des virus neurotropes. L'entérovirus A71 (EV-A71) est décrit comme un agent pathogène capable de migrer via les nerfs périphériques vers le cerveau par transport axonal rétrograde. Cependant, nous ne savons toujours pas si l'EV-A71 est capable d'envahir le SNC via la BHE. Dans cette thèse, nous avons utilisé un modèle in vitro de la BHE humaine co-cultivant des cellules endothéliales cérébrales (BLEC) et des péricytes. Grâce à ce modèle, nous avons montré que l'EV-A71 n'affecte pas les principales caractéristiques de la BHE telles que la perméabilité paracellulaire, car peu de cellules endotheliales sont infectées. Le virus infectieux est libéré principalement par le pôle luminal. Cependant, nous avons aussi détecté la libération de quelques particules virales infectieuses par le pôle baso-latéral et la présence d'ARN viraux dans ce compartiment baso-latéral. Ce travail ouvre des perspectives d'étude vers d'autres modes de franchissement de la BHE par l'EV-A71.

Mots-clés : Barrière hémato-encéphalique ; Entérovirus A71 ; Maladie pieds-mains-bouche ; Neuroinflammation ; Infection neurologique.

Abstract

The blood-brain barrier (BBB) formed by the brain microvasculature can be circumvented during the invasion of the central nervous system (CNS) by neurotropic viruses. Enterovirus A71 (EV-A71) is well reported as a pathogen capable of migrating to the brain through peripherical nerves via retrograde axonal transport. However, we still do not know whether EV-A71 is capable of invading the CNS through the BBB. In this thesis we used an in vitro model of the human BBB by co-culture brain-like endothelial cells (BLECs) and pericytes. With this model, we showed that EV-A71 does not affect the main characteristics of the BBB, such as paracellular permeability because few BLECs are productively infected. High amounts of infectious viruses are released from the luminal side. However, we also detected leakage of infectious viruses from the baso-lateral side and the presence of viral RNAs in the baso-lateral compartment. This work provides opportunities to the analyses of other mechanisms of BBB crossing by EV-A71.

Key words: Blood-brain barrier; Enterovirus A71; Hand, foot and mouth disease; Neuroinflammation; Neurological disease